Putative role of cGMP-dependent Protein Kinase G in Inherited Retinal Degeneration: Modulators and Biomarkers

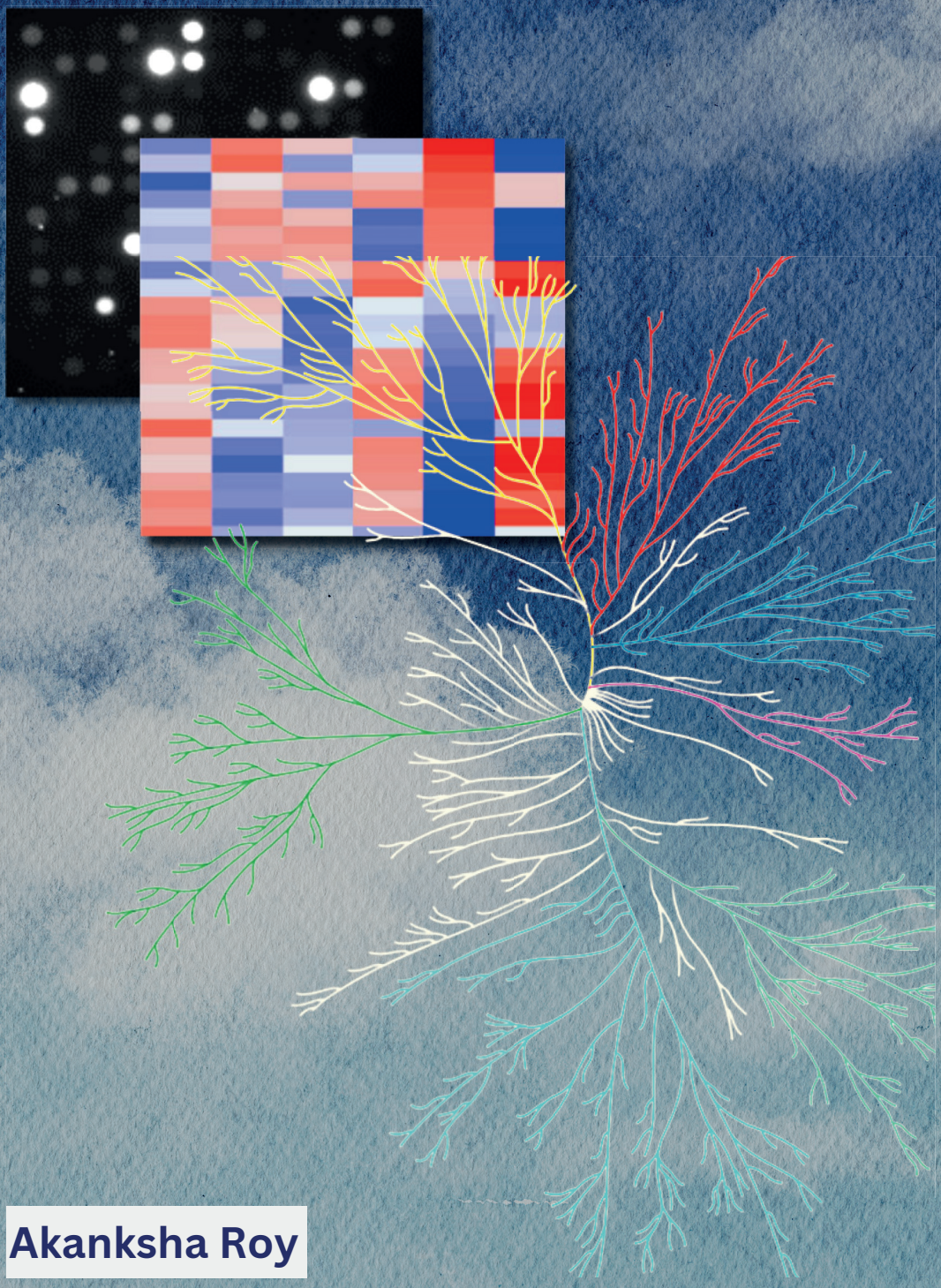

Akanksha Roy

Propositions

1. Unbiased multiplex kinome activity profiling in combination with cGMP-dependent Protein Kinase G (PKG) activity modulators identifies novel relevant downstream targets of PKG in retinal degeneration.
   (this thesis)

2. Studying PKG mediated CaMK-CREB signalling pathways provides novel biomarkers to characterize the effect of PKG inhibitors in clinical trials.
   (this thesis)

3. The assessment of the effect of genetic risk factors on healthy life years guides implementation of genetic-based clinical applications.

4. Technical innovations often provide the basis for insights in science that lead to further discoveries.

5. The importance of honesty and integrity still receives too little attention in academic training.

6. The COVID-19 pandemic demonstrated the importance of social interactions for personal well-being.

Proposition belonging to the thesis, entitled

Putative role of cGMP-dependent Protein Kinase G in Inherited Retinal Degeneration: Modulators and Biomarkers

Akanksha Roy
Wageningen, 25 October 2022

Putative role of cGMP-dependent Protein Kinase G in Inherited Retinal Degeneration: Modulators and Biomarkers

Akanksha Roy

Thesis Committee

Promotors

Prof. dr. ir. I.M.C.M. Rietjens
Professor of Toxicology
Wageningen University & Research

Prof. dr. ir. John P. Groten
Managing Director
PamGene International B.V.

Co-promotor

Dr. Tushar Tomar
Director, Scientific Research Services
PamGene International B.V.

Other members

Prof. dr. ir. Huub F.J. Savelkoul, Wageningen University & Research
Prof. dr. Einar Stefánsson, University of Iceland, Reykjavik, Iceland
Dr. Pieter A. van der Velden, Leiden University Medical Center, Leiden, Netherlands
Dr. Emiel P.C. van de Voorst, Maastricht University, Maastricht, Netherlands

This research was conducted under the auspices of the Graduate School VLAG (Advanced Studies in Food Technology, Agrobiotechnology, Nutrition and Health Sciences)

Putative role of cGMP-dependent Protein Kinase G in Inherited Retinal Degeneration:

Modulators and Biomarkers

Akanksha Roy

Thesis

Submitted in fulfilment of the requirements for the degree of doctor

at Wageningen University

by the authority of the Rector Magnificus,

Prof. Dr A.P.J. Mol,

in the presence of the Thesis Committee appointed by the Academic Board

to be defended in public

on Tuesday 25 October 2022 at 11.00 a.m. in the Groot Auditorium.

Akanksha Roy
Putative role of cGMP-dependent Protein Kinase G in Inherited Retinal Degeneration: Modulators and Biomarkers, 196 pages.

PhD thesis, Wageningen University, Wageningen, the Netherlands (2022)
With references, with summary in English

ISBN: 978-94-6447-429-9
DOI: https://doi.org/10.18174/578149

Table of contents

1

Chapter 1

General Introduction

Introduction

Inherited Retinal Degenerative diseases

Inherited Retinal Degenerative diseases (IRDs) are a group of neurodegenerative diseases which lead to progressive vision loss and eventual blindness in more than 2 million people worldwide [1]. IRDs are characterized by vast genetic heterogeneity with currently known mutations in over 300 genes and phenotypic heterogeneity with more than 20 IRD phenotypes [2]. Furthermore, different IRDs have shown overlapping clinical symptoms *e.g.* patients with Retinitis Pigmentosa (RP) might show clinical manifestations similar to other IRDs such as Leber Congenital Amaurosis and cone-rod dystrophy [3–5]. Also, mutations in the same gene might lead to different phenotypes. For instance, IRDs with *ABCA4* mutations have been associated with inherited macular degeneration, fundus flavimaculatus, generalized choriocapillaris dystrophy and rapid onset chorioretinopathy [6–10]. Of note, in 20-30% patients, IRDs might not be confined to just the eye but be associated with other non-ocular diseases *e.g.* in Usher Syndrome, patients experience hearing loss along with RP [3]. Since so many disease genes and contributing factors in the eye with various clinical phenotypes have been described for IRDs, this makes it difficult to devise generic treatments.

Retinitis Pigmentosa (RP) is one of the most prominent and most heterogenous IRDs with over 65 defective genes identified in the autosomal dominant, recessive and X-linked form of the disease (https://sph.uth.edu/retnet; information retrieved June 2022). During the onset of RP, rod photoreceptors in the retina, responsible for vision under dim light are primarily affected, followed by degeneration of cone photoreceptors. The disease manifests itself with the patients experiencing night vision problems and tunnel vision due to loss of rod cells that are present at the periphery of the retina (Fig. 1). With the progression of the disease, cone photoreceptors are also degenerated, leading to complete blindness [11].

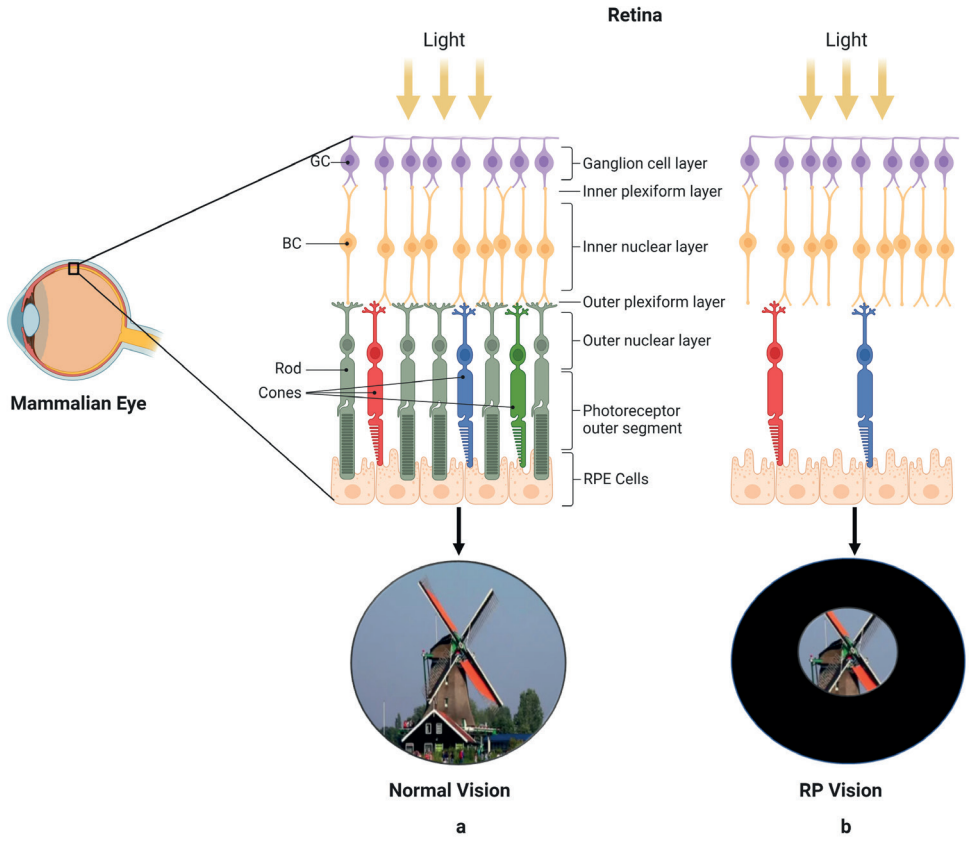

Figure 1: Schematic representation of the eye and organization of mammalian retina. Basic structure of the eyeball (Left). Representation of the layers of a portion of the a) healthy or b) RP retina in vertical section with healthy and tunnel vision respectively (Right). Rods are illustrated in grey and cones in red, blue, and green. RPE: Retinal Pigment Epithelium, BC: Bipolar Cell, GC: Ganglion Cell, and RP: Retinitis Pigmentosa *(Figure adapted from https://app.biorender.com/).*

Therapeutic approaches for IRDs

Current therapeutic interventions that might delay disease progression, include treatment with vitamin A, E or mineral supplements that could reduce oxidative damage to cones and preserve vision in patients [12]. Treatment with drugs like acetazolamide [13] or methazolamide [14] as oral medication, topical administration of dorzolamide [15], or slow-releasing intravitreal steroids [16] have also been reported to improve visual acuity in RP patients. Other treatments such as anti-VEGF systemic therapy that blocks vascular endothelial growth factor, vitrectomy which removes vitreous humor from the eye ball and LASER treatment have been applied with variable results in clinical trials [17]. Recently, Argus II, a retinal prosthesis system has obtained FDA approval to treat patients with advanced stage RP. It includes a miniature eye implant with patient-worn camera and processor that provides artificial vision to the patients [18]. However, the effect of disease progression on vision of patients with prosthesis still needs to be determined.

Besides treatments to reduce or delay symptoms of IRDs, there are also molecular approaches that make use of stem-cell or gene therapy-based therapeutic interventions in development for treatment of IRDs. Stem cell-based therapies are either derived from non-retinal sources or from endogenous retinal stem cells. The potential of non-retinal derived stem cell-based strategies include stem cells derived from bone marrow, adipose tissues or dental pulp [19–21]. The endogenous retinal stem cells, *eg.* Müller glia have been induced to differentiate into retinal progenitors which can transform into functional photoreceptors [22]. The RPE layer in human retina contains some stem cells that can mature into new RPE cells and cells with neuronal phenotype [23]. Similarly, ciliary epithelial-derived retinal stem cells can be made to differentiate *in vitro* into rhodopsin photoreceptors [24]. There are currently several clinical trials regarding stem cell transplantations in the eye underway [25].

Many gene-based therapies where functional genes are transferred are also available such as a recombinant AAV vector that was altered to carry the human *MERTK* gene (*hMERTK*), whose mutation is one of the known causes of IRDs. This vector restored vision in animal models for *MERTK*-associated RP [26]. In phase 1 clinical trials, a *RPE*-specific promoter, VMD2 was included and the *rAAV2-VMD2-hMERTK* was administered to six IRD patients with specific mutation in *MERTK* [27]. The gene therapy for MERTK did not cause any major side effect and improved visual acuity in three patients which was lost after two years. In another study, phase 1/2 clinical trials for 24 patients with AAV-X linked RP caused by *RPRG* mutation have been initiated [28]. Finally, in 2017, The US FDA approved the first AAV gene therapy product Luxturna® for *RPE65*-mutation-associated retinal dystrophy [29]. Luxturna™ *(voretigene neparvovec)* is the first gene therapy to treat an IRD indicated for children and adults with vision loss caused by mutations in both copies of the *rpe65* gene and sufficient viable retinal cells [30]. Nearly 60% of patients have severe forms of the disease, with severe visual impairment occurring shortly after birth [31]. As a one-time treatment, Luxturna™ restores vision and improves sight in children and adults with a sustained effect and favourable safety profile [32,33].

Despite these initial successes of gene-therapy, implementation of such treatments to clinical practice is challenging as every type of genetic defect requires a specific treatment. So, the gene-based therapies need to be tailor-made for a particular mutation for each IRD patient. In contrast, the stem-cell based therapies would be applicable to every patient irrespective of mutation as it is focused on replacement of photoreceptors. Needless to mention that both types of therapeutic interventions are very expensive. Another complicating factor in search of IRD therapies is the complex three-dimensional structure of the retina that comprises of more than 70 different, neuronal and non-neuronal cell types, each with a specific function, which further complicates the identification of key biological pathways responsible for clinical pathophysiology [34]. Therefore, there is a clear need to develop therapies targeting the common photoreceptor degradation pathways that can be applied at any stage of the disease in a mutation-independent manner.

The central role of 3',5'-cyclic guanosine monophosphate (cGMP) in cyclic nucleotide gated channel (CNGC) and cGMP-dependent Protein kinase G (PKG) signaling axis in IRDs

The high genetic heterogeneity and widely varying clinical phenotypes of IRDs hamper a detailed understanding of photoreceptor cell death mechanisms. Initially, the research on photoreceptor cell death was focused on apoptosis [35,36] but the current research has shifted to non-apoptotic cell death mechanisms which seem to be common to different IRD mutants. Key events of non-apoptotic degradation mechanism are the epigenetic factors such as activation of histone deacetylase, poly-ADP-ribose-polymerase as well as accumulation of second messenger signaling molecules such as 3',5'-cyclic guanosine monophosphate (cGMP) and Ca^{2+} involved in phototransduction cascade [37]. Aberrantly high levels of cGMP are associated with several mutations in several IRD-linked genes other than *pde6,* such as *cnga3, cngb1, cpfl1, rho, rpe65 etc.* [38]. The discovery of abnormal levels of cGMP, as one of the main constituents leading to photoreceptor cell death by activation of non-apoptotic cell death pathways, provides significant potential for development of novel neuroprotective strategies (Fig. 2).

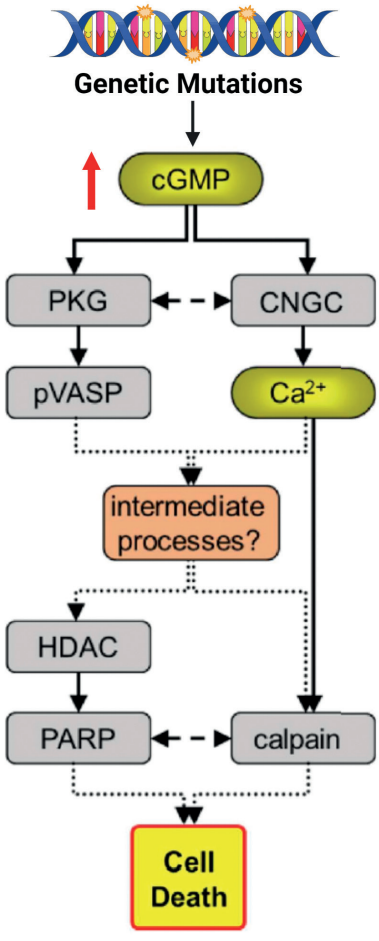

Figure 2: Diagram representing putative photoreceptor degradation mechanisms in IRDs: Several IRD-linked mutations increase cGMP concentration in photoreceptors which, opens the CNGCs and activates PKG. The elevated Ca^{2+} influx through CNGCs may trigger Calpain while PKG activity might be connected to HDAC and PARP activation. Together, the overactivation of these pathways leads to photoreceptor cell death. IRD, Inherited Retinal Degeneration; cGMP, 3',5'-cyclic guanosine monophosphate; PKG, cGMP-dependent Protein Kinase G; CNGC, cyclic nucleotide-gated channel; HDAC, histone deacetylase; PARP, poly-ADP-ribose-polymerase *(Figure adapted from Power et. al 2020)*.

In several IRD models, the photoreceptor cell death is linked to (abnormally) increased cGMP levels. Elevated cGMP over activates CNGCs and increases Ca^{2+} influx inside photoreceptors. Therefore, CNGCs have been targeted by different calcium channel blockers which slowed down photoreceptor degeneration and preserved visual acuity in *rd* mice with a mutation in *pde6* [39–42]. However, the calcium channel blockers need to be very specific as rods and cones express different isoforms of CNGCs, and should not affect the phototransduction cascade or any other Ca^{2+} signaling process in the cells [42]. The key role of CNGCs in IRDs was also confirmed in *rd1* or *rd10/Cngb1*$^{-/-}$ double knockouts, devoid of CNGCs, which improved rod photoreceptor viability [43,44]. Even though abolishing of CNGCs delayed rod photoreceptor death, it has been demonstrated that in a *Cngb1*$^{-/-}$ mice, simultaneous abolition of *prkg1* expression was necessary to have prolonged rod cell survival [45]. Moreover, role of CNGCs in photoreceptor cell death is not clear as other studies suggest Ca^{2+} signaling via voltage gated calcium channels instead to be responsible [46,47].

The interplay between cGMP and PKG signaling

Besides the CNGC axis, another major target of cGMP is cGMP-dependent Protein Kinase G (PKG), which is a Serine/Threonine Protein Kinase from the AGC kinase family. Mammalian PKG is encoded by *prkg1 gene*, which codes for splice variants PKG1α and PKG1β that differ in their first 80-100 amino acids and *prkg2 gene,* which codes for PKG2 [48]. PKG is a dimeric protein with each monomer containing an amino terminal, a regulatory and a catalytic domain on a single polypeptide chain. The regulatory domain consists of an N-terminal leucine zipper, a linker with an auto inhibitory sequence and two cGMP-binding sites. In absence of cGMP, the inhibitory regulatory domain binds to the catalytic domain with high affinity and the kinase remains inactive. Binding of cGMP to the four cGMP-binding sites on PKG, results in dissociation of the inhibitory and catalytic domain, which leads to structural changes and activates PKG (Fig. 3) [48].

Activated PKG then phosphorylates several proteins at Serine/Threonine amino acid position and mediates diverse downstream cellular pathways. In mammals, PKG1 mediates the feedback of the nitric oxide-signaling pathway [49], platelet activation and adhesion [50], smooth muscle contraction [51], cardiac function [52], insulin resistance, and mTOR signaling [53]. PKG1 also regulates aspects of the Central Nervous System like hippocampal and cerebral learning [54], circadian rhythm [55] etc. PKG2 controls cGMP-dependent translocation of CFTR in jejunum [56], mediates osteoblast anabolic response to mechanical stimulation by activation of kinases such as MAPK3/ERK1 and MAPK1/ERK2 [57]. Therefore, studying PKG interactions at kinome activity level is crucial.

A complete *pkg1* (α, β) knockdown in mice results in smooth muscle cell defects, intestinal dysfunctions, and dwarfism [58]. Normal muscle development can be initiated back by knock-in of murine *pkg1* (α, β) [59]. A *pkg2* knockdown in mice leads to defects in entrainment of the circadian rhythm [11]. PKG activity also plays a prominent role in cell death as PKG activation induces apoptosis in several types of cancer such as colon, breast, ovarian cancer, and also in some neuronal cells [11,60]. Based on immunohistochemical staining, PKG1 is localized in photoreceptor ONL and PKG2 in INL and GCL layers of the retina. *In vitro* and *in vivo* inhibition of PKG seems to have very strong protective effect on retinas of different murine IRD models such as *rd1, rd2, rd10*. Also, knockdown of *prkg1* was

shown to be necessary for sustained rod cell survival in CNG channel loss-of function mouse model [45]. In *rd1* mouse retina, photoreceptor cell death is linked to dysfunctional *pde6* which is involved in regulation of cGMP [61]. As mentioned earlier, increased cGMP is found in several other IRD models, and likely over activates PKG [38,62]. However, the cGMP/PKG signaling downstream targets and the specific isoforms of PKG involved in photoreceptor degeneration are still not clear.

Targeting PKG signaling

Besides the interplay between cGMP and signal transduction, the effects on PKG have also been postulated to be a promising target for controlling excessive cGMP, as PKG does not appear to be differentially expressed in rods and cones [63], and its inhibition is not likely to affect the phototransduction cascade. Several PKG inhibitors (such as KT5823 and N46) are able to target ATP binding sites on PKG. KT5823 lacks specificity and potency as it does not inhibit basal PKG activity in cells and may inhibit other kinases such as PKA, PKC [64]. Also, intravenous injection of N46 in rats successfully eased hyperalgesia and osteoarthritic pain by specific inhibition of PKG1α [65]. Another PKG inhibitor DT-2, binds to substrate-binding sites on PKG and inhibits its activity by competing with the substrates. Interestingly, DT-2 strongly inhibits PKG *in vitro* but loses specificity to inhibit PKG in cell homogenates and living cells [66]. The next class of PKG inhibitors, the inhibitory cGMP analogues are specific to cGMP binding sites on PKG.

The inhibitory cGMP analogues carry the common motif of a Rp-configured phosphorothioate where the exocyclic oxygen at equatorial position of 3',5'-cyclic phosphate is replaced by a sulphur and Rp defines the configuration of this moiety according to Cahn-Ingold-Prelog rules for Chiral atoms (Figure 3) [11].

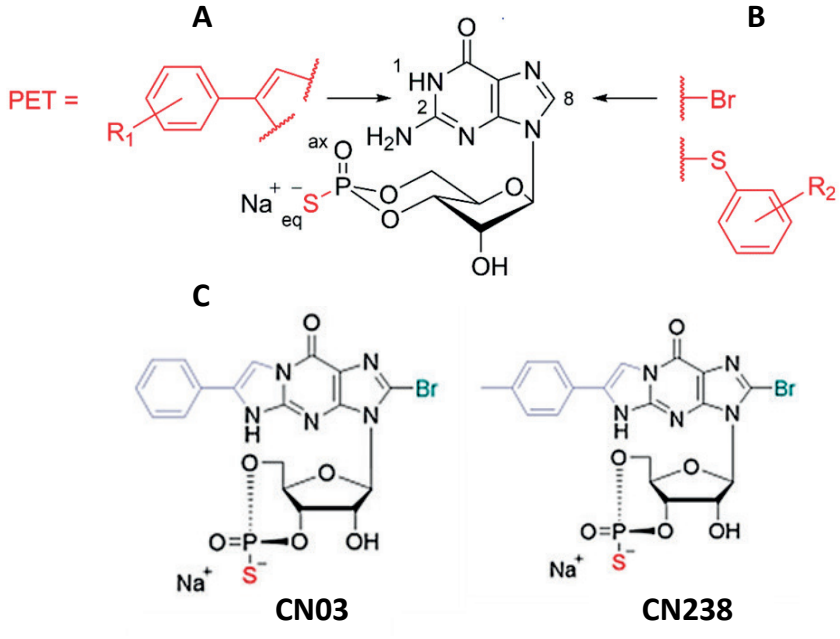

Figure 3: Schematic structure of Rp-cGMP analogues: Arrows show structural positions in Rp-cGMPs used for introduction of substituents to generate new Rp-cGMP structures with improved inhibitory potency for PKG1 or PKG2. (A) Position 1, N^2: Addition of β-phenyl-1,N^2-etheno-modification (PET) with varying additional substituents (R_1) [67,68]. (B) Position 8: Addition of halogens *eg.* bromine (Br) or sulphur (S)-connected aromatic ring systems with varying additional substituents (R2) [69,70]. (C) Structure of PKG inhibitors 8-Br-(β-phenyl-1,N^2-etheno) guanosine-3',5'-cyclic monophosphorothioate, Rp-isomer (Rp-8-Br-PET-cGMPS) CN03 and 8-Br-(4-methyl-β-phenyl-1,N^2-etheno) guanosine-3',5'-cyclic monophosphorothioate, Rp isomer (Rp-8-Br-pMe-PET-cGMPS) CN238. *(Figure adapted from Tolone et Al. 2019).*

These compounds are referred as Rp-cGMP analogues (Rp-cGMPs) and are able to bind to the cGMP-binding sites of PKGs but do not induce the conformational change required for activation of the catalytic subunit of PKG (Fig. 4). The inhibitory cGMP analogues, have been used to identify the non-apoptotic photoreceptor cell death mechanism triggered by excessive cGMP [71]. A pan-European collaboration of several collaborating research centers, the DRUGSFORD consortium, generated over 80 novel cGMP analogues that target and inhibit PKG. They generated and tested Rp-cGMP structures with introduction of a β-phenyl-1,N^2-etheno-modification (PET) moiety onto the Rp-cGMP backbone and its modifications (Fig. 3). This strategy led to a list of Rp-cGMP structures with improved lipophilicity and the ability to also block CNGCs. Systemic intraperitoneal injection of one of the selected liposome-formulated Rp-cGMPs (CN03), was able to provide photoreceptor protection in different IRD animal models [67]. This research has resulted in a new European and Marie Curie funded research initiative (*trans*Med) that also included the research described in this thesis. In the *trans*Med consortium, the studies are conducted with these

new cGMP analogues in more detail with a focus to identify novel targets and biological pathways affected by PKG inhibiting cGMP analogues.

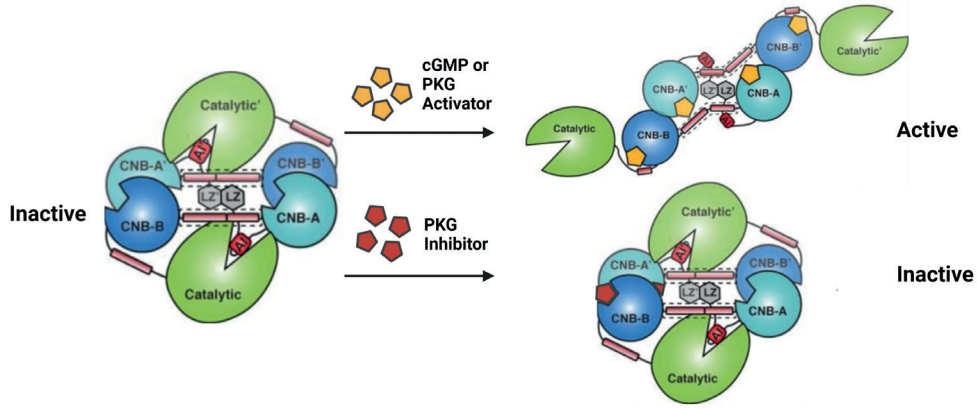

Figure 4: A schematic model of PKG activation or inhibition mediated by cGMP analogues. (Top) Binding of cGMP or a PKG Activator (cGMP analogue) to the four cGMP binding sites (CNBs) on PKG, induces a conformational change whereby the catalytic domain is released from the regulatory domain. (Bottom) Whereas, binding of a PKG Inhibitor (cGMP analogue) to the CNBs does not induce the conformational changes required for the activation of the kinase, resulting in a reversible inhibition of PKG *(Figure adapted from Kim et. al 2016).*

Lack of biomarker-based approach for target identification and therapy response in IRDs

Until now biomarker research that is applied in the field of IRD is related to disease prognosis and/or to assess the predictive effect of IRD treatment. Since the mechanism of action is seldomly known, most biomarkers approaches applied in IRD, particularly in RP, are phenotypical following the onset of the disease in the clinic and using a plethora of surrogate markers. Appropriate samples for biomarkers analysis in IRD can be largely taken from instance either (intra) retinal fluid or during imaging and by optic coherence topography (OCT) [72]. For RP with severe degeneration of rod/cone photoreceptors mutations in proteins associated with the classical components of the phototransduction cascade (rhodopsin and phosphodiesterase), cell signaling factors (such as *Crx, Nrl* or kinase signalling), and ion channels have been applied as a tool both in mice and human [11,69]. Also, since photoreceptors and/or retinal pigment epithelium represent the primary causes of RP development, previous studies have looked into the inflammatory response as a possible contributor (and biomarker) in the RP pathogenesis and found inflammatory cells and chemokines (interleukins, MCP) accumulate in the vitreous cavity of RP patients. This search into inflammatory factors and cell – and tissue viability is related to the photoreceptor cell death mechanisms and with a focus on non-apoptotic mechanisms of cell damage [38]. The possibility to assess inflammatory biomarkers (interleukins and TNF) in vitreal reflux samples (or even biopsies) have been proposed in grading pathological manifestation [72]. Again, searching for inflammatory markers may help to fine tune disease prognosis, however not to predict therapeutic outcome of Retinitis pigmentosa (RP). At present, perimetric and electroretinographic methods are the gold standards for diagnosing and monitoring RP and

assessing cone function [73]. These methods lack though the sensitivity to assess disease progression at the level of individual photoreceptor cells, where the vision loss accompanying the disease occurs [73]. To improve means for early diagnosing current research has shifted to new early markers of cell death pathways and preceding events, like epigenetic pathways, phototransduction signaling via cGMP and kinase signaling [53]. As previously indicated, the interplay between cGMP regulation and kinase signaling might contribute further to the homeostasis of the RP. Hence, better understanding of key pathways in the photoreceptor degeneration can facilitate the quest of finding robust translational and clinically relevant biomarkers.

Preclinical models to study IRDs

In order to study IRDs in a biological system, several retinal cell lines have been applied to study IRDs, however the number of photoreceptor cell lines used is rather limited *eg.* WERI-Rb1 and Y-79 cells [74,75]. These cell lines are derived from human retinoblastoma tumors and have limited characteristics of rod photoreceptors. For drug testing, techniques for *in vitro* differentiation of retinal stem cells derived from murine models to rod photoreceptor-like cell cultures already exist [67] but have high variability of cells that need to be isolated. One of the most widely used cell lines to study photoreceptor degeneration is 661W. It is derived from retinal tumors of a transgenic mouse line that expressed simian virus 40 T antigen under the control of human interphotoreceptor retinol-binding protein (IBRP) promotor [76]. 661W cells express photoreceptor precursors, cone specific and both rod and cone photoreceptor genes. These cells are modeled to mimic RD, by treatment with PDE6 inhibitor Zaprinast, which increases intracellular cGMP and Ca^{2+} concentration and induces cell death [77]. However, a cell line with high expression of rod-specific genes is necessary for high-throughput screening of drug candidates. Recently, a new *in vitro* model was developed from 661W cells to study Zaprinast treatment on rod-like cells. This cell line expressed *neural retina-specific leucine* which encodes the basic motif-leucine zipper transcription factor regulating rod-specific genes [78].

Murine models for quite a number of known genetic defects are available, the most well-known are *rd1*, *rd2,* and *rd10.* Especially the *rd1* mouse, discovered in 1924 and suffering from a mutation in exon 7 of *pde6β*, is arguably the oldest and most used animal model for IRD research. The photoreceptor degeneration starts around postnatal day (P) 10 and peaks at P12-P14 and is almost completed by P21 [79]. Mutations in *pde6β*-subunit also affects around 4-5% of human RP patients, therefore *rd1* is a very relevant model [80]. Another frequently used mice model, *rd10* carries a missense mutation in exon 13 of *pde6β*, which results in slower photoreceptor degeneration than what is observed in the *rd1* mouse model as in this *rd10* mouse model *pde6β* is still partially functional [79]. The rod cell degeneration starts at P16, peaks around P20-P25 and is completed by P45. In both the models, complete or partial loss of *pde6β* leads to an abnormal increase in cGMP levels which results in photoreceptor death [38].

To asses retinal cytotoxicity in RD models in several cell layers of the retina, a commonly used approach is the TUNEL assay. In this assay the *in situ* Terminal-deoxynucleotidyl-transferase dUTP-nick end-labelling (TUNEL) is analysed and in this way detects the dying cells by labelling DNA fragmentation [62]. It relies on the enzyme terminal deoxynucleotide

transferase that attaches to the 3'-hydroxyl terminus of DNA breaks and can be detected by a fluorescent label. In the present thesis the protective effect of the PKG inhibitor CN03 on photoreceptors in three IRD models was determined by the TUNEL assay [69]. With the TUNEL assay both necrotic as well apoptotic mechanism of cell toxicity can be taken into account [81].

In summary, besides *in vitro* cell models, *in vivo* murine models like *rd1* and *rd10* are frequently used in RD research and both type of models have been applied in the current thesis.

Analytical and biochemical methods for studying kinase signaling

As mentioned before, several mutations in IRDs convene to common cGMP driven PKG signaling routes, suggesting that targeting PKGs could provide a new, generic treatment intervention amenable for a larger group of patients. However, the pathways downstream of PKG in degenerating photoreceptors are nonetheless still poorly understood. Increased cGMP/PKG signaling has been associated with increased activity of poly-ADP-ribose-polymerase (PARP), histone deacetylase (HDAC), and calpain proteases, all known to be involved in photoreceptor cell death (17). However, to date there is no evidence that directly links these events to PKG. Techniques applying immunoblotting and enzyme-linked immunosorbent assays (ELISA) have been regularly used to detect the presence of specific kinases in cells and tissues at protein level. However, such techniques do not indicate protein activity, require a priori knowledge of the target and are hindered by limited availability of antibodies [37]. Another more holistic approach to identify kinases and other enzyme targets simultaneously in the retina tissues is proteome analysis through mass spectrometry (MS). The use of MS after affinity chromatography identified several new cGMP-interacting proteins such as Calmodulin Kinase IIα, Mitogen-Activated Protein Kinase 1/3, and Glycogen synthase kinase 3β in *rd1* mice retina [82]. Since, these proteomic-based methods use whole retinal lysates, they do not provide the single-cell resolution which can be obtained by *in situ* enzyme activity assays of proteins such as calpain, PARP, HDAC [38]. For instance, in the work of *Vighi et al.* [69], the immunohistochemistry marker phospho VASP was used to look into the activity of PKG in photoreceptor-like cells derived from *rd1* mice. The vasodilator-stimulated phosphoprotein (VASP) is a known PKG target studied in the retina and addition of a PKG inhibitor CN03 to photoreceptor-like cells, reduced phosphorylation at the Serine 239 position of VASP.

Assessing the active kinome in retina

Targeting PKGs could provide a new, generic treatment intervention amenable for a larger group of patients. A recent study by *Gonzalez-Medine et al. 2020*, revealed that over 73 approved small molecule kinase inhibitors developed for a single target, may have promiscuous structural moieties that allow for docking at the ATP-binding pocket of several other kinases [83]. Thus, single-kinase inhibitors exhibit a varying affinity towards multiple kinases. This variability in affinity for different kinases could provide advantages but also disadvantages when different signaling networks (*eg.* efficacy, toxicity) have to be taken into account. Many kinase inhibitors fail in early clinical trials due to the side effects of these drugs which could be determined earlier [84].

High throughput active kinome screening methods are thus needed to assess kinase inhibitors and their signaling networks in conjunction with evaluation of the toxicity *in vivo*. Also,

since PKG as a kinase, might have hundreds of substrates, the ones crucial in photoreceptor degeneration are unknown. To study kinase signaling *in toto* and applying new potent cGMP inhibitors, several multiplex analytical methods have been applied to measure signaling networks at the protein kinase activity level (active kinome).

The publicly available datasets that provide information about active kinomes are usually derived from MS-based phospho-peptide signatures [84]. However, these datasets only provide static and indirect information regarding protein function. Novel high-throughput technologies are being developed to study the active kinome. One of these technologies is the Kinobeads platform, where the bead surface is coated with broad-spectrum kinase inhibitors which allows determination of the degree of protein expression and phosphorylation of specific kinases [85]. This platform is often coupled with MS to quantify kinase expression. Still, this technology is limited by determination of only the kinases that bind to the beads and also requires a prior knowledge of protein kinase inhibitors or targets of the kinase of interest. Another active kinome platform is the KINOMEscan, which is a competitive binding assay designed to quantify binding characteristics of test compounds with up to 500 different kinases [86]. This assay is performed by running DNA-tagged kinases against ligands bound to beads. The movement of kinases occurs when its binding to ligands is disrupted by competition with test compounds and is detected by qPCR. The more kinase-test compound interaction, the more kinases move through the assay. KINOMEscan provides invaluable information about kinome profiling of isolated kinases but it does not account for kinase expression, activity, regulation, and interactions in a cellular context. The KINOMEscan can be considered as a biochemical assay of isolated protein kinases outside cellular context. This limitation is what constitutes the main difference between KINOMEscan and assays such as Kinobeads. A more highly sensitive and high throughput technology for kinase profiling is the Reverse Phase Protein Array (RIPA). The cells are immobilized on slides which are probed with primary antibodies followed by biotinylated secondary antibodies. This high throughput platform in addition to information on phosphorylation, also provides data on other post-translational modifications such as acetylation and glycosylation [87]. Major limitations of this platform are requirement of highly specific primary antibodies and a laborious sample-array printing process. All these high-throughput technologies mentioned till now do not directly measure the kinase activity within the biological sample.

Multiplex Peptide microarray platforms such as the Serine/Threonine Kinase (STK) or Protein Tyrosine Kinase (PTK) assay have also been frequently applied [84]. This method allows the real-time kinase activity profiling for hundreds of kinases present in complex biological samples [84]. Proteins targeted by recombinant kinases or by endogenous kinases in cells or tissues can be characterized by using these very sensitive (1-5 ug/array input) multiplex peptide microarrays [53,88]. On the microarrays 142 peptides derived from human phosphoproteome are immobilized on a porous 3D surface. The peptides are 13 amino acids in length and comprise a Serine/Threonine or Tyrosine amino acid residue. The kinases within the sample phosphorylate the peptides on microarrays. The phosphorylation at Serine/Threonine or Tyrosine position is detected by a primary antibody and then confirmed by a FITC-labeled secondary antibody. The images of the arrays are recorded at multiple exposure time and quantified by BioNavigator® software. Therefore, the multiplex peptide microarray technology not only allows identification of substrates of recombinant kinases, but also generation of hypotheses for kinases potentially active in complex mixtures of kinases. This is ascertained

by an in-house tool called 'Upstream Kinase Analysis' which integrates known interactions between the kinases and phosphorylation sites as mentioned in databases such as HPRD, PhosphoELM, PhosphositePLUS, Reactome, UniProt and provides a ranking of potential kinases [89].

The multiplex peptide microarray platforms have been successfully employed across multiple research domains such as cancer biology [90,91], immunology [92] and neuroscience [53,88]. The platform does not require isolation or immobilization of the protein kinases, as the sample is pumped back and forth over the peptides on the chip. It enables the study of any biological sample such as cell or tissue homogenates, for which the activity of endogenous kinases and their interacting partners is determined. Recombinant kinases can also be used on these microarrays to identify their novel substrates. Limitations of the multiplex peptide microarray platform include the limited number of peptides on the chip, and phosphorylation of the peptides by multiple kinases which requires further validation techniques to accurately determine the involved kinases.

Even though these are notable limitations, the multiplex peptide microarrays provide a powerful high-throughput profiling technique to measure the kinome activity in complex biological samples [84] and was applied in the current research to study kinome profiling in the retina.

Aim and Thesis Outline

The overall aim of the present project is to assess the role of cGMP-dependent protein kinase G (PKG) and its relationship to the health status and viability of the retina exposed to cGMP analogues. To this end two main objectives are defined:

1) To study the effect of novel PKG inhibitors on kinase signaling and viability in retinal cells, tissues and explants

2) To identify new biomarkers and biological pathways involved in kinase signaling and related to retinal degeneration

The thesis consists of introduction (Chapter 1), one review chapter (Chapter 2) and four research chapters (Chapter 3-6). **Chapter 1** comprises of brief introduction of the background and aim of the thesis. Considering the high heterogeneity of IRDs and no generic therapies yet available, a better understanding of the pathways leading to photoreceptor degeneration, particularly for cGMP-PKG kinase signaling may help to determine common targets and develop mutation-independent therapies for larger groups of IRD patients. Therefore, in **Chapter 2,** a literature review was performed to discuss the key biological pathways involved in photoreceptor cell death studied by transcriptomics, proteomics, and metabolomics techniques to identify potential therapeutic targets or biomarkers in IRDs.

As described above, several IRD-associated genetic defects affect cGMP levels and therefore PKGs have emerged as novel targets, and their inhibition has shown functional protection in IRDs. The development of such novel neuroprotective compounds warrants a better understanding of the pathways downstream of PKGs, that lead to photoreceptor degeneration. Since, a kinase has multiple substrates, in **Chapter 3**, the response of recombinant PKGs in

combination with PKG activity modulators was used on a multiplex peptide microarrays to identify novel substrates for PKG1 and PKG2, and use this information to identify critical PKG targets in the retina. The knowledge on modulation of PKG activity was applied to investigate the role of PKG1 and PKG2 in 661W retinal cells that are used as model for retinal degeneration. To better understand the mechanisms of photoreceptor cell death, in **Chapter 4**, the downstream effects of PKG and its phosphorylation targets in *rd1* murine retinal explants was explored. The PKG-mediated phosphorylation of specific peptides by kinases present in murine retinal explant lysates treated with the PKG inhibitor CN03, was measured on multiplex peptide microarrays. This was followed up by confirmation of novel PKG substrates in retina by immunohistochemistry. In **Chapter 5**, the unique proteins phosphorylated by PKG in *rd10* murine retinal explants were identified by multiplex peptide microarray technology and phosphoproteomics. The expression and localization of the identified proteins in retinal tissue and explants was examined by two techniques: immunohistochemistry and Western Blot. In **Chapter 6**, the effect of a novel PKG inhibitor (CN238) on photoreceptor viability and functionality was studied on *rd1* and *rd10* retinal explants. Multiplex peptide microarray analysis, Micro-electrode array recording, and Ca^{2+} imaging experiments identified potassium (K^+)-channel $K_v1.6$ as a possible mediator of PKG-dependent cell death. Given the important functions of potassium K_v-type channels for neuronal repolarization, these findings provide a rationale for the use of PKG-inhibitors as novel neuroprotective drugs with possible applications beyond the retina. Finally in **Chapter 7**, the main findings of this thesis are presented and discussed including a discussion of key findings and future prospectives. In summary, a schematic overview of the thesis lay out is shown in Figure 5.

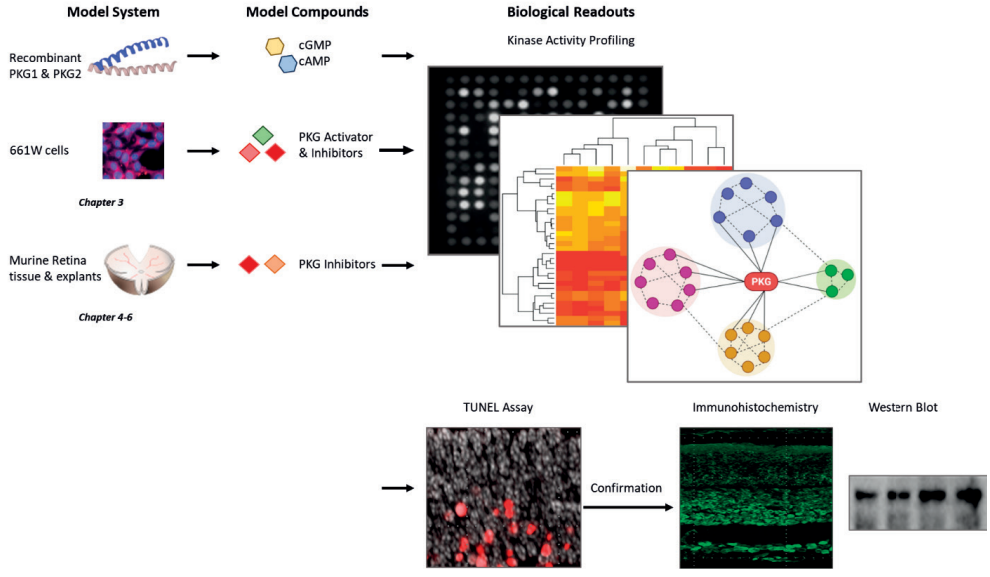

Figure 5: A schematic diagram of the thesis overview. In Chapter 3, kinase activity profiling is performed on recombinant PKG1, PKG2, and 661W cell lysate with PKG activity modulators (cGMP, cAMP, PKG activator, PKG inhibitors). In Chapters 4-6, the TUNEL assay and kinase activity profiling are performed on murine retinal tissue and explants treated with PKG inhibitors. The results are confirmed by immunohistochemistry and western blotting.

References

1. Lobanova ES, Finkelstein S, Li J, Travis AM, Hao Y, Klingeborn M, Skiba NP, Deshaies RJ, Arshavsky VY: **Increased proteasomal activity supports photoreceptor survival in inherited retinal degeneration**. *Nat Commun* 2018, **9**:1–11.
2. Chen TC, Huang DS, Lin CW, Yang CH, Yang CM, Wang VY, Lin JW, Luo AC, Hu FR, Chen PL: **Genetic characteristics and epidemiology of inherited retinal degeneration in Taiwan**. *npj Genomic Med* 2021, **6**:1–8.
3. Hartong D, Berson E, Dryja T: **Retinitis pigmentosa**. *Lancet* 2006, **368**:1795–1809.
4. Moore AT: **Cone and cone-rod dystrophies**. *J Med Genet* 1992, **29**:289.
5. Chung DC, Traboulsi EI: **Leber congenital amaurosis: Clinical correlations with genotypes, gene therapy trials update, and future directions**. *J Am Assoc Pediatr Opthalmology Strabismus* 2009, **13**:587–592.
6. Bauwens M, Garanto A, Sangermano R, Naessens S, Weisschuh N, De Zaeytijd J, Khan M, Sadler F, Balikova I, Van Cauwenbergh C, et al.: **ABCA4-associated disease as a model for missing heritability in autosomal recessive disorders: novel noncoding splice, cis-regulatory, structural, and recurrent hypomorphic variants**. *Genet Med* 2019, **21**:1761–1771.
7. Cremers FPM, Van De Pol DJR, Van Driel M, Den Hollander AI, Van Haren FJJ, Knoers NVAM, Tijmes N, Bergen AAB, Rohrschneider K, Blankenagel A, et al.: **Autosomal recessive retinitis pigmentosa and cone-rod dystrophy caused by splice site mutations in the Stargardt's disease gene ABCR**. *Hum Mol Genet* 1998, **7**:355–362.
8. Lambertus S, Van Huet RAC, Bax NM, Hoefsloot LH, Cremers FPM, Boon CJF, Klevering BJ, Hoyng CB: **Early-onset stargardt disease: Phenotypic and genotypic characteristics**. *Ophthalmology* 2015, **122**:335–344.
9. Bertelsen M, Zernant J, Larsen M, Duno M, Allikmets R, Rosenberg T: **Generalized choriocapillaris dystrophy, a distinct phenotype in the spectrum of ABCA4-associated retinopathies**. *Investig Ophthalmol Vis Sci* 2014, **55**:2766–2776.
10. Tanaka K, Lee W, Zernant J, Schuerch K, Ciccone L, Tsang SH, Sparrow JR, Allikmets R: **The Rapid-Onset Chorioretinopathy Phenotype of ABCA4 Disease**. *Ophthalmology* 2018, **125**:89–99.
11. Tolone A, Belhadj S, Rentsch A, Schwede F, Paquet-Durand F: **The cGMP pathway and inherited photoreceptor degeneration: Targets, compounds, and biomarkers**. *Genes (Basel)* 2019, **10**:1–16.
12. Zhao Y, Feng K, Liu R, Pan J, Zhang L, Lu X: **Vitamins and mineral supplements for retinitis pigmentosa**. *J Ophthalmol* 2019, doi:10.1155/2019/8524607.
13. Nigel Cox S, Hay E, Bird AC: **Treatment of Chronic Macular Edema with Acetazolamide**. *Arch Ophthalmol* 1988, **106**:1190–1195.
14. Fishman GA, Gilbert LD, Anderson RJ, Marmor MF, Weleber RG, Viana MAG: **Effect of Methazolamide on Chronic Macular Edema in Patients with Retinitis Pigmentosa**. *Ophthalmology* 1994, **101**:687–693.
15. Fishman GA, Apushkin MA: **Continued use of dorzolamide for the treatment of cystoid macular oedema in patients with retinitis pigmentosa**. *Br J Ophthalmol* 2007, **91**:743–745.
16. Mansour AM, Sheheitli H, Kucukerdonmez C, Sisk RA, Moura R, Moschos MM, Lima LH, Al-Shaar L, Arevalo JF, Maia M, et al.: **Intravitreal Dexamethasone Implant in Retinitis Pigmentosa-related Cystoid Macular Edema**. *Retina* 2018, **38**:416–423.
17. Chen C, Liu X, Peng X: **Management of Cystoid Macular Edema in Retinitis Pigmentosa: A Systematic Review and Meta-Analysis**. *Front Med* 2022, **9**.

18. Farvardin M, Afarid M, Attarzadeh A, Johari MK, Mehryar M, Hossein Nowroozzadeh M, Rahat F, Peyvandi H, Farvardin R, Nami M: **The Argus-II retinal prosthesis implantation; From the global to local successful experience**. *Front Neurosci* 2018, **12**:584.
19. Yu S, Tanabe T, Dezawa M, Ishikawa H, Yoshimura N: **Effects of bone marrow stromal cell injection in an experimental glaucoma model**. *Biochem Biophys Res Commun* 2006, **344**:1071–1079.
20. Tsuruma K, Yamauchi M, Sugitani S, Otsuka T, Ohno Y, Nagahara Y, Ikegame Y, Shimazawa M, Yoshimura S, Iwama T, et al.: **Progranulin, a Major Secreted Protein of Mouse Adipose-Derived Stem Cells, Inhibits Light-Induced Retinal Degeneration**. *Stem Cells Transl Med* 2014, **3**:42–53.
21. Mead B, Logan A, Berry M, Leadbeater W, Scheven BA: **Intravitreally transplanted dental pulp stem cells promote neuroprotection and axon regeneration of retinal ganglion cells after optic nerve injury**. *Investig Ophthalmol Vis Sci* 2013, **54**:7544–7556.
22. Osakada F, Ooto S, Akagi T, Mandai M, Akaike A, Takahashi M: **Wnt signaling promotes regeneration in the retina of adult mammals**. *J Neurosci* 2007, **27**:4210–4219.
23. Salero E, Blenkinsop TA, Corneo B, Harris A, Rabin D, Stern JH, Temple S: **Adult human RPE can be activated into a multipotent stem cell that produces mesenchymal derivatives**. *Cell Stem Cell* 2012, **10**:88–95.
24. Ballios BG, Clarke L, Coles BLK, Shoichet MS, Van Der Kooy D: **The adult retinal stem cell is a rare cell in the ciliary epithelium whose progeny can differentiate into photoreceptors**. *Biol Open* 2012, **1**:237–246.
25. Mead B, Berry M, Logan A, Scott RAH, Leadbeater W, Scheven BA: **Stem cell treatment of degenerative eye disease**. *Stem Cell Res* 2015, **14**:243–257.
26. Moore NA, Morral N, Ciulla TA, Bracha P: **Gene therapy for inherited retinal and optic nerve degenerations**. *Expert Opin Biol Ther* 2018, **18**:37–49.
27. Ghazi NG, Abboud EB, Nowilaty SR, Alkuraya H, Alhommadi A, Cai H, Hou R, Deng WT, Boye SL, Almaghamsi A, et al.: **Treatment of retinitis pigmentosa due to MERTK mutations by ocular subretinal injection of adeno-associated virus gene vector: results of a phase I trial**. *Hum Genet* 2016, **135**:327–343.
28. Moore NA, Morral N, Ciulla TA, Bracha P: **Gene therapy for inherited retinal and optic nerve degenerations**. *Expert Opin Biol Ther* 2018, **18**:37–49.
29. Lee JH, Wang JH, Chen J, Li F, Edwards TL, Hewitt AW, Liu GS: **Gene therapy for visual loss: Opportunities and concerns**. *Prog Retin Eye Res* 2019, **68**:31–53.
30. **Luxturna (voretigene neparvovec) Novartis Pharamceuticals. Approved EU SmPC**., 2018.
31. Zhu Y-Y: **Luxturna. BLA Clinical Review Memorandum.** 2017.
32. Russell S, Bennett J, Wellman JA, Chung DC, Yu ZF, Tillman A, Wittes J, Pappas J, Elci O, McCague S, et al.: **Efficacy and safety of voretigene neparvovec (AAV2-hRPE65v2) in patients with RPE65-mediated inherited retinal dystrophy: a randomised, controlled, open-label, phase 3 trial**. *Lancet* 2017, **390**:849–860.
33. Russell SR, Bennett J, Wellman J, Chung DC, High K, Yu Z-F, Tillman A, Maguire AM: **Three-year update for the phase 3 voretigene neparvovec study in biallelic RPE65 mutation–associated inherited retinal disease**. *Invest Ophthalmol Vis Sci* 2018, **59**:3900–3900.
34. Masland RH: **The neuronal organization of the retina**. *Neuron* 2012, **76**:266–280.
35. Marigo V: **Programmed cell death in retinal degeneration: Targeting apoptosis in photoreceptors as potential therapy for retinal degeneration**. *Cell Cycle* 2007, **6**:652–655.
36. Portera-Cailliau C, Sung CH, Nathans J, Adler R: **Apoptotic photoreceptor cell death in mouse models of retinitis pigmentosa**. *Proc Natl Acad Sci U S A* 1994, **91**:974–978.

37. Roy A, Hilhorst R, Groten J, Paquet-Durand F, Tomar T: **Technological advancements to study cellular signaling pathways in inherited retinal degenerative diseases**. *Curr Opin Pharmacol* 2021, **60**:102–110.
38. Arango-Gonzalez B, Trifunović D, Sahaboglu A, Kranz K, Michalakis S, Farinelli P, Koch S, Koch F, Cottet S, Janssen-Bienhold U, et al.: **Identification of a common non-apoptotic cell death mechanism in hereditary retinal degeneration**. *PLoS One* 2014, **9**:1–11.
39. Takano Y, Ohguro H, Dezawa M, Ishikawa H, Yamazaki H, Ohguro I, Mamiya K, Metoki T, Ishikawa F, Nakazawa M: **Study of drug effects of calcium channel blockers on retinal degeneration of rd mouse**. *Biochem Biophys Res Commun* 2004, **313**:1015–1022.
40. Vallazza-Deschamps G, Cia D, Gong J, Jellali A, Duboc A, Forster V, Sahel JA, Tessier LH, Picaud S: **Excessive activation of cyclic nucleotide-gated channels contributes to neuronal degeneration of photoreceptors**. *Eur J Neurosci* 2005, **22**:1013–1022.
41. Frasson M, Sahel JA, Fabre M, Simonutti M, Dreyfus H, Picaud S: **Retinitis pigmentosa: Rod photoreceptor rescue by a calcium-channel blocker in the rd mouse**. *Nat Med* 1999, **5**:1183–1187.
42. Das S, Chen Y, Yan J, Christensen G, Belhadj S, Tolone A, Paquet-Durand F: **The role of cGMP-signalling and calcium-signalling in photoreceptor cell death: perspectives for therapy development**. *Pflugers Arch Eur J Physiol* 2021, **473**:1411–1421.
43. Wang T, Tsang SH, Chen J: **Two pathways of rod photoreceptor cell death induced by elevated cGMP**. *Hum Mol Genet* 2017, **26**:2299–2306.
44. Wang T, Reingruber J, Woodruff ML, Majumder A, Camarena A, Artemyev NO, Fain GL, Chen J: **The PDE6 mutation in the rd10 retinal degeneration mouse model causes protein mislocalization and instability and promotes cell death through increased ion influx**. *J Biol Chem* 2018, **293**:15332–15346.
45. Wang T, Tsang SH, Chen J: **Two pathways of rod photoreceptor cell death induced by elevated cGMP**. *Hum Mol Genet* 2017, **26**:2299–2306.
46. Schön C, Paquet-Durand F, Michalakis S: **Cav1.4 L-type calcium channels contribute to calpain activation in degenerating photoreceptors of rd1 mice**. *PLoS One* 2016, **11**:e0156974.
47. Read DS, McCall MA, Gregg RG: **Absence of voltage-dependent calcium channels delays photoreceptor degeneration in rd mice**. *Exp Eye Res* 2002, **75**:415–420.
48. Kim JJ, Lorenz R, Arold ST, Reger AS, Sankaran B, Casteel DE, Herberg FW, Kim C: **Crystal Structure of PKG I:cGMP Complex Reveals a cGMP-Mediated Dimeric Interface that Facilitates cGMP-Induced Activation**. *Structure* 2016, **24**:710–720.
49. Francis SH, Busch JL, Corbin JD: **cGMP-dependent protein kinases and cGMP phosphodiesterases in nitric oxide and cGMP action**. *Pharmacol Rev* 2010, **62**:525–563.
50. Antl M, Von Brühl ML, Eiglsperger C, Werner M, Konrad I, Kocher T, Wilm M, Hofmann F, Massberg S, Schlossmann J: **IRAG mediates NO/cGMP-dependent inhibition of platelet aggregation and thrombus formation**. *Blood* 2007, **109**:552–559.
51. Tang M, Wang G, Lu P, Karas RH, Aronovitz M, Heximer SP, Kaltenbronn KM, Blumer KJ, Siderovski DP, Zhu Y, et al.: **Regulator of G-protein signaling-2 mediates vascular smooth muscle relaxation and blood pressure**. *Nat Med* 2003, **9**:1506–1512.
52. Prysyazhna O, Wolhuter K, Switzer C, Santos C, Yang X, Lynham S, Shah AM, Eaton P, Burgoyne JR: **Blood Pressure-Lowering by the Antioxidant Resveratrol Is Counterintuitively Mediated by Oxidation of cGMP-Dependent Protein Kinase**. *Circulation* 2019, **140**:126–137.

53. Roy A, Tolone A, Hilhorst R, Groten J, Tomar T, Paquet-Durand F: **Kinase activity profiling identifies putative downstream targets of cGMP/PKG signaling in inherited retinal neurodegeneration**. *Cell Death Discov* 2022, **8**:1–12.
54. Feil S, Zimmermann P, Knorn A, Brummer S, Schlossmann J, Hofmann F, Feil R: **Distribution of cGMP-dependent protein kinase type I and its isoforms in the mouse brain and retina**. *Neuroscience* 2005, **135**:863–868.
55. Manning BD: **Signalling protein protects the heart muscle from pressure-related stress**. *Nature* 2019, doi:10.1038/d41586-019-00245-3.
56. French PJ, Bijman J, Edixhoven M, Vaandrager AB, Scholte BJ, Lohmann SM, Nairn AC, De Jonge HR: **Isotype-specific activation of cystic fibrosis transmembrane conductance regulator-chloride channels by cGMP-dependent protein kinase II**. *J Biol Chem* 1995, **270**:26626–26631.
57. Rangaswami H, Marathe N, Zhuang S, Chen Y, Yeh JC, Frangos JA, Boss GR, Pilz RB: **Type II cGMP-dependent protein kinase mediates osteoblast mechanotransduction**. *J Biol Chem* 2009, **284**:14796–808.
58. Pfeifer A, Klatt P, Massberg S, Ny L, Sausbier M, Hirneiß C, Wang GX, Korth M, Aszódi A, Andersson KE, et al.: **Defective smooth muscle regulation in cGMP kinase I-deficient mice**. *EMBO J* 1998, **17**:3045–3051.
59. Jaumann M, Dettling J, Gubelt M, Zimmermann U, Gerling A, Paquet-Durand F, Feil S, Wolpert S, Franz C, Varakina K, et al.: **CGMP-Prkg1 signaling and Pde5 inhibition shelter cochlear hair cells and hearing function**. *Nat Med* 2012, **18**:252–259.
60. Quadri M, Comitato A, Palazzo E, Tiso N, Rentsch A, Pellacani G, Marconi A, Marigo V: **Activation of cGMP-Dependent Protein Kinase Restricts Melanoma Growth and Invasion by Interfering with the EGF/EGFR Pathway**. *J Invest Dermatol* 2021, doi:10.1016/j.jid.2021.06.011.
61. Han J, Dinculescu A, Dai X, Du W, Clay Smith W, Pang J: **Review: The history and role of naturally occurring mouse models with Pde6b mutations**. *Mol Vis* 2013, **19**:2579.
62. Power M, Das S, Schütze K, Marigo V, Ekström P, Paquet-Durand F: **Cellular mechanisms of hereditary photoreceptor degeneration – Focus on cGMP**. *Prog Retin Eye Res* 2020, **74**:100772.
63. Ekstrom PAR, Ueffing M, Zrenner E, Paquet-Durand F: **Novel In Situ Activity Assays for the Quantitative Molecular Analysis of Neurodegenerative Processes in the Retina**. *Curr Med Chem* 2014, **21**:3478–3493.
64. Burkhardt M, Glazova M, Gambaryan S, Vollkommer T, Butt E, Bader B, Heermeier K, Lincoln TM, Walter U, Palmetshofer A: **KT5823 inhibits cGMP-dependent protein kinase activity in vitro but not in intact human platelets and rat mesangial cells**. *J Biol Chem* 2000, **275**:33536–33541.
65. Sung YJ, Sofoluke N, Nkamany M, Deng S, Xie Y, Greenwood J, Farid R, Landry DW, Ambron RT: **A novel inhibitor of active protein kinase G attenuates chronic inflammatory and osteoarthritic pain**. *Pain* 2017, **158**:822.
66. Gambaryan S, Butt E, Kobsar A, Geiger J, Rukoyatkina N, Parnova R, Nikolaev VO, Walter U: **The oligopeptide DT-2 is a specific PKG i inhibitor only in vitro, not in living cells**. *Br J Pharmacol* 2012, **167**:826–838.
67. Vighi E, Trifunovic D, Veiga-Crespo P, Rentsch A, Hoffmann D, Sahaboglu A, Strasser T, Kulkarni M, Bertolotti E, Van Den Heuvel A, et al.: **Combination of cGMP analogue and drug delivery system provides functional protection in hereditary retinal degeneration**. *Proc Natl Acad Sci U S A* 2018, **115**:E2997–E3006.
68. Butt E, Pöhler D, Genieser HG, Huggins JP, Bucher B: **Inhibition of cyclic GMP-dependent protein kinase-mediated effects by (Rp)-8-bromo-PET-cyclic GMPS.** *Br J Pharmacol* 1995, **116**:3110–3116.

69. Vighi E, Trifunovic D, Veiga-Crespo P, Rentsch A, Hoffmann D, Sahaboglu A, Strasser T, Kulkarni M, Bertolotti E, Heuvel A Van Den, et al.: **Combination of cGMP analogue and drug delivery system provides functional protection in hereditary retinal degeneration**. *Proc Natl Acad Sci U S A* 2018, **115**:E2997–E3006.
70. Butt E, Eigenthaler M, Genieser HG: **(Rp)-8-pCPT-cGMPS, a novel cGMP-dependent protein kinase inhibitor**. *Eur J Pharmacol Mol Pharmacol* 1994, **269**:265–268.
71. Paquet-Durand F, Hauck SM, Veen T Van, Ueffing M, Ekström P: **PKG activity causes photoreceptor cell death in two retinitis pigmentosa models**. *J Neurochem* 2009, **108**:796–810.
72. Micera A, Balzamino BO, Di Zazzo A, Dinice L, Bonini S, Coassin M: **Biomarkers of Neurodegeneration and Precision Therapy in Retinal Disease**. *Front Pharmacol* 2021, **11**:601647.
73. Lassoued A, Zhang F, Kurokawa K, Liu Y, Bernucci MT, Crowell JA, Miller DT: **Cone photoreceptor dysfunction in retinitis pigmentosa revealed by optoretinography**. *Proc Natl Acad Sci* 2021, **118**.
74. Bogenmann E, Lochrie MA, Simon MI: **Cone cell-specific genes expressed in retinoblastoma**. *Science (80-)* 1988, **240**:76–78.
75. McFall RC, Sery TW, Makadon M: **Characterization of a New Continuous Cell Line Derived from a Human Retinoblastoma**. *Cancer Res* 1977, **37**:1003–1010.
76. Tan E, Ding XQ, Saadi A, Agarwal N, Naash MI, Al-Ubaidi MR: **Expression of cone-photoreceptor-specific antigens in a cell line derived from retinal tumors in transgenic mice**. *Investig Ophthalmol Vis Sci* 2004, **45**:764–768.
77. Comitato A, Subramanian P, Turchiano G, Montanari M, Becerra SP, Marigo V: **Pigment epithelium-derived factor hinders photoreceptor cell death by reducing intracellular calcium in the degenerating retina**. *Cell Death Dis* 2018, **9**:1–13.
78. Huang L, Kutluer M, Adani E, Comitato A, Marigo V: **New in vitro cellular model for molecular studies of retinitis pigmentosa**. *Int J Mol Sci* 2021, **22**:6440.
79. Sancho-Pelluz J, Arango-Gonzalez B, Kustermann S, Romero FJ, Van Veen T, Zrenner E, Ekström P, Paquet-Durand F: **Photoreceptor cell death mechanisms in inherited retinal degeneration**. *Mol Neurobiol* 2008, **38**:253–269.
80. Bayés M, Giordano M, Balcells S, Grinberg D, Vilageliu L, Martínez I, Ayuso C, Benítez J, Ramos-Arroyo MA, Chivelet P, et al.: **Homozygous tandem duplication within the gene encoding the β-subunit of rod phosphodiesterase as a cause for autosomal recessive retinitis pigmentosa**. *Hum Mutat* 1995, **5**:228–234.
81. Belhadj S, Hermann NS, Zhu Y, Christensen G, Strasser T, Paquet-Durand F: **Visualizing Cell Death in Live Retina: Using Calpain Activity Detection as a Biomarker for Retinal Degeneration**. *Int J Mol Sci* 2022, **23**:3892.
82. Rasmussen M, Welinder C, Schwede F, Ekström P: **The cGMP system in normal and degenerating mouse neuroretina: New proteins with cGMP interaction potential identified by a proteomics approach**. *J Neurochem* 2020, doi:10.1111/jnc.15251.
83. González-Medina M, Miljković F, Haase GS, Drueckes P, Trappe J, Laufer S, Bajorath J: **Promiscuity analysis of a kinase panel screen with designated p38 alpha inhibitors**. *Eur J Med Chem* 2020, **187**:112004.
84. Alganem K, Hamoud AR, Creeden JF, Henkel ND, Imami AS, Joyce AW, Ryan V WG, Rethman JB, Shukla R, O'Donovan SM, et al.: **The active kinome: The modern view of how active protein kinase networks fit in biological research**. *Curr Opin Pharmacol* 2022, **62**:117–129.
85. Cooper MJ, Cox NJ, Zimmerman EI, Dewar BJ, Duncan JS, Whittle MC, Nguyen TA, Jones LS, Ghose Roy S, Smalley DM, et al.: **Application of Multiplexed Kinase Inhibitor Beads to Study Kinome Adaptations in Drug-Resistant Leukemia**. *PLoS One* 2013, **8**:e66755.

86. Bastea LI, Hollant LMA, Döppler HR, Reid EM, Storz P: **Sangivamycin and its derivatives inhibit Haspin-Histone H3-survivin signaling and induce pancreatic cancer cell death**. *Sci Rep* 2019, **9**:1–10.
87. Gallagher RI, Espina V: **Reverse Phase Protein Arrays: Mapping the Path Towards Personalized Medicine**. *Mol Diagnosis Ther* 2014, **18**:619–630.
88. Roy A, Groten J, Marigo V, Tomar T, Hilhorst R: **Identification of novel substrates for cGMP dependent protein kinase (PKG) through kinase activity profiling to understand its putative role in inherited retinal degeneration**. *Int J Mol Sci* 2021, **22**:1–17.
89. Hilhorst R, Houkes L, Mommersteeg M, Musch J, Van Den Berg A, Ruijtenbeek R: **Peptide microarrays for profiling of serine/threonine kinase activity of recombinant kinases and lysates of cells and tissue samples**. *Methods Mol Biol* 2013, **977**:259–271.
90. Görte J, Danen E, Cordes N: **Therapy-Naive and Radioresistant 3-Dimensional Pancreatic Cancer Cell Cultures Are Effectively Radiosensitized by β1 Integrin Targeting**. *Int J Radiat Oncol Biol Phys* 2022, **112**:487–498.
91. Deville SS, Silva LFD, Vehlow A, Cordes N: **C-Abl tyrosine kinase is regulated downstream of the cytoskeletal protein synemin in head and neck squamous cell carcinoma radioresistance and DNA repair**. *Int J Mol Sci* 2020, **21**:7277.
92. Chirumamilla CS, Fazil MHUT, Perez-Novo C, Rangarajan S, de Wijn R, Ramireddy P, Verma NK, Vanden Berghe W: **Profiling activity of cellular kinases in migrating T-cells**. *Methods Mol Biol* 2019, **1930**:99–113.

2

Chapter 2

Technological advancements to study cellular signaling pathways in inherited retinal degenerative diseases

Akanksha Roy, Riet Hilhorst, John Groten, François Paquet-Durand and Tushar Tomar

Current Opinion in Pharmacology; 60 (2021): 102-110

Abstract

Inherited Retinal Degenerative Diseases (IRDs) are rare neurodegenerative disorders with mutations in hundreds of genes leading to vision loss, primarily due to photoreceptor cell death. This genetic diversity is impeding development of effective treatment options. Gene-based therapies have resulted in the first FDA approved drug (Luxturna®) for *RPE65*-specific IRD. Although currently explored in clinical trials, genomic medicines are mutation-dependent, hence suitable only for patients harbouring a specific mutation. Better understanding of the pathways leading to photoreceptor degeneration may help to determine common targets and develop mutation-independent therapies for larger groups of IRD patients. In this review, we discuss the key pathways involved in photoreceptor cell death studied by transcriptomics, proteomics, and metabolomics techniques to identify potential therapeutic targets in IRDs.

Introduction

IRDs are an important group of neurodegenerative diseases leading to progressive vision loss in more than 2 million people worldwide [1]. IRDs comprise of diseases associated with photoreceptor cell death, *e.g.,* Retinitis Pigmentosa (RP), Leber Congenital Amaurosis (LCA), rod or cone photoreceptor dystrophy. RP is one of the most prominent and heterogeneous IRDs. Initially, RP patients experience night vision problems due to the loss of rod photoreceptors (rods), followed by secondary degeneration of cone photoreceptors (cones), leading to so-called tunnel vision and eventually complete blindness [2]. RP associated with other neurological and congenital disorders, is named 'syndromic' RP, *e.g.* Usher syndrome involves hearing loss along with vision loss [3].

Around 270 disease genes have been described for IRDs, as well as copy number variations which makes it difficult to devise generic treatments [4]. Identification of genetic defects and advances in molecular genetics and gene-based therapies, have the potential to revolutionize the treatment of IRDs, as illustrated by the FDA approval of Luxturna® [5,6]. Clinical trials have proven the safety and efficiency of virus vector-based transfer of functional genes in IRDs [7]. Introduction of a functional *MERTK gene* [8] and *RPRG* gene [9] are currently investigated in clinical trials. Another recent breakthrough is genome editing with Clustered Regularly Interspaced Short Palindromic Repeats (CRISPR)-Cas [10]. Clinical trials have commenced for the first CRISPR Cas9-based *in vivo* treatment for LCA [11].

Despite these initial successes, implementation of such treatments to clinical practice is challenging as every type of genetic defect requires a specific treatment. Analysis of the genetic defects in IRDs has revealed that distinct mutations converge in common cellular signaling pathways, in which druggable targets might be identified that could benefit larger subgroups of patients [12]. Unraveling such pathways and their role in relation to diseased stage is complicated by the fact that the retina comprises of about 70 different cell types, both neuronal and non-neuronal, each with a specific function [13].

In this review, we will briefly discuss important routes associated with photoreceptor degradations in IRDs. In addition, we will focus on unbiased techniques employed to study gene expression, protein presence, protein activity, and metabolism in IRDs, leading to potential therapeutic targets or treatment options.

Key signaling pathways/targets known in IRDs

The high genetic heterogeneity and widely varying clinical phenotypes of IRDs hamper a detailed understanding of photoreceptor cell death mechanisms. Human tissues are not easy to procure, but several cell line models are available as well as animal models. Murine models for several known genetic defects are available, *e.g. rd1*, *rd2,* and *rd10* [14]. Especially the *rd1* mouse, discovered in 1924 [15] and suffering from a mutation in the *Pde6b* gene [16], is arguably the oldest and most used animal model. Initially, research into photoreceptor cell death mechanisms was focused on apoptosis [17,18], but currently attention has shifted to non-apoptotic cell death pathways and preceding events, like

epigenetic pathways, phototransduction signaling via cGMP, or energy metabolism (Figure 1) [12,19]. Regardless, of the causative mechanisms, the earlier a therapeutic intervention takes place, the better are the chances of preventing cell death.

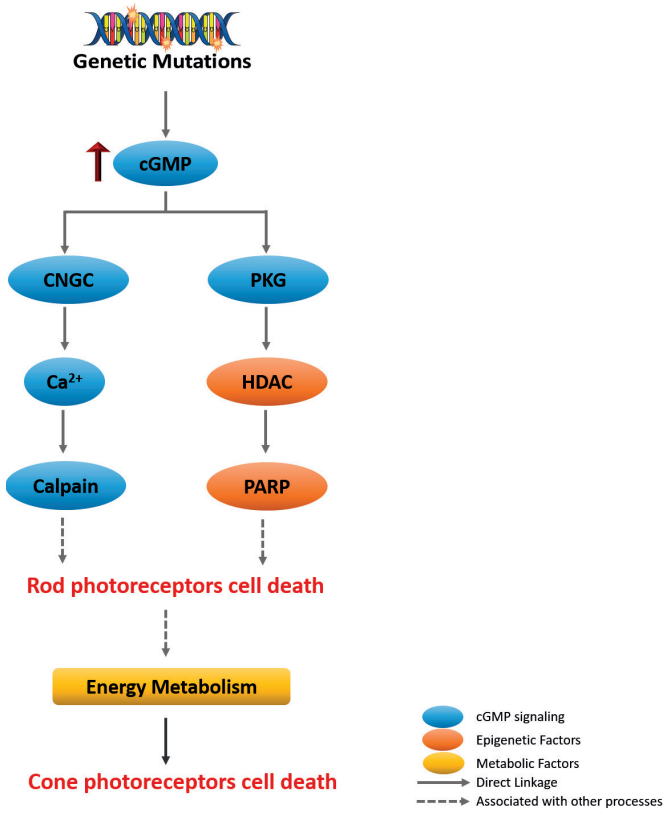

Figure 1- Putative photoreceptor degeneration mechanism in RP: Multiple IRD-linked mutations increase cGMP concentration, which opens CNGC and activates protein kinase G (PKG). Elevated Ca^{2+} influx through CNGCs may trigger calpain while PKG activity may be connected to HDAC and PARP activation. Together, the overactivation of these pathways lead to rod degradation, which eventually is followed by degradation of cones, possibly caused by changes in nutrient supply and energy metabolism.

Epigenetic processes

Epigenetic processes encompass events that affect the transcription of DNA without changing the DNA sequence. Epigenetic modifications like DNA methylation, modification of histones [histone (de)acetylation, (de)methylation and poly-ADP-ribosylation (PARylation)] are known to be directly associated with IRDs [12]. DNA hypermethylation in RP models of different species suggests a role in modulation of gene expression during photoreceptor degeneration [20,21]. The inhibition of DNA methyltransferase reduced photoreceptor cell death in *rd1* retinal explants and delayed their degeneration [20]. The histone deacetylase (HDAC) inhibitor Trichostatin-A showed a protective effect on rods and cones in *rd1* mice

[22]. Another HDAC inhibitor, valproic acid, either decreased or increased photoreceptor degeneration in murine RP models, therefore, use of valproic acid as a treatment option is doubtful [23,24]. One more epigenetic modification, PARylation due to excessive activity of (poly-ADP-ribose-polymerase) PARP may result in photoreceptor cell death which leads to loss of membrane integrity [25]. In retinal explants, PARylation was shown to colocalize with photoreceptor nuclei where HDAC activity was high [22]. Drugs targeting epigenetic processes in oncology are already FDA approved or in clinical trials [26,27]. Repurposing of these drugs to treat IRDs seems a promising option.

Phototransduction via cGMP driven pathways

Photon sensing in the photoreceptor cells is regulated by rapidly fluctuating levels of 3',5'-cyclic guanosine monophosphate (cGMP) [2]. In the dark, there is influx of Na^+ and Ca^{2+} into the photoreceptors due to opening of cyclic-nucleotide-gated channel (CNGC) by cGMP as well as continuous efflux of Na^+, K^+ and Ca^{2+} ions via a $Na^+/K^+/Ca^{2+}$ exchanger which leads to generation of 'dark current'. Light causes a conformational change of rhodopsin, which leads to activation of phosphodiesterase-6 (PDE6). PDE6 hydrolyzes cGMP, which causes closure of CNGCs, resulting in hyperpolarization. This leads to generation of an electro-chemical signal in response to light-stimuli which is transferred to 2nd order neurons as part of the vision process [2,28].

In IRD patients, recessive mutations have been identified in the *pde6b* subunit [29]. Accordingly, in the *Pde6b*-mutant *rd1* mouse, photoreceptor cell death was linked to elevated cGMP levels. Mutations in IRD related genes encoding for rhodopsin, CNGCs, Aryl hydrocarbon interacting protein like 1, or photoreceptor guanylyl cyclase also caused cGMP accumulation in the photoreceptors in murine models [2]. Although no explicit connection has been established between increased Ca^{2+} influx and photoreceptor degradation in IRD [30,31], knockdown of CNGCs delayed rod cell death, while knocking down of cGMP-dependent protein kinase G (PKG) alongside had a long-lasting protective effect on rod cell survival [32]. Increased PKG activity has been shown to cause photoreceptor cell death in murine RP models [14]. Since elevated cGMP levels are caused by multiple IRD mutations [19], understanding the cGMP driven pathways might provide new druggable targets.

Energy metabolism

The retina, notably the photoreceptor cells, is one of the most metabolically active tissues in the body [33]. Maintenance of the 'dark current' requires most of the energy but visual pigment recycling, synaptic activity, and biosynthesis of constituents for renewal of photoreceptor outer segments also demand a high energy input with cones incurring an even greater energy expenditure than rods [34]. Glycolysis seems to be predominant in the retina where glucose is converted to pyruvate and then to lactate under aerobic conditions (Warburg Effect) [35,36]. One hypothesis explaining the uptake of glucose or lactate by photoreceptors may be the 'astrocyte-neuron-lactate-shuttle' which would suggest that glia cells in the retina convert glucose into lactate, which would then be taken up by the photoreceptors [37,38]. However, it is presently not clear whether this hypothesis is valid for the retina as it is dependent on tissue type and metabolic context [39]. An alternative hypothesis proposes that photoreceptors rely mostly on glycolysis and provide the resultant lactate to the retinal pigment epithelial cells [40].

With the abundant energy demand in the retina, it seems likely that an impairment of energy metabolism would be detrimental to photoreceptor function and consequently to vision. The high metabolic activity is accompanied by the elevated production of reactive oxygen species, that cause mitochondrial damage. Mitochondrial dysfunction appears to be associated with retinal neurodegenerative diseases affecting photoreceptors, such as RP [41], age-related macular degeneration [42], diabetic retinopathy [43], but also concerns ganglion cells, such as in optic nerve atrophy [44]. There is converging evidence that bioenergetic dysfunction is a key pathogenic factor in secondary cone degeneration in RP [45,46].

Technologies to study cellular signaling pathways in IRDs

Although experimentally several treatments lead to retardation of photoreceptor degeneration, none of these have left the preclinical stage. Unbiased methods to identify gene expression, protein presence and its activity, as well as integration of multiple technologies are essential to understand the complexity of the retina and associated disorders.

Gene expression studies

Microarrays allow unbiased, high throughput screening of the expression of several thousands of genes, whereas real time-quantitative polymerase chain reaction (RT-qPCR) allows a targeted, quantitative, low throughput determination of expressed genes. Several microarray-based gene profiling studies in *rd1* murine model identified pathways like protein kinase C (PKC) signaling and JAK-STAT signaling pathway in association with photoreceptor cell death [47–49].

Both gene expression arrays and RT-PCR require many cells as input. Recent developments allow the determination of whole transcriptome profiles of individual cells. Differences in expression profiles were determined in murine retinas for microglia, monocytes and macrophages involved in neuroinflammatory response after onset of neurodegeneration [50]. Likewise, single-cell RNA sequencing of foveal and peripheral retinal samples of an autoimmune retinopathy patient revealed distinct transcriptional changes in glial cells [51]. These studies highlight the need for unbiased, high-throughput and high-dimensional molecular techniques for understanding the molecular complexity of different cell types in retina and IRDs. A major drawback of gene expression studies is that the mRNA detected may not be converted to proteins. Concordance between gene and proteins expression studies is low, underscoring the importance of studying signaling pathways at the protein level [52].

Protein presence and activity

Western blot and enzyme-linked immunosorbent assays can detect the presence of proteins in a sample, but these methods require *a priori* knowledge of the target and the availability of specific antibodies. Thus, non-discriminatory methods are imperative to make new discoveries related to changes in proteins. Moreover, the expression of a given protein does not *per se* reveal its activity, which may be dependent on its activation by upstream-signaling or the availability of suitable substrates. When the enzymatic activities of, for instance,

Ca^{2+}-dependent calpain-type proteases [53] or PARP-type enzymes [54] were studied in *rd1* mice, there was a strong disconnect with the corresponding gene and protein expression. While enzymatic activities of calpains and PARPs were strongly elevated in diseased *rd1* retina, no significant changes were detectable at the level of gene or protein expression. Therefore, it is important to also consider enzymatic activities as well as corresponding changes in metabolite spectrum and/or down-stream effectors and their post-translational modifications [55,56]. In this context, the understanding of protein phosphorylation, which often governs enzyme activity, and hence activities of the responsible kinases are of major importance.

Mass spectrometry-based methods for protein identification

Mass spectrometry-based protein identification techniques require no *a priori* knowledge about the targets and are sensitive, quick, and highly multiplexed. The technique requires quite high sample input (~ 1 mg), especially when enrichment for *e.g.*, ligands or post-translational modification is performed. Sample preparation is a crucial step for optimum results [57].

Mass spectrometry identified around 5,300 proteins differently expressed in *rd1* and control murine retinas [58], where key proteins of visual transduction cascade (PDE6A, PDE6B, ROM1, GNAT1, GRK1) were underrepresented in the diseased retina. Quantitative mass spectrometry applied to determine the composition of the protein degradation machinery in murine RP retina (PP23H Rhodopsin mutant) revealed that retinal degeneration can be significantly delayed by increasing the photoreceptor proteasomal activity [1]. In a recent study, affinity chromatography was performed to select potential cGMP-interacting proteins in *rd1* murine retinas [59]. This was followed by mass spectrometry, which identified ten known and twelve potentially new cGMP interacting partners (CaMKIIα, GSK3β, MAPK1/3, EPAC2, *etc.*). Since these studies utilized whole retina lysates, i.e., a heterogeneous sample with multiple cell types, it is not immediately clear whether the changes observed relate to retinal degeneration or to secondary or tertiary events. New developments in mass spectrometry may in the near future allow to profile at single cell resolution, for instance directly in the degenerating photoreceptors of the retina [60].

***In situ* enzyme activity assays**

To understand the photoreceptor degeneration mechanism, several biochemical assays have been adapted to determine the enzymatic activity of proteins such as calpain, PARP, and HDAC *in situ* [12]. Unfixed retinal cryosections, that still retain enzymatic activity, are incubated with specific probes (substrates), which are either directly or indirectly fluorescently labeled. These assays allow single-cell resolution and provide spatial information and reveal changes in enzymatic activity [61]. A limiting factor is the availability of specific substrates which must either be covalently linked to their target or precipitate upon modification so that the label remains in place.

Application to ten murine IRD models showed activation of calpain, PARP, HDAC and accumulation of cGMP and PAR in diseased photoreceptors, common to all the models [12]. Recently, the protective effect of the PKG inhibitor CN03 on photoreceptors of three RD models *in vivo* was determined using *in situ* TUNEL assay, providing evidence for their utility.

Multiplex microarray technology for protein activity determination

Enzyme activity is tightly regulated by transient modifications or interactions between proteins. Methods to determine enzyme activity are useful as proteases, kinases, and phosphatases play an important role in signal transduction. Multiplex microarrays, where up to 196 enzyme substrates are immobilized on a surface, allow real time detection of phosphorylation of specific peptide substrates for kinase activity of both recombinant enzymes and complex mixtures of kinases [62]. Detection of peptide phosphorylation with fluorescently labelled antibodies not only allows identification of substrates for recombinant kinases, but also generation of hypothesis for specific kinases potentially active in a complex mixture of other kinases. In a recent study, our group applied a multiplex peptide microarray platform to identify novel phosphorylation targets of PKG and to study kinase activity in retinal cell lysates [62].

Tools for metabolic studies

Initial metabolic studies were performed using Clark electrodes to determine oxygen consumption and Warburg apparatus to investigate metabolic pathways [63]. These methods were extended with tracer studies with radio-labeled precursors, assays for specific metabolites and, more recently, with liquid-chromatography combined with mass-spectrometry (LC-MS) to perform proteomics and metabolomics studies. A recent addition is the extracellular flux analyzer (Seahorse), that determines oxygen consumption as a measure of mitochondrial respiration and lactate formation as the result of glycolysis [64]. Mitochondrial metabolism can be quantified by measurement of oxygen consumption rate *in vivo* and *ex vivo* [65,66].

Towards pathway-specific therapeutic intervention in IRDs

Current advancement in multiplex technologies confirmed not only known targets in the pathways relevant for IRDs, but also added potentially druggable new targets as listed in Table 1. GSK-3 inhibition has been shown to provide protection to retinal ganglion cells and photoreceptors, thereby providing a potential target for treatment of IRDs [67,68] Drugs targeting GSK-3 kinase have entered clinical testing for Alzheimer's disease [69]. CN03, a cGMP analogue that inhibits PKG, was able to preserve photoreceptors in three different RD models *in vivo* [70]. Addressing the phototransduction pathway, QLT091001, a synthetic cis-retinoid with orphan drug status, restored visual function in animal models carrying mutations in the *Rpe65* gene [71]. In clinical trial QLT091001 improved visual function in patients with IRD, however it did not stop the progression of photoreceptor degradation completely [72].

Besides pathways targeting, recently transcriptome sequencing was combined with epigenetic profiling like 'genome-wide DNA methylation' and 'Assay for Transposase-Accessible Chromatin (ATAC) sequencing' of patient samples to reveal previously immeasurable molecular heterogeneity and potential therapeutic targets. For instance, integrated transcriptomics and epigenomics studies on retinal cells of age-related macular degeneration (AMD) patients revealed *HDAC11*, *SKI*, and *GTF2H4* as novel potential epigenetic targets [73,74]. Inhibition of sirtuin-6 (*SIRT6*), a histone deacetylase repressor

of glycolytic flux, reprogramed retinal cells toward enhanced glycolysis and delayed photoreceptor death in a murine RP model [75].

Metabolic interventions, such as administration of insulin or exposure to nucleoredoxin-like protein 1 (Rod-derived cone viability factor) may provide functional protection to cones, probably by increasing glucose entry into cones [45,76]. A proteomic analysis of liquid vitreous biopsies of a RP patient and a murine model with *Pde6a* mutations revealed key altered molecular pathways, particularly related to metabolism, at the onset of photoreceptor degeneration [77]. Metabolic therapy guided by liquid biopsy proteomics attenuated RP phenotype in murine model [77]. These results highlight the potential of personalizing future therapies in IRDs by translational proteomic approaches.

Table 1: Emerging therapeutic targets in IRDs with techniques used to identify them

Potential Targets	Techniques	IRD Model	Validation	(Pre)Clinical Status	Ref.
Genomic					
Tropomyosin-related kinase B (*TrkB*)	*In vivo* injection with the kinase antagonist	*rd10* mice	Histology, Optokinetic Tracking	Preclinical	[78]
Male germ cell-associated kinase (*MAK*)	CRISPR-Cas9	Induced pluripotent stem cells-derived photoreceptor precursor cells	RT-PCR	Preclinical	[79]
Mer receptor tyrosine kinase *(MER)*	CRISPR-Cas9	Royal College of Surgeon Rats	Electroretinogram response, Toxicology and Biodistribution studies	Phase-I clinical trial	[80,81]
	Light microscopy	*Mertk*$^{-/-}$ *Cx3cr1*$^{GFP/+}$*Ccr2*$^{RFP/+}$ transgenic mice	Immunohistochemistry, Flow Cytometry	Preclinical	[82]
Retinitis Pigmentosa GTPase regulator-interacting protein (*RPGRIP)*	AAV-based genomic therapy	*RPGRIP*$^{-/-}$ knockdown mice	Fundus examination, Immunohistochemistry, Electroretinography	Preclinical	[83]
Retinal pigment epithelium-specific 65KDa (*RPE65*)	AAV-based genomic therapy	Patients with biallelic *RPE65* mutation	Multi-luminance mobility test	FDA approved	[84]
Proteomic					
cGMP-dependent protein kinase (PKG)	Affinity Chromatography and mass spectrometry	*rd1, rd2, rd10* retina tissue	Proximity ligation assay	Preclinical	[59]
	TUNEL assay	Primary rod photoreceptor-like cells from *rd1*; *rd1, rd2, rd10* retina explants	Immunohistochemistry		[70]
	Immunohistochemistry	*rd1, rd2* retina explant and *rd1* mice	Western Blot		[14]
	Light microscopy	*Cngb1*$^{-/-}$ *Prkg1*$^{-/-}$ knockdown mice	Light microscopy (littermates at 4-5 months old)		[85]
Glycogen synthase kinase 3 (GSK-3)	TUNEL assay	*rd10* retina explants	TUNEL assay after treatment with N-methyl-D-aspartate	Preclinical	[67]

Potential Targets	Techniques	IRD Model	Validation	(Pre)Clinical Status	Ref.
Rhodopsin Kinase (RK)	Electrophysiology	*RK*$^{-/-}$ knockdown mice	TUNEL assay, Western Blot	Preclinical	[86]
Receptor-interacting protein kinase-3 (RIPK3)	qPCR, Western Blot	*rd10* retina tissue	Light microscopy, TUNEL assay	Preclinical	[87]
Serine/Threonine-protein kinase B-Raf (BRaf)	Affinity chromatography and mass spectrometry	*rd1, rd2, rd10* retina tissue	-	Preclinical	[59]
Calcium/Calmodulin-dependent protein kinase type IIα (CaMKIIα)	Affinity chromatography and mass spectrometry	*rd1, rd2, rd10* retina tissue	Proximity ligation assay	Preclinical	[59]
Poly-ADP-ribose-polymerase (PARP)	Immunostaining	*rd1* retina explant	Western Blot, TUNEL assay	Preclinical	[88]
	Immunohistochemistry	Retinal explants from ten different IRD-mutation murine models	-		[12]
cAMP response element-binding protein (CREB)	Immunohistochemistry	Retinal explants from ten different IRD-mutation murine models	-	Preclinical	[12]
Calpain	Immunohistochemistry	Retinal explants from ten different IRD-mutation murine models	-	Preclinical	[12]

Conclusion

The vast genetic heterogeneity in IRDs makes it difficult to identify common treatment approaches targeting photoreceptor degeneration. Therefore, integration of multiple technologies, ideally with spatial resolution at the single cell level, is essential to understand the complexity of IRDs. Investigation of pathways involved in phototransduction via cGMP signalling, energy metabolism, and epigenetics will likely facilitate identification of mutation-independent therapeutic targets. Treatments taking into account the cross-talk between different cell types in the retina and repurposing of clinically approved drugs might help to advance the development of effective drug interventions for IRDs.

Author contribution

Akanksha Roy: Writing - original draft preparation, Writing - review & editing, Visualization. **Riet Hilhorst**: Writing - review & editing. **John Groten**: Writing - review & editing. **François Paquet-Durand**: Writing - review & editing. **Tushar Tomar**: Conceptualization, Writing - original draft preparation, Writing - review & editing, Supervision.

Conflict of interests

Akanksha Roy, **John Groten**, and **Tushar Tomar** are currently employed and **Riet Hilhorst** is a previous employee of PamGene International B.V. The authors declare no conflict of interest.

Funding

This research was funded by European Union Horizon 2020 Research and Innovation Programme—*trans*Med under the Marie Curie grant agreement No. 765441 [(*trans*Med; H2020- MSCA-765441)].

References

1. Lobanova ES, Finkelstein S, Li J, Travis AM, Hao Y, Klingeborn M, Skiba NP, Deshaies RJ, Arshavsky VY: **Increased proteasomal activity supports photoreceptor survival in inherited retinal degeneration**. *Nat Commun* 2018, **9**:1–11.
2. Tolone A, Belhadj S, Rentsch A, Schwede F, Paquet-Durand F: **The cGMP pathway and inherited photoreceptor degeneration: Targets, compounds, and biomarkers**. *Genes (Basel)* 2019, **10**:1–16.
3. O'Neal, Teri B. EEL: **Retinitis Pigmentosa**. *StatPearls [Internet]* 2020,
4. Zampaglione E, Kinde B, Place EM, Navarro-gomez D, Maher M, Jamshidi F, Nassiri S, Mazzone JA, Finn C, Schlegel D, et al.: **Copy-number variation contributes 9 % of pathogenicity in the inherited retinal degenerations**. *Genet Med* 2020, **22**:1079–1087.
5. Russell S, Bennett J, Wellman JA, Chung DC, Yu ZF, Tillman A, Wittes J, Pappas J, Elci O, McCague S, et al.: **Efficacy and safety of voretigene neparvovec (AAV2-hRPE65v2) in patients with RPE65-mediated inherited retinal dystrophy: a randomised, controlled, open-label, phase 3 trial**. *Lancet* 2017, **390**:849–860.
6. **FDA approves novel gene therapy to treat patients with a rare form of inherited vision loss**. https://www.fda.gov/news-events/press-announcements/fda-approves-novel-gene-therapy-treat-patients-rare-form-inherited-vision-loss 2017.
7. Fuller-Carter PI, Basiri H, Harvey AR, Carvalho LS: **Focused Update on AAV-Based Gene Therapy Clinical Trials for Inherited Retinal Degeneration**. *BioDrugs* 2020, **34**:763–781.
8. Ghazi NG, Abboud EB, Nowilaty SR, Alkuraya H, Alhommadi A, Cai H, Hou R, Deng WT, Boye SL, Almaghamsi A, et al.: **Treatment of retinitis pigmentosa due to MERTK mutations by ocular subretinal injection of adeno-associated virus gene vector: results of a phase I trial**. *Hum Genet* 2016, **135**:327–343.
9. Moore NA, Morral N, Ciulla TA, Bracha P: **Gene therapy for inherited retinal and optic nerve degenerations**. *Expert Opin Biol Ther* 2018, **18**:37–49.
10. Doudna, Jennifer A. and EC: **The new frontier of genome engineering with CRISPR-Cas9**. *Science (80-)* 2014, **346**.
11. **First CRISPR therapy dosed**. https://doi.org/10.1038/s41587-020-0493-4. *Nat Biotechnol* 2020, **38**:382.
12. Arango-Gonzalez B, Trifunović D, Sahaboglu A, Kranz K, Michalakis S, Farinelli P, Koch S, Koch F, Cottet S, Janssen-Bienhold U, et al.: **Identification of a common non-apoptotic cell death mechanism in hereditary retinal degeneration**. *PLoS One* 2014, **9**:1–11.
13. Masland RH: **The neuronal organization of the retina**. *Neuron* 2012, **76**:266–280.
14. Paquet-Durand F, Hauck SM, Van Veen T, Ueffing M, Ekström P: **PKG activity causes photoreceptor cell death in two retinitis pigmentosa models**. *J Neurochem* 2009, **108**:796–810.
15. Keeler CE: **The inheritance of a retinal abnormality in white mice**. *Proc Natl Acad Sci U S A* 1924, **10**:329.
16. Bowes C, Li T, Danciger M, Baxter LC, Applebury ML, Farber DB: **Retinal degeneration in the rd mouse is caused by a defect in the β subunit of rod cGMP-phosphodiesterase**. *Nature* 1990, **347**:677–680.
17. Marigo V: **Programmed cell death in retinal degeneration: Targeting apoptosis in photoreceptors as potential therapy for retinal degeneration**. *Cell Cycle* 2007, **6**:652–655.
18. Portera-Cailliau C, Sung CH, Nathans J, Adler R: **Apoptotic photoreceptor cell death in mouse models of retinitis pigmentosa**. *Proc Natl Acad Sci U S A* 1994, **91**:974–978.

19. Power M, Das S, Schütze K, Marigo V, Ekström P, Paquet-Durand F: **Cellular mechanisms of hereditary photoreceptor degeneration – Focus on cGMP**. *Prog Retin Eye Res* 2020, **74**.
20. Farinelli P, Perera A, Arango-Gonzalez B, Trifunovic D, Wagner M, Carell T, Biel M, Zrenner E, Michalakis S, Paquet-Durand F, et al.: **DNA methylation and differential gene regulation in photoreceptor cell death**. *Cell Death Dis* 2014, **5**.
21. Wahlin KJ, Enke RA, Fuller JA, Kalesnykas G, Zack DJ, Merbs SL: **Epigenetics and cell death: DNA hypermethylation in programmed retinal cell death**. *PLoS One* 2013, **8**.
22. Sancho-Pelluz J, Alavi M V., Sahaboglu A, Kustermann S, Farinelli P, Azadi S, Van Veen T, Romero FJ, Paquet-Durand F, Ekström P: **Excessive HDAC activation is critical for neurodegeneration in the rd1 mouse**. *Cell Death Dis* 2010, **1**:1–9.
23. Mitton KP, Guzman AE, Deshpande M, Byrd D, DeLooff C, Mkoyan K, Zlojutro P, Wallace A, Metcalf B, Laux K, et al.: **Different effects of valproic acid on photoreceptor loss in Rd1 and Rd10 retinal degeneration mice**. *Mol Vis* 2014, **20**:1527–1544.
24. Todd L, Zelinka C: **Valproic acid for a treatment of retinitis pigmentosa: Reasons for optimism and caution**. *J Neurosci* 2017, **37**:5215–5217.
25. Newton F, Megaw R: **Mechanisms of photoreceptor death in retinitis pigmentosa**. *Genes (Basel)* 2020, **11**:1–29.
26. Mullard A: **FDA approves an inhibitor of a novel "epigenetic writer."** *Nat Rev* 2020, **19**:156–156.
27. Mirza MR, Pignata S, Ledermann JA: **Latest clinical evidence and further development of PARP inhibitors in ovarian cancer**. *Ann Oncol* 2018, **29**:1366–1376.
28. Zhang X, Cote RH: **cGMP signaling in vertebrate retinal photoreceptor cells.** *Front Biosci* 2005, **10**:1191–1204.
29. Mclaughlin ME, Sandberg MA, Berson EL, Dryja TP: **Recessive mutations in the gene encoding the B-subunit of rod phosphodiesterase in patients with retinitis pigmentosa**. *Nat Genet* 1993, **4**:130–134.
30. Pawlyk BS, Li T, Scimeca MS, Sandberg MA, Berson EL: **Absence of photoreceptor rescue with D-cis-diltiazem in the rd mouse**. *Investig Ophthalmol Vis Sci* 2002, **43**:1912–1915.
31. Barabas P, Peck CC, Krizaj D: **Do calcium channel blockers rescue dying photoreceptors in the pde6b rd1 mouse?** *Adv Exp Med Biol* 2010, **664**:491–499.
32. Wang T, Tsang SH, Chen J: **Two pathways of rod photoreceptor cell death induced by elevated cGMP**. *Hum Mol Genet* 2017, **26**:2299–2306.
33. Wong-Riley M: **Energy metabolism of the visual system**. *Eye Brain* 2010, **2**:99.
34. Okawa H, Sampath AP, Laughlin SB, Fain GL: **ATP Consumption by Mammalian Rod Photoreceptors in Darkness and in Light**. *Curr Biol* 2008, **18**:1917–1921.
35. Léveillard T, Sahel JA: **Metabolic and redox signaling in the retina**. *Cell Mol Life Sci* 2017, **74**:3649–3665.
36. Warburg O: **The metabolism of carcinoma cells 1**. *J Cancer Res* 1925, **9**:148–163.
37. Brooks GA: **The Science and Translation of Lactate Shuttle Theory**. *Cell Metab* 2018, **27**:757–785.
38. Pellerin L, Magistretti PJ: **Glutamate uptake into astrocytes stimulates aerobic glycolysis: A mechanism coupling neuronal activity to glucose utilization**. *Proc Natl Acad Sci U S A* 1994, **91**:10625–10629.
39. Dienel GA: **Lack of appropriate stoichiometry: Strong evidence against an energetically important astrocyte–neuron lactate shuttle in brain**. *J Neurosci Res* 2017, **95**:2103–2125.
40. Kanow MA, Giarmarco MM, Jankowski CSR, Tsantilas K, Engel AL, Du J, Linton JD, Farnsworth CC, Sloat SR, Rountree A, et. al.: **Biochemical adaptations of the retina and retinal pigment epithelium support a metabolic ecosystem in the vertebrate eye**. *Elife* 2017, **6**:e28899.

41. Moreno ML, Mérida S, Bosch-Morell F, Miranda M, Villar VM: **Autophagy dysfunction and oxidative stress, two related mechanisms implicated in retinitis pigmentosa**. *Front Physiol* 2018, **9**.
42. Jarrett SG, Boulton ME: **Consequences of oxidative stress in age-related macular degeneration**. *Mol Aspects Med* 2012, **33**:399–417.
43. Camara AKS, Lesnefsky EJ, Stowe DF: **Potential therapeutic benefits of strategies directed to mitochondria**. *Antioxidants Redox Signal* 2010, **13**:279–347.
44. Lenaers G, Neutzner A, Le Dantec Y, Jüschke C, Xiao T, Decembrini S, Swirski S, Kieninger S, Agca C, Kim US, et al.: **Dominant optic atrophy: Culprit mitochondria in the optic nerve**. *Prog Retin Eye Res* 2021, doi:10.1016/j.preteyeres.2020.100935.
45. Aït-Ali N, Fridlich R, Millet-Puel G, Clérin E, Delalande F, Jaillard C, Blond F, Perrocheau L, Reichman S, Byrne LC, et al.: **Rod-derived cone viability factor promotes cone survival by stimulating aerobic glycolysis**. *Cell* 2015, **161**:817–832.
46. Narayan DS, Chidlow G, Wood JPM, Casson RJ: **Investigations Into Bioenergetic Neuroprotection of Cone Photoreceptors: Relevance to Retinitis Pigmentosa**. *Front Neurosci* 2019, **13**:1234.
47. Hackam AS, Strom R, Liu D, Qian J, Wang C, Otteson D, Gunatilaka T, Farkas RH, Chowers I, Kageyama M, et al.: **Identification of Gene Expression Changes Associated with the Progression of Retinal Degeneration in the rd1 Mouse**. *Invest Ophthalmol Vis Sci* 2004, **45**:2929–2942.
48. Azadi S, Paquet-durand F, Medstrand P, Veen T Van, Ekström P: **Up-regulation and increased phosphorylation of protein kinase C (PKC) δ, μ and θ in the degenerating rd1 mouse retina**. *Mol Cell Neurosci* 2006, **31**:759–773.
49. He X, Sun D, Chen S, Xu H: **Activation of liver X receptor delayed the retinal degeneration of rd1 mice through modulation of the immunological function of glia**. *Oncotarget* 2017, **8**:32068–32082.
50. Ronning KE, Karlen SJ, Miller EB BM: **Molecular profiling of resident and infiltrating mononuclear phagocytes during rapid adult retinal degeneration using single-cell RNA sequencing**. *Sci Rep* 2019, **9**:1–12.
51. Voigt AP, Binkley E, Flamme-Wiese MJ, Zeng S, DeLuca AP, Scheetz TE, Tucker BA, Mullins RF, Stone EM: **Single-Cell RNA Sequencing in Human Retinal Degeneration Reveals Distinct Glial Cell Populations**. *Cells* 2020, **9**:438.
52. Franks A, Airoldi E, Slavov N: **Post-transcriptional regulation across human tissues**. *PLoS Comput Biol* 2017, **13**.
53. Paquet-Durand F, Azadi S, Hauck SM, Ueffing M, Van Veen T, Ekström P: **Calpain is activated in degenerating photoreceptors in the rd1 mouse**. *J Neurochem* 2006, **96**:802–814.
54. Paquet-Durand F, Silva J, Talukdar T, Johnson LE, Azadi S, Van Veen T, Ueffing M, Hauck SM, Ekström PAR: **Excessive activation of poly(ADP-ribose) polymerase contributes to inherited photoreceptor degeneration in the retinal degeneration 1 mouse**. *J Neurosci* 2007, **27**:10311–10319.
55. Nomura DK, Dix MM, Cravatt BF: **Activity-based protein profiling for biochemical pathway discovery in cancer**. *Nat Rev Cancer* 2010, **10**:630–638.
56. Weiss ER, Osawa S, Xiong Y, Dhungana S, Carlson J, McRitchie S, Fennell TR: **Broad spectrum metabolomics for detection of abnormal metabolic pathways in a mouse model for retinitis pigmentosa**. *Exp Eye Res* 2019, **184**:135–145.
57. Rose, Christopher M., Marta Isasa, Alban Ordureau, Miguel A. Prado, Sean A. Beausoleil, Mark P. Jedrychowski, Daniel J. Finley, J. Wade Harper and SPG: **Highly multiplexed quantitative mass spectrometry analysis of ubiquitylomes**. *Cell Syst* 2016, **3**:395–403.

58. Murenu E, Kostidis S, Lahiri S, Geserich AS, Imhof A, Giera M, Michalakis S: **Metabolic Analysis of Vitreous / Lens and Retina in Wild Type and Retinal Degeneration Mice**. *Int J Mol Sci* 2021, **22**:2345.
59. Rasmussen M, Welinder C, Schwede F, Ekström P: **The cGMP system in normal and degenerating mouse neuroretina: New proteins with cGMP interaction potential identified by a proteomics approach**. *J Neurochem* 2020, doi:10.1111/jnc.15251.
60. Labib M, Kelley SO: **Single-cell analysis targeting the proteome**. *Nat Rev Chem* 2020, **4**:143–158.
61. Ekstrom PAR, Ueffing M, Zrenner E, Paquet-Durand F: **Novel In Situ Activity Assays for the Quantitative Molecular Analysis of Neurodegenerative Processes in the Retina**. *Curr Med Chem* 2014, **21**:3478–3493.
62. Roy A, Groten J, Marigo V, Tomar T, Hilhorst R: **Identification of novel substrates for cGMP dependent protein kinase (PKG) through kinase activity profiling to understand its putative role in inherited retinal degeneration**. *Int J Mol Sci* 2021, **22**:1–17.
63. Clark JR, Leland C., Wolf R, Granger D and TZ: **Continuous recording of blood oxygen tensions by polarography**. *J Appl Physiol* 1953, **6**:189–193.
64. Pelgrom LR, van der Ham AJ, Everts B: **Analysis of TLR-induced metabolic changes in dendritic cells using the seahorse XFe96 extracellular flux analyzer**. In *Methods in Molecular Biology*. . Humana Press Inc.; 2016:273–285.
65. Stefánsson E, Olafsdottir OB, Eliasdottir TS, Vehmeijer W, Einarsdottir AB, Bek T, Torp TL, Grauslund J, Eysteinsson T, Karlsson RA, et al.: **Retinal oximetry: Metabolic imaging for diseases of the retina and brain**. *Prog Retin Eye Res* 2019, **70**:1–22.
66. Adlakha YK, Swaroop A: **Determination of mitochondrial oxygen consumption in the retina ex vivo: Applications for retinal disease**. In *Methods in Molecular Biology*. . Humana Press Inc.; 2018:167–177.
67. Marchena M, Villarejo-Zori B, Zaldivar-Diez J, Palomo V, Gil C, Hernández-Sánchez C, Martínez A, de la Rosa EJ: **Small molecules targeting glycogen synthase kinase 3 as potential drug candidates for the treatment of retinitis pigmentosa**. *J Enzyme Inhib Med Chem* 2017, **32**:522–526.
68. Biermann J, Grieshaber P, Goebel U, Martin G, Thanos S, Di Giovanni S, Lagrèze WA: **Valproic acid-mediated neuroprotection and regeneration in injured retinal ganglion cells**. *Investig Ophthalmol Vis Sci* 2010, **51**:526–534.
69. Tolosa E, Litvan I, Höglinger GU, Burn DJ, Lees A, Andrés M V., Gómez-Carrillo B, León T, Del Ser T, Gómez JC, et al.: **A phase 2 trial of the GSK-3 inhibitor tideglusib in progressive supranuclear palsy**. *Mov Disord* 2014, **29**:470–478.
70. Vighi E, Trifunovic D, Veiga-Crespo P, Rentsch A, Hoffmann D, Sahaboglu A, Strasser T, Kulkarni M, Bertolotti E, Heuvel A Van Den, et al.: **Combination of cGMP analogue and drug delivery system provides functional protection in hereditary retinal degeneration**. *Proc Natl Acad Sci U S A* 2018, **115**:E2997–E3006.
71. Palczewski K: **Retinoids for treatment of retinal diseases**. *Trends Pharmacol Sci* 2010, **31**:284–295.
72. Scholl HPN, Moore AT, Koenekoop RK, Wen Y, Fishman GA, Van Den Born LI, Bittner A, Bowles K, Fletcher EC, Collison FT, et al.: **Safety and proof-of-concept study of oral QLT091001 in retinitis pigmentosa due to inherited deficiencies of retinal pigment epithelial 65 protein (RPE65) or lecithin: Retinol acyltransferase (LRAT)**. *PLoS One* 2015, **10**.
73. Wang, Jie, Cristina Zibetti, Peng Shang, Srinivasa R. Sripathi, Pingwu Zhang, Marisol Cano TH et al.: **ATAC-Seq analysis reveals a widespread decrease of chromatin accessibility in age-related macular degeneration**. *Nat Commun* 2018, **9**:1–13.

74. Porter LF, Saptarshi N, Fang Y, Rathi S, Den Hollander AI, De Jong EK, Clark SJ, Bishop PN, Olsen TW, Liloglou T, et al.: **Whole-genome methylation profiling of the retinal pigment epithelium of individuals with age-related macular degeneration reveals differential methylation of the SKI, GTF2H4, and TNXB genes**. *Clin Epigenetics* 2019, **11**.
75. Zhang L, Du J, Justus S, Hsu CW, Bonet-Ponce L, Wu WH, Tsai YT, Wu WP, Jia Y, Duong JK, et al.: **Reprogramming metabolism by targeting sirtuin 6 attenuates retinal degeneration**. *J Clin Invest* 2016, **126**:4659–4673.
76. Punzo C, Kornacker K, Cepko CL: **Stimulation of the insulin/mTOR pathway delays cone death in a mouse model of retinitis pigmentosa**. *Nat Neurosci* 2009, **12**:44–52.
77. Wert KJ, Velez G, Kanchustambham VL, Shankar V, Evans LP, Sengillo JD, Zare RN, Bassuk AG, Tsang SH, Mahajan VB: **Metabolite therapy guided by liquid biopsy proteomics delays retinal neurodegeneration**. *EBioMedicine* 2020, **52**.
78. Hanif AM, Lawson EC, Prunty M, Gogniat M, Aung MH, Chakraborty R, Boatright JH, Pardue MT: **Neuroprotective effects of voluntary exercise in an inherited retinal degeneration mouse model**. *Investig Ophthalmol Vis Sci* 2015, **56**:6839–6846.
79. Burnight ER, Gupta M, Wiley LA, Anfinson KR, Tran A, Triboulet R, Hoffmann JM, Klaahsen DL, Andorf JL, Jiao C, et al.: **Using CRISPR-Cas9 to Generate Gene-Corrected Autologous iPSCs for the Treatment of Inherited Retinal Degeneration**. *Mol Ther* 2017, **25**:1999–2013.
80. Conlon TJ, Deng WT, Erger K, Cossette T, Pang J jing, Ryals R, Clément N, Cleaver B, McDoom I, Boye SE, et al.: **Preclinical potency and safety studies of an AAV2-mediated gene therapy vector for the treatment of MERTK associated retinitis pigmentosa.** *Hum Gene Ther Clin Dev* 2013, **24**:23–28.
81. Fowzan Alkuraya (Principal Investigator): **Trial of subretinal injection of rAAV2-VMD2-hMERTK**; King Khaled Eye Specialist Hospital; *ClincalTrials.gov Identifier: NCT01482195*.
82. Kohno H, Koso H, Okano K, Sundermeier TR, Saito S, Watanabe S, Tsuneoka H, Sakai T: **Expression pattern of Ccr2 and Cx3cr1 in inherited retinal degeneration**. *J Neuroinflammation* 2015, **12**:1–11.
83. Pawlyk BS, Smith AJ, Buch PK, Adamian M, Hong DH, Sandberg MA, Ali RR, Li T: **Gene replacement therapy rescues photoreceptor degeneration in a murine model of leber congenital amaurosis lacking RPGRIP**. *Investig Ophthalmol Vis Sci* 2005, **46**:3039–3045.
84. Maguire AM, Bennett J, Aleman EM, Leroy BP, Aleman TS: **Clinical Perspective: Treating RPE65-Associated Retinal Dystrophy**. *Mol Ther* 2021, **29**:442–463.
85. Chen CK, Burns ME, Spencer M, Niemi GA, Chen J, Hurley JB, Baylor DA, Simon MI: **Abnormal photoresponses and light-induced apoptosis in rods lacking rhodopsin kinase**. *Proc Natl Acad Sci U S A* 1999, **96**:3718–3722.
86. Murakami Y, Matsumoto H, Roh M, Suzuki J, Hisatomi T, Ikeda Y, Miller JW, Vavvas DG: **Receptor interacting protein kinase mediates necrotic cone but not rod cell death in a mouse model of inherited degeneration**. *Proc Natl Acad Sci U S A* 2012, **109**:14598–14603.
87. Sahaboglu A, Miranda M, Canjuga D, Avci-Adali M, Savytska N, Secer E, Feria-Pliego JA, Kayık G, Durdagi S: **Drug repurposing studies of PARP inhibitors as a new therapy for inherited retinal degeneration**. *Cell Mol Life Sci* 2020, **77**:2199–2216.

3

Chapter 3

Identification of novel substrates for cGMP dependent Protein Kinase (PKG) through kinase activity profiling to understand its putative role in inherited retinal degeneration

Akanksha Roy, John Groten, Valeria Marigo, Tushar Tomar and Riet Hilhorst

International journal of molecular sciences; 22 (3) (2021): 1180

Abstract

Inherited retinal degenerative diseases (IRDs), which ultimately lead to photoreceptor cell death, are characterized by high genetic heterogeneity. Many IRD-associated genetic defects affect 3′,5′-cyclic guanosine monophosphate (cGMP) levels. cGMP-dependent protein kinases (PKG1 and PKG2) have emerged as novel targets, and their inhibition has shown functional protection in IRDs. The development of such novel neuroprotective compounds warrants a better understanding of the pathways downstream of PKGs that lead to photoreceptor degeneration. Here, we used human recombinant PKGs in combination with PKG activity modulators (cGMP, 3′,5′-cyclic adenosine monophosphate (cAMP), PKG activator, and PKG inhibitors) on a multiplex peptide microarray to identify substrates for PKG1 and PKG2. In addition, we applied this technology in combination with PKG modulators to monitor kinase activity in a complex cell system, *i.e.* the retinal cell line 661W, which is used as a model system for IRDs. The high-throughput method allowed quick identification of *bona fide* substrates for PKG1 and PKG2. The response to PKG modulators helped us to identify, in addition to ten known substrates, about 50 novel substrates for PKG1 and/or PKG2 which are either specific for one enzyme or common to both. Interestingly, both PKGs are able to phosphorylate the regulatory subunit of PKA, whereas only PKG2 can phosphorylate the catalytic subunit of PKA. In 661W cells, the results suggest that PKG activators cause minor activation of PKG, but a prominent increase in the activity of cAMP-dependent protein kinase (PKA). However, the literature suggests an important role for PKG in IRDs. This conflicting information could be reconciled by cross-talk between PKG and PKA in the retinal cells. This must be explored further to elucidate the role of PKGs in IRDs.

Keywords
PKG, PKA, cGMP, cAMP, 661W, retinal degeneration, substrate identification, peptide microarray

Introduction

Inherited retinal degenerative diseases (IRDs) include a group of diseases that lead to severe vision impairment and blindness at a young age due to mutations affecting the functioning of the retina. Retinitis pigmentosa is one of the most prominent and most heterogenous IRD, with over 65 defective genes identified in the autosomal dominant, recessive, and X-linked forms of the disease [1]. During the onset of retinitis pigmentosa, rod photoreceptors, responsible for vision under dim light, are primarily affected. The disease manifests itself with the patients experiencing night vision problems and tunnel vision due to a loss of rod cells that are present at the periphery of the retina. With the progression of the disease, cone photoreceptors are also degenerated, leading to complete blindness [2].

The phototransduction pathway in retina is mediated by fluctuations in cGMP levels in the photoreceptors [2]. In the dark, high cGMP levels open cyclic nucleotide gated (CNG) ion channels. These non-specific channels lead to an influx of Na^+ and Ca^{2+} into the photoreceptors. At the same time, K^+ and Ca^{2+} are continuously extruded via a $Na^+/K^+/Ca^{2+}$ exchanger. The influx and efflux of ions via these two types of channels lead to generation of a dark current. Light disrupts the generation of the dark current. The absorption of photons induces conformational changes in rhodopsin (the visual pigment present in rod photoreceptors) which, through a series of steps, leads to the activation of phosphodiesterase-6 (PDE6). PDE6 hydrolyzes cGMP and prompts the closure of CNG channels, resulting in hyperpolarization due to the efflux of Ca^{2+} and K^+ by the $Na^+/K^+/Ca^{2+}$ exchanger, which sends a signal to the neuronal cells and ultimately to the brain for visual processing [2,3].

Mutations in the rod-specific PDE6 subunits α and β have been linked to high intracellular levels of cGMP, as cGMP is not hydrolyzed. For photoreceptor degeneration, three times higher cGMP levels have been reported in murine retinas with a PDE6 mutation [4,5]. Mutations in other genes encoding for rhodopsin, CNG ion channels, aryl hydrocarbon interacting protein-like 1 or photoreceptor guanylyl cyclase have also been identified to cause excessive cGMP accumulation in the photoreceptors [2,6]. cGMP opens the CNG ion channels and activates PKGs by binding to their regulatory sites. PKGs phosphorylate components of ion channels, G-proteins, and cytoskeleton proteins that regulate neuronal, cardiovascular, and intestinal functions [7]. Application of PKG inhibitors *in vivo* in retinas of the *rd1* mouse model resulted in photoreceptor protection [8]. Recently, it was demonstrated that *in vivo* application of a PKG inhibitor with a drug delivery system counteracted photoreceptor degeneration and preserved retina function in three IRD mouse models [9]. In addition, it has been shown in a CNG channel loss-of function mouse model that knocking out of *prkg1* encoding for PKG1 leads to sustained rod cell survival [10]. The correlation of PKG activation with cell death is corroborated by studies showing induction of apoptosis with PKG activation to stop tumor progression in colon cancers [11–13], breast cancers [14], ovarian cancers [15] and melanoma [16]. However, the signaling routes downstream of PKG1 and PKG2 that lead to cell death have not been identified yet. Since in this heterogeneous disease, many mutations convene in a common cGMP-driven PKG signaling route, targeting PKGs could provide a common treatment amenable for a larger group of patients. Therefore, identification of targets for PKG1 and PKG2 as well as their downstream signaling pathways might help to develop novel treatments for rare diseases such as IRDs, but also for various cancer types.

The aim of this study was to identify high-quality substrates for PKG1 and PKG2, and use this information to identify critical PKG targets in the retina. Since a kinase has multiple substrates, we used a peptide microarray with 142 serine/threonine containing peptides to determine preferred PKG1 or PKG2 substrates. PKG activity was modulated by known PKG specific inhibitors and activators that bind to the regulatory sites of cGMP-dependent protein kinases to identify novel and bona fide substrates for PKG1 and PKG2. We then applied the knowledge on modulation of PKG activity to investigate the role of endogenous PKG1 and PKG2 in 661W retinal cells that are also used as model for retinal degeneration [17,18]. We show that in a complex cellular environment, the PKG modulators only modestly increase the activity of cGMP-dependent kinases but strongly increase the activity of cAMP-dependent protein kinase A (PKA), a close relative of PKG.

Results

Modulation of PKG Activity and Substrate Identification

To identify substrates for PKGs, the effect of modulators (ATP, cGMP, cAMP, PKG activator and PKG inhibitors) on recombinant PKG1 and PKG2 was tested in a high throughput setting, using PamChip® 96 array plates. Each array comprises of 142 serine/threonine containing peptides which are derived from putative phosphorylation sites in the human phosphoproteome [19]. The peptide names consist of the protein they are derived from and the amino acid positions in that protein. First, incubations with or without ATP were performed to establish that the phosphorylation reaction for PKG1 and PKG2 is ATP-dependent (Supplementary Fig. S1). Next, a concentration series of recombinant PKG1 and PKG2 was tested on PamChip® arrays to determine the desired PKG input for this study (Supplementary Table S1). We found that the assay is linear with enzyme input; however, at a high concentration, the linearity is lost. Based on the results, we chose 0.5 ng PKG1 and 5 ng PKG2 per array as protein input concentration in all the following experiments.

Effect of cGMP and cAMP on PKG Activity

The phosphorylation activity of PKG1 and PKG2 on the peptides as a function of cGMP or cAMP concentration is shown in Fig. 1. PKG1 and PKG2 show a big overlap in substrate preference, although there are also differences. The phosphorylation signal intensity of four peptides each for PKG1 and PKG2 (ERF_519_531 and VASP_232_244 as substrates for both PKG1 and PKG2, CFTR_761_773 and F263_454_466 as substrates for PKG1 and CENPA_1_14 and H32_3_18 as substrates for PKG2) as a function of cGMP or cAMP concentration is shown in Fig. 1. Signal intensity for PKG1 and PKG2 started to increase around 100 nM cGMP and 1 µM cAMP.

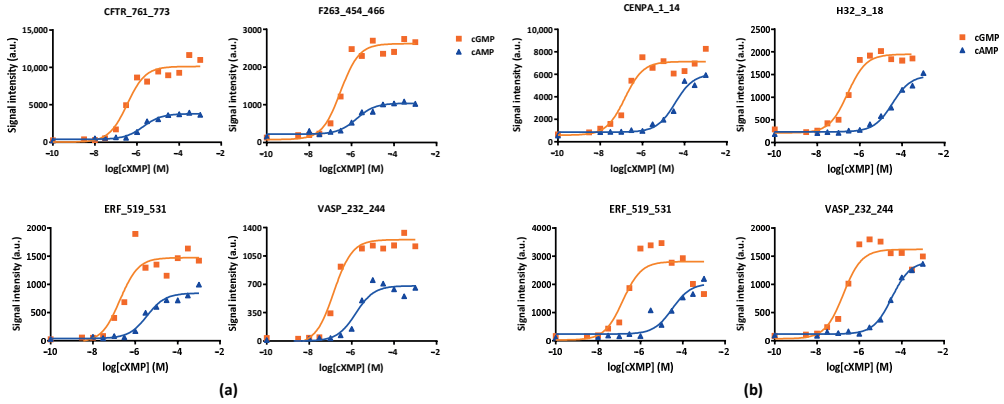

Figure 1. Effect of cGMP and cAMP concentrations on signal intensity of (**a**) PKG1 or (**b**) PKG2 on selected peptides. The signal intensity is the mean of triplicate measurements.

At saturating cGMP concentrations, the kinase activity increased about 30 times for PKG1 and 16 times for PKG2. Higher concentrations of cAMP were required to achieve a stimulation of activity. Maximal activity for cAMP-activated PKG1 was about half the value found with cGMP. For PKG2, the difference between the maximal activities with cGMP and cAMP was smaller (Fig. 1). Variation of cGMP and cAMP concentrations allowed the determination of the activation constants (Ka) for both PKG1 and PKG2 (Table 1). Ka values obtained for PKG1 (0.26 µM for cGMP and 22.4 µM for cAMP) were in good agreement with the data reported in the literature, but for PKG2, the measured Ka is higher than the reported values, which varied 20-fold for cGMP.

Table 1. Comparison of experimentally determined Ka values of cGMP and cAMP for PKG1 and PKG2 with literature values.

cXMP	PKG1 Ka (µM)		PKG2 Ka (µM)	
	Measured	Literature	Measured	Literature
cGMP	0.26	0.1–0.2 [20–24]	1.6	0.04–0.8 [20,24–26]
cAMP	22.4	7.6–39 [20,21]	27	~12 [20]

The response of PKGs to cGMP and cAMP also permits us to eliminate the effect of kinases that could be present as contaminants in the enzyme preparations. The activity of such kinases would not respond to the addition of these modulators. We excluded the peptides which already showed high signal intensity in the absence of cGMP or cAMP, with the signal either remaining constant or increasing further with elevated concentrations of cGMP or cAMP.

Effect of PKG Activator and Inhibitors on PKG Activity

To further classify the substrate preferences of PKG1 and PKG2, the effect of PKG activator 8-Br-cGMP, pan-PKG inhibitor Rp-8-pCPT-cGMPS (for both PKG1 and PKG2) and the PKG1 specific inhibitor Rp-8-Br-PET-cGMPS on the kinase activity was tested for three compound concentrations in the presence of cGMP. The modulation of PKG1 or PKG2 activity by these compounds is shown for the same four peptides (Fig. 2).

The addition of PKG activator resulted in a concentration-dependent increase in phosphorylation (Fig. 2a). The activator leads to a doubling of kinase activity for PKG1 and on average a 50% increase for PKG2. The effect was most prominent for the peptide ERF_519_531 (an ETS domain-containing transcription factor ERF). The addition of PKG1-specific inhibitor Rp-8-Br-PET-cGMP resulted in the inhibition of PKG1 kinase activity only, with no effect on PKG2 activity (Fig. 2b). On the other hand, the addition of pan-PKG inhibitor Rp-8-pCPT-cGMP resulted in a decrease in the kinase activity of both PKG1 and PKG2 for all four peptides (Fig. 2c). These data show that the PKG activity can be modified by the addition of PKG activity modulators and this change can be read out by phosphorylation changes on the peptides of the peptide microarray.

PKG1 and PKG2 Substrate Identification

First, peptides were selected for ATP-dependency—only those that showed a significant increase in signal upon addition of ATP at the highest concentrations of cGMP and cAMP were included in the analysis. Out of 142 peptides, 81 peptides showed statistically significant ($p \leq 0.05$) ATP-dependent phosphorylation by PKG1 and 92 by PKG2.

For substrate identification for the kinases, we devised a scoring system that included signal dependency on cGMP and cAMP concentration, phosphorylation induced by the PKG activator, and phosphorylation inhibited by PKG inhibitors (see Substrate Identification section of Materials and Methods and Supplementary Table S3 for assignment of scores). For PKG1, data for the specific PKG1 inhibitor, Rp-8-Br-PET-cGMPS were assessed and for PKG2, data for the pan-PKG inhibitor Rp-8-pCPT-cGMPs were used. The combined results obtained with the modulators amounted to a maximal value of ten and yielded a score indicating the preference of the kinases for each substrate. The substrates, their sequence, UniProt ID and scores for PKG1 and PKG2 are indicated in Table 2.

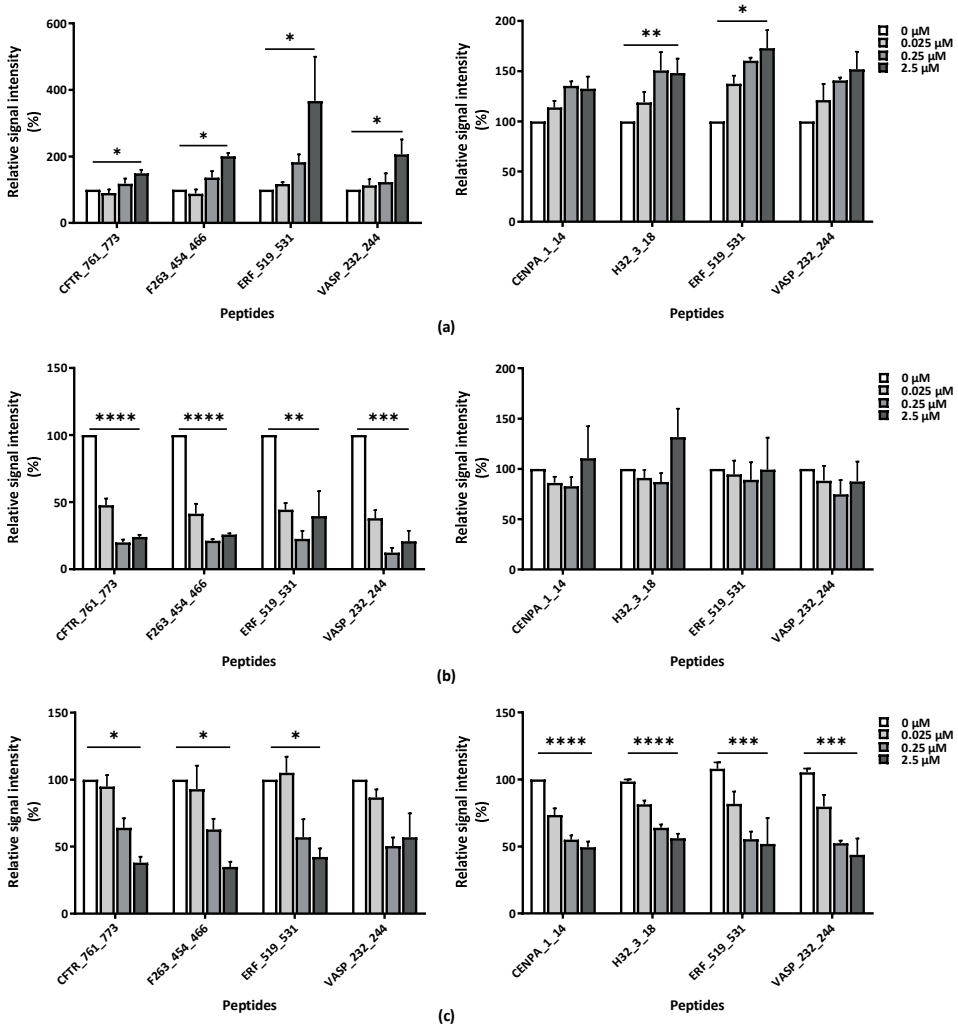

Figure 2. The effect of modulators on the activity of PKG1 (left) and PKG2 (right) for selected peptides: (**a**) PKG activator (8-Br-cGMP), (**b**) PKG1 Inhibitor (Rp-8-Br-PET-cGMPS), and (**c**) pan-PKG inhibitor (Rp-8-pCPT-cGMPS). The concentration of the modulators was varied as indicated in the legend in the presence of 0.2 µM cGMP. Relative signal intensity was measured in triplicate and expressed with respect to the condition without the modulator. The significant changes with modulators were determined with one-way ANOVA with significance indicated as * ($p \leq 0.05$), ** ($p \leq 0.01$), *** ($p \leq 0.001$) or **** ($p \leq 0.0001$).

Table 2. Peptide substrates for PKG1 and PKG2, their sequence, protein name, UniProtID and score. Scores for PKG1 and PKG2 range from 1 to 10. For sites already known to be phosphorylated by PKG1 or PKG2, the database containing this information is added. A—PhosphoSitePlus®, B—Human Protein Reference Database, C—UniProt. Color scheme according to the score—10–8: Good, 7–4: Intermediate and 3–0: Poor substrate.

Peptide ID	UniProt ID	Peptide Sequence	Description	PKG1 Score	PKG2 Score	Ref.
ERF_519_531	P50548	GEAGGPLTPRRVS	ETS domain-containing transcription factor ERF	10	9	
VASP_232_244	P50552	GAKLRKVSKQEEA	Vasodilator-stimulated phosphoprotein	10	8	A (PKG1)
CREB1_126_138	P16220	EILSRRPSYRKIL	cAMP response element-binding protein	10	6	A, B, C (PKG1)
CSF1R_701_713	P07333	NIHLEKKYVRRDS	Macrophage colony-stimulating factor 1 receptor precursor	10	7	
EPB42_241_253	P16452	LLNKRRGSVPILR	Erythrocyte membrane protein band 4.2	9	7	
GBRB2_427_439	P47870	SRLRRRASQLKIT	Gamma-aminobutyric acid receptor subunit beta-2 precursor	10	6	
GPSM2_394_406	P81274	PKLGRRHSMENME	G-protein-signaling modulator 2	10	7	
GRIK2_708_720	Q13002	FMSSRRQSVLVKS	Glutamate receptor, ionotropic kainate 2 precursor	10	4	
PDE5A_95_107	Q76074	GTPTRKISASEFD	cGMP-specific 3',5'-cyclic phosphodiesterase	10	6	
PTN12_32_44	Q05209	FMRLRRLSTKYRT	Tyrosine-protein phosphatase non-receptor type 12	10	5	
RS6_228_240	P62753	IAKRRRLSSLRAS	40S ribosomal protein S6	10	5	
RYR1_4317_4329	P21817	VRRLRRLTAREAA	Ryanodine receptor 1	9	5	
VTNC_390_402	P04004	NQNSRRPSRATWL	Vitronectin precursor	10	4	
CFTR_761_773	P13569	LQARRRQSVLNLM	Cystic fibrosis transmembrane conductance regulator	10	3	A, B (PKG1)
F263_454_466	Q16875	NPLMRRNSVTPLA	6-phosphofructo-2-kinase/fructose-2,6-biphosphatase 3	10	3	
KPB1_1011_1023	P46020	QVEFRRLSISAES	Phosphorylase b kinase regulatory subunit alpha, skeletal muscle isoform	9	3	
MYPC3_268_280	Q14896	LSAFRRTSLAGGG	Myosin-binding protein C, cardiac-type	10	4	
TY3H_65_77	P07101	FIGRRQSLIEDAR	Tyrosine 3-monooxygenase	9	3	
VASP_271_283	P50552	LARRRKATQVGEK	Vasodilator-stimulated phosphoprotein	8	3	A (PKG1)
ANXA1_209_221	P04083	AGERRKGTDVNVF	Annexin A1	7	9	
GPR6_349_361	P46095	QSKVPFRSRSPSE	Sphingosine 1-phosphate receptor GPR6	9	8	
KIF2C_105_118_S106G	Q99661	EGLRSRSTRMSTVS	Kinesin-like protein KIF2C	9	7	
ADDB_706_718	P35612	KKKFRTPSFLKKS	Beta-adducin	8	7	

Peptide ID	UniProt ID	Peptide Sequence	Description	PKG1 Score	PKG2 Score	Ref.
CAC1C_1974_1986	Q13936	ASLGRRASFHLEC	Voltage-dependent L-type calcium channel subunit α-1C	9	7	
KAP2_92_104	P13861	SRFNRRVSVCAET	cAMP-dependent protein kinase type II-alpha regulatory subunit	6	5	
KCNA2_442_454	P16389	PDLKKSRSASTIS	Potassium voltage-gated channel subfamily A member 2	9	7	
NCF1_296_308	P14598	RGAPPRRSSIRNA	Neutrophil cytosol factor 1	9	7	
MPIP1_172_184	P30304	FTQRQNSAPARML	M-phase inducer phosphatase 1	9	4	
ART_025_ CXGLRRWSLGGLRRWSL	Na	GLRRWSLGGLRRWSL	Peptide based on kemptide sequence	8	4	
CDN1A_139_151	P38936	GRKRRQTSMTDFY	Cyclin-dependent kinase inhibitor 1	6	3	
KCNA6_504_516	P17658	ANRERRPSYLPTP	Potassium voltage-gated channel subfamily A member 6	9	3	
ERBB2_679_691	P04626	QQKIRKYTMRRLL	Receptor tyrosine-protein kinase erbB-2 precursor	7	8	A (PKG2)
DESP_2842_2854	P15924	RSGSRRGSFDATG	Desmoplakin	8	7	
KCNA3_461_473	P22001	EELRKARSNSTLS	Potassium voltage-gated channel subfamily A member 3	8	7	
RAF1_253_265	P04049	QRQRSTSTPNVHM	RAF proto-oncogene serine/threonine-protein kinase	8	7	
RAP1B_172_184	P61224	PGKARKKSSCQLL	Ras-related protein Rap-1b precursor	7	7	
KAP3_107_119	P31323	NRFTRRASVCAEA	cAMP-dependent protein kinase type II-beta regulatory subunit	8	4	
TOP2A_1463_1475	P11388	RRKRKPSTSDDSD	DNA topoisomerase 2-alpha	6	5	
ADRB2_338_350	P07550	ELLCLRRSSLKAY	Beta-2 adrenergic receptor	8	4	
ANDR_785_797	P10275	VRMRHLSQEFGWL	Androgen receptor	6	4	
REL_260_272	Q04864	KMQLRRPSDQEVS	C-Rel proto-oncogene protein	6	4	
VASP_150_162	P50552	EHIERRVSNAGGP	Vasodilator-stimulated phosphoprotein	8	4	A (PKG1)
PTK6_436_448	Q13882	ALRERLSSFTSYE	Tyrosine-protein kinase 6	7	1	
KPCB_19_31_A25S	P05771	RFARKGSLRQKNV	Protein kinase C β	5	8	
PLM_76_88	O00168	EEGTFRSSIRRLS	Phospholemman precursor	7	7	
FRAP_2443_2455	P42345	RTRTDSYSAGQSV	FKBP12-rapamycin complex-associated protein (mTOR)	7	7	

Peptide ID	UniProt ID	Peptide Sequence	Description	PKG1 Score	PKG2 Score	Ref.
LIPS_944_956	Q05469	GFHPRRSSQGATQ	Hormone-sensitive lipase	7	7	A (PKG1)
PPR1A_28_40	Q13522	QIRRRRPTPATLV	Protein phosphatase 1 regulatory subunit 1A	4	7	
GYS2_1_13	P54840	MLRGRSLSVTSLG	Glycogen synthase, liver	5	4	
STK6_283_295	O14965	SSRRTTLCGTLDY	Serine/threonine-protein kinase 6 (Aurora A)	5	3	
PDPK1_27_39	O15530	SMVRTQTESSTPP	3-phosphoinositide-dependent protein kinase 1	3	9	
BAD_69_81	Q92934	IRSRHSSYPAGTE	Bcl2 antagonist of cell death	5	8	A (PKG1)
H2B1B_ 27_40	P33778	GKKRKRSRKESYSI	Histone H2B type 1-B	3	8	
NMDZ1_890_902	Q05586	SFKRRRSSKDTST	Glutamate [NMDA] receptor subunit zeta-1 precursor	4	8	
NOS3_1171_1183	P29474	SRIRTQSFSLQER	Nitric oxide synthase, endothelial	6	8	A (PKG1)
PLEK_106_118	P08567	GQKFARKSTRRSI	Pleckstrin	4	8	
H32_3_18	Q71DI3	RTKQTARKSTGGKAPR	Histone H3.2	4	9	
CENPA_1_14	P49450	MGPRRRSRKPEAPR	Histone H3-like centromeric protein A	3	7	
RBL2_655_667	Q08999	GLGRSITSPTTLY	Retinoblastoma-like protein 2	1	8	
KAPCG_192_206	P22612	VKGRTWTLCGTPEYL	cAMP-dependent protein kinase catalytic subunit γ	0	7	

We checked the Human Protein Reference Database (www.hprd.org), UniProt Knowledge base (www.uniprot.org), and PhosphoSitePlus® (www.phosphositeplus.org) for known PKG phosphorylation sites. Several peptides in Table 2 have already been reported as substrates for PKG1 and/or PKG2 such as VASP (S153, T278, S399), PDE5A_95_107 (cGMP-specific 3′, 5′-cyclic phosphodiesterase), RYR1_4317_4329 (ryanodine receptor 1), CFTR_761_773 (cystic fibrosis transmembrane conductance regulator), ERBB2_679_691 (receptor tyrosine kinase precursor), LIPS_944_956 (hormone-sensitive lipase) and BAD_69_81 (Bcl2 antagonist of cell death). In addition to these known substrates, novel PKG1 and PKG2 substrates were identified. PKG1 and PKG2 showed an overlap in substrate preference but also displayed differential preferences for substrates, as indicated by the scores. Fig. 1 and Fig. 2 show examples of good substrates for both PKG1 and PKG2 (ERF_519_531, VASP_232_244), substrates preferred by PKG1 (CFTR_761_773, F263_454_466) and substrates preferred by PKG2 (CENPA_1_14, H32_3_18).

The peptide sequences on PamChip® arrays can be present in more than one protein. Selection of only the UniProt ID of named peptide leads to loss of relevant biological information. To identify proteins that correspond to the peptides, the peptide sequences were blasted against the UniProt database of human proteins (see Materials and Methods,

Blast section). Only peptides with identical sequences (all amino acids identical) or similar sequences (having only conservative substitutions) were included (Table 3). Blasting yielded phosphosites with identical sequences in proteins such as the PKA subunits α and β proteins for KAPCG peptide, but also led to the identification of proteins with similar sequences, as for the PPR1A peptide. The threonine residue in this peptide was replaced by the serine residue in the protein phosphatase 1 regulatory subunit 1C.

Table 3. Extended list of proteins phosphorylated by PKG1 and or PKG2, (similarity = 1) after blasting of the peptides in Table 2.

Peptides on STK PamChip®			Hits after Blasting		
ID	UniProt ID	Sequence	Protein Name	UniProt ID	Sequence
KAPCG_192_206	P22612	VKGRTWTLCGTPEYL	cAMP-dependent protein kinase catalytic subunit α cAMP-dependent protein kinase catalytic subunit β	P17612 P22694	VKGRTWTLCGTPEYL VKGRTWTLCGTPEYL
KPCB_19_31_A25S	P05771	RFARKGSLRQKNV	Protein kinase C α type	P17252	RFARKGSLRQKNV
H32_3_18	Q71DI3	RTKQTARKSTGGKAPR	Histone H3.1 Histone H3.3 Histone H3.3C Histone H3.t	P68431 P84243 Q6NXT2 Q16695	RTKQTARKSTGGKAPR RTKQTARKSTGGKAPR RTKQTARKSTGGKAPR RTKQTARKSTGGKAPR
RAF1_253_265	P04049	QRQRSTSTPNVHM	Serine/Threonine-protein kinase A-Raf	P10398	QRIRSTSTPNVHM
PPR1A_28_40	Q13522	QIRRRRPTPATLV	Protein phosphatase 1 regulatory subunit 1C	Q8WVI7	QIRKRRPTPASLV
NCF1_296_308	P14598	RGAPPRRSSIRNA	Putative neutrophil cytosol factor 1C	A8MVU1	RGAPPRRSSIRNA
ADDB_706_718	P35612	KKKFRTPSFLKKS	α-adducin	P35611	KKKFRTPSFLKKS
RAP1B_172_184	P61224	PGKARKKSSCQLL	Ras-related protein Rap-1-b-like protein	A6NIZ1	PGKARKKSSCQLL
CREB1_126_138	P16220	EILSRRPSYRKIL	cAMP-responsive element modulator	Q03060	EILSRRPSYRKIL
DESP_2842_2854	P15924	RSGSRRGSFDATG	Plectin	Q15149	RAGSRRGSFDATG

Among the high scoring peptides identified, both PKG1 and PKG2 can phosphorylate the protein kinase PKCα and the regulatory subunit of protein kinase A (PKA). It was interesting to find that PKG2 but not PKG1, is able to phosphorylate the catalytic subunit of PKA, notably T198 in the PKA activation loop. This residue is conserved in the PKA α, β and γ catalytic subunits (www.phosphosite.org). PKG2 is also able to phosphorylate histones which play a prominent role in DNA repair and chromosomal stability [27]. On the other hand, PKG1 targets the serine/threonine-protein kinase A-Raf which regulates the mTOR signaling cascade, which is activated in tumors, insulin activation and in many other cellular processes [28]. mTOR (also known as FRAP) itself can be phosphorylated by both PKG1 and PKG2 on S2448, a site known to be phosphorylated by AKT1 and p70S6K (www.phosphosite.org).

As an additional check for the substrate quality, substrate motifs for PKG1 and PKG2 were determined (Supplementary Fig. S2). PKG1 showed a preference for substrates containing an R/K-R/K-X-S/T- motif. The R/K-R/K-X-S/T motif is also common to other members of the AGC kinase family, such as PKA [19]. PKG2 showed a preference for peptides with more positively charged amino acids at the N-terminal side, reflected in a G/R/K-X-K/G/R-X-R/K-R/K-X-S/T motif.

These experiments show that PKG1 and PKG2 respond differently to the addition of modulators with an increase or decrease in signal intensity. Furthermore, PKG1 and PKG2 have different substrate preference, which can be used to distinguish the two enzymes in a lysate, which is a complex mixture of many kinases. Knowledge of PKG1 and PKG2 substrates, in combination with their response to the modulators was used further to study the activity of PKGs in the retinal murine cell line 661W. 661W immortalized cone photoreceptor precursor cells are derived from the retinal tumor of a mouse expressing SV40 T antigen under the control of a photoreceptor specific promoter [29] and have been used as a cell model for retinal ciliopathies such as retinitis pigmentosa [17,18]. The role of PKG1 and PKG2 in retinal degeneration has not been elucidated yet.

Modulation of Kinase Activity in Retinal 661W Cells

Effect of Modulators on Kinase Activity in 661W Cells

To study the effect of elevated cGMP on endogenous PKG1 and PKG2 activity and its downstream effects, we investigated PKG activity in the photoreceptor cell line, 661W. Cells were grown and lysed as described in Materials and Methods. The addition of modulators to a lysate *ex vivo* in an on-chip assay is expected to assess the effect on endogenous PKG1 and PKG2 activity and determine their contribution to kinase activity in the lysate.

We first compared the kinase profile of 661W cell lysate with those of the recombinant PKGs at 100 µM cGMP, as is visualized in a scatter plot (Fig. 3a, 3b). The correlation coefficient between the kinase activity profile of the cells and recombinant PKG1 and PKG2 was 0.75 and 0.71, respectively. This is a relatively low correlation and it suggests a prominent role for kinases other than only the PKG family in the cells.

The kinase activity in the cells was analyzed as function of the concentration of cGMP and cAMP, resulting in increased phosphorylation signal intensities on many peptides. The kinases in the lysate showed a stronger response to cAMP than to cGMP. Relative increases in phosphorylation signal intensities for three peptides with the highest signals in 661W cells at 1 µM concentration of cGMP or cAMP are shown in Fig. 3c, as well as for VASP_150_162. The peptide VASP_150_162 is one of the three VASP peptides that is phosphorylated by PKGs and frequently used as a read out for PKG activity in studies on retinal degeneration [9]. The peptide phosphorylation increased at lower concentrations of cAMP than of cGMP. The Ka of cGMP in the 661W cell lysate was found to be around 10 µM for peptides that responded to these compounds, as is illustrated with the peptide VASP_150_162 in Fig. 3d. For recombinant PKG1 and PKG2, the Ka was 0.2 and 1.6 µM, respectively (Table 1). For cAMP, the Ka in cell lysate was around 0.1 µM (Fig. 3e), whereas for recombinant PKG1 and PKG2, Ka values of 7.6 and 39 µM, respectively, were found (Table 1). These results indicate that the kinase activity in the cell lysate was more responsive to cAMP than to

cGMP. Addition of increasing concentrations of PKG activator resulted in increased kinase activity starting from 0.1 µM with a Ka of about 2.6 µM (Fig. 3f). The value of PKG activator reported to activate PKGs is between 0.01 and 1 µM [20], much lower than the value found in the 661W cell lysate. The addition of PKG inhibitors (PKG1 specific and pan–PKG) at concentrations where recombinant PKG1 and/or PKG2 activity was strongly inhibited did not lead to statistically significant inhibition of the kinase activity in the 661W lysate on any of the peptides on the array.

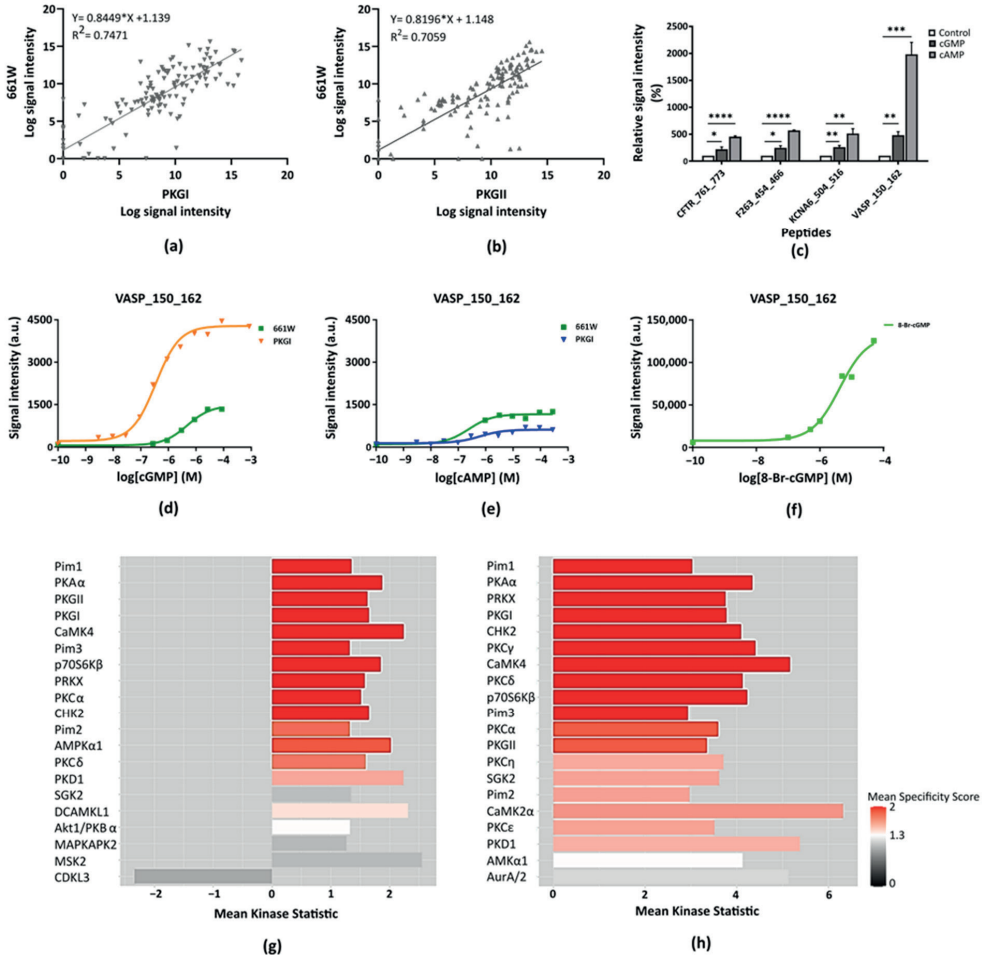

Figure 3. (**a**,**b**) Scatter plot of signal intensities of 661W cell lysate and the recombinant kinases PKG1 (**a**) and PKG2 (**b**) at 100 µM cGMP. (**c**) Modulation of kinase activity by 1 µM cGMP and cAMP in 661W cell lysate for selected peptides. Relative signal intensity was measured in triplicate and expressed with respect to the condition without the modulator. The significance of changes with cGMP and cAMPs was determined by Unpaired *T*-test with significance indicated as * ($p \leq 0.05$), ** ($p \leq 0.01$) and *** ($p \leq 0.001$), **** ($p \leq 0.0001$). (**d**,**e**) Modulation of phosphorylation of the peptide VASP_150_162 for recombinant PKG1 and 661W cell lysate with an increase in cGMP (**d**) and cAMP (**e**) concentrations. The relative signal intensity of VASP_150_162 is plotted against log concentration of cGMP (left) or cAMP (right). Data points are the mean of three replicates. (**f**) Modulation of kinase activity for peptide VASP_150_162 in 661W cell lysate with increasing concentrations of PKG Activator 8-Br-cGMP (n = 1). (**g**,**h**) Kinases predicted by upstream kinase analysis to be activated in 661Wcells at 1 µM cGMP (**g**) or cAMP (**h**).

Not PKG but PKA Is Modulated in 661W Cells

Since the concentrations of cGMP, cAMP, and PKG activator where modulation of kinase activity in 661W lysate is observed are not in line with the concentrations required to activate recombinant PKG and the inhibitors have no effect on signal intensity, this may indicate that a different (or additional) cyclic nucleotide binding kinase is activated in the cells. Therefore, to assess the type of kinases differentially activated in the cells, upstream kinase analysis was performed comparing cell lysate with and without cGMP or cAMP. In the upstream kinase analysis, the kinases most likely to be able to phosphorylate the peptide sequences on the array are identified (see Materials and Methods section). The kinases hypothesized to be activated in cGMP and cAMP condition in 661W cells in comparison with untreated control are shown in Fig. 3g, 3h. In both analyses, Pim1 ranked highest. Although this kinase is able to phosphorylate many peptides, it does not respond to cyclic nucleotides, and therefore was excluded. Among the cyclic nucleotide binding kinases, the upstream kinase analysis suggested the kinases PKA, PKG1 and PKG2 as most likely affected in both cGMP and cAMP conditions. A possible activation of PKA is substantiated by the fact that the Ka values of cGMP, cAMP, and PKG activator obtained in 661W lysate match those reported for PKA activation [20].

To check the hypothesis that PKA rather than PKG is activated in 661W cells with the addition of PKG activity modulators, we first performed a substrate identification for the recombinant PKA catalytic subunit α on the STK PamChip®. This was done both in the presence and absence of PKA inhibitor peptide (PKAi). The substrates were identified on the basis of their activation and inhibition in the presence of ATP and PKAi, respectively. The set of PKA substrates showed a big overlap with the PKG substrates (Supplementary Table S2). All peptides shown in Fig. 3c were found to be good PKA substrates, and also VASP_150_162. To investigate whether PKA is active in the 661W lysate, we added the PKAi to the cell lysate supplemented with cGMP or cAMP. The addition of PKAi to the lysate decreased phosphorylation of the PKA substrates when compared with the control (lysate without PKA inhibitor) (Fig. 4a, 4b). However, the addition of PKAi did not result in significant inhibition of the signal intensity on peptides ERF_519_531 and H32_3_18, which are not PKA substrates.

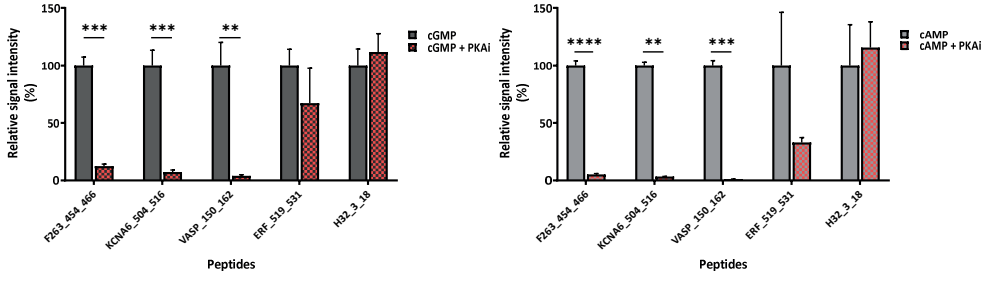

Figure 4. Phosphorylation of selected peptides by 661W cell lysate in the presence of either (**a**) cGMP (10 µM) or (**b**) cAMP (0.1 µM) with and without PKAi (1 µM). The significance of changes in cGMP and cAMPs was determined by unpaired T-tests with significance indicated as * ($p \leq 0.05$), ** ($p \leq 0.01$), *** ($p \leq 0.001$) and **** ($p \leq 0.0001$).

We also checked the possibility that PKAi inhibits PKG1 and PKG2 activity by incubating the recombinant PKGs with 1 μM PKAi. Neither PKG1 nor PKG2 were inhibited by PKAi (Supplementary Fig. S3). We checked the effect of the modulators on the peptide VASP_232_244, ERF_519_531 and H32_3_18 that are good substrates for PKG1 and or PKG2 (Table 2). The peptide VASP_232_244 had no signal in 661W lysates, and addition of modulators did not have any effect. These data too are in agreement with a low activity of PKG1 and PKG2 in the 661W lysate. However, phosphorylation signals are present on the peptides ERF_519_531 and H32_3_18. Since PKG activity is low in the 661W lysate, the phosphorylation of these peptide must be due to activity of other kinases. S10 site of H32 is also known to be phosphorylated by AuroraA (www.uniprot.org).

The Ka values for cGMP, cAMP and 8-Br-cGMP and the lack of inhibition by PKG inhibitors, in addition to the strong inhibitory effect by PKAi, confirm that PKA is present at high concentrations in 661W cells.

Discussion

The genetic heterogeneity in the IRD group of diseases severely limits the development of mutation-specific treatments [2]. Therefore, it is imperative to identify targets where several disease-associated pathways convene for the design of treatments addressing an extended group of IRD patients. PKG has emerged as a promising target for the treatment of IRDs as its inhibition leads to photoreceptor preservation [8,9]. Therefore, identification of PKG substrates and their downstream signaling pathways in photoreceptors might help to find generic, new targets for the treatment of IRDs. More insight on the effect of PKG modulators on PKGs will not only be beneficial in IRDs but also for cancer research, as PKG activators have been shown to reduce cell proliferation, activate cell death and limit cell invasion in different cancer cell models [11–16].

Here, we identified novel substrates for PKG1 and PKG2 in a multiplex assay using a peptide microarray, which allowed investigation of the phosphorylation of the 142 peptides present on one array. The substrates for PKG1 and PKG2 were selected on the basis of a series of strict criteria: response to ATP, cGMP, cAMP, PKG activator and inhibitors, as assessed by statistical analysis, quality of the fit for cAMP and cGMP, and effect size and direction for the activators and inhibitors. Peptides were scored for each criterion. This approach resulted in the confirmation of several known PKG substrates such as VASP (S153, T278, S399), CREB, PDE5A, CFTR (see Table 2) for PKG1 and PKG2 and identification of novel substrates, that, to the best of our knowledge, have not been described before. We identified good substrates for PKG1 and PKG2 (e.g., VASP_232_244, ERF_519_531, GPR6_349_361) and substrates preferred by either one of the kinases (e.g., CFTR_761_773, F263_454_466 for PKG1, and H32_3_18 and RBL2_655_667 for PKG2) (Table 2). Data obtained on the peptide micro-array confirmed the Ka values for cGMP and cAMP reported for the two enzymes. Comparison of PKG substrates with substrates for PKA revealed also differences in substrate preference between the PKG's and PKA. The response to cyclic nucleotides, 8-Br-cGMP, and PKG inhibitors is also different for the PKGs and PKA [20]. Furthermore, we confirmed that PKAi is a nM inhibitor for PKA, and showed that it does not inhibit PKG1 and PKG2 at μM

concentrations. These compounds, in combination with a peptide microarray were shown to be valuable tools to distinguish PKG1 and PKG2 from PKA activity in a complex environment like a cell lysate.

Role of PKG Activation in Retinal Cells

In the 661W cell lysate, a multitude of kinases are present. Peptides on the microarray can be phosphorylated by many serine-threonine kinases, which makes elucidation of the role of PKG complicated. To overcome this limitation, we decided to make use of specific PKG1 or PKG2 modulators that can be added to the cell lysate, to activate or inhibit the protein kinase G family. In 661W retinal cell lysate, addition of both cGMP and cAMP resulted in an increase in the overall kinase activity (Fig. 3c). As compared to studies using purified, recombinant PKGs, a higher cGMP concentration was required in the cell lysate to activate these kinases. The Ka of cGMP in the cell lysate was determined to be around 10 μM, which is close to the Ka for cGMP reported for the PKA family [20]. The Ka for cAMP in the cell lysate was reached at a much lower concentration level, i.e. 0.1 μM, but, again, this is also closer to the cAMP concentration required to activate PKA [20, 21]. Activation by 8-Br-cGMP also occurred at a concentration more likely to activate PKA than PKGs [20]. Furthermore, we found that PKG inhibitors did not significantly change kinase activity of the lysates, whereas the addition of a PKA inhibitor resulted in a pronounced inhibitory effect of the kinase activity on the peptide micro array. From the recombinant PKGs study, the three VASP peptides on PamChip® were found to be substrates for PKG1 and PKG2. VASP_232_244, which is not phosphorylated by PKA but is phosphorylated by PKGs, had a very low signal intensity in the lysate. These observations suggest that with the addition of PKG modulators in the cell lysate, PKA activity is affected. These experimental data indicate that the main body of PKA in 661W lysate is present in an inactive form, and it becomes activated by the addition of kinase modulators. Gene expression studies show that a high concentration of PKA catalytic subunit α is present in 661W cells [17]. Our experimental data suggest that PKG is present at a low concentration in the cell lysate, because it is hardly activated or inhibited by these modulators, or at least is effectively shielded (and thus not exposed) to these modulators. Previous studies reported that both PKG1 and PKG2 are present in the 661W cells [30] and the gene expression analysis of the cone receptor cells has shown a high expression of PKG2 [17]. The expression of PKA catalytic subunit β and PKG1 is low in this cell line [17]. Our experiments indicate that PKG activity in 661W can only be modulated to a limited extent, whereas PKA activity responds highly to all PKG modulators tested. This may prompt us to reconsider the role of PKA in retinal degeneration and in future research investigate putative interactions between PKA and PKG.

PKG inhibitors and knockdown of PKG have been shown to delay retinal degeneration and therewith indicate a clear role for PKG. The role for PKG in retinal degeneration is based on its high affinity for cGMP. However, our data show that PKA can also be activated by cGMP, albeit at higher concentrations, in the range of those needed to open CNG channels [31]. Evidence for involvement of PKG comes from quite a number of studies. In RD mouse models, Paquet-Durand et al. showed, using immunofluorescence, co-localization of cGMP and PKG, inferring a role for PKG in retinal degeneration [8]. Phosphorylation of VASP at S238 is used as read out for PKG activity in several murine RP model-based studies [8,9].

However, our cell line studies revealed that the addition of PKG modulators can also affect the activity of PKA. Substrate identification showed that PKG2 (Table 3), and not PKG1, is able to activate PKA catalytic subunits α, β, and γ by phosphorylating T198 in the activation loop, which is conserved in all three PKA subunits. It has also been shown that PKG phosphorylates PKA regulatory subunit I α, which activates PKA in eukaryotic cells [32]. The addition of PKAi to the cell lysate confirms the interrelationship between PKG and PKA and the key function of PKA. Therefore, the cross talk between PKG and PKA, *i.e.*, PKG is activated by cGMP and activates PKA, might provide a plausible explanation for the predominant effect of PKA via the cGMP axis. In such an environment, the conventional route of PKA activation through the cAMP stimulus might be bypassed by the cGMP route. Based on our novel finding revealing the prominent PKA activity, the interplay of PKG and PKA axis in retina cells should be taken into account when studying the molecular events during retinal degeneration, and optimized conditions where PKA is not activated should be considered.

Conclusion

PKG has emerged as a crucial target to design treatment for a highly heterogeneous group of IRDs. Here, we used peptide microarrays with PKG modulators for high throughput substrate identification of PKG1 and PKG2. We were able to determine substrates specific for each kinase, and found a large overlap between substrates for both PKGs. We also showed that these modulators stimulate PKA activity in retinal cells.

Materials and Methods

Materials: PKG1α (full length human recombinant protein type α) was obtained from Millipore and PKG2 (full length human recombinant protein) was obtained from Thermo Fischer Scientific. PKA catalytic subunit alpha and PKA inhibitor peptide (PKAi) were from Merck. PKG activator (8-Br-cGMP) and PKG inhibitors (Rp-8-Br-PET-cGMPS, Rp-8-pCPT-cGMPS) were provided by BIOLOG Life Science Institute (Bremen, Germany). cGMP and cAMP sodium salts were purchased from Sigma-Aldrich. The immortalized murine retinal photoreceptor precursor cells 661W [31,32] were generously provided by Dr. Muayyad Al-Ubaidi (University of Houston, Houston, Texas, USA). Dulbecco's modified Eagle medium (DMEM), fetal bovine serum (FBS), penicillin, and streptomycin were purchased from Gibco. Mammalian protein extraction reagent (M-PER™) buffer, Halt™ protease and phosphatase inhibitor cocktails and the Coomassie Plus (Bradford) assay kit were purchased from Thermo Fischer Scientific.

Cell Culture and Lysis: 661W cells were cultured in DMEM supplemented with 10% FBS, 100 U/mL penicillin, and 100 μg/mL streptomycin. The cells were maintained at 37 °C in a humidified atmosphere of 5% CO_2. At 80% confluency (passage number 19), the medium was removed and cells were washed with ice cold PBS. The cells were lysed with lysis buffer (MPER with 1:100 phosphatase inhibitor cocktail and protease inhibitor cocktail) for 15 min on ice. The lysate was centrifuged at 16,000× g for 15 min at 4 °C. The supernatant was

immediately aliquoted, flash-frozen, and stored at −80 °C. The protein content of the lysate was determined using the Bradford Protein Assay [33].

Kinase Activity Measurements: Kinase activity of recombinant kinases and cell lysates was determined on STK PamChip® arrays (product # 87,102), each comprising 142 peptides derived from human proteins, according to the instructions of the manufacturer (PamGene International B.V., 's-Hertogenbosch, North Brabant, The Netherlands). An antibody mix detects the phosphorylated Ser/Thr amino acid residues, which is confirmed by addition of FITC-conjugated secondary antibody [19].

The assay mix consisted of protein kinase buffer (PamGene International BV. 's-Hertogenbosch, North Brabant, The Netherlands), 0.01% BSA, STK primary antibody mix and recombinant protein or lysate. The protein amount used in the assays was 0.5 ng/array for PKG1, 5ng/array for PKG2, 1 ng/array for PKA and 0.5 µg/array for 661W cell lysate, unless indicated otherwise. The cyclic nucleotide concentration range varied from 3.3 nM to 1 mM for cGMP or to 3.3 mM for cAMP. For PKG activator or inhibitors, a concentration range from 0.025 to 2.5 µM was used [20]. The effect of PKG activator or inhibitors was tested in the presence of 0.2 µM cGMP. In all experiments, 400 µM ATP was present. A total assay volume of 40 µL was applied per array.

Instrumentation: All experiments were performed in triplicate on a PamStation® on which up to 96 assays can be performed simultaneously (PamGene International B.V., 's-Hertogenbosch, North Brabant, The Netherlands). To prevent aspecific binding to the arrays, the PamChips® were blocked with 2% BSA by pumping it up and down 30 times through the array. The chips were then washed 3 times with Protein Kinase buffer and assay mix was applied. The assay mix was pumped up and down the arrays for 60 min. The arrays were washed 3 times and the detection mix comprising of FITC labeled secondary antibody was applied on the PamChips®. The signals were recorded at multiple exposure times by a CCD camera [34].

Data Analysis: Signals on all peptides at all exposure times were quantified by BioNavigator® software version 6.3.67.0 (PamGene International B.V., 's-Hertogenbosch, North Brabant, The Netherlands). For each peptide on the array, the software calculates a single value for images obtained at multiple exposure times (exposure time scaling) [34]. Statistical methods such as T-tests and one-way ANOVA were used to compare two or more groups. Bionavigator® software was used for data visualization and statistical analysis. The graphs were made with GraphPad Prism 9 software (GraphPad Software, San Diego, California, USA).

To identify kinases that are able to phosphorylate the peptide sequences on the array, upstream kinase analysis was performed [34]. The phosphorylation changes between two groups were compared and linked to kinases known to phosphorylate these sites (upstream kinases). The knowledge base is compiled from experimental data from several databases and theoretical interactions (PhosphoNet). The result provides a list of kinases that might be differentially active.

Blast: Peptide sequences were blasted in UniProt against human proteins using the PAM30 substitution matrix [35]. Similarity was defined as the ratio of the PAM30 score for a retrieved sequence and the original sequence. Peptides with a similarity score equal to 1 were included.

Substrate Identification: Results obtained in experiments with the different modulators were assessed using a scoring system for each experiment. The 142 peptides were first scored on the basis of statistically significant ($p \leq 0.05$) ATP-dependent phosphorylation by PKG1 or PKG2 in the presence of cGMP. In the next step, the peptides were scored for a statistically significant increase in phosphorylation by PKG1 or PKG2 with increasing cGMP or cAMP concentration ($p \leq 0.05$ between lowest and highest concentrations). The quality of the fit ($R^2 > 0.8$) for cAMP and cGMP for each peptide was also included in the scoring. Next, the peptides were scored for statistically significant activation or inhibition in response to PKG activator or PKG inhibitors, respectively. Noise on signals was eliminated by checking for the expected direction of change and size of the fold change. To identify the best substrates for PKG1 and PKG2, all scores were combined in one value. Based on the score, the peptides were classified as good, intermediate, or poor substrates for PKG1 and or PKG2 (see Table S3).

Substrate Motifs: Seq2Logo 2.0 was used to generate substrate motifs based on the sequences listed in Table 2. For this purpose, the peptide sequences from Table 2 were aligned relative to the target Ser residue and only residues from position −5 to +5 were considered. To account for differences in signal intensity, a weight corresponding to the relative signal intensity was applied when entering sequences into the program.

Author contribution

Conceptualization and methodology—A.R., R.H. and J.G.; formal analysis and data curation—A.R. and R.H.; writing, original draft preparation—A.R.; review and editing—A.R., R.H., J.G., T.T., V.M.; supervision—J.G. and R.H.; resources, project administration and funding acquisition—J.G. All authors have read and agreed to the published version of the manuscript.

Conflict of interests

A.R., J.G. and T.T. are currently employed and R.H is a previous employee of PamGene International B.V. The authors declare no conflict of interest.

Funding

This research was funded by European Union Horizon 2020 Research and Innovation Programme—*trans*Med under the Marie Curie grant agreement No. 765441 (*trans*Med; H2020-MSCA-765441).

References

1. **Retinal Information Network (RetNet). Available online: https://sph.uth.edu/retnet** (accessed on 18 November 2020).
2. Tolone A, Belhadj S, Rentsch A, Schwede F, Paquet-Durand F: **The cGMP pathway and inherited photoreceptor degeneration: Targets, compounds, and biomarkers**. *Genes* 2019, **10**:1–16.
3. Zhang X, Cote RH: **cGMP signaling in vertebrate retinal photoreceptor cells.** *Front Biosci* 2005, **10**:1191–1204.
4. Lolley RN, Farber DB, Rayborn ME, Hollyfield JG: **Cyclic gmp accumulation causes degeneration of photoreceptor cells: Simulation of an inherited disease**. *Science (80-)* 1977, **196**:664–666.
5. Farber DB, Lolley RN: **Cyclic guanosine monophosphate: Elevation in degenerating photoreceptor cells of the C3H mouse retina**. *Science (80-)* 1974, **186**:449–451.
6. Power M, Das S, Schütze K, Marigo V, Ekström P, Paquet-Durand F: **Cellular mechanisms of hereditary photoreceptor degeneration – Focus on cGMP**. *Prog Retin Eye Res* 2020, **74**:100772.
7. Hofmann F, Feil R, Kleppisch T, Schlossmann J: **Function of cGMP-dependent protein kinases as revealed by gene deletion**. *Physiol Rev* 2006, **86**:1–23.
8. Paquet-Durand F, Hauck SM, Veen T Van, Ueffing M, Ekström P: **PKG activity causes photoreceptor cell death in two retinitis pigmentosa models**. *J Neurochem* 2009, **108**:796–810.
9. Vighi E, Trifunovic D, Veiga-Crespo P, Rentsch A, Hoffmann D, Sahaboglu A, Strasser T, Kulkarni M, Bertolotti E, Heuvel A Van Den, et al.: **Combination of cGMP analogue and drug delivery system provides functional protection in hereditary retinal degeneration**. *Proc Natl Acad Sci U S A* 2018, **115**:E2997–E3006.
10. Wang T, Tsang SH, Chen J: **Two pathways of rod photoreceptor cell death induced by elevated cGMP**. *Hum Mol Genet* 2017, **26**:2299–2306.
11. Hoffmann D, Rentsch A, Vighi E, Bertolotti E, Comitato A, Schwede F, Genieser HG, Marigo V: **New dimeric cGMP analogues reduce proliferation in three colon cancer cell lines**. *Eur J Med Chem* 2017, **141**:61–72.
12. Browning DD: **Protein kinase G as a therapeutic target for the treatment of metastatic colorectal cancer**. *Expert Opin Ther Targets* 2008, **12**:367–376.
13. Deguchi A, Thompson WJ, Weinstein IB: **Activation of protein kinase G is sufficient to induce apoptosis and inhibit cell migration in colon cancer cells**. *Cancer Res* 2004, **64**:3966–3973.
14. Fallahian F, Karami-Tehrani F, Salami S, Aghaei M: **Cyclic GMP induced apoptosis via protein kinase G in oestrogen receptor-positive and -negative breast cancer cell lines**. *FEBS J* 2011, **278**:3360–3369.
15. Leung EL, Wong JC, Johlfs MG, Tsang BK, Fiscus RR: **Protein kinase G type Iα activity in human ovarian cancer cells significantly contributes to enhanced Src activation and DNA synthesis/cell proliferation**. *Mol Cancer Res* 2010, **8**:578–591.
16. Vighi E, Rentsch A, Henning P, Comitato A, Hoffmann D, Bertinetti D, Bertolotti E, Schwede F, Herberg FW, Genieser HG, et al.: **New cGMP analogues restrain proliferation and migration of melanoma cells**. *Oncotarget* 2018, **9**:5301.
17. Wheway G, Nazlamova L, Turner D, Cross S: **661W photoreceptor cell line as a cell model for studying retinal ciliopathies**. *Front Genet* 2019, **10**:308.
18. Comitato A, Subramanian P, Turchiano G, Montanari M, Becerra SP, Marigo V: **Pigment epithelium-derived factor hinders photoreceptor cell death by reducing intracellular calcium in the degenerating retina**. *Cell Death Dis* 2018, **9**:1–13.

19. Hilhorst R, Houkes L, Mommersteeg M, Musch J, Van Den Berg A, Ruijtenbeek R: **Peptide microarrays for profiling of serine/threonine kinase activity of recombinant kinases and lysates of cells and tissue samples**. *Methods Mol Biol* 2013, **977**:259–271.
20. Poppe H, Rybalkin SD, Rehmann H, Hinds TR, Tang XB, Christensen AE, Schwede F, Genieser HG, Bos JL, Doskeland SO, et al.: **Cyclic nucleotide analogs as probes of signaling pathways [1]**. *Nat Methods* 2008, **5**:277–278.
21. Lorenz R, Bertinetti D, Herberg FW: **cAMP-dependent protein kinase and cGMP-dependent protein kinase as cyclic nucleotide effectors**. In *Non-canonical cyclic nucleotides*. . 2015:105–122.
22. Kim JJ, Lorenz R, Arold ST, Reger AS, Sankaran B, Casteel DE, Herberg FW, Kim C: **Crystal Structure of PKG I:cGMP Complex Reveals a cGMP-Mediated Dimeric Interface that Facilitates cGMP-Induced Activation**. *Structure* 2016, **24**:710–720.
23. Francis SH, Poteet-Smith C, Busch JL, Richie-Jannetta R, Corbin JD: **Mechanisms of autoinhibition in cyclic nucleotide-dependent protein kinases.** *Front Biosci* 2002, **7**:580–592.
24. Francis SH, Blount MA, Zoraghi R, Corbin JD: **Molecular properties of mammalian proteins that interact with cGMP: Protein kinases, cation channels, phosphodiesterases, and multi-drug anion transporters**. *Front Biosci* 2005, **10**:2097–2117.
25. Campbell JC, Kim JJ, Li KY, Huang GY, Reger AS, Matsuda S, Sankaran B, Link TM, Yuasa K, Ladbury JE, et al.: **Structural basis of cyclic nucleotide selectivity in cGMP-dependent Protein Kinase II**. *J Biol Chem* 2016, **291**:5623–5633.
26. Pöhler D, Butt E, Meißner J, Müller S, Lohse M, Walter U, Lohmann SM, Jarchau T: **Expression, purification, and characterization of the cGMP-dependent protein kinases Iβ and II using the baculovirus system**. *FEBS Lett* 1995, **374**:419–425.
27. Williamson EA, Wray JW, Bansal P, Hromas R: **Overview for the histone codes for DNA repair**. In *Progress in Molecular Biology and Translational Science*. . 2012:207–227.
28. Laplante M, Sabatini DM: **mTOR signaling at a glance**. *J Cell Sci* 2009, **122**:3589–3594.
29. Tan E, Ding XQ, Saadi A, Agarwal N, Naash MI, Al-Ubaidi MR: **Expression of cone-photoreceptor-specific antigens in a cell line derived from retinal tumors in transgenic mice**. *Investig Ophthalmol Vis Sci* 2004, **45**:764–768.
30. Mencl S, Trifunović D, Zrenner E, Paquet-Durand F: **PKG-dependent cell death in 661W cone photoreceptor-like cell cultures (experimental study)**. In *Retinal Degenerative Diseases*. . 2018:511–517.
31. Lincoln TM, Cornwell TL: **Intracellular cyclic GMP receptor proteins**. *FASEB J* 1993, **7**:328–338.
32. Haushalter KJ, Casteel DE, Raffeiner A, Stefan E, Patel HH, Taylor SS: **Phosphorylation of protein kinase a (PKA) regulatory subunit RI by protein kinase g (PKG) primes PKA for catalytic activity in cells**. *J Biol Chem* 2018, **293**:4411–4421.
33. Zor T, Selinger Z: **Linearization of the Bradford protein assay increases its sensitivity: Theoretical and experimental studies**. *Anal Biochem* 1996, **236**:302–308.
34. Chirumamilla CS, Fazil MHUT, Perez-Novo C, Rangarajan S, de Wijn R, Ramireddy P, Verma NK, Vanden Berghe W: **Profiling activity of cellular kinases in migrating T-cells**. *Methods Mol Biol* 2019, **1930**:99–113.
35. Pearson WR: **Selecting the right similarity-scoring matrix**. *Curr Protoc Bioinforma* 2013, **43**:3–5.

Supplementary Materials

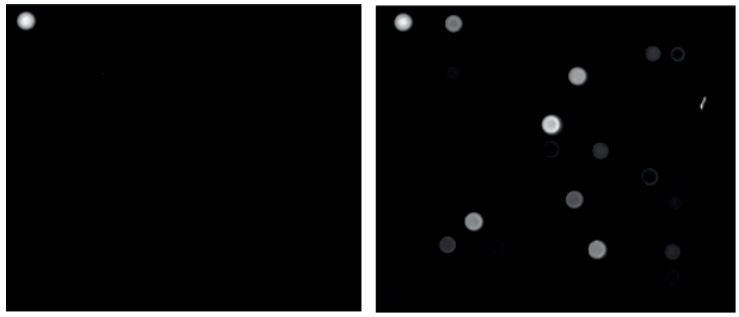

Fig. S1- Phosphorylation of peptide microarray by PKG1 as function of ATP and cGMP. ATP (0μM, left and 400 μM, right) and cGMP (0 μM, left and 400 μM, right)

Table S1- Relative signal intensity of peptide substrates as function of enzyme (PKG1 or PKG2) concentration

PKG1 (ng/array)	F263_454_466	VASP_232_244
0.5	100	100
1	170	217
2.5	275	282
5	297	323

PKG2 (ng/array)	F263_454_466	VASP_232_244
5	100	100
10	186	122
20	321	141
30	134	75

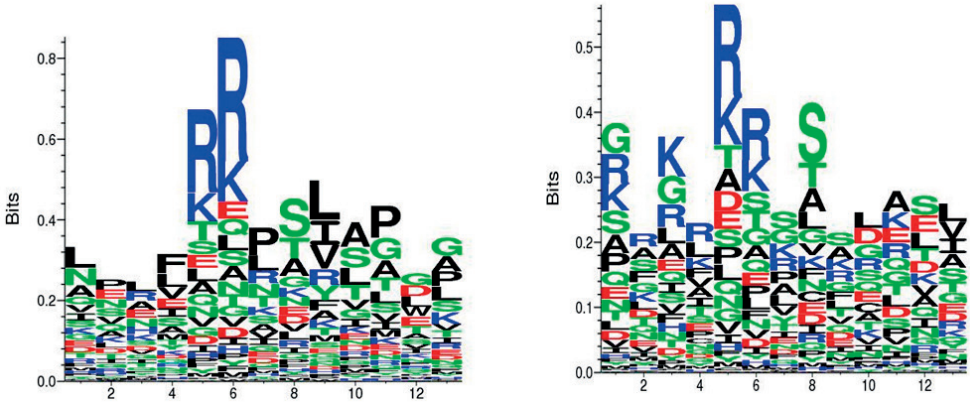

Fig. S2- Substrate Logo of PKG1 (left) and PKG2 (right)

Table S2: List of PKA substrates

Peptides	PKA Relative Signal Intensity
CFTR_761_773	100
F263_454_466	63
KCNA6_504_516	51
GBRB2_427_439	46
MYPC3_268_280	43
GRIK2_708_720	41
KAP3_107_119	36
TOP2A_1463_1475	29
VTNC_390_402	27
TY3H_65_77	26
STK6_283_295	20
CFTR_730_742	18
NCF1_296_308	17
CDN1A_139_151	16
RS6_228_240	16
SCN7A_898_910	16
CAC1C_1974_1986	15
PTN12_32_44	14
KAP2_92_104	13
KPB1_1011_1023	13
VASP_150_162	12
ADRB2_338_350	10

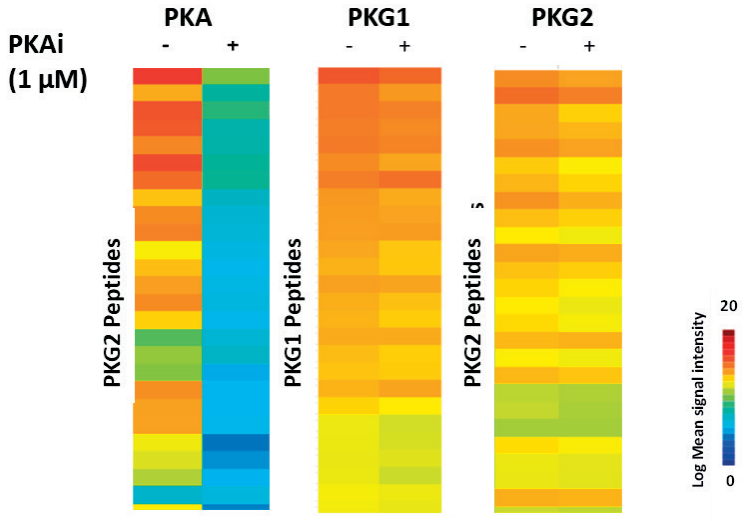

Fig S3- Effect of PKA inhibitor (PKAi) in the kinase activity of recombinant PKA, PKG1 and PKG2. PKA inhibitor reduced kinase activity of recombinant PKA but not of recombinant PKG1 and PKG2.

Table S3 PKG1 and PKG2 substrate scoring

	p value	Log Fold Change	EC_{50} Fit
cGMP	1	1	1
cAMP	1	1	1
8-Br-cGMP	**1**	**1**	
Rp-8-Br-PET-cGMPS	1	1	
Rp-8-pCPT-cGMPS	1	1	

All the experiments were performed on PamChip® 96 plate. The PamChip® 96 contains 96 identical arrays grouped on 24 strips each containing 4 arrays. Every array consists of 142 serine/threonine containing peptides. To minimize the variation between experiments performed on different days and on different PamChip® 96 plates, the experiment setup comprised of a control on each strip with variable concentrations of the modulators on the remaining three arrays of every strip. The effect of modulators was analyzed within each strip and paired with One-Way ANOVA. First, the peptides were selected for ATP dependency. Only the peptides that showed significant increase in phosphorylation with ATP were included in the scoring. The scoring of the peptides for PKG1 or PKG2 was based on the following parameters with 1 point assigned for every condition met (p value ≤ 0.05 for all the conditions, Log fold change> +2 for cGMP or cAMP, > +0.5 for PKG activator and > -0.5 for PKG Inhibitors, and EC_{50} fit R^2> 0.8). For PKG1, the inhibitor Rp-8-Br-PET-cGMPS which is more specific for PKG1 was used and for PKG2, the Rp-8-pCPT-cGMPS inhibitor was used.

4

Chapter 4

Kinase activity profiling identifies putative downstream targets of cGMP/PKG signaling in inherited retinal neurodegeneration

Akanksha Roy*, Arianna Tolone*, Riet Hilhorst, John Groten, Tushar Tomar and François Paquet-Durand

*Authors contributed equally

Cell death discovery; 8 (1) (2022): 1-12

Abstract

Inherited retinal diseases (IRDs) are a group of neurodegenerative disorders that lead to photoreceptor cell death and eventually blindness. IRDs are characterised by a high genetic heterogeneity, making it imperative to design mutation-independent therapies. Mutations in a number of IRD disease genes have been associated with a rise of cyclic 3',5'-guanosine monophosphate (cGMP) levels in photoreceptors. Accordingly, the cGMP-dependent protein kinase (PKG) has emerged as a new potential target for the mutation-independent treatment of IRDs. However, the substrates of PKG and the downstream degenerative pathways triggered by its activity have yet to be determined. Here, we performed kinome activity profiling of different murine organotypic retinal explant cultures (diseased *rd1* and wild-type controls) using multiplex peptide microarrays to identify proteins whose phosphorylation was significantly altered by PKG activity. In addition, we tested the downstream effect of a known PKG inhibitor CN03 in these organotypic retina cultures. Among the PKG substrates were potassium channels belonging to the K_v1 family (KCNA3, KCNA6), cyclic AMP-responsive element-binding protein 1 (CREB1), DNA topoisomerase 2-α (TOP2A), 6-phosphofructo-2-kinase/fructose-2,6-biphosphatase 3 (F263), and the glutamate ionotropic receptor kainate 2 (GRIK2). The retinal expression of these PKG targets was further confirmed by immunofluorescence and could be assigned to various neuronal cell types, including photoreceptors, horizontal cells, and ganglion cells. Taken together, this study confirmed the key role of PKG in photoreceptor cell death and identified new downstream targets of cGMP/PKG signaling that will improve the understanding of the degenerative mechanisms underlying IRDs.

Keywords
cGK1, cGK2, apoptosis, retinitis pigmentosa, *rd1* murine model, retinal explants, KCNA6, F263

Introduction

Inherited retinal degeneration (IRD) relates to a genetically highly heterogeneous group of neurodegenerative diseases causing photoreceptor cell death and eventually blindness (1,2). To this day, in almost all cases, these diseases are untreatable. Causative mutations have been identified in over 300 different disease genes (https://sph.uth.edu/retnet; information retrieved October 2021), calling for the development of mutation-independent therapies. Mutations in more than 20 IRD disease genes have been linked to increased levels of cyclic 3',5'-guanosine monophosphate (cGMP) in photoreceptors (3) and are thought to affect at least 30% of IRD patients (4). A key effector of cGMP-signaling is cGMP-dependent protein kinase (PKG), the overactivation of which may trigger photoreceptor cell death (5,6).

Mammals possess two different genes encoding for PKG, *prkg1* and *prkg2* (7). Splicing of *prkg1* leads to two distinct isoforms – PKG1α and PKG1β – which differ in first 80 to 100 amino acids in their N-terminal. The *prkg2* gene gives rise to only one isoform called PKG2. PKGs exist as a homodimer and binding of cGMP to one of the four cGMP binding sites induces a conformational change which activates the kinase (7). Activated PKG phosphorylates numerous cellular proteins at serine/threonine amino acid positions, which in turn regulates numerous cellular pathways. In mammals, PKG1 regulates smooth muscle contraction (8), platelet activation and adhesion (9), cardiac function (10), feedback of the NO-signaling pathways (11), and various processes in the central nervous system, such as hippocampal and cerebellar learning (12). PKG2 is involved in translocation of CFTR channels in jejunum (13) and regulation of bone growth by activation of kinases such as MAPK3/ERK1 and MAPK1/ERK2 in mechanically stimulated osteoblasts (14).

Intriguingly, PKG also plays an important role in cell death, which has been ascertained, for instance, through studies where PKG activation inhibited tumour progression in colon cancers, breast cancers, ovarian cancers and melanoma (15,16). Furthermore, PKG seems to play a central role in photoreceptor degeneration (17–19). In the *rd1* mouse retina, a well characterised model for IRD, photoreceptor cell death is triggered by abnormally high concentrations of retinal cGMP. This event is linked to dysfunction of phosphodiesterase 6 (PDE6) – involved in the regulation of intracellular cGMP levels – caused by a nonsense mutation in the rod *Pde6b* gene (20). Increased cGMP signaling has been found in several other models for IRDs (4,17) and is likely to over-activate PKG (3). *In vitro* and *in vivo* pharmacological inhibition of PKG showed strong photoreceptor protection in *rd1* retina as well as in the retina of *rd2* and *rd10* mouse models (3,21). Together, these studies suggest a key role for PKG activity in cGMP-mediated cell death and highlight PKG as a potential common target for strategies aiming to reduce photoreceptor degeneration.

The pathways downstream of PKG in degenerating photoreceptors are nonetheless still poorly understood. Increased cGMP/PKG signaling has been associated with increased activity of poly-ADP-ribose-polymerase (PARP), histone deacetylase (HDAC), and calpain proteases, all known to be involved in photoreceptor cell death (17). However, to date there is no evidence that directly links these events to PKG. Intracellular changes of known PKG targets such as vasodilator-stimulated phosphoprotein (VASP) and cAMP response element-binding protein (CREB) have been observed in dying photoreceptors (19,22,23).

While this can be a direct consequence of excessive cGMP/PKG signalling, these targets may also be phosphorylated by or have phosphorylation sites for other kinases, including cAMP-dependent protein kinase (PKA), characterised by substrate motifs similar to those of PKG (24). A better insight into the downstream effects of PKG and its phosphorylation targets is needed to understand the mechanisms of photoreceptor cell death and to, furthermore, guide the development of both new neuroprotective strategies and biomarker applications.

Using multiplex peptide microarrays, PamChips®, we measured PKG1- and PKG2- mediated phosphorylation of specific peptides by kinases in the lysates of murine retinal explant cultures treated or not with the PKG inhibitor CN03 (21). We identified several new PKG substrates potentially connected to IRD and confirmed their retinal expression in murine tissue. This study thus provides the groundwork for future studies aimed at the elucidation of cGMP/PKG-dependent cell death pathways.

Results

PKG inhibition reduces photoreceptor cell death in rd1 retinal explants

To investigate potential targets of PKG and their possible role in photoreceptor cell death, we used the PKG inhibitor CN03 on *rd1* organotypic retinal explant cultures. CN03 is a cGMP analogue, and as such is able to bind to cGMP binding sites on PKG, without inducing the conformational changes required for kinase activation (25). This culminates in reversible and competitive inhibition of PKG. In previous studies, CN03 showed marked protection of photoreceptors in retinal explants derived from the *rd1* mouse model (21,26). We therefore collected wild-type (WT) and *rd1* retinal explants treated or not with 50 µM CN03, using a treatment paradigm based on the aforementioned studies. Thus, retinas were explanted at postnatal (P) day 5 when photoreceptor degeneration had not yet started. The CN03 treatment was given at P7 and P9 and cultures were terminated at P11. The latter time-point corresponds to the beginning of *rd1* photoreceptor cell death (27), and is thus well suited to assess the protective effects of a given compound and to study events downstream of abnormal cGMP/PKG signalling. We confirmed the protective effects of CN03, by characterising the degree of cell death using the TUNEL assay (Fig. 1). CN03-treated retinas showed marked photoreceptor protection as previously reported (21).

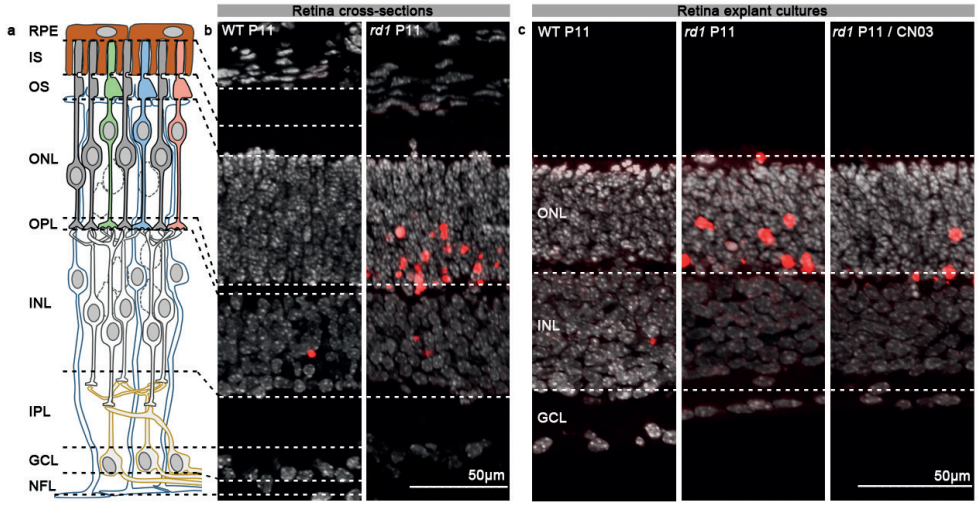

Figure 1: CN03-mediated photoreceptor protection in *rd1* P11 retinal explants. **a**) Diagram showing retinal layers: RPE=retina pigment epithelium, IS=inner segment, OS=outer segment, ONL=outer nuclear layer, OPL=outer plexiform layer, INL=inner nuclear layer, IPL=inner plexiform layer, GCL=ganglion cell layer, NFL=nerve fibre layer**. b**) Retina cross-sections derived from WT and *rd1* P11 mice. **c**) Sections derived from WT and *rd1* P11 retinal explant cultures untreated or treated from P7 to P11 with 50 µM CN03. In both **b** and **c**: TUNEL assay (red) indicated dying cells, DAPI (grey) was used as nuclear counterstain. P=postnatal day.

Serine/Threonine Kinase (STK) activity in rd1 retinal explants

To evaluate possible differences in kinase profiles of the murine retinal explant samples (*rd1*, n=8; WT, n=5), we used PamChip® peptide microarray-based Serine/Threonine Kinase (STK) activity assays (24). The overall STK activity between the samples is represented as heatmap (Supplementary Fig. S1a). A violin plot was used to visualize the phosphorylation signal intensity of the peptides and its distribution within the same sample groups (Fig. 2a). Increased phosphorylation was observed for 43% of the total 142 peptides in *rd1* retinal explants, indicating higher kinase activity in *rd1* NT when compared to WT (Fig. 2b). The peptides, SRC8_CHICK_423_435, RBL2_959_971, CDN1B_151_163 and RADI_559_569 showed significantly higher phosphorylation (p<0.05) in *rd1* explants than in wild type controls. Using the upstream kinase analysis tool of the BioNavigator® software, the peptides with increased phosphorylation were linked to kinases that are most likely to be responsible for phosphorylation of these peptides (See Data Analysis, Materials and Methods Section). The kinase statistics and kinase score were calculated as a metrics for identifying highly active kinases. The kinases that were predicted to be more active in *rd1* explants include CaMK4, PKG1, PKG2, PKAα, and Pim1 (Table 1). In order to present relative kinome activity profiles of retinal explants (*rd1 vs*. WT), kinase score and kinase statistics were used in color coding branches and nodes on the phylogenetic tree of protein kinase families (Fig. 2 c).

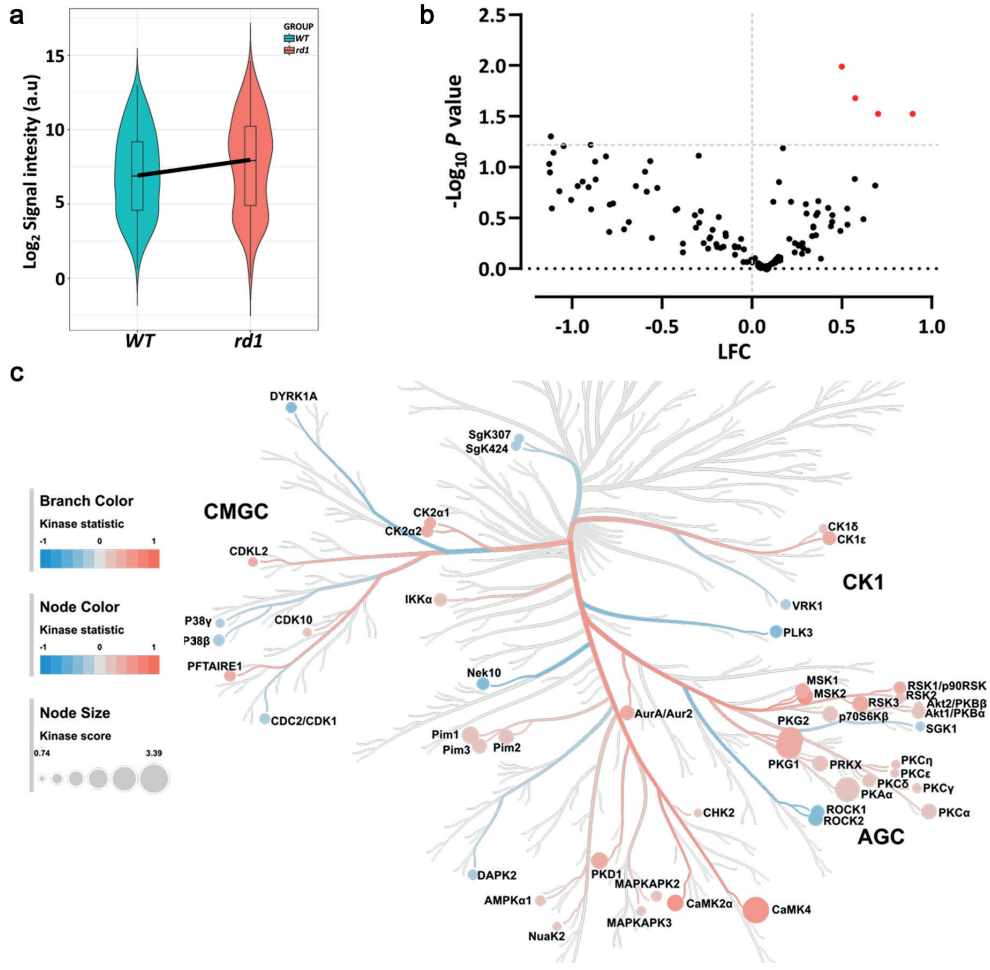

Figure 2. Serine/Threonine Kinase (STK) activity in untreated retinal explants. Organotypic retinal explants derived from wild-type (WT) and *rd1* mice (WT, n=5; *rd1*, n=8) were maintained in culture medium from P5 till P11. The kinase activity of their lysates was measured on PamChip® Serine/Threonine kinase (STK) arrays. **a**) Violin plot showing the global phosphorylation of the peptides on PamChip® STK array as Log_2 signal intensity and their intensity value distribution, when comparing WT to *rd1* explants. The thick line connects the average values of each group. **b**) Volcano plot representing Log Fold Change (LFC) and $-Log_{10}$ *p*-value for peptide phosphorylation. Red dots indicate significantly changed phosphopeptides (*p*-value < 0.05), black dots represent peptides with no significant alteration in phosphorylation. **c**) The high-ranking kinases were visualized in a kinome phylogenetic tree, where branch and node color are encoded according to the kinase statistic, with values > 0 (in red) representing higher kinase activity in *rd1* retinal explants. The node size is encoded by the kinase score, that ranks kinases based on their significance and specificity in terms of sets of peptides used for the corresponding kinase.

Table 1. Upstream kinase analysis results for *rd1 vs*. WT (top) and *rd1* CN03 *vs*. *rd1* (bottom). The Kinase Statistic shows the overall change of the peptide set that represents a given kinase. Positive values indicate higher kinase activity in *rd1*, while negative values indicate lower activity, *e.g*., in *rd1* CN03. The Kinase Score includes the sum of significance and specificity scores (Scores > 1.5 shown in the table).

	rd1 vs. WT retinal explants		
Rank	**Kinase Name**	**Kinase Score**	**Kinase Statistic**
1.	CaMK4	3.39	0.46
2.	PKG1	3.23	0.32
3.	PKG2	3.16	0.30
4.	PKAα	3.09	0.26
5.	Pim1	2.02	0.19
6.	p70S6Kβ	1.78	0.24
7.	CaMK2α	1.92	0.46
8.	RSK1/p90RSK	1.92	0.42
9.	MSK2	1.89	0.52
10.	PKD1	1.95	0.43
11.	PKCα	1.77	0.23
12.	Pim2	1.70	0.21
13.	PRKX	1.82	0.23
14.	ROCK2	1.69	-0.37
15.	MSK1	1.71	0.36
16.	Pim3	1.68	0.18

	CN03-treated *rd1 vs.* control *rd1* retinal explants		
Rank	**Kinase Name**	**Kinase Score**	**Kinase Statistic**
1.	PKAα	3.60	-0.40
2.	Pim1	3.50	-0.40
3.	PKG2	3.70	-0.40
4.	PKG1	3.20	-0.40
5.	CaMK4	3.30	-0.50
6.	PKCα	3.10	-0.40
7.	Pim3	3.00	-0.40
8.	PRKX	3.00	-0.40
9.	p70S6Kβ	2.90	-0.40
10.	PKCδ	2.70	-0.40
11.	CK2α2	3.70	-0.60
12.	RSK3	2.80	-0.50
13.	RSK2	2.90	-0.50
14.	PKCθ	2.30	-0.40
15.	MSK2	2.40	-0.60
16.	PKCε	2.10	-0.40
17.	MAPKAPK3	2.20	-0.40
18.	PKCγ	2.10	-0.40
19.	MSK1	2.20	-0.50
20.	PKD1	2.20	-0.50
21.	CHK2	2.10	-0.40
22.	Pim2	1.90	-0.30
23.	MAPKAPK2	2.10	-0.40

	CN03-treated *rd1 vs.* control *rd1* retinal explants		
Rank	**Kinase Name**	**Kinase Score**	**Kinase Statistic**
24.	SGK2	1.90	-0.40
25.	AMPKα1	1.80	-0.40
26.	PKN1	2.10	-0.40
27.	PKCη	1.80	-0.40
28.	CK2α	2.30	-0.40
29.	RSK1	1.80	-0.40
30.	AurA/Aur2	1.70	-0.50
31.	PRKY	1.80	-0.40
32.	Akt1	1.70	-0.30
33.	DCAMKL1	1.70	-0.50
34.	PKCβ	1.70	-0.40
35.	Akt2	1.70	-0.30
36.	COT	2.60	-0.40
37.	PKCI	1.60	-0.40
38.	RSKL1	1.60	-0.40

STK activity in rd1 retinal explants treated with PKG Inhibitor CN03

As we found a higher phosphorylation of peptides in *rd1* explants, when compared to WT explants, and with a clear role for PKGs observed, we sought to investigate the effect of the PKG inhibitor CN03 on the STK activity. The PKG inhibitor CN03 significantly decreased photoreceptor cell death (*cf*. Fig. 1). The overall STK activity profiles for treated and untreated *rd1* retinal explants are shown in a heatmap (Supplementary Fig. S1b). The distribution of phosphorylated peptides for both the samples is represented by a violin plot (Fig. 3a). Phosphorylation decreased for approximately 80% of the 142 peptides present on the STK PamChip®. Fourteen peptides were identified whose phosphorylation decreased significantly ($p<0.05$) in *rd1* CN03 as compared to untreated *rd1* (Fig. 3b). Table 2 shows peptides that displayed lower phosphorylation (22 peptides, $p<0.1$) in CN03 treated *rd1* retina than untreated controls, *p*-value, names of the proteins they are derived from, with their UniProt IDs, substrate score of PKG1 and PKG2, and localization within the retina.

The designation of the peptides as PKG1- or PKG2- substrates is based on our recent studies where we ranked the peptides on the STK PamChip® according to their preference for PKG1 and or PKG2 (24). This preference was based on the substrate phosphorylation by recombinant PKG1 or PKG2 in response to PKG activity modulators (ATP, cGMP, cAMP, PKG activator, PKG inhibitors). In the present study, fourteen of the peptides in Table 2, are substrates for both PKG1 and PKG2 and three for PKG1 only. Among those peptides, KCNA6_504_516, NCF1_296_308, GRIK2_708_720, VTNC_390_402, ADRB2_338_350, BRCA1_1451_1463, RYR1_4317_4329, KCNA3_461_473 and VASP_150_162 have been verified to be present in the retina based on literature data.

We subsequently linked the phosphorylated peptides to the putative upstream kinases and found that kinase activity of particularly PKAα, Pim1, PKG1, PKG2, CaMK4 was suggested to be reduced by CN03 treatment (Table 1, Fig. 3c,). Notably, these were the same kinases

that were predicted to be more active in the diseased *rd1* explants in comparison to WT explants, indicating specific targeting by CN03 (Fig. 2c).

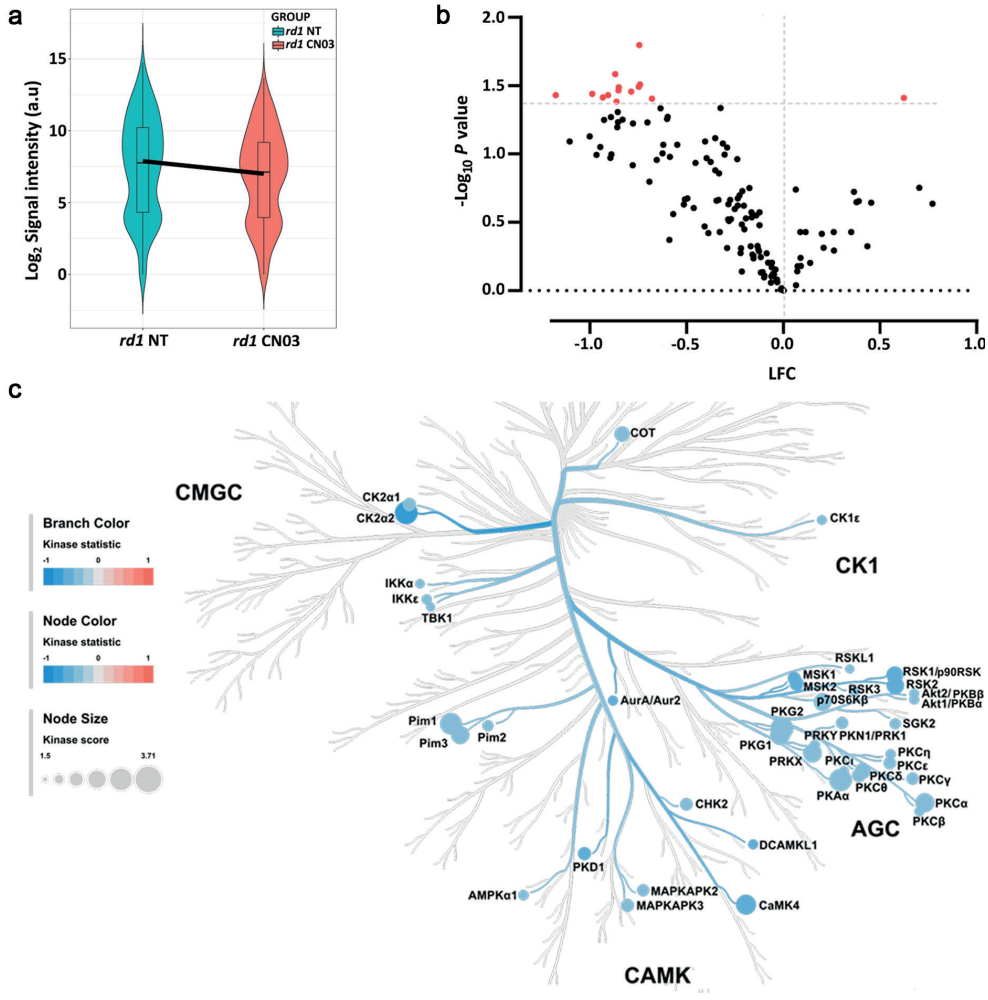

Figure 3. Serine/Threonine Kinase (STK) activity in response to PKG inhibition in retinal explants. Retinal explant cultures were either non-treated (NT) or treated with 50 µM CN03 (*rd1* NT, n=8; *rd1* CN03, n=10). The kinase activity of retinal explant lysates was measured on PamChip® Serine/Threonine kinase (STK) arrays. **a**) Violin plot showing the global phosphorylation of peptides on the PamChip® STK array as Log_2 signal intensity and their intensity value distribution, when comparing *rd1* NT to *rd1* CN03 treated explants. The thick line is connecting the average values of each group. **b**) Volcano plot representing Log Fold Change (LFC) and $-Log_{10}$ *p* value for peptide phosphorylation. Red dots indicate significantly changed phosphopeptides with *p* value < 0.05 and black dots represent phosphopeptides with no significant alteration in phosphorylation. **c**) The high-ranking kinases are visualized in a kinome phylogenetic tree, where branch and node color are encoded according to the kinase statistic, with values < 0 (in blue) representing lower kinase activity in *rd1* retinal explants treated with CN03. The node size is encoded by the kinase score, that ranks kinases based on their significance and specificity in terms of sets of peptides used for the corresponding kinase.

Table 2. Differentially phosphorylated peptides (*p<0.1*) *in rd1* untreated *vs. rd1* CN03 treated retinal explant cultures. The table shows the peptide name, name of the protein that the peptide is derived from, its UniProt ID, *p* value, PKG1 and PKG2 substrate score, and localization in the retina with reference. The scores for PKG1, PKG2 are as described in (24), and range from 0 (no substrate) to 10 (very good substrate). Colour scheme for the PKG specificity score: 10–8: Good, 7–4: Intermediate, and 3–1: Poor substrate, 0: no substrate (24). For proteins previously detected in the mouse retina, the reference is added. The expression of proteins printed in bold was studied using immunodetection (*cf*. Fig. 5).

S. No.	ID	UniProt ID	Protein name	*p* value	PKG1 score	PKG2 score	Localisation	Ref.
1.	IKBA_26_38	P25963	NF-kappa-B inhibitor alpha	0.016	0	0	ONL, INL, GCL	(28)
2.	GBRB2_427_439	P47870	Gamma-aminobutyric acid receptor subunit beta-2 precursor	0.026	10	6		
3.	PTN12_32_44	Q05209	Tyrosine-protein phosphatase non-receptor type 12	0.031	10	5		
4.	KCNA6_504_516	**P17658**	**Potassium voltage-gated channel subfamily A member 6**	**0.032**	**9**	**3**	**GCL**	(29)
5.	NCF1_296_308	P14598	Neutrophil cytosol factor 1	0.032	9	7	GCL	(30)
6.	CREB1_126_138	**P16220**	**cAMP response element-binding protein**	**0.034**	**10**	6	**ONL, INL, GCL**	
7.	GRIK2_708_720	**Q13002**	**Glutamate receptor, ionotropic kainate 2 precursor**	**0.035**	**10**	4	**INL, IPL**	(31)
8.	NCF1_321_333	P14598	Neutrophil cytosol factor 1	0.036	0	0		
9.	EPB42_241_253	P16452	Erythrocyte membrane protein band 4.2	0.037	9	7		
10.	VTNC_390_402	P04004	Vitronectin precursor	0.037	10	4	RPE, ONL, GCL	(32)
11.	ADRB2_338_350	P07550	Beta-2 adrenergic receptor	0.039	8	4	Müller cells	(33)
12.	BRCA1_1451_1463	P38398	Breast cancer type 1 susceptibility protein	0.039	0	0		(34)
13.	TOP2A_1463_1475	**P11388**	**DNA topoisomerase 2-alpha**	**0.039**	6	5	**GCL**	
14.	MPIP3_208_220	P30307	M-phase inducer phosphatase 3	0.041	0	0		
15.	CDC2_154_169	P06493	Cell division control protein 2 homolog	0.046	0	0		
16.	KAP3_107_119	P31323	cAMP-dependent protein kinase type II-beta regulatory subunit	0.046	8	4		
17.	MYPC3_268_280	Q14896	Myosin-binding protein C, cardiac-type	0.049	10	4		
18.	RYR1_4317_4329	P21817	Ryanodine receptor 1	0.053	9	5	ONL, INL, GCL	(35)
19.	TY3H_65_77	P07101	Tyrosine 3-monooxygenase	0.054	9	3		
20.	KCNA3_461_473	**P22001**	**Potassium voltage-gated channel subfamily A member 3**	**0.055**	**8**	7	**ONL, IPL**	(29)
21.	F263_454_466	**Q16875**	**6-phosphofructo-2-kinase/fructose-2,6-biphosphatase 3**	**0.059**	10	3	INL, GCL	
22.	VASP_150_162	P50552	Vasodilator-stimulated phosphoprotein	0.081	8	4	ONL	(23)

Putative biological pathways involved in retinal degeneration

To identify possible associations of the kinases with biological pathways that are activated in retinal degeneration as represented by *rd1* explants, we performed an analysis of relevant biochemical pathways using the Kyoto Encyclopedia of Genes and Genomes database (KEGG; Version 2021).

Pathway analysis of kinase activity in *rd1 vs.* WT explants yielded as the major associated pathways Neurotrophin signaling pathway, proteoglycans in cancer, circadian entrainment, insulin resistance, HIF-1 signaling pathway, long-term potentiation, FMAPK signaling (Fig. 4a). After treatment of *rd1* explants with CN03, the high scoring pathways *i.e.*, insulin resistance, mTOR, MAPK signaling, long-term potentiation, circadian entrainment, and HIF-1 signaling (Fig. 4b) were the same as found in Fig. 4a.

To identify the putative kinases involved in retinal degeneration, based on the *rd1* model and PKG inhibitor CN03 treatment, we compared the kinase list derived from each comparison as represented in a Venn diagram (Fig. 4c). Here, almost 77% of kinases with high activity in *rd1* as compared to WT were overlapping with the kinases showing reduced activity in *rd1* retinal explants treated with CN03.

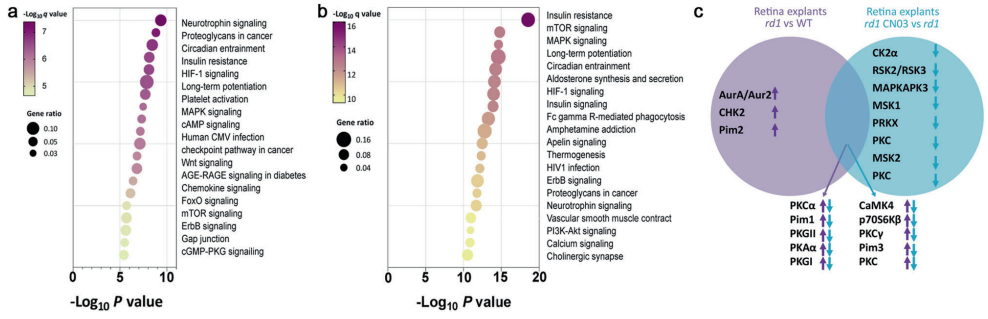

Figure 4. Biological pathways involved in retinal degeneration. Key biological pathways with potentially higher activity in *rd1* **(a)** and lower activity in *rd1* treated with CN03 **(b)**. Pathways are ranked according to their *p*-values and colored by their *q*-values. A *q* value is the *p*-value adjusted for multiple testing using the Benjamini-Hochberg procedure (36,37). The node size indicates the gene ratio, *i.e.,* the percentage of total genes or proteins in the given KEGG pathways (only input genes or proteins with at least one KEGG pathway were included in the calculation). **c)** The overlap between kinases changed in *rd1* NT *vs*. WT and *vs. rd1* treated with CN03 respectively (Fig. 2c, 3c), is visualized in a Venn Diagram. Here, increased or reduced activity of a kinase is indicated by arrows pointing up- or down-wards, respectively.

PKG target validation for retinal localization

Next, we tested whether the proteins corresponding to the peptides that were differentially phosphorylated in the three retinal explant groups (*i.e.*, WT, *rd1*, and *rd1*/CN03) were present in the retina. While some of these proteins had already previously been shown to be present in mouse retina (Table 2), we performed immunostaining on retinal tissue sections derived from P11 WT mice to assess the retinal expression and cellular localization

for six proteins with high PKG preference (Table 2), that might potentially be connected to photoreceptor degeneration.

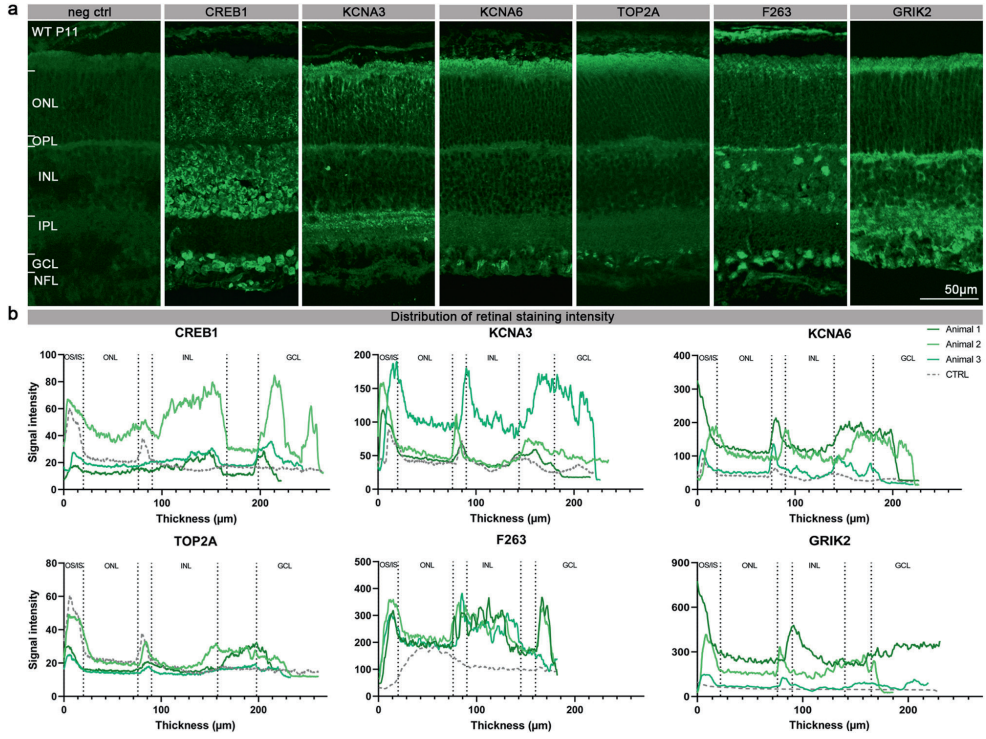

Figure 5: Presence and localisation of PKG target proteins in the retina. (a) The panel shows retinal cross-sections derived from P11 WT mice and stained with secondary antibody for negative control (neg. ctrl.), anti-CREB1, anti-KCNA3, anti-KCNA6, anti-TOP2A, anti-F263, or anti-GRIK2. **(b)** The localisation of CREB1, KCNA3, KCNA6, TOP2A, F263, and GRIK2 in the retina of WT mice is illustrated by a signal distribution plot along vertical sections across the retina. Antibody labelling obtained on stained retinal tissue sections from three different animals is represented in different shades of green, while the negative control is represented in grey. OS/IS=outer segment/inner segment, ONL=outer nuclear layer, OPL=outer plexiform layer, INL=inner nuclear layer, IPL=inner plexiform layer, GCL=ganglion cell layer, NFL=nerve fiber layer.

The analysis of the WT retinal sections immunostained for cyclic AMP-responsive element-binding protein 1 (CREB1) showed abundant expression in the INL as well as the GCL (Fig. 5). The potassium voltage-gated channel subfamily A, member 3 (K_v1.3; KCNA3) was found to be localised in the ONL, possibly in photoreceptor axons, and in two discrete sublamina of the IPL (38), where the synapses between bipolar cell axons and ganglion cell dendrites reside. The potassium voltage-gated channel subfamily A, member 6 (K_v1.6; KCNA6) was prominently expressed in the ganglion cell layer (GCL) and the nerve fibre layer (NFL). DNA topoisomerase 2-α (TOP2A) expression was restricted to the GCL. 6-phosphofructo-2-kinase/fructose-2,6-biphosphatase 3 (F263) – an enzyme involved in the control of glycolytic flux (39) appeared to be present in the OPL, likely in horizontal cells, as well as in the GCL.

Finally, staining with the antibody directed against glutamate ionotropic receptor kainate 2 (GRIK2) confirmed its presence in the INL and GCL, in line with previous findings (31). Taken together, the immunostaining data as well as the signal intensity in the distribution plots confirmed the retinal expression of several of the discovered PKG targets (24) (Fig. 5a, 5b). Furthermore, the differences in phosphorylation of these targets between WT, *rd1*, and *rd1*/CN03 retinas (Fig. 2, Fig.3) may suggest a potential role for these PKG substrates in the mechanism leading to photoreceptor cell death.

Discussion

Excessive activity of PKG has been directly linked to retinal degeneration and its inhibition has been shown to provide photoreceptor protection in several *in vivo* IRD models (3,21). Yet, at present it is still unclear how PKG exerts its detrimental effects and what are the protein targets that, when phosphorylated by PKG, mediate photoreceptor cell death. Here, we combined PKG inhibitor treatment with multiplex peptide microarray technology and immunohistochemistry to identify novel PKG phosphorylation targets in the retina.

PKG inhibition mediates photoreceptor neuroprotection

Over-activation of PKG has been connected to neuronal cell death in different experimental settings and conditions, including in human neuroblastoma derived cell cultures (40), peripheral nerve injury (41), and in photoreceptor degeneration in IRD (6,42). For photoreceptor degeneration an excessive accumulation of cGMP was already established in the 1970s and while it had already then become evident that high cGMP-levels were cytotoxic (43,44), it was unclear how cGMP would exert its negative effects. Research initially focussed on a proposed detrimental role of cyclic-nucleotide-gated (CNG) channels (45,46), however, in recent years it has become increasingly obvious that PKG-signaling plays a major role in photoreceptor degeneration (3,47). Our study, showing that the inhibitory cGMP analogue CN03 reduces photoreceptor cell death, is in line with earlier studies in which PKG inhibitors were found to preserve photoreceptor viability and functionality in a variety of models for inherited photoreceptor degeneration (3,21). Nevertheless, what protein targets of PKG exactly are responsible for its cell death promoting effects is unclear. Since PKG may phosphorylate hundreds of substrates it is important to identify those relevant for degeneration in a tissue and cell type specific context (48).

PKG inhibition and peptide microarray technology for the prediction of PKG phosphorylation targets

To identify the biological pathways leading to photoreceptor cell death, the kinase activity of retinal samples was studied on the PamChip® microarray platform, which allowed investigating the phosphorylation status of 142 peptides simultaneously. The *rd1* retinal explants showed an overall increased phosphorylation of peptides, indicating a higher kinase activity and the possible involvement of kinases from the AGC and CAMK families. Substrates to both isoforms of PKG; PKG1 and PKG2 showed higher signals in *rd1* retina indicating increased phosphorylation (Table 2). The specific inhibition of PKG activity with the inhibitor CN03 in organotypic retina explants allowed to profile kinase activity and response to PKG inhibition using PamChip® technology. CN03 treatment showed a decrease

in peptide phosphorylation with significantly reduced signal on seventeen peptides. Among the significantly regulated peptides, CREB1_126_38 has already been reported as PKG1 substrate (24). VASP, another well-known PKG substrate (21,24), was also affected, but ranked much lower on our substrate list (rank 22), suggesting that in a retinal context PKGs may prefer other substrates.

Recent studies identified additional cGMP-interacting proteins such as PKAs, PKCs, and CaMKs as upregulated in IRD retinas, which might be interesting in developing new therapeutic targets (49,50). These recent findings corresponded well with our results where we identified these same kinases as activated in *rd1* diseased retinal explants and repressed by the PKG inhibitor CN03. The significant difference in phosphorylation between untreated *rd1* and CN03-treated *rd1* retinal explants indicates that PKG inhibition influenced phosphorylation of these peptides, whose corresponding proteins are therefore candidate PKG targets *in situ* and may play a role in the mechanism of photoreceptor cell death. We focused on those peptides for which PKG has a high preference, *i.e*., peptides with a high PKG score (Table 2), and confirmed the presence of the corresponding proteins in the retina by either literature data or by additional immunofluorescence analysis.

Novel targets for PKG in the neuroretina

One of the identified targets in our analysis was KCNA6, which, together with KCNA3 (rank 20 based on *p* value, Table 2), belongs to the K_v1 family of voltage-dependent potassium channels. The K_v1 family mainly consists of channels with a slow and delayed activation. Immunoreactivity studies revealed expression of both KCNA3 and KCNA6 in the mouse retina (29), which is in line with our immunofluorescence results. The K_v1 family is involved in the regulation of progression through cell cycle checkpoints by defining the membrane potential and ensuring the driving force for calcium and chloride entry. Surprisingly, these proliferation-related channels also appear to play a role in regulating cell death, making them interesting for our study (51). It has been shown that within a few minutes of apoptosis induction KCNA3 is inhibited by the cluster of differentiation 95 (CD95) *via* tyrosine phosphorylation (52). Other studies have shown the activation of KCNA3 at an early stage of apoptosis, as well as its contribution to a decrease in apoptotic volume, also known as 'cell shrinkage' in lymphocytes (53). In the retina, inhibition of KCNA1 and KCNA3 *in vivo* was protective for retinal ganglion cells (RGCs) after optic nerve axotomy (54). The localization of KCNA6 and KCNA3 in the WT mouse retina and their differential phosphorylation by PKG in *rd1* and CN03 treated *rd1* retinal explant cultures suggest a role in photoreceptor cell death. Past studies on the involvement of K_v1 channels in cell death, although conflicting, strengthen this idea (51–53). Establishing whether PKG-mediated phosphorylation of K_v1 channels involves activation or inhibition of these channels would help shed light on their contribution to photoreceptor death.

Among the various differentially phosphorylated substrates located in the retina of both *rd1* and WT, CREB1 is a known target of PKG (55,56). CREB1 is a transcription factor implicated in neuronal survival (57) and constitutively expressed in different types of human cancer (58). As shown by the *ex vivo* results, CREB1 is widely distributed in the mouse retina. Furthermore, through upstream kinase analysis we predicted the activation of several other kinases such as CaMK4, PKC theta, and PKA, known to target CREB (59–61). Thus,

the abnormal activity of PKG as well as that of the other kinases can lead to increased CREB1 phosphorylation, in contrast to previous studies in which downregulation of CREB1 was associated with photoreceptor degeneration in both *rd1* and *rd10* mice (22,62). The increase in activity of kinases that phosphorylate CREB combined with an increase in CREB peptide phosphorylation in *rd1* may be due to the activation of parallel signals after the cellular insult: the induction of cell death and the activation of a CREB1-directed survival program (63).

Other PKG targets that we have identified and localized in the retina include vitronectin (VTNC) and F263. VTNC is a cell adhesion protein, upregulated in inflammation and traumatized tissues (64) and a major component of extracellular deposits specific to age-related macular degeneration (AMD) (65). In the same study, VTNC mRNA expression has been found distributed in the various layers of the human retina. Its high phosphorylation in *rd1* explants might be linked to increased inflammation, which is an early phenomenon observed for degenerative retinal disorders such as RP, AMD, and diabetic retinopathy (DR) (66). If so, VTNC would have the potential to be a predictive biomarker for certain retinal degenerative diseases.

6-phosphofructo-2-kinase/fructose-2,6-biphosphatase 3 or F263 is a pro-glycolytic enzyme. Its activation following excitotoxic stimulation has been associated with neuronal cell death (67). Furthermore, dysregulation of the HIF-1 - F263 pathway has been proposed as crucial for two key aspects of the pathogenesis of DR, namely angiogenesis and neurodegeneration (68). With *ex vivo* analysis we localized F263 in GCL and INL while it was not detected in ONL. The identification of F263 as a target of PKG and its high phosphorylation in *rd1* compared to WT may suggest a change in retinal energy metabolism during degeneration and may also help to understand the mechanism of aerobic glycolysis in the retina, which remains relatively poorly understood to date (69).

Metabolic pathways in the retina regulated by PKG

The pathway analysis showed insulin resistance and mTOR as important pathways inhibited by CN03. mTOR is a serine/threonine kinase which regulates protein synthesis, cellular metabolism and autophagy (70). The mTOR pathway regulates neurogenesis in the eye and is crucial to normal development of retina and the optic nerve (71). Activated mTOR signaling has been shown to be involved in retinal neurodegenerative diseases such as DR and AMD (72,73). Treatment with the mTOR inhibitor rapamycin, improved mitochondrial dysfunction and provided neuroprotection to 661W cells, a cellular model that shares certain features with photoreceptors (74). Similarly, inhibition of the mTOR/PARP-1 axis leads to photoreceptor protection against light-induced photoreceptor cell death (70). However, the targeting of this pathway axis in IRD as treatment strategy is still contentious as there are also studies that show mTOR stimulation delays cone cell death in IRD (75,76).

Among the peptides whose phosphorylation was high in untreated *rd1* retinal explants and significantly decreased in CN03-treated *rd1* retinal explants was F263. The protein F263 is a key regulator of glycolysis (77). Photoreceptors metabolize glucose through aerobic glycolysis (the 'Warburg effect') to satisfy their very high energy demand for the maintenance of the dark current, as well as for the recycling of visual pigments and the renewal of photoreceptor

OS (78,79). As a consequence of the high energy demand, the retina has an elevated oxygen consumption, probably the highest in the body, and is therefore particularly prone to oxidative stress and reactive oxygen species (ROS)-induced mitochondrial damage (80). The high phosphorylation of F263 found in the *rd1* retina may be linked to an abnormal increase in metabolic activity in the retina resulting in mitochondrial damage. Considering that mitochondrial dysfunction has been associated with RP (80), the identification of F263 as a substrate of PKG and its possible role in the degeneration process could help to clarify the metabolic state of the diseased retina.

Conclusion

Using multiplex peptide microarray technology, we provide further evidence for the likely involvement of PKG in degenerating *rd1* photoreceptors *in vitro* and confirmed the already known neuroprotective effects of the PKG inhibitor CN03 (21). Importantly, we identified several novel downstream PKG targets that might play a role in cGMP/PKG-mediated photoreceptor degeneration. This will form the basis for future studies, which may further elucidate the role of PKG target phosphorylation, as well as the beneficial effects of CN03. Our work could likewise be employed to develop novel diagnostic and therapeutic biomarkers for retinal degenerative diseases. For example, the use of phospho-specific antibodies may allow to confirm a reduction of target phosphorylation and *in situ* studies may allow to localize in which cellular compartment such changes occurred. Finally, our results further connect several metabolic pathways with retinal degeneration, including insulin, mTOR, and HIF-1 signaling, which in future studies may help to understand the complex mechanisms behind photoreceptor cell death.

Materials and Methods

Animals: C3H Pde6b$^{rd1/rd1}$ (*rd1*) and congenic C3H wild-type (WT) mice were housed under standard light conditions, had free access to food and water, and were used irrespective of gender. All procedures were performed in accordance with the law on animal protection issued by the German Federal Government (Tierschutzgesetz) and approved by the institutional animal welfare office of the University of Tübingen.

cGMP analogues synthesis. Synthesis of the cyclic nucleotide analogue CN03 was performed by Biolog Life Science Institute GmbH & Co. KG according to previously described methods (21) (https://patentscope.wipo.int/search/en/detail.jsf?docId=WO2018010965)

Organotypic retinal explant cultures: Preparation of organotypic retinal cultures derived from *rd1* (n = 10) and C3H (n= 5) animals chosen randomly out of three different litters was performed as described previously (26,81). Animals were sacrificed at postnatal day (P)5. Eyes were rapidly enucleated and incubated in R16 serum-free, antibiotic-free culture medium (07491252A; Gibco) with 0.12% proteinase K (21935025; ICN Biomedicals Inc.) for 15 min at 37°C. Subsequently, eyes were incubated in 20% foetal bovine serum (FCS) (F7524; Sigma) in order to block proteinase K activity. This step was followed by rinsing

in R16 medium. Under a laminar-flow hood and sterile conditions, the anterior segment, lens, vitreous, sclera, and choroids were removed from the eyes. The retina with the RPE still attached was cut in four points resembling a four-leaf clover and transferred to a culture membrane insert (3412; Corning Life Sciences) in a six-well culture plates with completed R16 medium with supplements (26). The retinal explants were incubated at 37°C in a humidified 5% CO2 incubator and left undisturbed for 48h. At P7 and P9 medium was changed *i.e*. with replacement of the full volume of the complete R16 medium, 1mL per dish, with fresh medium. In this context, half of the retinal explants were treated with CN03 at 50 µM (dissolved in water), while the other half was kept as untreated control. For retinal explant lysis, culturing was stopped at P11, retinal explants were snap frozen in liquid nitrogen and stored at -80 °C. For retinal explants cross-sectioning preparation, culturing was stopped at P11 by 45 min fixation in 4% paraformaldehyde (PFA), cryoprotected with graded sucrose solutions containing 10, 20, and 30% sucrose, embedded in optimal cutting temperature compound (Tissue-Tek) and then cut into 12µm sections.

TUNEL assay: Representative results showing the protective effects of CN03 on photoreceptor cell death at a concentration of 50 µM, were obtained using terminal deoxynucleotidyl transferase dUTP nick end labelling (TUNEL) assay (82) (based on in Situ Cell Death Detection Kit, 11684795910, red fluorescence; Sigma-Aldrich) on sections derived from *rd1* and C3H retinal explant cultures. DAPI (Vectashield Antifade Mounting Medium with DAPI; Vector Laboratories) was used as blue fluorescence nuclear counterstain. Images were captured using 7 Z-stacks with maximum intensity projection (MIP) on a Zeiss Axio Imager Z1 ApoTome Microscope MRm digital camera (Zeiss, Oberkochen, Germany) with a 20x APOCHROMAT objective. The excitation (λ_{Exc}) / emission (λ_{Em}.) characteristics of the filter sets used for the fluorophores were as follows: DAPI (λ_{Exc}. = 369 nm, λ_{Em}. = 465 nm) and TMR red (λ_{Exc} = 562 nm, λ_{Em} = 640 *nm*). Adobe Photoshop (CS5Adobe Systems Incorporated, San Jose, CA) was used for image processing.

Materials for retinal explant lysis: Mammalian protein extraction reagent (M-PER™), Halt™ protease and phosphatase inhibitor cocktails and the Coomassie Plus (Bradford Assay) kit were purchased from Thermo Fischer Scientific.

Retinal explant Lysis: The retinal explant samples were lysed with lysis buffer (MPER with 1:100 phosphatase inhibitor cocktail and protease inhibitor cocktail reagents) for 30 mins on ice. The lysate was centrifuged at 16 000 x *g* for 15 min at 4 °C. The supernatant was immediately aliquoted, flash frozen, and stored at -80 °C. The protein content of the lysate was measured using the Bradford Protein Assay (83).

Kinase activity measurements: The kinase activity for the retina lysates was determined on STK PamChip® with four arrays, each array comprising of 142 peptides derived from the human phosphoproteome, according to the instructions of the manufacturer (PamGene International B.V., 's-Hertogenbosch, North Brabant, The Netherlands). The peptide names consist of the protein they are derived from and the first and last amino acid positions in that protein. The phosphorylated Serine/Threonine amino acid residues are detected by a primary antibody mix, which is then made visible by addition of FITC-conjugated secondary antibody (84). The assay mix consisted of protein kinase buffer (PamGene International BV.

's-Hertogenbosch, North Brabant, The Netherlands), 0.01% BSA, STK primary antibody mix, ATP (400 μM) and retina tissue lysate (0.25 μg protein/array).

Instrumentation for kinase activity measurements: All experiments were performed on PamStation12® where up to 12 assays can be performed simultaneously (PamGene International B.V., 's-Hertogenbosch, North Brabant, The Netherlands). To prevent unspecific antibody binding, the PamChips® were first blocked with 2% BSA, by pumping it up and down 30 times through the arrays. The chips were then washed three times with Protein Kinase Buffer and assay mix was applied. The assay mix was pumped up and down through the arrays for 60 mins. Afterwards, the arrays were washed and FITC labelled secondary antibody mix was applied on the arrays. The images of the arrays were recorded at multiple exposure times (85).

Data analysis: The signal intensity of each peptide spot on the array for each time point was quantified by BioNavigator® software version 6.3.67.0 (PamGene International B.V., 's-Hertogenbosch, North Brabant, The Netherlands). For each spot, the signal intensity at the different exposure times was combined to a single value by exposure time scaling (85). The resulting values were $\log_2$ transformed and the overall differences in STK profile between *rd1* NT *vs*. WT or *rd1* CN03 *vs*. *rd1* NT were visualized as heatmaps and violin plots which were generated in R software (R version 4.0.2, The R Foundation for Statistical Computing). For heatmaps, hierarchal clustering of peptides was performed using the average-linkage method and clustering was shown as dendrograms on the y-axis of heatmaps. Unpaired *t*-tests were used to determine significant differences ($p < 0.05$) in phosphorylation intensity between the groups. Results were represented as volcano plots (GraphPad Prism version 9.2.0).

Upstream kinase analysis: Information on kinases that could be responsible for peptide phosphorylation differences between the two sample groups was obtained through the STK Upstream Kinase Analysis tool of BioNavigator® (85). This software integrates known interactions between kinases and the phosphorylation sites as provided in databases such as HPRD, PhosphoELM, PhosphositePLUS, Reactome, UniProt to provide a peptide set for each kinase (fingerprint) and predicts the kinases differentially active between the groups. The results of this analysis are described by two parameters: The Kinase Statistic, indicating the size and direction of the change for each kinase and the Kinase Score, ranking the kinases by the likelihood of this kinase being involved.

The Kinase Statistic depicts the overall change of the peptide set that represents a kinase. For instance, a larger positive value indicates a larger kinase activity in either *rd1* explants in comparison to WT or CN03 treated explants in comparison to untreated explants. The Kinase Score is the result of two permutation analyses. The Kinase Score is calculated by addition of the Significance Score and the Specificity Score. The Significance Score indicates the significance of the change represented by the Kinase Statistic between two groups (using 500 permutations across sample labels). The Specificity Score indicates the specificity of the Kinase Statistic with respect to the number of peptides used for predicting the corresponding kinase (using 500 permutations across target peptides).

The kinases are ranked by the Kinase Score. The highest-ranking predicted kinases from the significant STK peptide sets are represented on a phylogenetic tree of the human protein kinase family generated in Coral, a web-based application http://phanstiel-lab.med.unc.edu/CORAL/) (86).

Pathway analysis: Pathway analysis was performed in Enrichr (https://maayanlab.cloud/Enrichr/), which is a comprehensive resource for curated gene sets and a search engine that accumulates biological knowledge for further biological discoveries (36,37). We used differentially phosphorylated peptides and predicted upstream kinases as input list for Enrichr analysis. Visualization was performed in GraphPad Prism (version 9) using known matrices from the analysis.

Histology: For retinal cross-section preparation, the eyes were marked nasally and cornea, iris, lens, and vitreous were carefully removed. The remaining eyecups were fixed in 4% PFA for 2 h at room temperature. Incubation with graded sucrose solutions was performed for cryoprotection. Eyes were embedded in Tissue-Tek and cut into 14 µm sections. Immunostaining was performed on retinal cross-sections derived from 3 different mice by incubating with primary antibody against CREB1 (1:200; Proteintech), KCNA3 (1:200; Alomone labs), KCNA6 (1:300; Alomone labs), F263 (1:100; Abcam), TOP2A (1:500; Proteintech), GRIK2 (1:100; Invitrogen) diluted in blocking solution at 4 °C overnight. The negative control was obtained by incubating the retinal cross-sections at 4 °C overnight with the blocking solution devoid of the primary antibody. Alexa Fluor 488 antibody was used as secondary antibody. Sections were mounted with DAPI. Images were captured using 9 Z-stacks with maximum intensity projection (MIP) on a Zeiss Axio Imager Z1 ApoTome Microscope MRm digital camera (Zeiss, Oberkochen, Germany) with a 20x APOCHROMAT objective. The excitation (λ_{Exc}) / emission (λ_{Em}.) characteristics of the filter sets used for the fluorophores were as follows: DAPI (λ_{Exc}. = 369 nm, λ_{Em}. = 465 nm) and AF488 (λ_{Exc} = 490 nm, λ_{Em} = 525 nm). Adobe Photoshop (CS5Adobe Systems Incorporated, San Jose, CA) was used for image processing.

Histological image analysis: Fluorescence intensity data were generated from images of retinal sections derived from 3 different wild-type (WT) P11 mice, using the image profiling function included in the Zen software (Zeiss). Based on the fluorescence intensity data, a signal intensity distribution plot was generated in which each antibody was compared to its corresponding negative control (Figure 5 b). To account for the high variability inherent to immunostaining, the relative signal intensity was also calculated (Figure S 2). The bar graphs represent the ratio of the mean signal intensity for a single antibody (antigen) in a given retinal layer divided by the negative control value. The ratios obtained are expressed as mean ± SD. Graphs were prepared using Prism 8 for Windows (GraphPad Software).

Acknowledgements

We thank Norman Rieger for excellent technical assistance and Rik de Wijn, Savithri Rangarajan, and Liesbeth Houkes for helpful discussion on data analysis.

Author contribution

Conceptualization, JG, TT and FPD; methodology, AR, AT; writing—original draft preparation, AR, AT, RH, TT, JG and FPD; writing—review and editing, AR, AT, RH, TT, JG and FPD; supervision, JG, TT and FPD; funding acquisition, JG and FPD.

Conflict of interests

AR, TT, RH, JG are current or former employees of PamGene International B.V., 's-Hertogenbosch, The Netherlands. FPD is shareholder of the company Mireca Medicines, Tübingen, Germany, which intends to forward clinical testing of CN03.

Funding

This research was funded by European Union Horizon 2020 Research and Innovation Programme—*trans*Med under the Marie Curie grant agreement No. 765441 (*trans*Med; H2020-MSCA-765441).

Data availability

The datasets used and/or analysed during the current study are available from the corresponding author on reasonable request.

References

1. Galan A, Chizzolini M, Milan E, Sebastiani A, Costagliola C, Parmeggiani F: **Good Epidemiologic Practice in Retinitis Pigmentosa: From Phenotyping to Biobanking**. *Curr Genomics* 2011, **12**:260–266.
2. Farrar GJ, Carrigan M, Dockery A, Millington-Ward S, Palfi A, Chadderton N, Humphries M, Kiang AS, Kenna PF, Humphries P: **Toward an elucidation of the molecular genetics of inherited retinal degenerations**. *Hum Mol Genet* 2017, **26**:R2–R11.
3. Paquet-Durand F, Hauck SM, Van Veen T, Ueffing M, Ekström P: **PKG activity causes photoreceptor cell death in two retinitis pigmentosa models**. *J Neurochem* 2009, **108**:796–810.
4. Power M, Das S, Schütze K, Marigo V, Ekström P, Paquet-Durand F: **Cellular mechanisms of hereditary photoreceptor degeneration – Focus on cGMP**. *Prog Retin Eye Res* 2020, **74**:100772.
5. Paquet-Durand F, Hauck SM, Veen T Van, Ueffing M, Ekström P: **PKG activity causes photoreceptor cell death in two retinitis pigmentosa models**. *J Neurochem* 2009, **108**:796–810.
6. Koch M, Scheel C, Ma H, Yang F, Stadlmeier M, Glück AF, Murenu E, Traube FR, Carell T, Biel M, et al.: **The cGMP-dependent protein kinase 2 contributes to cone photoreceptor degeneration in the Cnga3-deficient mouse model of achromatopsia**. *Int J Mol Sci* 2021, **22**:52.
7. Lorenz R, Bertinetti D, Herberg FW: **cAMP-dependent protein kinase and cGMP-dependent protein kinase as cyclic nucleotide effectors**. In *Non-canonical cyclic nucleotides*. . 2015:105–122.
8. Tang M, Wang G, Lu P, Karas RH, Aronovitz M, Heximer SP, Kaltenbronn KM, Blumer KJ, Siderovski DP, Zhu Y, et al.: **Regulator of G-protein signaling-2 mediates vascular smooth muscle relaxation and blood pressure**. *Nat Med* 2003, **9**:1506–1512.
9. Antl M, Von Brühl ML, Eiglsperger C, Werner M, Konrad I, Kocher T, Wilm M, Hofmann F, Massberg S, Schlossmann J: **IRAG mediates NO/cGMP-dependent inhibition of platelet aggregation and thrombus formation**. *Blood* 2007, **109**:552–559.
10. Prysyazhna O, Wolhuter K, Switzer C, Santos C, Yang X, Lynham S, Shah AM, Eaton P, Burgoyne JR: **Blood Pressure-Lowering by the Antioxidant Resveratrol Is Counterintuitively Mediated by Oxidation of cGMP-Dependent Protein Kinase**. *Circulation* 2019, **140**:126–137.
11. Francis SH, Busch JL, Corbin JD: **cGMP-dependent protein kinases and cGMP phosphodiesterases in nitric oxide and cGMP action**. *Pharmacol Rev* 2010, **62**:525–563.
12. Feil S, Zimmermann P, Knorn A, Brummer S, Schlossmann J, Hofmann F, Feil R: **Distribution of cGMP-dependent protein kinase type I and its isoforms in the mouse brain and retina**. *Neuroscience* 2005, **135**:863–868.
13. French PJ, Bijman J, Edixhoven M, Vaandrager AB, Scholte BJ, Lohmann SM, Nairn AC, De Jonge HR: **Isotype-specific activation of cystic fibrosis transmembrane conductance regulator-chloride channels by cGMP-dependent protein kinase II**. *J Biol Chem* 1995, **270**:26626–26631.
14. Rangaswami H, Marathe N, Zhuang S, Chen Y, Yeh JC, Frangos JA, Boss GR, Pilz RB: **Type II cGMP-dependent protein kinase mediates osteoblast mechanotransduction**. *J Biol Chem* 2009, **284**:14796–808.
15. Tolone A, Belhadj S, Rentsch A, Schwede F, Paquet-Durand F: **The cGMP pathway and inherited photoreceptor degeneration: Targets, compounds, and biomarkers**. *Genes (Basel)* 2019, **10**:1–16.
16. Quadri M, Comitato A, Palazzo E, Tiso N, Rentsch A, Pellacani G, Marconi A, Marigo V: **Activation of cGMP-Dependent Protein Kinase Restricts Melanoma Growth and Invasion by Interfering with the EGF/EGFR Pathway**. *J Invest Dermatol* 2021, doi:10.1016/j.jid.2021.06.011.

17. Arango-Gonzalez B, Trifunović D, Sahaboglu A, Kranz K, Michalakis S, Farinelli P, Koch S, Koch F, Cottet S, Janssen-Bienhold U, et al.: **Identification of a common non-apoptotic cell death mechanism in hereditary retinal degeneration**. *PLoS One* 2014, **9**:1–11.
18. Farber DB, Park S, Yamashita C: **Cyclic GMP-phosphodiesterase of rd retina: Biosynthesis and content**. *Exp Eye Res* 1988, **46**:363–374.
19. Sancho-Pelluz J, Arango-Gonzalez B, Kustermann S, Romero FJ, Van Veen T, Zrenner E, Ekström P, Paquet-Durand F: **Photoreceptor cell death mechanisms in inherited retinal degeneration**. *Mol Neurobiol* 2008, **38**:253–269.
20. Han J, Dinculescu A, Dai X, Du W, Clay Smith W, Pang J: **Review: The history and role of naturally occurring mouse models with Pde6b mutations**. *Mol Vis* 2013, **19**:2579.
21. Vighi E, Trifunovic D, Veiga-Crespo P, Rentsch A, Hoffmann D, Sahaboglu A, Strasser T, Kulkarni M, Bertolotti E, Heuvel A Van Den, et al.: **Combination of cGMP analogue and drug delivery system provides functional protection in hereditary retinal degeneration**. *Proc Natl Acad Sci U S A* 2018, **115**:E2997–E3006.
22. Paquet-Durand F, Azadi S, Hauck SM, Ueffing M, Van Veen T, Ekström P: **Calpain is activated in degenerating photoreceptors in the rd1 mouse**. *J Neurochem* 2006, **96**:802–814.
23. Trifunović D, Dengler K, Michalakis S, Zrenner E, Wissinger B, Paquet-Durand F: **cGMP-dependent cone photoreceptor degeneration in the cpfl1 mouse retina**. *J Comp Neurol* 2010, **518**:3604–3617.
24. Roy A, Groten J, Marigo V, Tomar T, Hilhorst R: **Identification of novel substrates for cGMP dependent protein kinase (PKG) through kinase activity profiling to understand its putative role in inherited retinal degeneration**. *Int J Mol Sci* 2021, **22**:1–17.
25. Zhao J, Trewhella J, Corbin J, Francis S, Mitchell R, Brushia R, Walsh D: **Progressive cyclic nucleotide-induced conformational changes in the cGMP-dependent protein kinase studied by small angle x-ray scattering in solution**. *J Biol Chem* 1997, **272**:31929–31936.
26. Belhadj S, Tolone A, Christensen G, Das S, Chen Y, Paquet-Durand F: **Long-term, serum-free cultivation of organotypic mouse retina explants with intact retinal pigment epithelium**. *J Vis Exp* 2020, **2020**:1–13.
27. Sahaboglu A, Paquet-Durand O, Dietter J, Dengler K, Bernhard-Kurz S, Ekström PAR, Hitzmann B, Ueffing M, Paquet-Durand F: **Retinitis pigmentosa: Rapid neurodegeneration is governed by slow cell death mechanisms**. *Cell Death Dis* 2013, **4**:e488–e488.
28. Zeng HY, Tso MOM, Lai S, Lai H: **Activation of nuclear factor-κB during retinal degeneration in rd mice**. *Mol Vis* 2008, **14**:1075.
29. Höltje M, Brunk I, Große J, Beyer E, Veh RW, Bergmann M, Große G, Ahnert-Hilger G: **Differential distribution of voltage-gated potassium channels Kv 1.1-Kv1.6 in the rat retina during development**. *J Neurosci Res* 2007, **85**:19–33.
30. Dvoriantchikova G, Grant J, Santos ARC, Hernandez E, Ivanov D: **Neuronal NAD(P)H oxidases contribute to ROS production and mediate RGC death after Ischemia**. *Investig Ophthalmol Vis Sci* 2012, **53**:2823–2830.
31. Vila A, Whitaker CM, O'Brien J: **Membrane-associated guanylate kinase scaffolds organize a horizontal cell synaptic complex restricted to invaginating contacts with photoreceptors**. *J Comp Neurol* 2017, **525**:850–867.
32. Anderson DH, Hageman GS, Mullins RF, Neitz M, Neitz J, Ozaki S, Preissner KT, Johnson L V.: **Vitronectin gene expression in the adult human retina**. *Investig Ophthalmol Vis Sci* 1999, **40**:3305–3315.

33. Cammalleri M, Dal Monte M, Amato R, Lapi D, Bagnoli P: **Novel Insights into Beta 2 Adrenergic Receptor Function in the rd10 Model of Retinitis Pigmentosa**. *Cells* 2020, **9**:2060.
34. Ganguly A, Shields CL: **Differential gene expression profile of retinoblastoma compared to normal retina**. *Mol Vis* 2010, **16**:1292.
35. Huang W, Xing W, Ryskamp DA, Punzo C, Križaj D: **Localization and phenotype-specific expression of ryanodine calcium release channels in C57BL6 and DBA/2J mouse strains**. *Exp Eye Res* 2011, **93**:700–709.
36. Xie Z, Bailey A, Kuleshov M V., Clarke DJB, Evangelista JE, Jenkins SL, Lachmann A, Wojciechowicz ML, Kropiwnicki E, Jagodnik KM, et al.: **Gene Set Knowledge Discovery with Enrichr**. *Curr Protoc* 2021, **1**:e90.
37. Kuleshov M V., Jones MR, Rouillard AD, Fernandez NF, Duan Q, Wang Z, Koplev S, Jenkins SL, Jagodnik KM, Lachmann A, et al.: **Enrichr: a comprehensive gene set enrichment analysis web server 2016 update**. *Nucleic Acids Res* 2016, **44**:W90–W97.
38. Celesia GG, DeMarco PJ: **Anatomy and physiology of the visual system**. *J Clin Neurophysiol* 1994, **11**:482–492.
39. Lu Y, Zhang L, Zhu R, Zhou H, Fan H, Wang Q: **PFKFB3, a key glucose metabolic enzyme regulated by pathogen recognition receptor TLR4 in liver cells**. *Ther Adv Endocrinol Metab* 2020, **11**:2042018820923474.
40. Canzoniero LMT, Adornetto A, Secondo A, Magi S, Dell'Aversano C, Scorziello A, Amoroso S, Di Renzo G: **Involvement of the nitric oxide/protein kinase G pathway in polychlorinated biphenyl-induced cell death in SH-SY 5Y neuroblastoma cells**. *J Neurosci Res* 2006, **84**:692–697.
41. González-Forero D, Portillo F, Gómez L, Montero F, Kasparov S, Moreno-López B: **Inhibition of resting potassium conductances by long-term activation of the NO/cGMP/protein kinase G pathway: A new mechanism regulating neuronal excitability**. *J Neurosci* 2007, **27**:6302–6312.
42. Xu J, Morris L, Thapa A, Ma H, Michalakis S, Biel M, Baehr W, Peshenko I V., Dizhoor AM, Ding XQ: **cGMP accumulation causes photoreceptor degeneration in CNG channel deficiency: Evidence of cGMP cytotoxicity independently of enhanced CNG channel function**. *J Neurosci* 2013, **33**:14939–14948.
43. Farber DB, Lolley RN: **Cyclic guanosine monophosphate: Elevation in degenerating photoreceptor cells of the C3H mouse retina**. *Science (80-)* 1974, **186**:449–451.
44. Lolley RN, Farber DB, Rayborn ME, Hollyfield JG: **Cyclic gmp accumulation causes degeneration of photoreceptor cells: Simulation of an inherited disease**. *Science (80-)* 1977, **196**:664–666.
45. Paquet-Durand F, Beck S, Michalakis S, Goldmann T, Huber G, Mühlfriedel R, Trifunović D, Fischer MD, Fahl E, Duetsch G, et al.: **A key role for cyclic nucleotide gated (CNG) channels in cGMP-related retinitis pigmentosa**. *Hum Mol Genet* 2011, **20**:941–947.
46. Barabas P, Peck CC, Krizaj D: **Do calcium channel blockers rescue dying photoreceptors in the pde6b rd1 mouse?** *Adv Exp Med Biol* 2010, **664**:491–499.
47. Ma H, Butler MR, Thapa A, Belcher J, Yang F, Baehr W, Biel M, Michalakis S, Ding XQ: **cGMP/protein kinase G signaling suppresses inositol 1,4,5-trisphosphate receptor phosphorylation and promotes endoplasmic reticulum stress in photoreceptors of cyclic nucleotide-gated channel-deficient mice**. *J Biol Chem* 2015, **290**:20880–20892.
48. Makhoul S, Walter E, Pagel O, Walter U, Sickmann A, Gambaryan S, Smolenski A, Zahedi RP, Jurk K: **Effects of the NO/soluble guanylate cyclase/cGMP system on the functions of human platelets**. *Nitric Oxide - Biol Chem* 2018, **76**:71–80.

49. Rasmussen M, Welinder C, Schwede F, Ekström P: **The cGMP system in normal and degenerating mouse neuroretina: New proteins with cGMP interaction potential identified by a proteomics approach**. *J Neurochem* 2020, doi:10.1111/jnc.15251.
50. Roy A, Hilhorst R, Groten J, Paquet-Durand F, Tomar T: **Technological advancements to study cellular signaling pathways in inherited retinal degenerative diseases**. *Curr Opin Pharmacol* 2021, **60**:102–110.
51. Bachmann M, Li W, Edwards MJ, Ahmad SA, Patel S, Szabo I, Gulbins E: **Voltage-Gated Potassium Channels as Regulators of Cell Death**. *Front Cell Dev Biol* 2020, **8**:1571.
52. Szabò I, Gulbins E, Apfel H, Zhang X, Barth P, Busch AE, Schlottmann K, Pongs O, Lang F: **Tyrosine phosphorylation-dependent suppression of a voltage-gated K+ channel in T lymphocytes upon Fas stimulation**. *J Biol Chem* 1996, **271**:20465–20469.
53. Storey NM, Gómez-Angelats M, Bortner CD, Armstrong DL, Cidlowski JA: **Stimulation of Kv1.3 Potassium channels by death receptors during apoptosis in Jurkat T lymphocytes**. *J Biol Chem* 2003, **278**:33319–33326.
54. Koeberle PD, Schlichter LC: **Targeting KV channels rescues retinal ganglion cells in vivo directly and by reducing inflammation**. *Channels* 2010, **4**:337–346.
55. Butt E, Abel K, Krieger M, Palm D, Hoppe V, Hoppe J, Walter U: **cAMP- and cGMP-dependent protein kinase phosphorylation sites of the focal adhesion vasodilator-stimulated phosphoprotein (VASP) in vitro and in intact human platelets**. *J Biol Chem* 1994, **269**:14509–14517.
56. Nagai-Kusuhara A, Nakamura M, Mukuno H, Kanamori A, Negi A, Seigel GM: **cAMP-responsive element binding protein mediates a cGMP/protein kinase G-dependent anti-apoptotic signal induced by nitric oxide in retinal neuro-glial progenitor cells**. *Exp Eye Res* 2007, **84**:152–162.
57. Finkbeiner S: **CREB couples neurotrophin signals to survival messages**. *Neuron* 2000, **25**:11–14.
58. Sakamoto KM, Frank DA: **CREB in the pathophysiology of cancer: Implications for targeting transcription factors for cancer therapy**. *Clin Cancer Res* 2009, **15**:2583–2587.
59. Azadi S, Paquet-durand F, Medstrand P, Veen T Van, Ekström P: **Up-regulation and increased phosphorylation of protein kinase C (PKC) δ, μ and θ in the degenerating rd1 mouse retina**. *Mol Cell Neurosci* 2006, **31**:759–773.
60. Gonzalez GA, Montminy MR: **Cyclic AMP stimulates somatostatin gene transcription by phosphorylation of CREB at serine 133**. *Cell* 1989, **59**:675–680.
61. Bito H, Deisseroth K, Tsien RW: **CREB phosphorylation and dephosphorylation: A Ca2+- and stimulus duration-dependent switch for hippocampal gene expression**. *Cell* 1996, **87**:1203–1214.
62. Dong E, Bachleda A, Xiong Y, Osawa S, Weiss ER: **Reduced phosphoCREB in Müller glia during retinal degeneration in rd10 mice**. *Mol Vis* 2017, **23**:90.
63. Lonze BE, Ginty DD: **Function and regulation of CREB family transcription factors in the nervous system**. *Neuron* 2002, **35**:605–623.
64. Preissner KT, Seiffert D: **Role of vitronectin and its receptors in haemostasis and vascular remodeling**. *Thromb Res* 1998, **89**:1–21.
65. Biasella F, Plössl K, Karl C, Weber BHF, Friedrich U: **Altered protein function caused by AMD-associated variant rs704 links vitronectin to disease pathology**. *Investig Ophthalmol Vis Sci* 2020, **61**:2.
66. Arroba AI, Campos-Caro A, Aguilar-Diosdado M, Valverde ÁM: **IGF-1, inflammation and retinal degeneration: A close network**. *Front Aging Neurosci* 2018, **10**:203.

67. Burmistrova O, Olias-Arjona A, Lapresa R, Jimenez-Blasco D, Eremeeva T, Shishov D, Romanov S, Zakurdaeva K, Almeida A, Fedichev PO, et al.: **Targeting PFKFB3 alleviates cerebral ischemia-reperfusion injury in mice**. *Sci Rep* 2019, **9**:1–13.
68. Min J, Zeng T, Roux M, Lazar D, Chen L, Tudzarova S: **The Role of HIF1α-PFKFB3 pathway in Diabetic Retinopathy**. *J Clin Endocrinol Metab* 2021, doi:10.1210/clinem/dgab362.
69. Hurley JB: **Retina Metabolism and Metabolism in the Pigmented Epithelium: A Busy Intersection**. *Annu Rev Vis Sci* 2021, **7**.
70. Pan YR, Song JY, Fan B, Wang Y, Che L, Zhang SM, Chang YX, He C, Li GY: **MTOR may interact with PARP-1 to regulate visible light-induced parthanatos in photoreceptors**. *Clin Experiment Ophthalmol* 2020, **48**:1072–1084.
71. Avet-Rochex A, Carvajal N, Christoforou CP, Yeung K, Maierbrugger KT, Hobbs C, Lalli G, Cagin U, Plachot C, McNeill H, et al.: **Unkempt Is Negatively Regulated by mTOR and Uncouples Neuronal Differentiation from Growth Control**. *PLoS Genet* 2014, **10**:e1004624.
72. Sinha D, Valapala M, Shang P, Hose S, Grebe R, Lutty GA, Zigler JS, Kaarniranta K, Handa JT: **Lysosomes: Regulators of autophagy in the retinal pigmented epithelium**. *Exp Eye Res* 2016, **144**:46–53.
73. Nakahara T, Morita A, Yagasaki R, Mori A, Sakamoto K: **Mammalian Target of Rapamycin (mTOR) as a Potential Therapeutic Target in Pathological Ocular Angiogenesis**. *Biol Pharm Bull* 2017, **40**:2045–2049.
74. Fan B, Li FQ, Zuo L, Li GY: **mTOR inhibition attenuates glucose deprivation-induced death in photoreceptors via suppressing a mitochondria-dependent apoptotic pathway**. *Neurochem Int* 2016, **99**:178–186.
75. Petit L, Punzo C: **mTORC1 sustains vision in retinitis pigmentosa**. *Oncotarget* 2015, **6**:16786.
76. Punzo C, Kornacker K, Cepko CL: **Stimulation of the insulin/mTOR pathway delays cone death in a mouse model of retinitis pigmentosa**. *Nat Neurosci* 2009, **12**:44–52.
77. Porporato PE, Dhup S, Dadhich RK, Copetti T, Sonveaux P: **Anticancer targets in the glycolytic metabolism of tumors: A comprehensive review**. *Front Pharmacol* 2011, **2**:49.
78. Zhang R, Shen W, Du J, Gillies MC: **Selective knockdown of hexokinase 2 in rods leads to age-related photoreceptor degeneration and retinal metabolic remodeling**. *Cell Death Dis* 2020, **11**:1–15.
79. Léveillard T, Sahel JA: **Metabolic and redox signaling in the retina**. *Cell Mol Life Sci* 2017, **74**:3649–3665.
80. Moreno ML, Mérida S, Bosch-Morell F, Miranda M, Villar VM: **Autophagy dysfunction and oxidative stress, two related mechanisms implicated in retinitis pigmentosa**. *Front Physiol* 2018, **9**:1008.
81. Caffé AR, Ahuja P, Holmqvist B, Azadi S, Forsell J, Holmqvist I, Söderpalm AK, Van Veen T: **Mouse retina explants after long-term culture in serum free medium**. *J Chem Neuroanat* 2002, **22**:263–273.
82. Loo DT: **In situ detection of apoptosis by the TUNEL assay: An overview of techniques**. *Methods Mol Biol* 2011, doi:10.1007/978-1-60327-409-8_1.
83. Zor T, Selinger Z: **Linearization of the Bradford protein assay increases its sensitivity: Theoretical and experimental studies**. *Anal Biochem* 1996, **236**:302–308.
84. Hilhorst R, Houkes L, Mommersteeg M, Musch J, Van Den Berg A, Ruijtenbeek R: **Peptide microarrays for profiling of serine/threonine kinase activity of recombinant kinases and lysates of cells and tissue samples**. *Methods Mol Biol* 2013, **977**:259–271.

85. Chirumamilla CS, Fazil MHUT, Perez-Novo C, Rangarajan S, de Wijn R, Ramireddy P, Verma NK, Vanden Berghe W: **Profiling activity of cellular kinases in migrating T-cells**. *Methods Mol Biol* 2019, **1930**:99–113.
86. Metz KS, Deoudes EM, Berginski ME, Jimenez-Ruiz I, Aksoy BA, Hammerbacher J, Gomez SM, Phanstiel DH: **Coral: Clear and Customizable Visualization of Human Kinome Data**. *Cell Syst* 2018, **7**:347–350.

Supplementary Figures

a

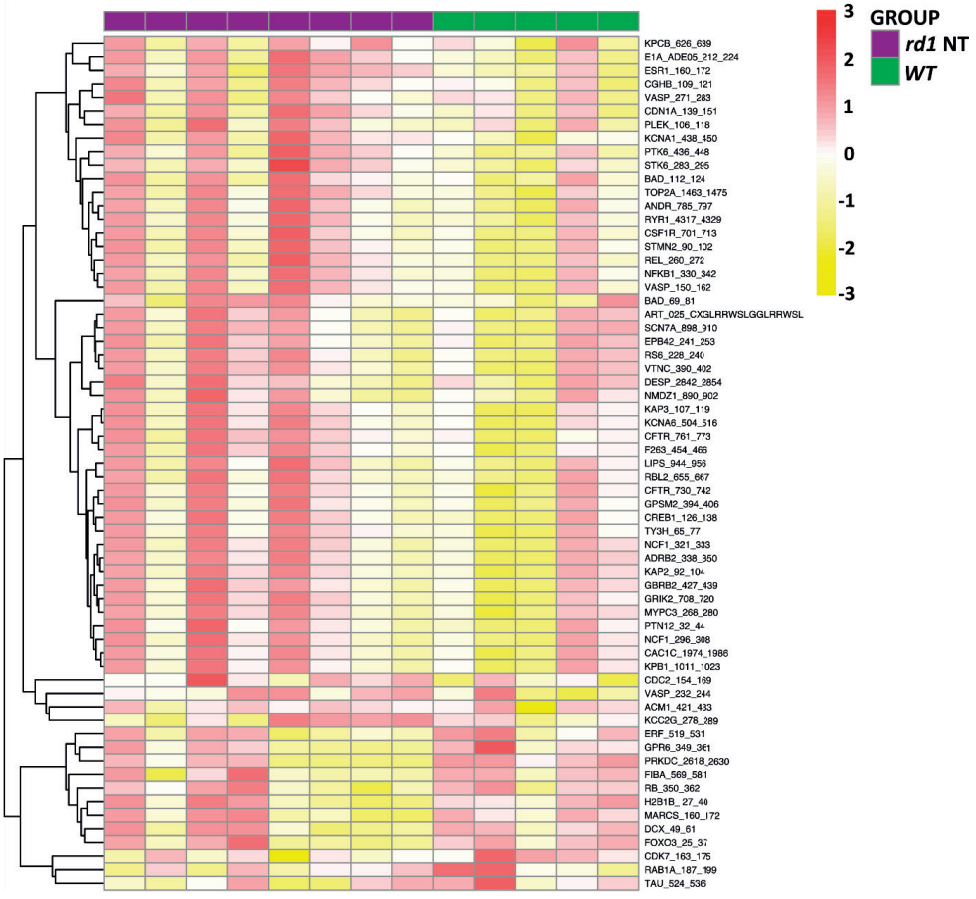

b

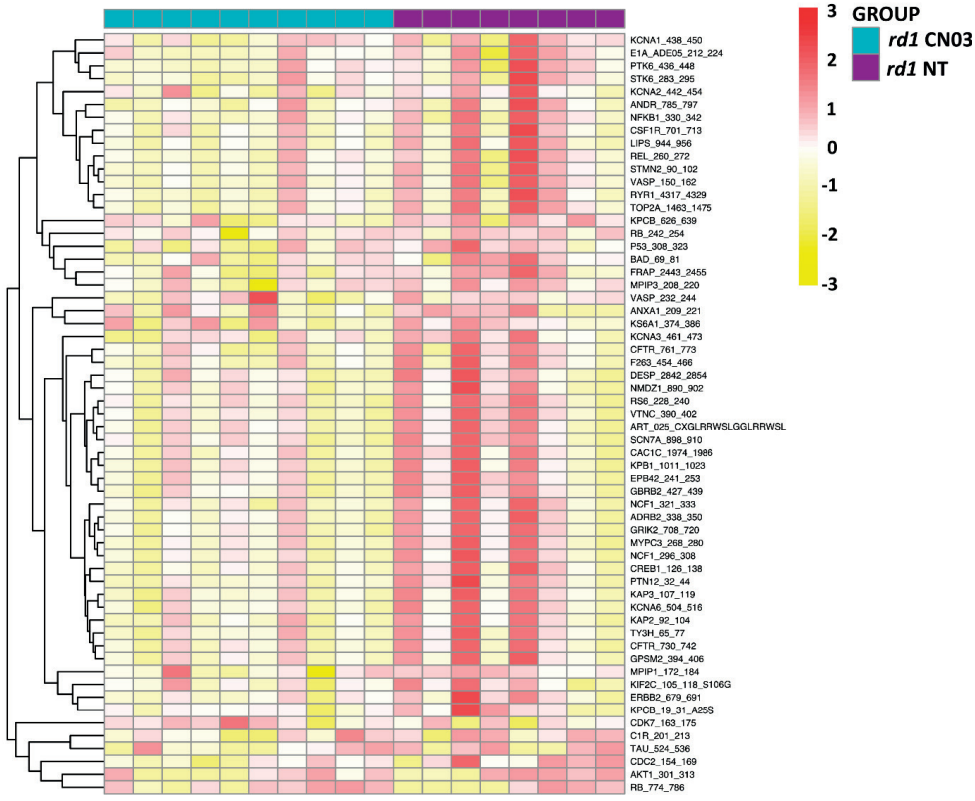

Figure S1. Heatmap representing the overall serine/threonine kinase activity in retinal explants. a) Comparison of protein phosphorylation between *rd1* vs. WT retinal explant cultures. **b**) comparison of CN03 treated *vs*. non-treated (NT) *rd1* retinal explant cultures. The phosphorylated peptides are clustered hierarchically as explained in 'Data Analysis' section (red=high phosphorylation; yellow=low phosphorylation).

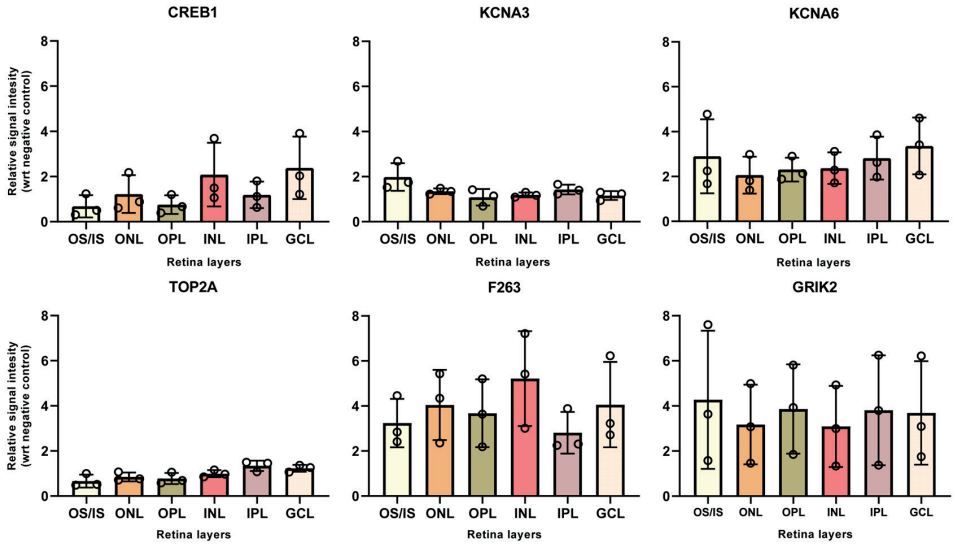

Figure S2. Bar graph representing the relative signal intensity of individual antibodies in different retina layers. The relative signal intensity was calculated as the ratio of the average intensity of the single antibody in a single retina layer divided by the negative control. The analysis was performed from retinal cross-sections derived from n=3 P11 WT mice. Mean with ± SD. OS/IS=outer segment/inner segment, ONL=outer nuclear layer, OPL=outer plexiform layer, INL=inner nuclear layer, IPL=inner plexiform layer, GCL=ganglion cell layer.

5

Chapter 5

Integrative kinase activity profiling and phosphoproteomics of retinal explants during cGMP dependent retinal degeneration

Akanksha Roy*, Jiaming Zhou*, Merijn Nolet, Charlotte Welinder, Yu Zhu, François Paquet-Durand, John Groten, Tushar Tomar and Per Ekström

*Authors contributed equally

Submitted

Abstract

Inherited retinal degenerative diseases (IRDs) are a group of rare diseases that lead to progressive vision loss due photoreceptor degeneration and eventual blindness. Overactivation of cGMP-dependent protein kinase G (PKG), one of the key effectors of cGMP-signalling, has been shown to be involved in photoreceptor cell death in IRD. This PKG has been extensively studied in murine IRD models to assess the pathophysiology behind the retina degeneration. However, there is currently very little insight into what happens at the level of PKG based phosphorylation and downstream events in these IRD models, including *rd10*. The fact that PKG is a serine/threonine kinase (STK) with several hundred potential phosphorylation target provides for a complex cellular signaling pattern during IRDs. In this study we carried out a parallel kinome activity analysis and a phosphoproteomic profiling of *rd10* retinal explant cultures. To enable a focus on PKG related events, *rd10* explants treated with a PKG inhibitor (CN03). The kinome activity results showed that CN03 treatment resulted in an overall decrease in phosphorylation of peptides with a significant decrease in phosphorylation of seven peptides including CREB1 which is a known PKG substrate. The Phosphoproteomics data showed both inhibited and activated peptides. Integration of both datasets resulted in a common biological network altered due to PKG inhibition and includes kinases predominantly from the AGC and CaMK families of kinases (*e.g.* PKG1, PKG2, PKA, CaMKs, RSKs, AKTs, SGKs, and PKD1) as well as associated pathways (e.g. Intracellular signaling by second messengers, Calcium-induced signalling, calmodulin-induced events, MAPK targets and CREB phosphorylation). From the identified peptides and pathways that showed reduced phosphorylating activity, 3 substrates (CREB, CaMK4 and CaMK2) were selected and validated for their presence, activity and localization by immunohistochemical analysis and immunoblotting using *ex vivo* analysis of the *rd10 retina*. In summary, integrative analysis of the kinome activity and phosphoproteomic data revealed known as well as several novel validated PKG substrates in murine IRD model which will provide the basis for improved understanding of biological pathways involved in cGMP-mediated photoreceptor degeneration. Moreover, these results merits exploration of validated PKG targets like phopho-CREB and Phospho-CaMKs as novel (surrogate) biomarkers for determining the effect of clinical PKG-targeted treatment for IRDs.

Keywords
rd10, PKG, CREB, CaMK, Phosphoproteomics, kinome activity profiling

Introduction

Inherited Retinal Degenerative diseases (IRDs) are rare neurodegenerative disorders that are characterized by progressive vision loss, primarily due photoreceptor cell death. Mutations in over 300 genes have been identifiedfor IRDs (https://sph.uth.edu/retnet; information retrieved July 2022), making it imperative to design mutation-independent therapies. Accumulation of cyclic 3',5'-guanosine monophosphate (cGMP) has emerged as a potential and crucial link in more than 20 IRD disease genes affecting at least 30% of IRD patients (1,2). Overactivation of cGMP-dependent protein kinase G (PKG), one of the key effectors of cGMP-signalling, is likely to be involved in photoreceptor cell death (2–4). The most frequently used murine model to study IRDs is *rd1* with a point mutation in exon 7 of the gene for the beta subunit of phosphodiesterase 6 (*pde6b*). The PDE6 enzyme is essential for the proper functioning of the photoreceptor since it hydrolyses cGMP in response to incoming light and as such governs phototransduction. The mutation renders PDE6 non-functional, which results in accumulation of cGMP and subsequent photoreceptor death (1,2,9-11). The *rd1* cell death peaks at postnatal (P) day 12 - P14 (5), while in the *rd10* mouse, another *pde6b* mutation based IRD model with a missense mutation in exon 13 and an overall slower rate of photoreceptor degeneration, cell death peaks around P18 - P22. This means that the retinal structure and function are kept over a longer period of time in *rd10* animals compared to *rd1*, and also that the *rd10* photoreceptor degeneration does not overlap with the retina's developmental apoptosis (6). Together, this makes the *rd10* mice a very attractive model for studying the pathophysiology behind the degeneration, as well as for testing of protective treatments (4).

Much is already known about the structural and functional aspects of the *rd10* degeneration, since this have previously been extensively characterized, including the activation of survival pathways (7–10). Possible alterations to the *rd10* retinal proteome proteome at pre-, peak- and post-degenerative time points (P14, P21 and P28, respectively) have also been addressed (6). A recent gene expression analysis of *rd10* at peak cell death established cGMP-related genes to be affected along with dysregulation of transcription factors that regulate stress response, apoptotic factor production, ion channel activity, optic nerve signal transduction, metabolism, and intracellular homeostasis (11). However, there is currently very limited insight into what happens in the *rd10* retina at the level of PKG based phosphorylation, in spite of the clear degeneration involvement of this kinase in several IRD models, including *rd10* (1,2,4). An increased knowledge of these aspects would hence be most helpful when it comes to describing and understanding the degeneration machinery.

The fact that PKG is a serine/threonine kinase (STK) with likely several hundred potential phosphorylation target provides for a very complex cellular signaling during IRDs and makes it difficult to find targets or biomarkers relevant for photoreceptor cell death. To overcome this hurdle, we here performed a parallel kinome activity analysis and a phosphoproteomic profiling of *rd10* retinal explant cultures. To enable a focus on PKG related events, *rd10* explants treated with a PKG inhibitor (CN03) were compared with untreated ones. Based on the profiling of kinome activity and phosphoproteomic data, several novel PKG substrates were identified and validated for their expression and location in both retinal tissues and explants. This study not only increases our knowledge of the cGMP/PKG-dependent

photoreceptor degeneration mechanism, including suggestions of markers for PKG-based therapies, but also provides a strong foundation for future studies of this and other related questions.

Results

PKG inhibition significantly reduces photoreceptor cell death in rd10 retinal explants

To establish the link of PKG inhibition and its protective effect on *rd10* photoreceptors, *rd10* retinal explants were treated with the well-established PKG inhibitor CN03, which binds to the cGMP-binding sites of PKG and competitively inhibits its activation (4, 5). The retinas of wild type (WT) and *rd10* mice were explanted at P8, when photoreceptor degeneration had not yet started, and CN03 treatment was given to the *rd10* explants from P10 until P18, when the culture was terminated. The photoreceptor cell death was characterized by the TUNEL assay (Fig. 1a), which labels dead cells. There was a significant 20-fold increase in TUNEL positive cells in *rd10* outer nuclear layer (ONL) compared to that of WT explants, proving the validity of the chosen model. Notably, CN03-treatment significantly reduced TUNEL positive cells up to 10-fold in comparison with untreated *rd10*, indicating a protective effect of PKG inhibition against retinal cell death (Fig. 1b).

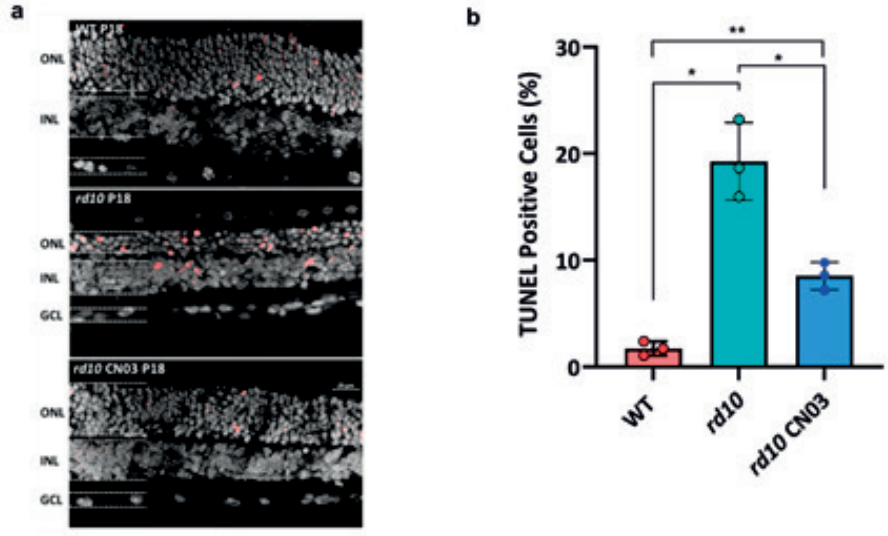

Figure 1: CN03-mediated photoreceptor protection in *rd10* P18 retinal explants: a) Retinal cross-sections derived from WT and *rd10* P18 explant cultures untreated or treated from P8 to P18 with 50 µM CN03. The TUNEL assay (red) indicated dying cells, DAPI (grey) was used as nuclear counterstain. P = postnatal day; ONL = outer nuclear Layer; INL = inner nuclear layer; GCL = ganglion cell layer **b)** Graph representing percentage of TUNEL positive cells for WT and *rd10* untreated or CN03-treated retinal explants. n = 3 different retinal explants per genotype/condition and error bars indicate SD. Significance levels were determined by one-way ANOVA with Dunnett multiple comparisons and significance indicated as * ($p \leq 0.05$) and ** ($p \leq 0.01$);

PKG inhibition reduces Serine/Threonine Kinase activity in rd10 retinal explants

As PKG inhibition significantly decreased photoreceptor cell death in *rd10* retinal explants, the kinase activity profiles of P18 *rd10* and P18 CN03-treated *rd10* retina were determined on multiplex peptides microarrays, known as PamChip® STK arrays. The overall kinome activity was decreased in CN03 treated retinal explants (Fig. 2a). Phosphorylation decreased by around 52% of the 142 peptides on the PamChip® STK arrays. Phosphorylation of seven peptides, namely, CAC1C_1974_1986, ESR1_160_172, PLM_76_88, CREB1_126_138, PTK6_436_448, TOP2A_1463_1475, RBL2_655_667, CGHB_109_121, and STK_283_295, significantly ($p < 0.05$) decreased in *rd10* treated with CN03, whereas phosphorylation of the peptide H2B1B_27_40 increased significantly in the untreated *rd10* retinal explants (Fig. 2b, 2c). Next, the changes in peptide phosphorylation between the two groups were linked to kinases potentially involved in that change by the Upstream Kinase Analysis tool of BioNavigator® software (for details, refer to 'Kinase activity measurements by kinome array' in the Materials and methods section). The Kinase Score and Kinase Statistic were calculated as metrics to identify the kinases with potentially lowered activity. The majority of the linked kinases came from the Ca^{2+}/calmodulin-stimulated kinase (CaMK), casein kinase 1 (CK1) and protein kinase A, G, and C (AGC) families, such as CaMK4, PKAα, CK1ε, CDKL1, PKD1, PKG1, PKG2, and were suggested to have reduced activity by CN03 treatment (Table 1). The relative kinome activity profile of the retinal explants (*rd10 vs*. *rd10* CN03) was represented on a phylogenetic tree of the protein kinase families with color coding of the branches according to Kinase Statistic (Fig. 2d). Here, blue color represents decreased kinase activity in *rd10* CN03 treated retinal explants.

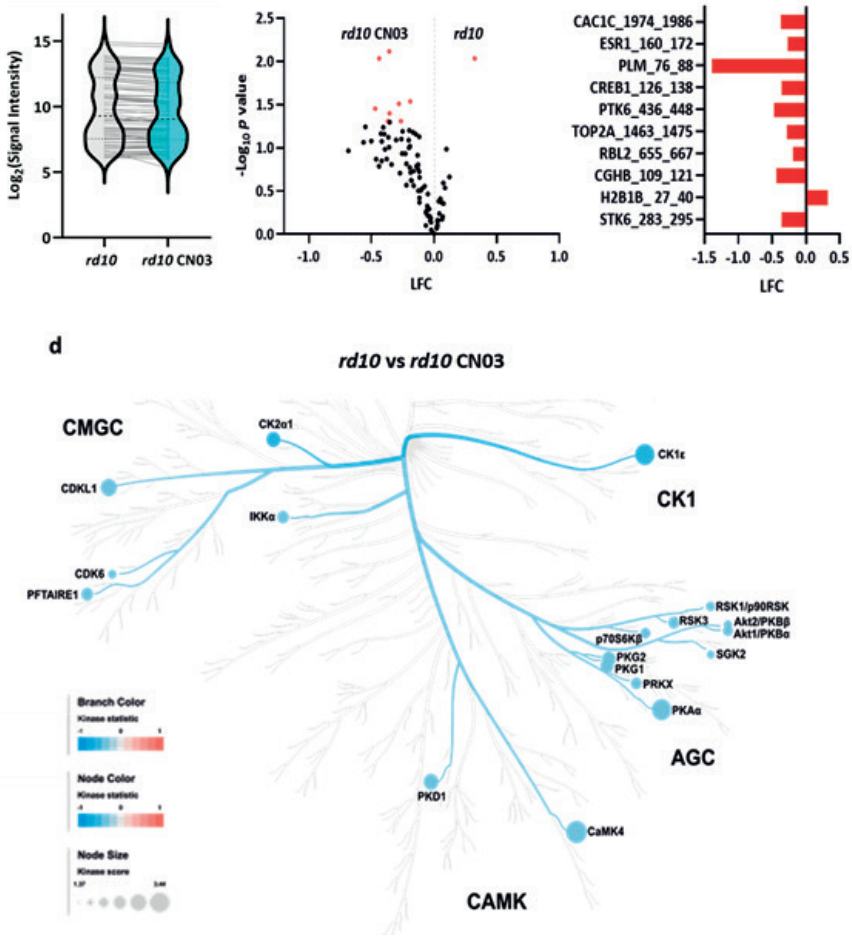

Figure 2: Serine/Threonine Kinase (STK) activity in *rd10* retinal explants in response to PKG inhibition. Retinal explant cultures were either treated with 50 µM CN03 or untreated. The kinase activity of retinal lysates was measured on PamChip® Serine/Threonine Kinase (STK) arrays. **a)** Violin plot representing phosphorylation signal intensity of all the peptides on PamChip® STK arrays as Log_2 signal intensity and their intensity value distribution when comparing *rd10* to *rd10* CN03 treated retinal explants. **b)** Volcano plot showing Log Fold Change (LFC) and $-Log_{10}$ *p* value of phosphorylated peptides. Red dots represent significantly phosphorylated peptides ($p < 0.05$) by Paired t-Test and black dots represent peptides with no significant phosphorylation. **c)** The significantly phosphorylated peptides are represented as bar plot with their respective LFC. **d)** The predicted kinases whose activities were most likely to be altered by the CN03 treatment (refer Table 1) are visualized as a kinome phylogenetic tree where the branch and node color are encoded by Kinase Statistic, with values < 0 (in blue) representing decreased kinase activity in *rd10* CN03 treated retinal explants. The node size is indicated by Kinase Score which is based on specificity and selectivity of that kinase for a particular peptide.

Table 1: Upstream kinase analysis results for *rd10 vs. rd10* CN03. The Kinase Score includes the sum of significance and specificity scores (Score ≥ 1.2 shown in the table). The Kinase Statistic shows the overall change of the peptide set that represents a given kinase. Negative values of Kinase Statistic indicate lower activity in *rd10* CN03. For details refer Material and Method section.

Rank	Kinase Name	Kinase Uniprot ID	Kinase Score	Kinase Statistic
1	CaMK4	Q16566	3.44	-0.43
2	PKAα	P17612	3.26	-0.31
3	CK1ε	P49674	3.24	-0.52
4	CDKL1	Q00532	2.72	-0.42
5	PKD1	Q15139	2.52	-0.42
6	PKG2	Q13237	2.32	-0.31
7	CK2α	P68400	2.39	-0.47
8	PKG1	Q13976	2.27	-0.31
9	PFTAIRE1	O94921	2.04	-0.44
10	IKKα	O15111	2.00	-0.43
11	PRKX	P51817	1.87	-0.30
12	RSK1/p90RSK	Q15349	1.94	-0.39
13	Akt1/PKBα	P31749	1.72	-0.30
14	P70S6Kβ	Q9UBS0	1.72	-0.31
15	RSK3	Q15418	1.58	-0.34
16	mTOR/FRAP	P42345	1.60	-0.37
17	CDK6	Q00534	1.47	-0.35

PKG inhibition alters the phosphoproteome of rd10 retinal explants

To investigate how PKG affected also proteins not represented by the peptides on the chip, we undertook a global phosphoproteomics approach on retinal tissue in which the PKG activity had been inhibited. Proteins from explants treated with CN03 or untreated were extracted after explant homogenization and precipitation of the soluble fraction, followed by phosphorylated peptide enrichment (based on an Fe-NTA Phosphopeptide Enrichment Kit; see Materials and Methods for all details), and then analysed with mass spectrometry (MS). In this way 992 proteins with 597 phosphorylated peptides and 1002 phosphorylation sites were identified. After selection (details in Materials and Methods), 711 phosphorylated sites in 263 proteins were compared from CN03 treated and untreated counterparts, and 85 phosphorylated sites of 50 proteins were identified to be significantly different between the two groups (Fig. 3a), with 28 and 66 phosphorylations being decreased and increased, respectively (Fig. 3b). Some of these proteins, and particularly those with reduced phosphorylation, could be potential cGMP-PKG dependent substrates. Tables 2 and 3 lists the proteins whose phosphorylation was either reduced or increased by the CN03 treatment, respectively.

As several of the affected sites also may be linked to other kinases, we performed in addition an upstream kinase analysis to reveal possible changes in kinome profiling. This identified 28 kinases with altered activities. For kinases with proposed lower activities by CN03 treatment, the mitogen-activated protein kinase (MAPK) family took up the major part, including MAPK1, MAPK3, and MAPK14, whereas calcium/calmodulin-dependent protein kinase II alpha (CaMK2a), MAPK14 and tyrosine-protein kinase ZAP-70 (ZAP70) decreased

most. By contrast, we observed 20 kinases with higher activities from varied kinase groups, among which ribosomal protein S6 kinaseβ-1 (RPS6KB1 or p70S6 kinase), cyclin-dependent kinase 2 (CDK2), and FYN proto-oncogene (FYN) increased most (Fig. 3c).

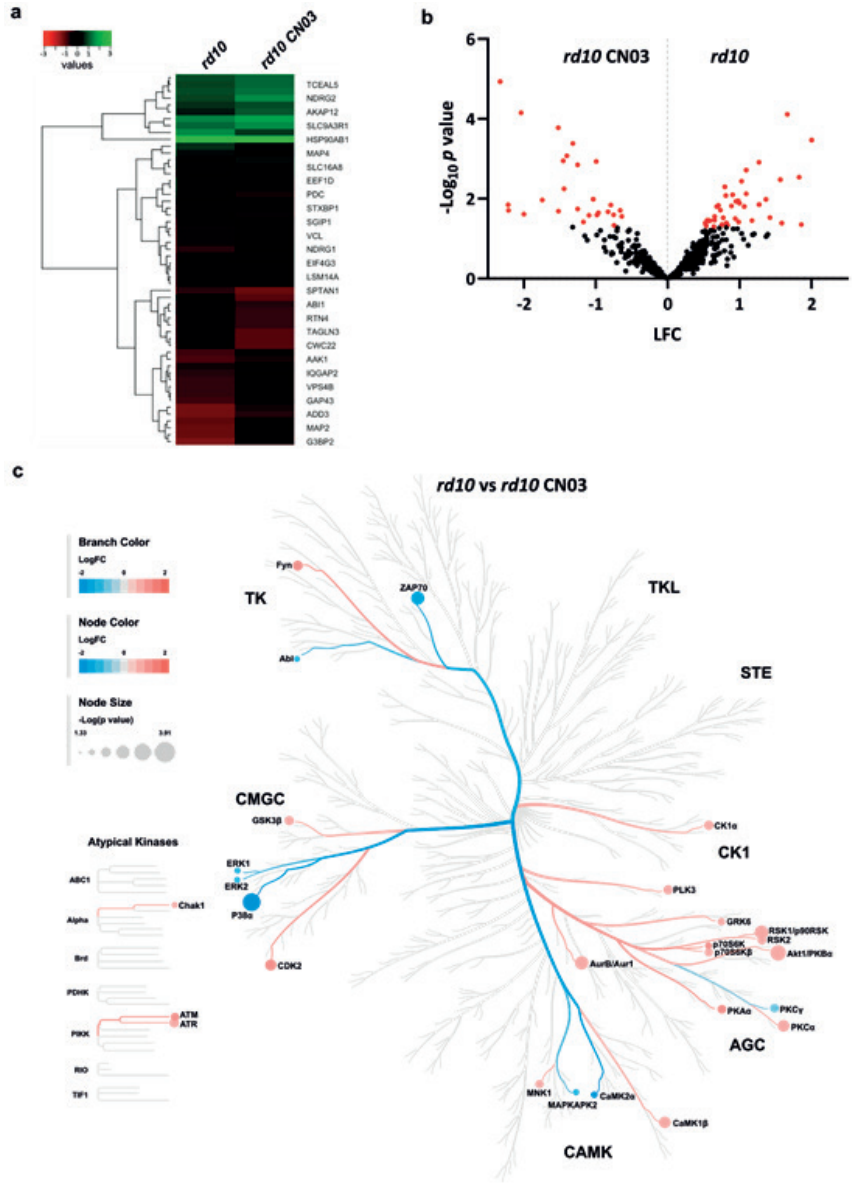

Figure 3: Phosphorylated sites in *rd10* retinal explants in response to PKG inhibition. Retinal explant cultures were either treated with 50 µM CN03 or untreated, followed by phosphopeptide enrichment and mass spectrometry analysis. **a)** Heatmap representing proteins with significantly different phosphorylated sites as Log_2 signal intensity. **b)** Volcano plot showing Log Fold Change (LFC) and $-Log_{10}$ *p* value of phosphorylated sites. Red dots represent significantly phosphorylated sites ($p < 0.05$) and black dots represent peptides with no significant phosphorylation. **c)** The predicted kinases with significantly altered activities are visualized as a kinome phylogenetic tree, where the

branch and node color are encoded by Fold Change, with values < 0 (in blue) and > 0 (in red) representing kinase activity as decreased or increased respectively in *rd10* CN03 retinal explants.

Table 2: Proteins whose phosphorylation decreased after CN03 treatment of *rd10* retinal explants, as detected by phosphoproteomics. The table shows selected proteins with decreased phosphorylation from *rd10* retinal explants after CN03 treatment. The retinal explant cultures were either treated with 50 µM CN03 or left untreated, followed by phosphorylated peptide enrichment and mass spectrometry analysis (MS). For selection of proteins refer to MS analysis in Materials and Methods section.

S. no	Uniprot ID	Gene symbol	Protein description	Position	Fold Change	P value
1	P27816	MAP4	microtubule associated protein 4	352S, 354T	-2.33	1.17E-05
2	Q9UQ35	SRRM2	serine/arginine repetitive matrix 2	1097S	-2.04	7.04E-05
3	Q9UI15	TAGLN3	transgelin 3	163S	-1.52	1.68E-04
4	P17600-1	SYN1	synapsin I	568S	-1.32	4.17E-04
5	Q9UJU6	DBNL	drebrin like	278T	-1.40	8.52E-04
6	Q9UJU6	DBNL	drebrin like	277S	-1.45	1.13E-03
7	Q13813	SPTAN1	spectrin alpha, non-erythrocytic 1	1217S	-0.99	1.16E-03
8	Q9HCG8	CWC22	CWC22 spliceosome associated protein homolog	903S	-1.25	1.43E-03
9	Q13427	PPIG	peptidylprolyl isomerase G	685S	-1.44	5.69E-03
10	P27816	MAP4	microtubule associated protein 4	841S, 688S	-1.03	1.03E-02
11	P20941	PDC	phosducin	54S	-1.74	1.08E-02
12	P46821	MAP1B	microtubule associated protein 1B	2252S	-2.22	1.42E-02
13	Q8WY54	PPM1E	protein phosphatase, Mg2+/Mn2+ dependent 1E	545S	-0.79	1.43E-02
14	Q9P2E9	RRBP1	ribosome binding protein 1	786S	-1.25	1.80E-02
15	P13637	ATP1A3	ATPase Na+/K+ transporting subunit alpha 3	10S	-2.21	1.96E-02
16	Q9H3Q1	CDC42EP4	CDC42 effector protein 4	64S	-0.66	1.97E-02
17	P29692	EEF1D	eukaryotic translation elongation factor 1 delta	133S	-1.52	2.06E-02
18	O00499	BIN1	bridging integrator 1	332S	-0.83	2.14E-02
19	Q9NQC3	RTN4	reticulon 4	344S	-0.96	2.26E-02
20	Q92597	NDRG1	N-myc downstream regulated 1	356T	-2.00	2.44E-02
21	Q15773	MLF2	myeloid leukemia factor 2	237S	-0.75	2.53E-02
22	Q8IZP0	ABI1	abl interactor 1	183S	-0.98	2.55E-02
23	P46821	MAP1B	microtubule associated protein 1B	2068S	-1.09	2.62E-02
24	P61764	STXBP1	syntaxin binding protein 1	516S	-0.64	2.76E-02
25	Q9UQ35	SRRM2	serine/arginine repetitive matrix 2	1077S	-1.17	3.85E-02
26	P46821	MAP1B	microtubule associated protein 1B	1775S	-0.75	4.65E-02

Table 3: Proteins whose phosphorylation increased after CN03 treatment of *rd10* retinal explants, as detected by phosphoproteomics. The table shows selected proteins with increased phosphorylation from *rd10* retinal explants after CN03 treatment. The retinal explant cultures were either treated with 50 µM CN03 or left untreated, followed by phosphorylated peptide enrichment and mass spectrometry analysis (MS). For selection of proteins refer to MS analysis in Materials and Methods section.

S no.	Uniprot ID	Gene symbol	Protein description	Position	Fold Change	P value
1	Q7Z4V5	HDGFL2	HDGF like 2	635S	1.67	7.74E-05
2	P11137	MAP2	microtubule associated protein 2	1654S, 1650T	2.00	3.42E-04
3	P46821	MAP1B	microtubule associated protein 1B	1934T	1.27	1.23E-03
4	Q9UEY8	ADD3	adducin 3	679S, 681S, 683S	1.09	1.91E-03
5	Q9UN86-2	G3BP2	G3BP stress granule assembly factor 2	227T	1.83	2.92E-03
6	Q9ULU8	CADPS	calcium dependent secretion activator	88S. 89S	1.57	3.33E-03
7	Q9UDY2	TJP2	tight junction protein 2	1136S	1.03	3.65E-03
8	Q8N111	CEND1	cell cycle exit and neuronal differentiation 1	9S, 10S	0.80	5.06E-03
9	O75351	VPS4B	vacuolar protein sorting 4 homolog B	102S	1.09	7.59E-03
10	Q02952	AKAP12	A-kinase anchoring protein 12	584S, 583T	0.90	8.04E-03
11	Q08J23	NSUN2	NOP2/Sun RNA methyltransferase 2	723S, 717T	0.81	8.40E-03
12	Q9NXV6	CDKN2AIP	CDKN2A interacting protein	168S, 169S	1.37	1.04E-02
13	Q13576	IQGAP2	IQ motif containing GTPase activating protein 2	16S	0.98	1.13E-02
14	Q5VTR2	RNF20	ring finger protein 20	136S, 138S	0.95	1.17E-02
15	P17677	GAP43	growth associated protein 43	103S	1.00	1.30E-02
16	Q9UN36	NDRG2	NDRG family member 2	332S, 330T	1.27	1.40E-02
17	Q2M2I8	AAK1	AP2 associated kinase 1	936S	0.71	1.47E-02
18	Q9Y4F1	FARP1	FERM, ARH/RhoGEF and pleckstrin domain protein 1	373S	0.89	1.53E-02
19	Q5H9L2	TCEAL5	transcription elongation factor A like 5	120S, 124S, 117T	0.69	1.58E-02
20	Q8ND56	LSM14A	LSM14A mRNA processing body assembly factor	182S, 183S	1.07	1.59E-02
21	O00567	NOP56	NOP56 ribonucleoprotein	543S	0.74	1.95E-02
22	P09651	HNRNPA1	heterogeneous nuclear ribonucleoprotein A1	4S, 6S	0.65	2.82E-02
23	Q9BVG4	PBDC1	polysaccharide biosynthesis domain containing 1	184S	1.43	2.96E-02
24	O95907	SLC16A8	solute carrier family 16 member 8	422S, 428S	0.77	3.00E-02
25	Q9UQ35	SRRM2	serine/arginine repetitive matrix 2	454S	0.94	3.13E-02
26	O14745	SLC9A3R1	SLC9A3 regulator 1	283S, 285S, 286S, 288T	0.65	3.47E-02
27	P46821	MAP1B	microtubule associated protein 1B	1792Y	0.55	3.48E-02
28	P08238	HSP90AB1	heat shock protein 90 alpha family class B member 1	255S	0.57	3.50E-02
29	Q04637	EIF4G1	eukaryotic translation initiation factor 4 gamma 1	1597S	1.17	3.52E-02
30	Q9H6Z4	RANBP3	RAN binding protein 3	57S, 58S	0.58	3.57E-02
31	Q8ND76	CCNY	cyclin Y	324S, 326S	0.99	3.83E-02
32	Q9BQI5	SGIP1	SH3GL interacting endocytic adaptor 1	409T	0.52	4.07E-02
33	O43432	EIF4G3	eukaryotic translation initiation factor 4 gamma 3	267S	0.82	4.08E-02
34	Q7Z4V5	HDGFL2	HDGF like 2	366S, 367S	1.59	4.09E-02
35	P46821	MAP1B	microtubule associated protein 1B	1788S, 1789S, 1793S	0.53	4.25E-02
36	P21964	COMT	catechol-O-methyltransferase	260S, 261S	0.76	4.42E-02
37	Q92597	NDRG1	N-myc downstream regulated 1	366T	1.86	4.45E-02
38	Q9UQ35	SRRM2	serine/arginine repetitive matrix 2	962S, 964S, 963T	0.83	4.68E-02
39	P18206	VCL	vinculin	290S	0.54	4.80E-02
40	P35579	MYH9	myosin heavy chain 9	1943S	0.64	5.00E-02

Potential biological pathways involved in retinal degeneration

Next, we integrated kinase activity profiling data with phosphoproteomics to identify possible common networks of kinases and biological pathways. The predicted kinase list from both datasets (Table S1, S2) were entered into STRING database (12) to find common networks and their connections (Fig. 4). The highest-ranking network of kinases common to both types of generated data were PKG1, PKG2, CaMK4, CaMK2A, MAPKs, AKTs, and RSKs amongst others. In order to link this kinase-based network to a more biological context, we performed a pathway analysis using the Reactome database; Version 2016. Here, the major associated pathways with potentially altered activity after CN03 treatment in *rd10* explants were intracellular signaling by second messengers, calcium induced signalling, calmodulin induced events, MAPK targets, CREB phosphorylation, and RAS activation. Notably, we also

observed pathways like cell cycle activation and suppression of apoptosis among the top predicted ones, which supports the protective effect of PKG inhibitors in cGMP-mediated retinal degeneration.

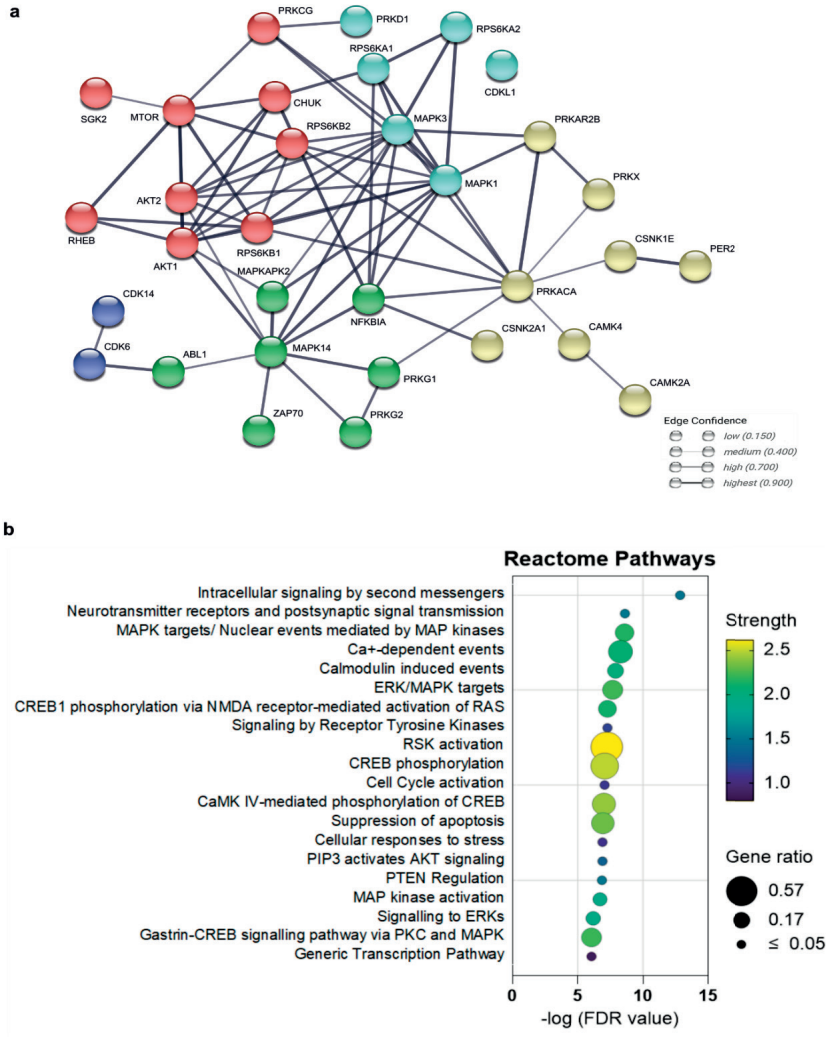

Figure 4: Pathways and network analysis based on integrated kinase analysis of phosphoproteomics and kinome activity profiles of CN03 treated *rd10* retinal explants. a) Network of kinases with potentially altered activity in *rd10* treated with CN03. **b)** Key biological pathways with potentially altered activity in *rd10* treated with CN03. False discovery rate (FDR) is the p value adjusted for multiple testing using the Benjamini Hochberg procedure and measures significance of enrichment. Pathways are ranked according to their FDR values and colored by their strength. Strength describes how large the enrichment effect is and is calculated as Log10(no. observed proteins/ no. of expected proteins). The node size indicates the gene ratio, *i.e.*, the percentage of total genes or proteins in the given Reactome pathways (only input genes or proteins with at least one Reactome pathway were included in the calculation).

Confirmation of CaMKs and CREB expression and activity in murine retina

Based on the kinome profiling and phosphoproteomics results as well as pathway analysis, key proteins (CREB, CaMK2 and CaMK4) corresponding to the peptides that were differentially phosphorylated in *rd10* CN03 compared with untreated *rd10* retinal explants were tested. Immunostaining was performed for retinal sections derived from WT and *rd10* P18 mice (Fig. 5). CaMK2 was found to be expressed in OPL, INL, IPL, and GCL (outer plexiform layer, inner nuclear layer, inner plexiform layer, and ganglion cell layer, respectively) for both WT and *rd10*, with perhaps slightly weaker signal intensity in *rd10* INL. Phosphorylated CaMK2 (pCaMK2, at threonine 287) was located in INL and GCL in WT and *rd10*, with stronger presence in *rd10*. The signal intensity of pCREB predominantly increased in OPL, INL, IPL, and GCL and more so in *rd10* than WT. In contrast, CaMK4 was more abundantly present in OPL, INL, IPL and GCL of WT than *rd10*. Phosphorylated CaMK4 (pCaMK4, at threonine 196/200) showed increased signal intensity in the ONL of WT than *rd10*. Therefore, the localization of the selected PKG targets was confirmed in WT and *rd10* retina tissue with much higher signal intensity of the proteins CREB and CaMK2 in *rd10* as expected. Since an abnormal high level of cGMP, as well as its dependent PKG activity, are mainly observed in photoreceptors, a focused comparison of the fluorescence signal of these proteins was performed within the ONL between these two strains. As seen in Fig. 5, there was no difference for CaMK2, while the signals of pCaMK2 and phosphorylated CREB (pCREB, at Serine 133) were stronger in *rd10* than in WT. By contrast, a higher signal for CaMK4 and its phosphorylation was observed in WT. Taken together, this shows that the *rd10* degeneration has differential effects on the selected players.

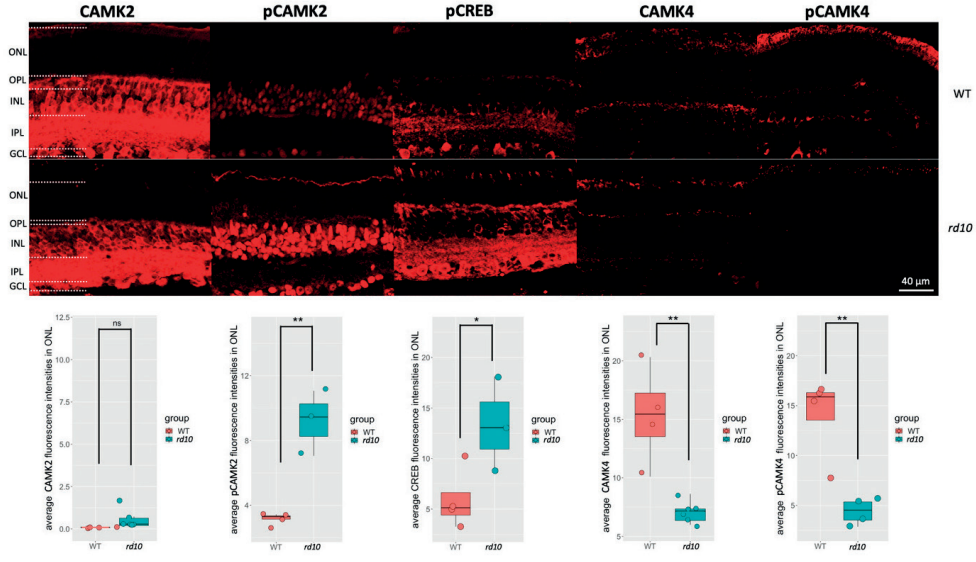

Figure 5: Presence and localization of PKG target proteins in WT and *rd10* retina by immunofluorescence. The panels show retinal cross-sections derived from WT (top) and *rd10* (bottom) P18 mice and stained with secondary antibody for anti-CAMK2, anti-pCAMK2, anti-CAMK4, anti-pCaMK4 or anti-pCREB. ONL: Outer nuclear layer, OPL: Outer plexiform layer, INL: Inner nuclear layer, IPL: Inner plexiform layer, and GCL: Ganglion cell layer.

In order to further analyze and quantify the activation of the selected targets CaMK2, CaMK4, and CREB, we performed immunoblotting of *in vivo* retinas and/or whole retinal explant lysates was performed using antibodies for the activated variants, *i.e.* pCaMK2, pCaMK4, and pCREB (Fig. 6). This allowed us to make strict WT - *rd10* comparisons, as well as to see what the CN03 treatment did to the activation state in the *rd10* explants. For the WT - *rd10* comparisons, there was increased phosphorylation for both pCREB and pCaMK2 for *rd10*, with a significant change for pCaMK2, whereas pCaMK4 was significantly higher in WT. In the CN03 treated *vs.* untreated comparisons, CN03 treatment was found to decrease the pCREB level, but increase that of pCaMK4. The WT vs. *rd10* comparison therefore replicated the ONL results for pCaMK4 from the corresponding immunostainings, where pCaMK4 was higher in WT (Figure 5). The CN03 treatment of the explants then appeared to have at least to some extent normalized the pCaMK4 situation of the *rd10*, since the treated explants displayed an increased presence of the pCaMKIV signal, *i.e.* being more like WT in the WT vs *rd10* comparison.

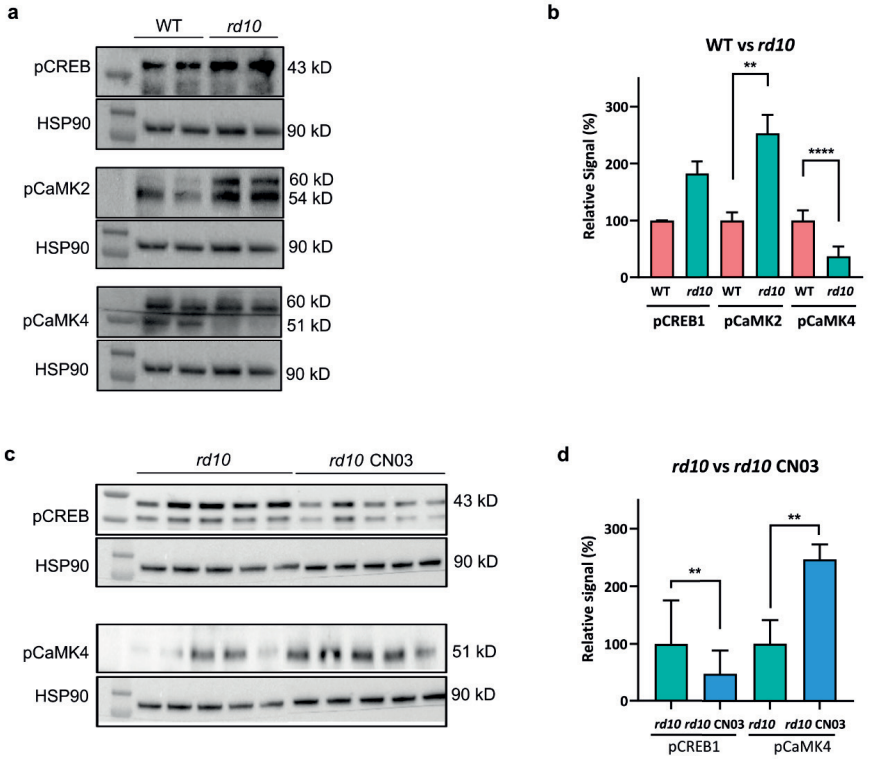

Figure 6: Confirmation of PKG target proteins in retina by Western Blot. a) Representative Western blots showing protein levels for the PKG targets pCREB (at 43 kD), pCMAK2 (at 54 kD), pCAMK4 (at 51 kD) in the retina. **b**) Quantitative analysis with n ≥ 3 tissues for each group. First row of each blot is marker lane. **c**) Protein levels for PKG targets pCREB and pCAMK4 in retinal explants either untreated or treated with CN03 (50μM). **d**) Quantitative analysis of ≥ 5 retinal explants for each group. First row of each blot is marker lane. The significant differences between the groups was determined by unpaired Student's t-test with significance indicated as ** ($p \leq 0.01$) and **** ($p \leq 0.0001$).

Discussion

PKG has emerged as a common target to treat IRDs as its inhibition provides photoreceptor protection in several *in vivo* and *ex vivo* IRD models (1,4,8). However, the proteins targeted by PKG and the affected biological pathways are still unknown. Several mutations in IRDs converge on common cGMP driven PKG signaling routes, suggesting that targeting PKGs could provide a new, common treatment that may benefit a large number of IRD patients. But since PKG as a kinase might have hundreds of substrates, the ones crucial in photoreceptor degeneration need to be elucidated.

Studies into kinase signaling and the use of new potent cGMP inhibitors have revealed incidental, new targets for IRD. For instance, in the work of *Vighi et al.* the immunohistochemistry marker phospho VASP was used to look into the activity of PKG in photoreceptor-like cells derived from *rd1* mice (3). Addition of a PKG inhibitor CN03 to photoreceptor-like cells, reduced phosphorylation at the Serine 239 position of PKG-target VASP. Besides individual target specific approaches, more holistic approaches like MS-centric proteome analysis or kinome substrate-specific peptide microarray has been implemented to identify novel kinases and other enzyme targets simultaneously in the retina (18, 28). With the help of the omics (kinomics and proteomics) approaches, several new cGMP-interacting proteins were found such as CaMK2a, MAPK1/3, and Glycogen synthase kinase 3β (18) as well as potential downstream signaling nodes such as calcium/potassium channel and VASP axis (18, 28) in *rd1* mice retina were identified. However, the careful integration of such omics data generated from one and the same experimental study has not been performed so far and such an integrative approach would offer several advantages to investigate biological pathways in a more comprehensive manner. As such it would provide better understanding of the molecular mediators at the protein level as well as post-translational modifications like phosphorylation levels that regulate the underlying cGMP-mediated retinal degeneration pathways. Therefore, in this study, we sought to investigate the signaling routes downstream of PKG related to photoreceptor cell death by combining kinase activity profiling and phosphoproteomics to identify potential novel PKG targets which are relevant for the photoreceptor degeneration in IRD. In addition, such identified kinases or proteins may serve as potential biomarkers for PKG targeted therapy and its response.

Toxicity of increased cGMP has been linked to photoreceptor degeneration and is a common feature of several IRD related genes (14,15). The cGMP targets of the photoreceptors include cGMP gated ion channels (CNGCs) and PKG, although several other proteins are likely to interact with cGMP (14). Knockdown of only CNGCs does not result in complete photoreceptor protection, whereas down also the PKG provides a long-lasting protective effect (16), which together with the protective effects of PKG inhibition (1,4,8) underlines the importance of PKG in the degeneration process. Our study confirmed that PKG inhibition leads to significant decrease in photoreceptor cell death for the *rd10* model, so to devise mutation-independent therapies for IRDs it is essential to identify the targets and downstream pathways affected by PKG.

The multiplex kinase activity profiling identified several peptides with decreased phosphorylation after PKG inhibition. Of these peptides, CAC1C_1974_1986, CREB1_126_138, PLM_76_88, PTK6_436_448, RBL2_655_667, STK6_283_295 and TOP2A_1463_1475 have been reported as PKG1 and/or PKG2 substrates (17). Interestingly, H2B1B_27_40, the only peptide that had higher phosphorylation in *rd10* untreated explants, was also identified as a potential good PKG2 substrate in the same study. The decrease in peptide phosphorylation due to CN03 treatment was linked to potential kinases such as CaMK4, PKGs and PKA. These kinases have been determined to be upregulated in *rd* retinas and are also identified as potential cGMP-interacting proteins through MS-based proteomics analysis (18). It is thus possible that the proteins corresponding to the mentioned peptides are important PKG targets during the *rd10* photoreceptor degeneration.

The kinase activity profiling makes use of 3D microarray chips with a number of defined substrate peptides to known STK. To allow for the detection of also other, not yet defined substrates, we in addition performed a phosphoproteomic analysis. Here we detected 28 phosphorylations (on 26 proteins) to be reduced after PKG inhibition. According to the kinase profiling study, these decreased phosphorylations may link to reduced kinase activities that were regulated by the cGMP-PKG system. We noticed that some kinases from the MAPK family, including ERK1, ERK2 and p38 (Figure 3c), decreased under CN03 treatment. The MAPK family plays a key role in cell proliferation, differentiation and stress response and the ERK kinases are involved in signaling cascades and transmission of extracellular signals to intracellular targets (19). PKG mediated-signaling has been determined to be necessary *e.g.* for prolonged activation of MAPK in invertebrate associative memory (20), and our finding of PKG inhibitor-mediated reduction in ERKs and p38 MAPK therefore indirectly indicated that cGMP-PKG upregulated the activities of these kinases, likely having detrimental effects during degeneration. In turn this is consistent with a recent report that pharmacological ERK1/2 inhibition had protective effects towards photoreceptor degeneration (21). Interestingly, our results regarding CaMK2α in *rd10* are very compatible with previous work on the likewise cGMP connected *rd1* model, that was obtained by independent methods involving 2D-gel electrophoresis-based proteomics and which concluded increased CaMK2α activity in *rd1* compared to WT (22). Our kinome profiling suggested reduced CaMK2α activity after PKG inhibition in *rd10*, and consequently this would fit with PKG being responsible for the increased CaMK2α activity in *rd1* (22). Moreover, the previous work showed that phosducin, a photoreceptor specific CaMK2α substrate, had increased phosphorylation in *rd1,* whereas we here demonstrated by our phosphoproteomics approach that PKG inhibition reduces phosducin phosphorylation. Time events to describe the (de) phosphorylation of phosducin are therefore needed to shed some more light on its interplay with CaMK targets and their phenotypic readouts in the mice models. However, both the studies indicate that these data make a strong argument for a CaMK2α involvement downstream of PKG in photoreceptor degeneration.

In addition to proteins with reduced phosphorylation, we identified 66 phosphorylated sites that were upregulated when PKG was inhibited, suggesting that the cGMP-PKG system could also negatively regulate other kinases. For the kinases with higher activities under CN03 treatment as suggested by the kinome profiling, some of them have been proven to promote cellular survival, such as three members of ribosomal S6 kinase (RSK) family,

including Ribosomal Protein S6 Kinase B1 (RPS6KB1, highest activity), Ribosomal Protein S6 Kinase B2 (RPS6KB2) and Ribosomal Protein S6 Kinase A1 (RPS6KA1). These kinases prolong cellular wellbeing in a manner of constitutive Bcl-2-associated death promoter (BAD) phosphorylation and protection from BAD-modulated cell death (23). Also, AKT Serine/Threonine Kinase 1 (AKT1) (24) and Glycogen synthase kinase-3β (GSK-3β) (25), with known survival effects, showed higher activities after PKG inhibition. It is noteworthy that GSK-3β was recently shown to be a potential cGMP interacting protein in the proteomics analysis of the retina in *rd* models (18), and future investigations may reveal whether such interactions entail a PKG mediated regulation of the GSK-3β activity. One general interpretation of the kinase activation data could be that the cGMP dependent photoreceptor death involves PKG inhibition of kinases with anti-cell death function during retinal degeneration.

Based on integration of results from kinase activity profiling and phosphoproteomics, CREB1, CaMK2 and CaMK4 were selected as targets for further analyses. CREB1 is a known PKG substrate (17) and it stimulates transcription on binding to DNA cAMP response element and is involved in neuronal survival (26) and different cancers (27). In our previous study, CREB1 was identified to have increased phosphorylation activity in *rd1* retinal explants and was confirmed as one of the potential PKG targets (28). Based on the *in vitro* studies shown in the present report, phosphorylation of CREB1 is decreased by CN03 treatment, supporting further the idea that this step is PKG mediated. CREB1 is targeted by the kinase CaMK2, which is a downstream effector of Ca^{2+} signaling and is activated by increased levels of intracellular Ca^{2+} (29). PKG has also been shown to a activate calmodulin and CaMK2 dependent intracellular mechanism, which stimulates the cardiac ATP-dependent potassium channels in cardiomyocytes (30). As mentioned above, CaMK2 has been demonstrated to have increased activity in *rd1* photoreceptors (22) and reactivation of CAMK2 has been reported to have a protective effect on retinal ganglion cells in glaucoma (32). 'Calmodulin induced events' was identified as one of the major biological pathways potentially affected by CN03 treatment, and calmodulin is a major Ca^{2+} binding protein which activates CaMK2. Calmodulin is also involved in cell death, as its inhibition has been reported to prevent apoptosis in neuronal cells (33,34). CREB1 is also targeted by another kinase, CaMK4, which is in alignment with the results of our upstream kinase analysis and where CaMK4 is one of the kinases with potentially decreased activity due to PKG inhibition. However, both immunofluorescence, which showed a presence mainly in the photoreceptor segments as in a previous study (35), and our immunoblotting results suggested CaMK4 to have higher expression and activity in the WT retina as compared to the *rd10* retina, which was matched by an increased phosphorylation by PKG inhibition in *rd10* explants. CaMK4 promotes neural survival (36) and is reduced in neurodegenerative diseases, such as amyotrophic lateral sclerosis (37). It is thus possible that CaMK4 exerts some neuroprotective effects, that may involve activation of anti-apoptotic gene expression via its substrate NF-kappa B (38). Since CaMKs and CREB1 were also identified as potentially proteins with reduced phosphorylation after CN03 treatment in the *rd1* model (28), the PKG-meditated CaMKs-CREB1 signaling appears as a promising target to develop potential biomarkers for retinal disease progression and therapy response.

In summary, the effect of PKG inhibitor treatments showed a significant overlap in both *rd10* models and previously reported data in *rd1*. The major common peptides with significantly

decreased phosphorylation were CREB1 and TOP2A and kinases potentially involved in differential phosphorylation were PKG1, PKG2, and CaMK4. Still for the *rd10* model reported here, it seems that the CN03 treatment resulted in a lower number of peptides affected when compared to its treatment in *rd1* (28). The difference in number of differentially phosphorylated peptides in both models could be attributed to a distinctive rate of photoreceptor degeneration in *rd1* or *rd10* and the fact that the time point chosen for CN03 treatment was not identical in both models. A straightforward head-to-head comparison of PKG targets in both *rd* models is advised to investigate the expression of these potential PKG targets with time in degenerating *rd1* and *rd10* retinas. Since, for *rd10* at day 18 still some residual PDE6 activity is left, this might be the reason why there were no significant changes observed in differential phosphorylation of peptides with CN03 treatment in *rd1* (harvested around day 10) and *rd10* (harvested around day 20). These time events should be addressed in future studies assessing retinal degeneration.

In the present study we combined multiplex peptide microarray technology and phosphoproteomics, to identify novel targets downstream of cGMP/PKG signaling, and a selection of these were then confirmed by immuno-based techniques. Our results therefore provide new insights in understanding cGMP-mediated retinal degenerative diseases and could also be employed in designing new therapies as well as biomarkers for their treatment.

Materials and Methods

Organotypic retinal explant cultures: Retinas from P8 *rd10* and *wt* mice were used to generate explants following the standard protocol as previously described (13). Mice were euthanized and eyes rapidly enucleated and incubated in R16 medium (07491252A, Gibco, Waltham, MA) and treated for 15 min with 0.12 % proteinase K (21935025, ICN Biomedicals Inc, Irvine, CA), the activity of which was subsequently blocked by 10% fetal bovine serum (F7524, Sigma, Darmstadt, Germany) followed by rinsing in R16 medium. In a sterile environment under a laminar-flow hood, the retina with the retinal pigment epithelium (RPE) attached was separated from the eyes and the anterior segment, lens, vitreous, sclera and choroids were removed. The retina was then incised to give a four-leaf clover shape and transferred to a culture membrane insert (3412; Corning Life Sciences, Corning, NY), with the RPE directly facing the inserts. The inserts with the explants were then put into six-well culture plates (83.3920, Sarstedt, Nümbrecht, Germany) with 1.5 mL serum-free R16 medium with supplements added to each well (Paquet-Durand et al., 2009), incubated at 37°C with a CO_2 level of 5%, and with the medium replaced every second day. Retinas were selected randomly for either treatment or control. For the *rd10* retinas, the first 2 days in culture were without any treatment, and after this, *i.e.* at a time that equals P10, the cultures were exposed to 50 µM Rp-8-Br-PET-cGMPS (a.k.a. CN03 [4], PKG inhibitor; Cat. No.: P 007, Biolog, Bremen, Germany), respectively, with their corresponding untreated controls receiving an equal amount of solvent (water). The end point of the whole culturing procedure was after another eight days of culture, *i.e.* equivalent to P18. The same paradigm (P8 + 10 days) was applied to the *wt* without any treatments. All retinal explant samples were collected for kinome activity microarray measurements or phosphoproteomic based analyses, or fixed, sectioned and used for microscopy-based analyses.

Cryosection and immunohistochemistry: Retinal tissues from *rd10* and *wt in vivo* at P18, as well as P18 cultured explants, were treated with 4% formaldehyde for 2 h, washed 4 × 15 min in phosphate-buffered saline (PBS), cryoprotected in PBS + 10% sucrose for overnight at 4 °C and subsequently with PBS + 25% sucrose for 2 h. After embedding, 12 µm thick retinal cross-sections were cut and collected from a HM560 cryotome (Microm, Walldorf, Germany). The sections were stored in -20 °C for later usage. Cryosections were used for immunohistochemistry as described before (15). Briefly, the cryosections were dried in room temperature for 15 minutes and rehydrated in PBS. They were then blocked with 1% BSA +0.25% Triton X100 + 5% goat serum in PBS in room temperature for 45 min. Primary antibodies were diluted with 1% BSA and 0.25% Triton X100 in PBS (PTX) and incubated at 4°C for overnight; a no primary antibody control ran in parallel. After the incubation the sections were washed 3 × 5 min each in PTX and incubated with a goat anti-rabbit IgG (H+L) cross-adsorbed secondary antibody with Alexa Fluor 594 (#A11037, ThermoFisher) at 1:400 dilution in PTX. After 3 x 5-min PBS washes the sections were mounted with Vectashield DAPI (Vector, Burlingame, CA, USA).

TUNEL assay: To evaluate the neuroprotective effects of CN03 on photoreceptor death a fluorescent terminal deoxynucleotidyl transferase dUTP nick end labelling (TUNEL) assay (#11687495910, Roche Diagnostics, Basel, Switzerland) was performed following the manufacturer's instructions, and used on cryosections generated from *rd10* and *wt* retinal explant cultures.

Microscopy and image processing: A Zeiss Imager Z1 Apotome Microscope (Zeiss, Oberkichen, Germany), with a Zeiss Axiocam digital camera was used for the microscopy-based observations. In the further processing image generation and contrast enhancement were performed identically for all images via use of the ZEN2 software (blue edition). The immunostaining and TUNEL was analysed for staining differences via three sections from three to six animals for each condition, after which the fluorescent intensities of positive cells randomly distributed within in the selected area of interest (outer nuclear layer, ONL, *i.e.* the photoreceptor layer) was assessed. Fluorescence intensity was captured and analysed by the ImageJ software (version 1.53a, NIH, Maryland, USA), where the freehand selection function was used to target the ONL, with the fluorescence intensity calculated with the measure function. The values of all sections from the same animal were averaged before further use.

Materials for retinal explant lysis: Mammalian protein extraction reagent (M-PER™), Halt™ protease and phosphatase inhibitor cocktails and the Coomassie Plus (Bradford Assay) kit were all purchased from Thermo Fischer Scientific.

Retinal explant lysis: Whole retinal explant lysates were prepared in Lysis Buffer (M-PER with 1:100 Protease and Phosphatase Inhibitor cocktails), such that the samples were lysed for 30 minutes on ice followed by centrifugation (16 000 x g for 15 min at 4°C). The supernatant was subsequently divided into aliquots, snap frozen and stored a -80°C until further processing. Protein quantification was performed with Bradford Assay as per the manufacturer's instructions

Kinase activity measurements by kinome array: Kinase Activity profiling was performed on Serine/Threonine Kinase (STK) PamChips®, where each chip comprises of four arrays with 142 Serine/Threonine containing immobilized-peptides which are derived from human phosphoproteome, according to instructions of the manufacturer (PamGene International B.V., 's-hertogenbosch, The Netherlands). Briefly an assay mix was prepared with 0.25 µg of protein lysate, protein kinase buffer (proprietary, PamGene), 0.01% BSA, STK primary antibody mix (proprietary, PamGene), and 400 µM ATP. Firstly, the PamChips® were placed in PamStation12® system and blocked with 2% BSA. Subsequently, assay mix containing active kinases was added and pumped back and forth through PamChip® wells in order to facilitate interactions between the active kinases and the 142 immobilized consensus phospho peptide sequences. The presence of peptides phosphorylated by kinases present in the retinal lysate and their extend of phosphorylation were assessed with an FITC-conjugated secondary antibody targeting towards the primary STK antibody cocktail (40,41). The images of the arrays were recorded at multiple exposure times and the signal intensity of each peptide was quantified by BioNavigator® software version 6.3.67.0 (PamGene International B.V., 's-Hertogenbosch, North Brabant, The Netherlands). The signal intensity at multiple time points was combined to a single value and log2 transformed. The overall differences in the *rd1* untreated (*rd1* NT) and CN03-treated (*rd1* CN03) samples STK peptide phosphorylation profiles were visualized as violin plots (GraphPad Prism version 9.2.0). Significant differences *($p < 0.05$)* in phosphorylation intensity between the two groups were determined by Paired t-test and results represented as volcano plots (GraphPad Prism version 9.2.0). The kinases that might be responsible for differences in the peptide phosphorylation between the treated and untreated retinal samples were ascertained by the STK Upstream Kinase Analysis tool of BioNavigator®. This software combines information of kinase interaction with phosphorylation sites from databases such as HPRD, PhosphoELM, PhosphositePLUS, Reactome, UniProt (41). The highest-ranking predicted kinases based on their Kinase Score (Significance and Specificity Score) were represented on a phylogenetic tree of the human protein kinase family (Coral, http://phanstiel-lab.med.unc.edu/CORAL/) (42).

Sample preparation for MS: Each retinal explant was homogenized separately in a buffer (50 mM Tris-HCl, 50 mM NaCl, 1 mM EDTA, 5 mM NaH2PO4, 1 mM DL-Dithiothreitol [DTT]), supplemented with phosphatase inhibitors (Lot No, 33041800, Roche, Basel, Switzerland, 1 tablet per 10 mL buffer) using a homogenizer (Knotes Glass Company, Vineland, NJ). The homogenate was then centrifuged at 10000 x g for 5 min at 4°C, after which the soluble fraction was collected, with the concentration measured by Bio-Rad Protein Reagent Assay Kit (Cat. No.: #5000113, #5000114, #5000115, Bio-Rad, Hercules, CA).

For each separated sample, 150 µg of proteins were reduced with DTT to a final concentration of 10 mM and heated at 56°C for 30 min followed by alkylation with iodoacetamide for 30 min at room temperature in the dark, to a final concentration of 20 mM. Subsequently, samples were precipitated with ice cold ethanol for overnight at -20°C, followed by centrifugation at 14000 x g for 10 min, after which the pellets were resuspended in 100 mM ammonium bicarbonate and sonicated for 20 cycles of 15 sec on, 15 sec off, using a Bioruptor (Diagenode, Denville, NJ). A digestion was then performed by adding trypsin (Sequencing Grade Modified Trypsin, Part No. V511A, Promega, Madison, WI) at a ratio of 1:50 to the samples and incubated for overnight at 37°C after which it was stopped

by 5 µL 10% trifluoroacetic acid (TFA). The Pierce High-Select Fe-NTA Phosphopeptide Enrichment Kit (Cat. No.: A32992; Thermo Fischer Scientific, Waltham, MA) was used to enrich phosphopeptides according to the manufacturer's protocol. The phosphopeptides were run to dryness in a Speed Vac and resolved in 2% acetonitrile (ACN) and 0.1% TFA to a peptide concentration of 0.25 µg/µL.

MS acquisition and analysis: LC-MS detection was performed on a Tribrid mass spectrometer Fusion (Thermo Fischer Scientific) according to Rasmussen et al (18). Briefly, for each sample, 1 µg of the peptides was injected into the LC-MS. Peptides were concentrated on an Acclaim PepMap 100 C18 precolumn (75 µm x 2 cm, Cat. No.: 164941, Thermo Fischer Scientific) for subsequent separation on an Acclaim PepMap RSLC column (75 µm x 25 cm, C18, 2 µm, 100 Å, nanoViper, Cat. No.: 164941, Thermo Fischer Scientific) at a temperature of 45°C and a flow rate of 300 nL/min. Solvent A (0.1% formic acid in water) and solvent B (0.1% formic acid in ACN) were used to create a nonlinear gradient for elution of the peptides. The gradient was constructed such that the percentage of solvent B was maintained at 3% for 3 min, increased from 3% to 30% for 90 min and then increased to 60% for 15 min and then increased to 90% for 5 min to be kept at 90% for another 7 min to wash the column.

The Orbitrap Fusion was operated in the positive data-dependent acquisition (DDA) mode. The peptides were introduced into the LC-MS via stainless steel Nano-bore emitter (OD 150 µm, ID 30 µm) with the spray voltage set to 2 kV and the capillary temperature to 275°C. Full MS survey scans from m/z 350-1350 with a resolution of 120,000 were performed in the Orbitrap detector. The automatic gain control (AGC) target was set to 4 × 105 with an injection time of 50 ms. The most intense ions (up to 20) with charge states 2-5 from the full scan MS were selected for fragmentation in the Orbitrap. The MS2 precursors were isolated with a quadrupole mass filter set to a width of 1.2 m/z. Precursors were fragmented by high-energy collision dissociation (HCD) at a normalized collision energy (NCE) of 30%. The resolution was fixed at 30000 and for the MS/MS scans, the values for the AGC target and injection time were 5 × 104 and 54 ms, respectively. The duration of dynamic exclusion was set to 45s and the mass tolerance window was 10 ppm.

The raw DDA data were analysed with Proteome Discoverer™ Software (Version 2.5, Thermo Fisher Scientific). Peptides were identified using both SEQUEST HT (Tabb, 2015) and Mascot (Perkins, Pappin, Creasy and Cottrell, 1999) against UniProtKB mouse database (UP000000589 plus isoforms). The search was performed with the following parameters applied: static modification: cysteine carbamidomethylation and dynamic modifications: N-terminal acetylation. Phosphorylation (S, T, Y) was set as variable for the phosphopeptide analysis. Precursor tolerance was set to 10 ppm and fragment tolerance was set to 0.05 ppm. Up to two missed cleavages were allowed and Percolator was used for peptide validation at a q-value of maximum 0.05. Extracted peptides were used to identify and quantify them by label-free relative quantification. The extracted chromatographic intensities were used to compare peptide abundance across samples.

The MS results were processed via Perseus software (version 1.6.0.7, Tyanova et al., 2016). The protein intensities were log2 transformed and the missing values were replaced from a normal distribution was performed though data imputation by using the following settings:

width 0.3 and downshift 0. The further bioinformatics analysis of these processed data was done via the web-based tool Phosphomatics (https://phosphomatics.com/, Hornbeck et al., 2014; UniProt: a worldwide hub of protein knowledge, 2018). A two-sample Student's t-test (two-tailed) was performed to compare phosphorylated site levels between the *rd10* explants with PKG inhibition and their counterparts. A p-value of 0.05 was defined as the cut-off.

Integrative kinome network and Pathway analysis: to Performing integrative network analysis we use String database (https://string-db.org/), which is a comprehensive resource for curated organism-wide protein associations and implement to integrate all known and predicted associations between proteins, including both physical interactions as well as functional associations (44). We used differentially predicted upstream kinases from kinome activity microarray data (n=17 from Table 1) and MS-centric phosphoproteome data (n=28 from Supplementary table S1) as input for String DB network analysis. For network analysis, only medium confidence (0.04 for interaction score) and Markov cluster algorithm (MCL) was applied with default settings.

The biological pathways that might be affected between untreated and CN03-treated *rd10* samples were determined in Reactome Pathways analysis (https://reactome.org/) (45), where same differentially predicted upstream kinases were used as input list as that of network analysis. Visualization was performed in GraphPad Prism (version 9.2.0) using known matrices from the analysis.

Western Blot: *20 μg* of retinal explant lysate per sample per lane were loaded and separated on 4-20% Mini-PROTEAN® TGX Stain-Free® Protein Gels (Bio-Rad, Cat. #4568096) at 150V and 40A for 50-60 minutes in 1x Tris/Glycine/SDS (TGS) buffer (Bio-Rad, #1610732). All proteins were transferred to Trans-Blot Turbo Mini 0.2 µm PVDF Membrane (Bio-Rad, Cat. #1704156) using the Trans-Blot Turbo Transfer System (Bio-Rad). Trans-Blot system was set to run for 7 minutes at 1,3A and 25V per blot. For staining, the membrane was blocked for 1 h at room temperature (RT) with 5% low-fat milk (ELK, Campina) in PBST (Phosphate buffered saline with 0.1% Tween-20) or with 5% BSA in PBST for phospho-proteins. Before adding primary antibody, the membrane was washed 3x times PBST. The membrane was incubated overnight at 4^{o}C with primary antibody dilutions in 5% skim milk in PBST according to Suppletmentary table S2. The membrane was washed extensively with PBST in the following day. Subsequently the membranes were re-probed with appropriate HRP-conjugated secondary antibodies (refer supplementary table S2) for 1 h at RT. The chemiluniscence HRP signal was detected with SuperSignal™ West Festo Maximum Sensitivity Substrate kit (Thermo Fisher, Cat. #34094) using a ChemiDoc™ Touch Imaging System (Bio-Rad) equipped with Quantity One/ChemiDoc XRS software. The ratio of the optical density of the protein to the internal control (β-actin or HSP-90) was obtained and was expressed as ratio or percentage of the control value in the Figures.

Acknowledgements

We thank Liesbeth Houkes and Liesbeth Hovestad for excellent technical assistance as well as Peter Linders for helpful discussion on data analysis. We thank the Center for Translational Proteomics at Medical Faculty, Lund University for generating phosphoproteomic data. We also like to thank Prof. Ivonne Rietjens for her valuable discussion. This research was funded by the European Union Horizon 2020 Research and Innovation Programme- *trans*Med under the Marie Curie grant agreement No. 765441 (*trans*Med; H2020- MSCA-765441). In addition Per Ekström received funding from Stiftelsen för Synskadade i f.d. Malmöhus län, Kronprinsessan Margaretas Ar-betsnämnd för synskadade, and Ögonfonden.

Conflict of interest

AR, TT, JG are current or former employees of PamGene International B.V., 's-Hertogenbosch, The Netherlands. PE and FPD are shareholders of the company Mireca Medicines, Tübingen, Germany, which intends to forward clinical testing of PKG inhibitor CN03.

References

1. Power M, Das S, Schütze K, Marigo V, Ekström P, Paquet-Durand F: **Cellular mechanisms of hereditary photoreceptor degeneration – Focus on cGMP**. *Prog Retin Eye Res* 2020, **74**:100772.
2. Koch M, Scheel C, Ma H, Yang F, Stadlmeier M, Glück AF, Murenu E, Traube FR, Carell T, Biel M, et al.: **The cGMP-dependent protein kinase 2 contributes to cone photoreceptor degeneration in the Cnga3-deficient mouse model of achromatopsia**. *Int J Mol Sci* 2021, **22**:52.
3. Vighi E, Trifunovic D, Veiga-Crespo P, Rentsch A, Hoffmann D, Sahaboglu A, Strasser T, Kulkarni M, Bertolotti E, Heuvel A Van Den, et al.: **Combination of cGMP analogue and drug delivery system provides functional protection in hereditary retinal degeneration**. *Proc Natl Acad Sci U S A* 2018, **115**:E2997–E3006.
4. Paquet-Durand F, Hauck SM, Veen T Van, Ueffing M, Ekström P: **PKG activity causes photoreceptor cell death in two retinitis pigmentosa models**. *J Neurochem* 2009, **108**:796–810.
5. Sancho-Pelluz J, Arango-Gonzalez B, Kustermann S, Romero FJ, Van Veen T, Zrenner E, Ekström P, Paquet-Durand F: **Photoreceptor cell death mechanisms in inherited retinal degeneration**. *Mol Neurobiol* 2008, **38**:253–269.
6. Ly A, Merl-Pham J, Priller M, Gruhn F, Senninger N, Ueffing M, Hauck SM: **Proteomic Profiling Suggests Central Role of STAT Signaling during Retinal Degeneration in the rd10 Mouse Model**. *J Proteome Res* 2016, **15**:1350–1359.
7. Gargini C, Terzibasi E, Mazzoni F, Strettoi E: **Retinal organization in the retinal degeneration 10 (rd10) mutant mouse: A morphological and ERG study**. *J Comp Neurol* 2007, **500**:222–238.
8. Barhoum R, Martínez-Navarrete G, Corrochano S, Germain F, Fernandez-Sanchez L, de la Rosa EJ, de la Villa P, Cuenca N: **Functional and structural modifications during retinal degeneration in the rd10 mouse**. *Neuroscience* 2008, **155**:698–713.
9. Phillips MJ, Otteson DC, Sherry DM: **Progression of neuronal and synaptic remodeling in the rd 10 mouse model of retinitis pigmentosa**. *J Comp Neurol* 2010, **518**:2071–2089.
10. Samardzija M, Wariwoda H, Imsand C, Huber P, Heynen SR, Gubler A, Grimm C: **Activation of survival pathways in the degenerating retina of rd10 mice**. *Exp Eye Res* 2012, **99**:17–26.
11. Wei C, Li Y, Feng X, Hu Z, Paquet-Durand F, Jiao K: **RNA Biological Characteristics at the Peak of Cell Death in Different Hereditary Retinal Degeneration Mutants**. *Front Genet* 2021, **12**.
12. Szklarczyk D, Gable AL, Nastou KC, Lyon D, Kirsch R, Pyysalo S, Doncheva NT, Legeay M, Fang T, Bork P, et al.: **The STRING database in 2021: Customizable protein-protein networks, and functional characterization of user-uploaded gene/measurement sets**. *Nucleic Acids Res* 2021, **49**:D605–D612.
13. Paquet-Durand F, Hauck SM, Van Veen T, Ueffing M, Ekström P: **PKG activity causes photoreceptor cell death in two retinitis pigmentosa models**. *J Neurochem* 2009, **108**:796–810.
14. Vighi E, Trifunovic D, Veiga-Crespo P, Rentsch A, Hoffmann D, Sahaboglu A, Strasser T, Kulkarni M, Bertolotti E, Van Den Heuvel A, et al.: **Combination of cGMP analogue and drug delivery system provides functional protection in hereditary retinal degeneration**. *Proc Natl Acad Sci U S A* 2018, **115**:E2997–E3006.
15. Lolley RN, Farber DB, Rayborn ME, Hollyfield JG: **Cyclic gmp accumulation causes degeneration of photoreceptor cells: Simulation of an inherited disease**. *Science (80-)* 1977, **196**:664–666.
16. Arango-Gonzalez B, Trifunović D, Sahaboglu A, Kranz K, Michalakis S, Farinelli P, Koch S, Koch F, Cottet S, Janssen-Bienhold U, et al.: **Identification of a common non-apoptotic cell death mechanism in hereditary retinal degeneration**. *PLoS One* 2014, **9**:1–11.

17. Wang T, Tsang SH, Chen J: **Two pathways of rod photoreceptor cell death induced by elevated cGMP**. *Hum Mol Genet* 2017, **26**:2299–2306.
18. Roy A, Groten J, Marigo V, Tomar T, Hilhorst R: **Identification of novel substrates for cGMP dependent protein kinase (PKG) through kinase activity profiling to understand its putative role in inherited retinal degeneration**. *Int J Mol Sci* 2021, **22**:1–17.
19. Rasmussen M, Welinder C, Schwede F, Ekström P: **The cGMP system in normal and degenerating mouse neuroretina: New proteins with cGMP interaction potential identified by a proteomics approach**. *J Neurochem* 2020, doi:10.1111/jnc.15251.
20. Guo Y, Pan W, Liu S, Shen Z, Xu Y, Hu L: **ERK/MAPK signalling pathway and tumorigenesis (Review)**. *Exp Ther Med* 2020, **19**:1997–2007.
21. Michel M, Green CL, Eskin A, Lyons LC: **PKG-mediated MAPK signaling is necessary for long-term operant memory in Aplysia**. *Learn Mem* 2011, **18**:108–117.
22. Ding XY, Gu RP, Tang WY, Shu QM, Xu GZ, Zhang M: **Effect of Phosphorylated-Extracellular Regulated Kinase 1/2 Inhibitor on Retina from Light-induced Photoreceptor Degeneration**. *Chin Med J (Engl)* 2018, **131**:2836–2843.
23. Shimamura A, Ballif BA, Richards SA, Blenis J: **Rsk1 mediates a MEK-MAP kinase cell survival signal**. *Curr Biol* 2000, **10**:127–135.
24. Jomary C, Cullen J, Jones SE: **Inactivation of the akt survival pathway during photoreceptor apoptosis in the retinal degeneration mouse**. *Investig Ophthalmol Vis Sci* 2006, **47**:1620–1629.
25. Liu M, Huang X, Tian Y, Yan X, Wang F, Chen J, Zhang Q, Zhang Q, Yuan X: **Phosphorylated GSK-3β protects stress-induced apoptosis of myoblasts via the PI3K/Akt signaling pathway**. *Mol Med Rep* 2020, **22**:317–327.
26. Finkbeiner S: **CREB couples neurotrophin signals to survival messages**. *Neuron* 2000, **25**:11–14.
27. Sakamoto KM, Frank DA: **CREB in the pathophysiology of cancer: Implications for targeting transcription factors for cancer therapy**. *Clin Cancer Res* 2009, **15**:2583–2587.
28. Roy A, Tolone A, Hilhorst R, Groten J, Tomar T, Paquet-Durand F: **Kinase activity profiling identifies putative downstream targets of cGMP/PKG signaling in inherited retinal neurodegeneration**. *Cell Death Discov* 2022, **8**:1–12.
29. Junho CVC, Caio-Silva W, Trentin-Sonoda M, Carneiro-Ramos MS: **An Overview of the Role of Calcium/Calmodulin-Dependent Protein Kinase in Cardiorenal Syndrome**. *Front Physiol* 2020, **11**:735.
30. Chai Y, Zhang DM, Lin YF: **Activation of cGMP-dependent protein kinase stimulates cardiac ATP-sensitive potassium channels via a ROS/calmodulin/CaMKII signaling cascade**. *PLoS One* 2011, **6**:e18191.
31. Hauck SM, Ekström PAR, Ahuja-Jensen P, Suppmann S, Paquet-Durand F, van Veen T, Ueffing M: **Differential modification of phosducin protein in degenerating rd1 retina is associated with constitutively active Ca2+ /calmodulin kinase II in rod outer segments**. *Mol Cell Proteomics* 2006, **5**:324–336.
32. Bito H, Deisseroth K, Tsien RW: **CREB phosphorylation and dephosphorylation: A Ca2+- and stimulus duration-dependent switch for hippocampal gene expression**. *Cell* 1996, **87**:1203–1214.
33. Guo X, Zhou J, Starr C, Mohns EJ, Li Y, Chen EP, Yoon Y, Kellner CP, Tanaka K, Wang H, et al.: **Preservation of vision after CaMKII-mediated protection of retinal ganglion cells**. *Cell* 2021, **184**:4299–4314.
34. Fan W, Agarwal N, Kumar MD, Cooper NGF: **Retinal ganglion cell death and neuroprotection: Involvement of the CaMKIIα gene**. *Mol Brain Res* 2005, **139**.

35. Goebel DJ: **Selective blockade of CaMKII-α inhibits NMDA-induced caspase-3-dependent cell death but does not arrest PARP-1 activation or loss of plasma membrane selectivity in rat retinal neurons**. *Brain Res* 2009, **1256**.
36. Tsumura T, Murata A, Yamaguchi F, Sugimoto K, Hasegawa E, Hatase O, Nairn AC, Tokuda M: **The expression of Ca2+/calmodulin-dependent protein kinase I in rat retina is regulated by light stimulation**. *Vision Res* 1999, **39**:3165–3173.
37. Pérez-García MJ, Gou-Fabregas M, De Pablo Y, Llovera M, Comella JX, Soler RM: **Neuroprotection by neurotrophic factors and membrane depolarization is regulated by calmodulin kinase IV**. *J Biol Chem* 2008, **283**:4133–4144.
38. Gou-Fabregas M, Ramírez-Núñez O, Cacabelos D, Bahi N, Portero M, Garcera A, Soler RM: **Calpain activation and CaMKIV reduction in spinal cords from hSOD1G93A mouse model**. *Mol Cell Neurosci* 2014, **61**:219–225.
39. Bae JS, Jang MK, Hong SH, An WG, Choi YH, Kim H Do, Cheong JH: **Phosphorylation of NF-κB by calmodulin-dependent kinase IV activates anti-apoptotic gene expression**. *Biochem Biophys Res Commun* 2003, **305**:1094–1098.
40. Hilhorst R, Houkes L, Mommersteeg M, Musch J, Van Den Berg A, Ruijtenbeek R: **Peptide microarrays for profiling of serine/threonine kinase activity of recombinant kinases and lysates of cells and tissue samples**. *Methods Mol Biol* 2013, **977**:259–271.
41. Chirumamilla CS, Fazil MHUT, Perez-Novo C, Rangarajan S, de Wijn R, Ramireddy P, Verma NK, Vanden Berghe W: **Profiling activity of cellular kinases in migrating T-cells**. *Methods Mol Biol* 2019, **1930**:99–113.
42. Metz KS, Deoudes EM, Berginski ME, Jimenez-Ruiz I, Aksoy BA, Hammerbacher J, Gomez SM, Phanstiel DH: **Coral: Clear and Customizable Visualization of Human Kinome Data**. *Cell Syst* 2018, **7**:347–350.
43. Xie, Haohuan, Wen Zhang, Mei Zhang, Tasneem Akhtar, Young Li, Wenyang Yi XS et al.: **Chromatin accessibility analysis reveals regulatory dynamics of developing human retina and hiPSC-derived retinal organoids**. *Sci Adv* 2020, **6**:eaay5247.
44. Kuleshov M V., Jones MR, Rouillard AD, Fernandez NF, Duan Q, Wang Z, Koplev S, Jenkins SL, Jagodnik KM, Lachmann A, et al.: **Enrichr: a comprehensive gene set enrichment analysis web server 2016 update**. *Nucleic Acids Res* 2016, **44**:W90–W97.

Supplementary Data

Supplementary table S1: Kinase analysis from MS-based phosphoproteomics results for *rd10* vs *rd10* CN03

Rank	Kinase Name	Kinase Uniprot ID	Log(fold change)	-log10(p-val)
1	MAPK14	Q16539	-1.68	3.91
2	AKT1	P31749	0.76	3.41
3	RPS6KA1	Q15418	0.79	3.00
4	AURKB	Q96GD4	0.73	2.96
5	ZAP70	P43403	-1.43	2.91
6	PRKCA	P17252	0.59	2.55
7	PNCK	Q6P2M8	0.69	2.54
8	CDK2	P24941	1.11	2.45
9	FYN	P06241	1.01	2.18
10	ATR	Q13535	0.90	2.10
11	GSK3B	P49841	0.57	2.04
12	CSNK1A1	P48729	0.57	2.04
13	PLK3	Q9H4B4	0.57	2.04
14	PRKACA	P17612	0.95	1.91
15	PRKCG	P05129	-0.64	1.89
16	RPS6KA3	P51812	0.58	1.88
17	MKNK1	Q9BUB5	0.65	1.80
18	RPS6KB2	Q9UBS0	0.65	1.80
19	ATM	Q13315	0.95	1.77
20	GRK6	P43250	0.65	1.61
21	RPS6KB1	P23443	1.27	1.47
22	CAMK2A	Q9UQM7	-1.74	1.46
23	MAPKAPK2	P49137	-0.96	1.41
24	MAPK1	P28482	-0.98	1.34
25	MAPK3	P27361	-0.98	1.34
26	ABL1	P00519	-0.98	1.34
27	TRPM7	Q96QT4	0.64	1.33
28	CSNK2B	P67870	0.64	1.33

Supplementary table S2: List of antibodies used in Western blotting

Target protein	Antibody	Molecular weight	Supplier	Catalogue no.	Dilution
HSP90	HSP 90a/b (F08)	90 kD	Santa cruz biotechnologies	sc-13119	1:500
pCREB	Phospho-CREB (Ser133; F.959.4)	43 kDa	ThermoFisher Scientific	MA5-11192	1:1000
pCAMK2	Phospho-CaMKII beta/gamma/delta (Thr287)	54/60 kDa	ThermoFisher Scientific	PA5-37833	1:1000
pCaMK4	Anti-phospho-CaMK4 (pThr196/200)	51 kDa	Sigma Aldrich	SAB4504122	1:500
secondary antibody: HSP90	Anti-mouse-HRP	-	Santa cruz biotechnologies	SC-2005	1:50000
secondary antibody: pCREB, pCaMK2 and pCaMK4	Anti-Rabbit-HRP	-	Cell Signaling Technology	7074S	1:50000

6

Chapter 6

Retinal degeneration: Multilevel protection of photoreceptor and ganglion cell viability and function with the novel PKG inhibitor CN238

Arianna Tolone*, Wadood Haq*, Akanksha Roy, Alexandra Fachinger, Andreas Rentsch, Friedrich W. Herberg, Frank Schwede, Tushar Tomar, John Groten and François Paquet-Durand

*Authors contributed equally

Submitted

Abstract

Hereditary retinal degeneration (RD) is often associated with excessive cGMP-signaling in photoreceptors. Previous research has shown that inhibition of cGMP-dependent protein kinase G (PKG) can slow down the loss of photoreceptors in different RD animal models. In this study, we identified a novel PKG inhibitor, the cGMP analogue CN238, with strong protective effects on photoreceptors in retinal degeneration *rd1* and *rd10* mutant mice. In long-term organotypic retinal explants, CN238 preserved *rd1* and *rd10* photoreceptor viability and function. Surprisingly, in explanted retinae, CN238 also protected retinal ganglion cells from axotomy-induced retrograde degeneration and preserved their functionality. Furthermore, analysis of kinase activity-dependent protein phosphorylation patterns in *rd10* retinal explants after CN238 treatment revealed a reduced phosphorylation of the PKG target Kv1.6. Using calcium imaging on *rd10* acute retinal explants, we showed that CN238 inhibits Kv1.6 suggesting a possible role in retinal ganglion cell degeneration. Together, these results confirm the strong neuroprotective capacity of PKG inhibitors for both photoreceptors and retinal ganglion cells, thereby significantly broadening their potential applications for the treatment of retinal diseases and possibly neurodegenerative diseases in general.

Keywords
Apoptosis, neuroprotection, retinitis pigmentosa, cGMP, cGK1, Kv1.3, Kv1.6, functional vision preservation, microelectrode array recording, ERG

Introduction

Photoreceptor degeneration is a hallmark of retinal degenerative diseases (RD), a group of retinal dystrophies characterized by primary dysfunction and degeneration of photoreceptor cells, leading to visual loss and eventually blindness [1] . Because of the genetic heterogeneity of RD-type diseases, no effective therapies are currently available [2]. While the mechanisms causing photoreceptor degeneration are far from being fully understood, high levels of cyclic guanosine monophosphate (cGMP) are known to trigger non-apoptotic photoreceptor cell death in many RD disease models [3,4]. Two commonly used models for studying RD are *rd1* and *rd10* mice, which are characterized by a nonsense (*rd1*) and a missense (*rd10*) mutation in the gene encoding for the β-subunit of rod phosphodiesterase (PDE) 6 [5]. Lack of PDE6 activity leads to an accumulation of cGMP in photoreceptors [6,7] and emerging RD neuroprotection strategies include targeting pathways downstream of cGMP [3,4].

The prototypic cellular target of cGMP is protein kinase G (PKG), a serine/threonine kinase that exists as a homodimer of two subunits, each consisting of an N-terminal dimerization domain, an auto-inhibitory sequence, two cGMP binding sites, and a C-terminal kinase domain. Three isoforms of PKG have been identified in mammals: PKG1α, PKG1β and PKG2. Binding of cGMP to PKG induces the release of the C-terminal catalytic domain from the auto-inhibitory sequence, activating PKG [8]. cGMP-signaling activates PKG, which, when over-activated, is likely to play a key role in triggering cell death [4,9-13]. In the retina, exceedingly high cGMP levels, as well as strong PKG activation were causally linked to photoreceptor cell death [6,7,14], highlighting PKG as a target for the treatment of RD-type diseases.

In an effort to develop new drugs for the treatment of RD, a number of cGMP analogues designed to inhibit PKG have been synthetized [15,16]. These compounds bear an Rp-configured phosphorothioate, which enables them to antagonize the activation of PKG by binding to the cGMP binding sites in the regulatory domain, without liberating the catalytic domain [17]. A previous study showed that the *in vivo* treatment with the cGMP analogue CN03, rescued photoreceptor viability and function in the genetically distinct *rd1*, *rd2*, and *rd10* animal models [16]. These results confirmed cGMP/PKG-signaling as a common target for the mutation-independent treatment of different RD-type diseases. Since then, a 2nd generation of promising and potent cGMP analogues have been developed, but their biochemical properties and neuroprotective efficacy have not been examined thus far.

Here, we identified a novel cGMP analogue with strong photoreceptor-protective effects in organotypic retinal explant cultures derived from *rd1* and *rd10* mice. When long-term *rd10* and wild-type (WT) retinal cultures were studied using micro-electrode arrays (MEAs), this compound revealed a preservation of photoreceptor responses and, surprisingly, also showed increased retinal ganglion cell (RGC) activity. Increased photoreceptor and RGC viability in treated specimens was confirmed by histological analysis. Furthermore, combination of PamChip® multiplex peptide microarray analysis, MEA recording, and calcium imaging experiments identified the outward rectifying K^+-channel Kv1.6 as a possible mediator of PKG-dependent cell death. Given the important functions of KV-type channels

for neuronal repolarization, these findings provide a rationale for the use of PKG-inhibitors as novel neuroprotective drugs with possible applications beyond the retina.

Results

Novel PKG inhibitors protect rd1 photoreceptors

Cyclic nucleotide (CN) analogues of cGMP (Fig. S1) were previously generated in the context of the EU project DRUGSFORD (HEALTH-F2-2012-304963) and amongst others tested for their protective effects in primary rod-like cells. Here, we selected cGMP analogues that shared structural similarities with the retinoprotective compounds **CN003** and **CN004** [16], which served as reference compounds. Structure wise all compounds featured a cGMPS backbone containing a sulfur-modified phosphate function with Rp-configuration, which confers PKG inhibitory properties [17]. Further modifications were introduced on the nucleobase moiety at positions 8 (R_1) and 1, N^2 (R_2, R_3). While both reference compounds contain a so-called PET-group (β- **p**henyl- 1, N^2- **et**heno) at 1, N^2, this group is either lacking (**CN226**), substituted with an additional methyl-group (**CN238**), or replaced through the heteroaromatic furan ring (**CN007**). At position 8 the residue in **CN226** contains a phenyl ring as present in reference compound **CN004**, however, a different, slightly larger linker has been introduced and said phenyl ring is unsubstituted. **CN007** and **CN238**, in turn, share the same bromide function as in the reference compound **CN003**. A compound concentration of 50 µM was used, based on previous *in vitro* results obtained with the reference compounds [16].

We initially tested the cGMP analogues on organotypic retinal explant cultures derived from *rd1* mouse. The loss of function of PDE6 in *rd1* results in primary loss of rods already during development, with a peak around P13 and almost complete loss at P18 [28]. Therefore, in *rd1* explants treatment with cGMP analogues started at P7 and ended at P11, *i.e*., at the onset of manifest retinal degeneration [29], a time-point well suited for establishing possible protective effects.

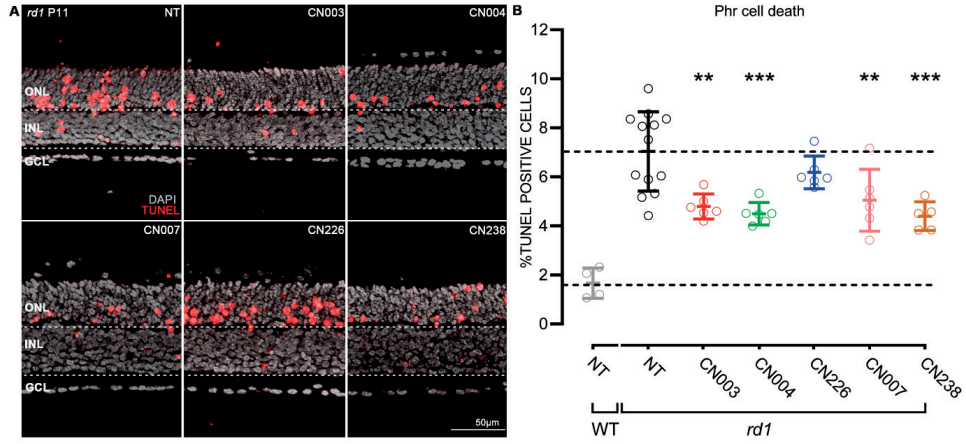

Figure 1: Retinoprotective effects of novel PKG inhibitors on *rd1* P11 organotypic retinal explant cultures. (**A**) Postnatal (P) day 11 *rd1* retinal explant cultures treated for four days with 50 µM of different cGMP analogues. TUNEL assay (red) indicated dying cells, DAPI (grey) was used as nuclear counterstain. (**B**) Quantification of TUNEL positive cells in the outer nuclear layer (ONL) of sections from A. Cell death rate in NT WT retina shown for comparison. A cell death rate lower than in the non-treated (NT) *rd1* retina was interpreted as evidence for photoreceptor protection. Compounds CN003 and CN004 had previously been established as photoreceptor protective [16] and were used for reference. Testing was performed on n = 4 to 12 different retinae from different animals. Error bars: mean with SD. Statistical analysis was performed using one-way ANOVA followed by the Dunnett´s multiple comparison test; significance levels were: $^{**}P \leq 0.01$, $^{***}P \leq 0.001$. INL = inner nuclear layer, GCL = ganglion cell layer.

As a readout for the effects of cGMP analogue treatments, we performed TUNEL assays on sections obtained from treated and non-treated (NT) specimens (Fig. 1A). We considered any reduction in the percentage of TUNEL positive cells in the ONL as indicative of a decrease in photoreceptor degeneration. When compared to *rd1* NT (100%), retinae treated with the compounds CN007, CN226, and CN238 (NT = 7.03 ± 1.61; CN007 = 5.04 ± 1.26; CN226 = 6.18 ± 0.66; CN238 = 4.39 ± 0.50) showed a relative reduction of TUNEL positive cells of ≈32%, ≈17%, and ≈40%, respectively. The reference compounds CN003 and CN004 (CN003 = 4.79 ± 0.50; CN004 = 4.49 ± 0.45) confirmed their previously seen protective effects [16] (Fig. 1B).

We then assessed the efficacy of the most promising compound CN238 to inhibit the PKG isoforms PKG1α, PKG1β, and PKG2. As references in this characterization, we included the previous lead compound CN003, as well as the compound CN226 as a "negative control" since it had not shown protection in *rd1* retinal explants (Supplementary Fig. S3). This analysis indicated a slightly increased potency of CN238 towards PKG1 and PKG2 and furthermore revealed this compound to have partial agonistic effects on PKG1α at high concentrations. This suggests that CN238 was modulating or dampening PKG1α activity rather than completely blocking it. On the other hand, analysis of the efficacy of CN226 showed that it was only weakly inhibiting PKG1β and PKG2, and that it did, in fact, activate PKG1α, in line with our results on *rd1* retinal explants (*cf*. Supplementary Fig. S1).

PKG inhibition preserves viability and function of photoreceptors in rd10 retinal explants
To assess the validity of these results across different animal models, we further tested the most promising compound CN238 and the reference compound CN003 on organotypic retinal explant cultures derived from *rd10* mice. As in *rd1* animals, the *rd10* mutation affects the gene encoding for the β-subunit of rod PDE6, however, in *rd10* photoreceptors the PDE6 enzyme retains some residual activity, delaying the onset of photoreceptor degeneration until P18 [3,4]. The culturing and treatment paradigms were adjusted accordingly, and *rd10* retinae were cultured from either P9 to P17 or P19, or from P12 till P24. As in the *rd1* situation, and to allow the retinal explant to adapt to culture conditions, drug treatments were begun two days after explantation.

While the TUNEL assay gives a count of the number of dying cells at a given age, the number of mutant photoreceptors still surviving compared to the number of photoreceptors in an age-matched NT retina, gives the integral of cells preserved until a given time-point (Fig. 2A). We therefore analyzed the number of photoreceptor rows to assess the long-term effects of the compounds. When CN003 and CN238 were tested on *rd10* retina in treatments reaching until P17 or P19 there was no statistically significant rescue, likely because of the comparatively late onset of *rd10* degeneration around P18. At P24, however, a clear and highly significant rescue of *rd10* photoreceptors was observed, with an increase in the photoreceptor row counts of ≈55% and ≈46% in samples treated with CN003 and CN238 (NT = 3.86 ± 1.01; CN003 = 6.01 ± 0.87; CN238 = 5.64 ± 0.32), respectively (Fig. 2B).

To determine whether the increased photoreceptor survival seen with PKG inhibition also translated into improved retinal function, we performed electrophysiological recordings of *rd10* retinal explants employing a micro-electrode array (MEA) system and white light LED stimulator to apply 500 ms full-field light flashes. The method allowed for the selective assessment of photoreceptor functionality by recording light-elicited micro-electroretinograms (μERG). In this analysis, we included the compound that performed best in the retinal cell death assay, CN238 (*cf*. Fig. 1), along with the previous lead compound CN003, as well as CN226, which served as additional “negative” control.

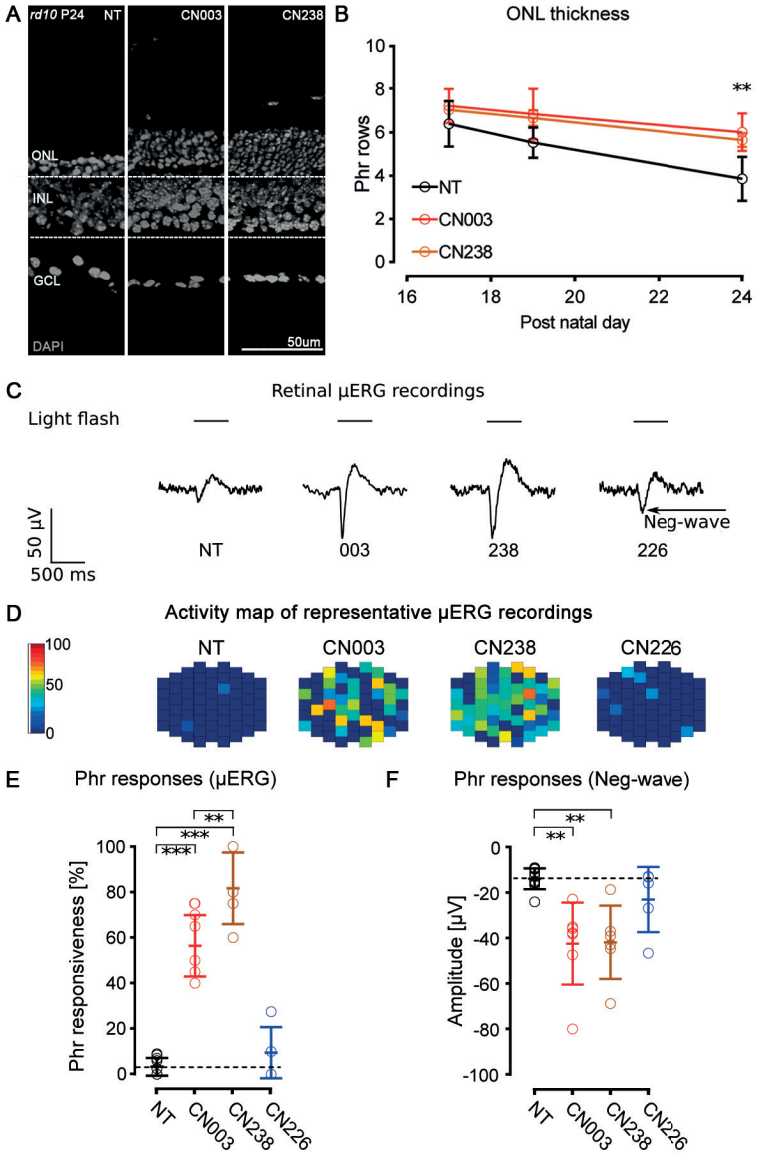

Figure 2: CN238 preserves photoreceptor viability and function in *rd10* retina: Organotypic retinal explant cultures derived from *rd10* mice were treated with cGMP analogues at 50 µM concentration. (**A**) Representative sections of post-natal (P) day 24 *rd10* retinal cultures treated or non-treated (NT) and stained with DAPI (grey). (**B**) *rd10* retinal explants were treated for varying times until either P17, P19, or P24, and photoreceptor rows were quantified. Row counts above NT were interpreted as evidence for photoreceptor protection. Testing was performed on n = 5 different retinae from different animals. (**C**) Representative µERG traces of NT and treated *rd10* retinal explants. The single-electrode data represents the integrated signal of multiple photoreceptors above a given electrodes recording field. The strength of the light-evoked photoreceptor hyperpolarization is indicated by the initial negative deflection (neg.-wave) of the µERG (arrow). (**D**) Activity map of representative µERG recordings across the 59 electrodes of the MEA, indicating the reactivity to light in spatial context. Each pixel corresponds to a recording electrode and the color from blue to red (*i.e.*, 0 to 100) encodes the increasing intensity of the negative deflection of the recorded µERG. (**E**) Quantification of retinal light responsiveness as percentage of MEA electrodes

displaying µERG negative deflections ≥ 1.75-fold average baseline. Testing was performed on n = 5 different retinae from different animals. (**F**) Average amplitudes of negative deflection in µERG recordings. Error bars: mean with SD. Statistical testing: one-way ANOVA with Dunnett´s multiple comparison test; significance level: $^{**}P \leq 0.01$. INL = inner nuclear layer, Phr = photoreceptor, µERG = micro-electroretinogram, GCL = ganglion cell layer, MEA = micro-electrode array.

As shown in representative µERG traces (Fig. 2C), after 12 days of *in vitro* culture the PKG inhibitors CN003 and CN238 strongly increased the amplitudes of light-induced retinal responses, when compared to NT and CN226. In particular, the initial negative deflection of the µERG (Figure 2C, arrow), indicated a light-induced hyperpolarization of photoreceptors (*i.e.*, the a-wave in a conventional ERG) and thus their functional preservation with drug treatment. For each retina, recordings were obtained from two different areas located dorsally and ventrally from the center and averaged (each recording area: 340 X 280 µm; 59 electrodes at 40 µm spacing). Since each of the MEA electrode captured the integrated signal of multiple photoreceptors within an electrode´s recording range, the total span of the MEA recording field allowed an estimation of the overall light-sensitivity of a given retinal explant. We considered a light-induced negative µERG deflection exceeding respective threshold (1.75-fold ≥ calculated average control baseline) to indicate light-responsiveness and drew activity maps for the MEA electrodes showing light responses (Fig. 2D). We then expressed the number of electrodes showing such a response as percent of the total (Fig. 2E). This analysis revealed that NT retina, and CN226 treated retina, displayed almost no response to light (NT = 3.3% ± 3.9; CN226 = 9.5% ± 11.2), while CN003 (56.4% ± 13.5), and even more so CN238 (81.7% ± 15.7), strongly and significantly increased light responsiveness of treated retinal explants (Fig. 2E). In other words, treatment with CN003 or CN238 dramatically increased the retinal area responding to light by ≈ 17- or ≈ 25- times, respectively, when compared to NT. Compared to CN003, CN238 increased retinal responsiveness by yet another ≈ 45%, suggesting a further improvement of photoreceptor function and/or the density of the photoreceptors activating a given MEA electrode.

As an additional measure of photoreceptor functionality, we quantified the amplitudes of the initial negative µERG deflection, as a measure for the light-induced photoreceptor hyperpolarization. When compared to NT, retinal explants treated with CN003 or CN238 on average displayed a significantly stronger hyperpolarization response to light (NT: -13.6 µV ± 4.6; CN003: -42.1 µV ± 18.0; CN238: -41.5 µV ± 16.1). In contrast, CN226 treatment had only a minor effect on response amplitudes (-22.7 µV ± 14.3) and/or the density of the photoreceptors activating a given MEA electrode (Fig. 2F).

Taken together, we have established that the PKG inhibitors CN003 and CN238 preserved not only the viability of photoreceptor cells but also their functionality. In these comparisons the effects of the novel compound CN238 were at least equal, if not superior, to the previous lead compound CN003.

CN238 prevents axotomy-induced degeneration of retinal ganglion cells

The MEA recordings of treated *rd10* retinal explants revealed another feature that was entirely unexpected: During the retinal explantation procedure the optic nerve is transected, and this axotomy leads to rapid degeneration and loss of most RGCs within 4-7 days of *in*

vitro culture [30-32]. Accordingly, in NT *rd10* retinal explants, cultured for 12 days *in vitro*, RGC spiking activity was virtually extinguished, and this was also true for CN226 treated explants. Yet, explants treated with CN003 or CN238 showed a very remarkable preservation of light-stimulus correlated RGC spiking activity (Fig. 3A).

Similar to the analysis shown above for photoreceptor responses (µERG), we assessed the light responsiveness of RGCs across the entire surface of the MEA chip, from two different central recording areas. Here, light-induced RGC spike responses were considered to be stimulus correlated, if post stimulus activity (600 ms) exceeded the average of pre stimulus activity (500 ms, 100 ms bin, see methods for details). While RGC light responsiveness in NT and CN226 treated cultures was nearly absent (NT = 3.3% ± 4.9; CN226 = 1.5% ± 1.4), it was strongly and highly significantly increased in CN003 and CN238 treated retina (CN003 = 53.6% ± 15.5; CN238: 49.2% ± 8.8) (Fig. 3B). Thus, in comparison to NT the area of the retina showing light responses at the RGC level was ≈ 16- or ≈ 15-times larger after CN003 or CN238 treatment, respectively.

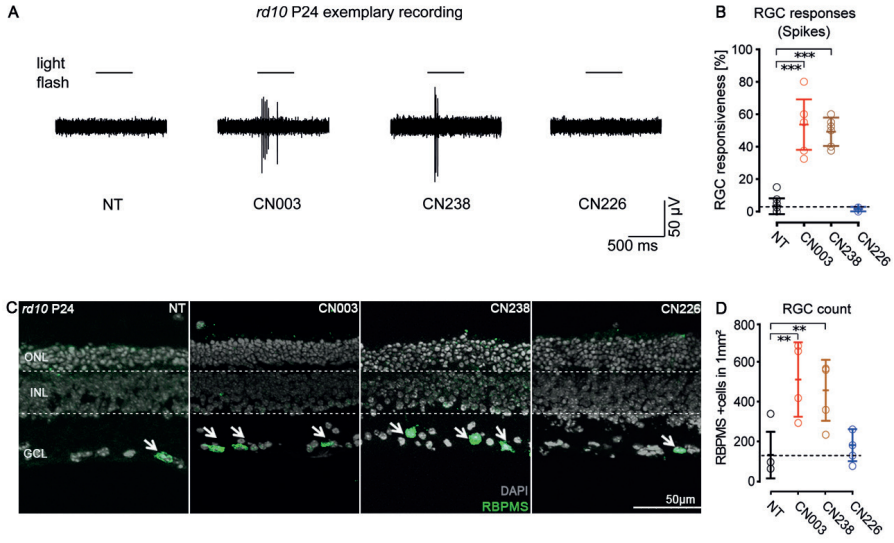

Figure 3: CN238 improves RGC viability and function in *rd10*. (**A**) Representative light-correlated RGC spike MEA recordings performed on P24 *rd10* retinal explants. *rd10* retinas were treated from post-natal day (P) 14 to P24 with 50 µM of CN003, CN238, or CN226, and compared to non-treated (NT) retinal explants. (**B**) Quantification of light-evoked *rd10* RGC activity in NT and treated explants (percentage of MEA electrodes detecting light-correlated spike-activity). (**C**) Sections derived from recorded *rd10* retinal explant cultures were stained with DAPI (grey) and RBPMS (green). (**D**) Quantification of RBPMS positive cells in *rd10* P24 retinal explant sections. Error bars indicate SD; statistical analysis in B, D: one-way ANOVA followed by Dunnett´s multiple comparison test; levels of significance: **P* ≤ 0.05, ***P* ≤ 0.01, ****P* ≤ 0.001. ONL = outer nuclear layer, INL = inner nuclear layer, Phr = photoreceptor, µERG = micro-electroretinogram, GCL = ganglion cell layer, MEA = micro-electrode array.

We then used the very same retinal explants from which the MEA recordings were obtained for a histological workup, to assess the survival and physical presence of RGCs. To this end, we employed labelling for the RNA-binding protein with multiple splicing (RBPMS), a protein that is expressed in about 60% of RGCs [33] (Fig. 3C). The quantification of RBPMS positive cells per mm^2 in the four experimental groups yielded very low RGC counts in NT and CN226 treated retina (NT = 134.1/mm^2 ± 117.3; CN226 = 184.1 ± 81.06), while CN003 and CN238 treated explants displayed significantly larger numbers of RGCs (CN003 = 514.4 ± 187.7; CN238 = 460.3 ± 153.6). Compared to NT, retinal explants treated with CN003 and CN238 showed 3.8- and 3.4-fold higher numbers of RBPMS positive cells, respectively. In line with the previous experiments, the compound CN226 did not preserve the viability of RGCs (Fig. 3D).

The magnitude of the rescue effect on axotomized RGCs raised the question whether this was a direct effect on RGCs or whether perhaps the preservation of *rd10* photoreceptors had indirectly enhanced the survival of *rd10* RGCs. To address this question, we extended our investigation to WT retinal explants, cultured for 12 days *in vitro*, from P12 to P24, treated or not with CN238. The light-induced hyperpolarization response in the µERG obtained from P24 WT explants did not seem to differ between NT and CN238 treated retina, however, the RGC spiking activity was virtually absent in NT, but present after CN238 treatment (Supplementary Fig. S4A). The overall photoreceptor activity was obviously higher in WT than *rd10* explants, yet even in the WT situation CN238 treatment improved light responsiveness somewhat (NT = 61.7 ± 45.9 %; CN238 = 98.9 ± 2.6 %) (Supplementary Fig. S4B). In line with this, the light-response amplitude in terms of negative deflection of the µERG was also increased in CN238 treated explants compared to NT (NT = -26.2 ± 20.5 µV; CN238 = -79.0 ± 36.9 µV) (Supplementary Fig. S4C). The most striking effect of CN238 on WT retina was, however, observed at the level of RGC light-responsiveness: While NT retina showed nearly no light correlated activity, CN238 treatment largely preserved RGC light-induced spiking activity across the whole retinal explant (NT = 0.8 ± 2.0 %; CN238 = 78.3 ± 30.6 %) (Fig. S4D). In relative terms CN238 had thus increased WT RGC functionality by a striking ≈ 95-times.

Further confirmation came from an investigation of WT RGC viability with RBPMS staining, which showed RGCs survival 2.3-fold higher in retinae treated with CN238 (NT = 163.9/mm^2 ± 96.4; CN238 = 379.3 ± 97.7) (Supplementary Fig. S4E and S4F). In addition, we assessed photoreceptor survival in NT and CN238 treated samples, without detecting significant photoreceptor loss (Supplementary Fig. S4G). These findings thus confirmed the formidable capacity of CN238 to preserve RGC activity despite the axotomy caused by the explantation procedure. This data on WT retina also demonstrated that the RGC protection was independent of photoreceptor degeneration.

Effects of cGMP-mediated inhibition of PKG in retinal ganglion cells

In a recent study, we measured the ability of active serine/threonine kinases (*i.e.,* PKG1 and PKG2) to phosphorylate specific peptides on lysed samples of explant cultures either treated with the PKG inhibitor CN003 or untreated [34]. When compared to WT, several voltage-dependent potassium channels belonging to the Kv1 family (*i.e.,* Kv1.3 and Kv1.6) showed increased phosphorylation in untreated *rd1* retinal explant cultures. This phosphorylation was significantly reduced in retinas treated with CN003.

The K_v1 family consists mainly of slow-activating and inactivating delayed rectifier channels [35]. Immunoreactivity studies revealed the expression of Kv1.2, Kv1.3 and Kv1.6 in mouse [36] and rat [35] RGCs. An *In vivo* study showed that a few members of the Kv1 family contribute to degeneration of RGCs after optic nerve axotomy [36].

Considering these findings and recent studies identifying Kv1.3, and Kv1.6 as PKG targets [37], we evaluated possible differences in Kv1 channel phosphorylation in *rd1* P11 retinal explant samples treated with CN003 or CN238 using PamChip® peptide microarray-based Serine/Threonine Kinase (STK) activity assays. This analysis showed decreased phosphorylation for approximately 56% of the 142 peptides on STK PamChip® (Figure 4A). Twenty-one peptides were identified whose phosphorylation significantly decreased in *rd10* CN238 compared to untreated *rd10*, with a significant decrease in the phosphorylation of Kv1.3 and Kv1.6 ($p<0.05$) in treated retinae, indicating reduced kinase activity (Fig. 4B).

We then mapped the localization of Kv1.3 and Kv1.6 channels in the adult mouse retina. To this end we stained retinal cross-sections and flat mounted retinas of P24 WT mice for anti-Kv1.3 and anti-Kv1.6 antibodies. This procedure revealed intense Kv1.3 staining in the ONL, inner plexiform layer (IPL) and nerve fiber layer (NFL). Kv1.6 immunoreactivity was detected in the photoreceptor OS, IPL, and NFL. Furthermore, both Kv1.3 and Kv1.6 antibodies co-localized with anti-SMI32, recognizing non-phosphorylated epitopes of neurofilament proteins (Fig. 4C).

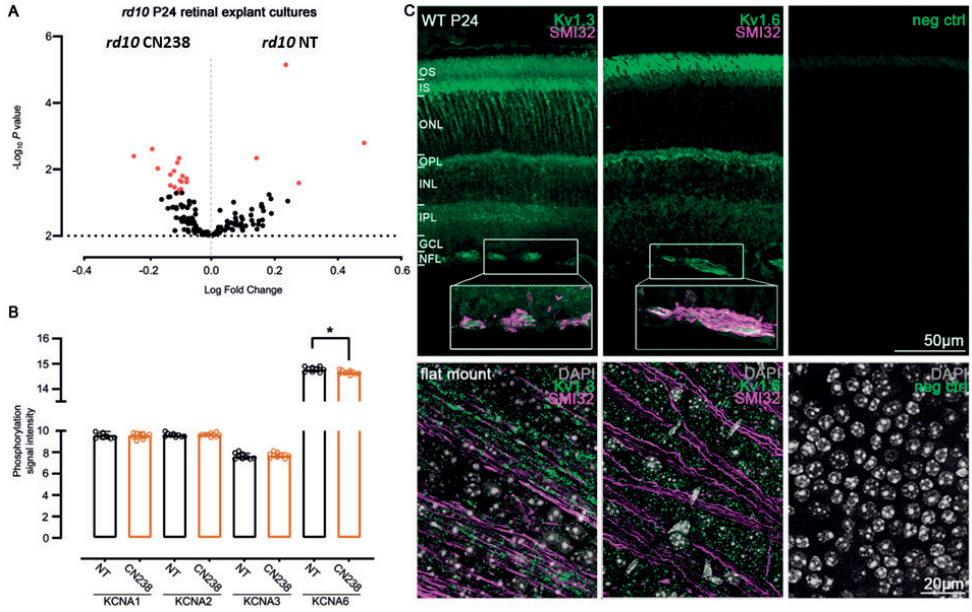

Figure 4: Localization and phosphorylation status of Kv1.3 and Kv1.6 in the mouse retina at P24. (**A**) Volcano plot representing Log Fold Change (LFC) and $-Log_{10}$ *p*-value for peptide phosphorylation. Red dots indicate significantly changed phosphopeptides (*p*-value < 0.05), black dots represent peptides with no significant alteration in phosphorylation. (**B**) Bar graph showing the phosphorylation of Kv1.1, Kv1.2, Kv1.3, and Kv1.6 peptides on the PamChip® STK array as signal intensity in *rd10* NT and *rd10* treated with CN238 treated explants with significant difference ($p < 0.05$) determined by Unpaired t-test. (**C**) Retina cross-sections and Flat mounted retinas derived from WT P24 mice stained with DAPI (grey), anti-SMI32 (magenta) anti-KCNA3 and anti-KCNA6 (all green). OS = outer segment, IS = inner segment, ONL = outer nuclear layer, OPL = outer plexiform layer, INL = inner nuclear layer, IPL = inner plexiform layer, GCL = ganglion cell layer, NFL = nerve fiber layer, P postnatal day.

CN238 inhibits Kv1-mediated calcium extrusion

To investigate a correlation between the reduction of Kv1.6 phosphorylation (PamChip® data) in CN238-treated cultures and the impact of CN238 on retinal function, we performed MEA-based µERG recordings on acute retinal explants of WT mice in the presence of CN238, its corresponding PKG-activator CN056, and the selective inhibitor of Kv1.3 and Kv1.6 Margatoxin (Fig. 5A).

The light-induced hyperpolarization in µERG (negative a-wave deflection, Fig. 5A, 5B) of acute retinal explants exposed to Margatoxin did not differ from control (ctr: -88.76 ± 14.08 and Mrg: -79.59 ± 10.91 µV). In contrast, in explants exposed to CN238 (-16.18 ± 8.6 µV) and CN056 (-39.46 ± 10.73 µV), light-induced hyperpolarization significantly decreased 5.5- and 2.4-fold compared with control (Fig. 5B). In addition, we evaluated the correlated response of RGCs to retinal light stimulation. While the light-correlated responses of RGCs in the CN056 groups were almost identical to those in the control groups (CN056: 77.53 ± 40.46 and ctr: 75.14 ± 34.29 spike count), they were significantly reduced in the Margatoxin

(4-fold) and CN238 (7-fold) groups (Fig. 5C, Mrg: 19.02 ± 9.86 and CN238: 10.54 ± 8.51 spike count), suggesting an abolition of spike generation due to Kv antagonization.

To validate the light-induced responses of RGCs (retinal network mediated RGC responses), we evaluated RGC responses directly elicited by potassium chloride (KCl) stimulation (calcium-imaging recordings) on acute retinal explants of an adult blind *rd10* mouse in the presence of CN238, the PKG activator CN056, the selective Kv1.3 and Kv1.6 inhibitor Margatoxin or in the absence of a compound as control (Fig. 5D). The Margatoxin and CN238 data revealed a significant decay in the clearance of the intracellular Ca^{2+} (at 90 s: mrg 2.04-fold and CN238 1.84-fold higher than ctr (4.28 ± 0.30); at 180 s: Mrg 4.81-fold and CN238 2.34-fold higher than ctr (1.26 ± 0.13)), intruded upon KCl-stimulus, while CN056 mediated similar responses to those found in the control groups (Fig. 5E), suggesting an inhibition of Kv-mediated calcium extrusion.

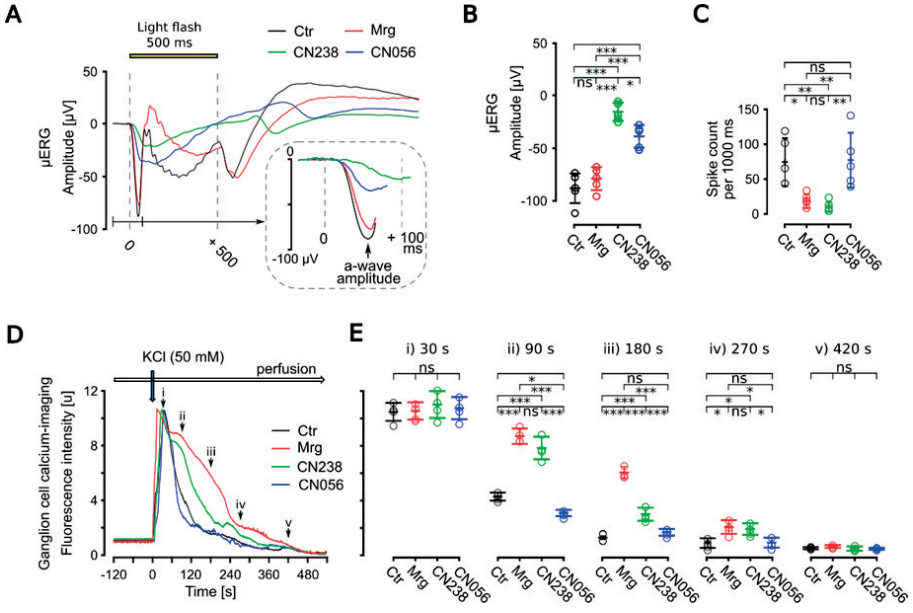

Figure 5: Effects of PKG-modulators on retinal photoreceptors and ganglion cells. Multi-electrode array recordings of light-stimulation induced retinal responses (wild type mouse, n = 5 retina) under control condition and in presences of Margatoxin (Mrg, 50 nM), CN238 (50 µM) and CN056 (50 µM): representative micro-electroretinogram (µERG) traces (**A**), µERG a-wave amplitude (**B**) and ganglion cell spike (**C**). Calcium-imaging recording of KCl-induced ganglion cells responses (blind rd10 mouse, n = 4 retina, 200 cells per retinal recording) under control condition and in presences of Mrg, CN238 and CN056 (same concentrations as A-C): representative KCL-evoked (50 mM) ganglion cell traces (**D**) and values of intracellular calcium clearance at respective five time points (30, 90, 180, 270 and 420 s) post stimulation (**E**). Error bars indicate SD; statistical analysis: one-way ANOVA followed by Dunnett´s multiple comparison test; levels of significance: **P* ≤ 0.05, ***P* ≤ 0.01, ****P* ≤ 0.001.

Discussion

The excessive accumulation of cGMP in photoreceptors has long since been established as a trigger for the loss of photoreceptors in rare, RD-type diseases [6,14]. Here, using the novel inhibitory cGMP-analogue CN238, we validate PKG as the critical effector of cGMP-dependent cell death. Unexpectedly, the protective effect of PKG inhibition extended beyond photoreceptors to axotomized retinal ganglion cells, neurons whose degeneration is underlying common retinal diseases such as glaucoma and diabetic retinopathy. Importantly, a drug-mediated rescue of axotomized RGCs of the magnitude seen in this study has not been reported before. This emphasizes the general importance of PKG for neuronal cell death and highlights PKG inhibition as a new therapeutic approach for the treatment of neurodegenerative diseases in general.

cGMP analogues as PKG inhibitors

Analogues of cGMP carrying an Rp-configurated phosphorothioate modification were first described as exceptionally potent and selective PKG inhibitors in the early 1990s [15,38]. While clinically used kinase inhibitors typically block the ATP-binding site present on all kinases [39,40], cGMP analogues target the cGMP-binding site present only on PKG, *i.e.*, its physiological activation mechanism, thereby affording an extraordinary selectivity for PKG.

With CN238, we identified a cGMP analogue PKG inhibitor that preserved photoreceptor viability and function in *rd1* and *rd10* retina. This novel compound was found to have improved potency when compared to the reference compound CN003, a known PKG inhibitor with protective effects in *rd1*, *rd2*, and *rd10* mice *in vivo* [16].

Both cGMP analogues are characterized by the ß-phenyl-1, N^2-etheno (PET) group [41] and differ only by the additional methyl group in CN238. Interestingly, the compound CN007 which carried a similar N^2-etheno modification was moderately photoreceptor protective, while CN226, which lacked such a R_2-R_3 modification (Figure 1), did not afford photoreceptor protection in *rd1* retina. This lack of efficacy was corroborated by the studies on *rd10* retina where CN226 showed significantly less preservation of photoreceptor function than CN003 or CN238.

The PET-group enhances the lipophilicity of Rp-cGMPS analogues, making it easier for the compounds to reach their target site inside the cell. In addition, the PET-group may bestow the ability to inhibit cyclic nucleotide gated ion (CNG) channels, albeit with an efficacy that is ≈ 2-3 log units lower than for PKG inhibition [41]. Although, CNG channel activity was for many years considered to be a driver of photoreceptor degeneration [42,43], numerous studies in the last two decades explored the use of CNG-channel blockers, essentially without tangible results. Moreover, a recent study found that the selective block of CNG channels with L-*cis*-diltiazem increased rather than prevented photoreceptor cell death [44]. These conflicting results would suggest that while CNG channels inhibition alone did not slow the rate of cell death, the presence of the PET- group in cGMP inhibitory PKG analogues appears to play a role in the efficacy of the compounds. This could imply both that PET modification and thus large lipophilic substituents may contribute to the inhibitory

effect of the compounds, but also that synergistic action on multiple events downstream of cGMP signaling is promising for RD treatment development.

Effect of PKG inhibitors on photoreceptor function

The PKG inhibitors CN003 and CN238 robustly preserved the function of *rd10*-mutant photoreceptors as assessed via retinal recording of MEA µERG field-potentials. Each of the 59 MEA electrodes covered an area of approx. 80 μm^2, meaning that the field potentials recorded likely originated from thousands of photoreceptors [22]. Likewise, the amplitude of the initial negative deflection in the µERG represents the sum response of a large number of photoreceptors in a given recording field. Moreover, the recording of µERGs at different retinal locations allowed the creation of spatial activity maps for light responsiveness, both for treated and untreated tissues. The comparison of such maps of *rd10* retina revealed large differences between CN003/CN238 treated and untreated specimens, not only in terms of amplitudes of negative µERG deflections but also in terms of the areas of the retina showing responses to light flashes. This in turn demonstrates the magnitude of the photoreceptor protection over a large retinal area, an effect that was corroborated by the histological examination of the retina.

PKG inhibition affords multilevel neuronal protection

The deleterious effects of high cGMP on photoreceptor viability were established already in the 1970s [6,14]. Yet, the role of PKG as a necessary and sufficient mediator of cGMP-dependent photoreceptor cell death was recognized only more recently [4,7]. Accordingly, a systematic screening of PKG targeting cGMP analogues in various *in vitro* and *in vivo* models identified CN003 as a compound that afforded strong functional protection of *rd1*-, *rd2*-, and *rd10*- mutant photoreceptors [16].

The finding that PKG inhibition with either CN003 or CN238, in addition to photoreceptor protection, also prevented the demise of RGCs in both WT and *rd10* long-term retinal explant cultures was entirely unexpected. The transection of the optic nerve is a massive insult, known to cause rapid RGC function loss and degeneration [31,32]. Instead, our MEA recordings indicated striking preservation of RGC function, concomitant with a marked and significant increase in morphological RGC survival. A recent MEA study on retinal explant cultures found that in WT retina RGC activity gradually decreased to essentially zero within a culture period of 14 days. More importantly, RGC responses to light stimulation were no longer observed beyond 7 days of culture [30], a result that corresponds to our observations on both WT and *rd10* retina.

To investigate whether RGCs survival was somehow related to photoreceptor rescue, WT retinal explant cultures were treated with CN238 and compared with untreated specimens. Also, in treated WT retina the MEA recordings revealed strong RGC responses correlated to light stimuli. Immunohistochemical analysis, using the RGC marker RBPMS [33,45] and performed on the recorded retinal explants, demonstrated the strongly improved RGC survival after CN238 treatment. Remarkably, the number of RBPMS positive RGCs in both *rd10* and WT untreated retinal explants were approximately equal. Furthermore, in WT retina, the comparison of the number of photoreceptors in a row did not show any difference between the CN238-treated and untreated groups. These results suggest that in

both the WT and the *rd10* situation, long-term retinal explant cultures display a loss of RGCs over time and that their rescue by CN238 is independent of photoreceptor survival. The failure of the cGMP analogue CN226 to preserve RGCs viability and function in *rd10* retinal explants indicates that RGC survival is connected to PKG inhibition.

The very marked RGC protection seen with CN003 and CN238 makes these compounds attractive for therapy development beyond photoreceptor diseases. Indeed, RGC degeneration is a hallmark of several retinal diseases with only limited treatment options to date. This includes glaucoma [46], diabetic retinopathy [47], exudative age-related macular degeneration [48], and non-exudative age-related macular degeneration [49]. How exactly PKG inhibition may afford RGC neuroprotection is not clear at present, yet numerous earlier studies have invoked detrimental effects of nitric oxide synthase and nitric oxide (NO) on RGCs [50,51] also in optic nerve injury [52]. Since, NO activates soluble guanylyl cyclase to produce cGMP and activate PKG [53] increased NO production in injured RGCs will likely also cause overactivation of PKG, providing a rationale for the use of PKG inhibitors for RGC neuroprotection. The axotomy-induced degeneration of ganglion cells resembles a Wallerian-like retrograde degeneration [54,55]. The fact that PKG inhibition significantly reduces this type of degeneration thus indicates that PKG inhibitors may be applicable even more broadly in neurodegenerative conditions characterized by axonal damage, such as spinal cord injury or multiple sclerosis.

PKG inhibition and RGC survival: a possible link

Whether *in vivo* or *in vitro*, optic nerve damage triggers a degeneration process that results in RGC death accompanied by a gradual loss of RGC activity [30,56]. Several *in vivo* studies reported that inhibition of the voltage-dependent potassium channels Kv1.1 and Kv1.3 rescued RGC after optic nerve axotomy [36,57,58]. It is intriguing that recently, Roy and collaborators identified some members of the Kv1 family (*i.e.,* Kv1.3, Kv1.2, and Kv1.6) as potential substrates of PKG1 and PKG2 in 661W cells [37]. Furthermore, in a parallel study, we measured the ability of PKG1 and PKG2 to phosphorylate certain substrates in retinal explant samples derived from *rd1* and WT, treated or not with CN003. Among the different substrates highly phosphorylated in *rd1* but not in WT were Kv1.3 and Kv1.6 channels. Interestingly, treatment with CN003 reduced this phosphorylation significantly [34].

By immunofluorescence staining on cross sections and flat mounts of retinas from WT P24 mice we localized Kv1.3 and Kv1.6 in the ONL and the NFL which is consistent with previous observations on the distribution of potassium channels in the mammalian retina [35,59]. The NFL tract proximal to the RGC soma consists of unmyelinated axons characterized by mitochondria-rich varicosities and a high level of Na^+/K^+-ATPase [60]. These peculiarities suggest a high energy demand in this area of the NFL [61]. Analysis of the kinase activity in retinal explants cultures derived from *rd10* P24 mice confirmed reduced phosphorylation of the Kv1.6 channel in CN238-treated retinas compared to untreated retinas. In addition, results obtained from calcium-imaging on acute retinal explants derived from adult *rd10* mice confirmed that CN238 exerts Margatoxn-like effects on Kv1.3 and Kv1.6. In fact, the slowing of Ca^{2+} release extracellularly by both Margatoxin and CN238 suggests that the latter inhibits Kv1 channels. Thus, hyperactivation of PKG in RGCs directly or indirectly increases phosphorylation of its targets Kv1.3 and Kv1.6, increasing K^+ efflux from these channels. The

greater the K^+ efflux from the cell, the greater the ionic imbalance between the inside and outside of the cell. This would lead to an increase in the activity of the Na^+/K^+ pump [62] and thus to higher energy consumption which would gradually lead the cell to death. Similarly, in photoreceptors, a high loss of K^+ caused by PKG through Kv1.3 and Kv1.6 could increase ATP-dependent Na^+/K^+ exchanger (NKX) activity in the inner segment (IS), possibly leading to cell death. However, MEA recordings on acute retinal explant derived from adult WT mice did not indicate a modulation of photoreceptor light-induced response by CN238 through Kv1 channels. In a follow-up study, it would be interesting to determine whether the use of specific inhibitors or knockdown of Kv1 channels could produce protective effects like those mediated by CN238 or CN003 on photoreceptors and RGCs in organotypic retinal explant cultures. This would help to better understand the impacts of Kv1 channel modulation by PKG in both cell types but also to throw light on the potential beneficial effects that cGMP analogues might have on RGCs other than photoreceptors.

Conclusion

While there has been tremendous progress in the development of new forms of therapy for RD, including gene, molecular and stem cell-based therapies [63,64], as well as retinal prostheses [65], there is still an important unmet medical need for more broadly applicable therapies that may benefit large groups of RD-patients. Our results support the idea that PKG/cGMP signaling is involved in photoreceptor degenerative processes [4] and identify CN238 as a second-generation drug candidate with protective effects on photoreceptors survival and function in two mouse models for RD *in vitro*. However, further studies need to be conducted to assess whether the protective effects of CN238 can be extended to other models for RD characterized by abnormal cGMP signaling. In addition, the protective effect on RGCs in the explant culture system opens new perspectives for the use of PKG inhibitors for the treatment of common retinal diseases, including glaucoma.

Materials and Methods

Animals: C3H *Pde6b*$^{rd1/rd1}$ (*rd1*), congenic C3H *Pde6b*$^{+/+}$ wild-type (C3H), C57BL/6J wild-type (C57) and C57BL/6J *Pde6b*$^{rd10/rd10}$ (*rd10*) mice were housed under standard light conditions, had free access to food and water, and were used irrespective of gender. All procedures were performed in accordance with the ARVO declaration for the use of animals in ophthalmic and vision research and the law on animal protection issued by the German Federal Government (Tierschutzgesetz) and were approved by the institutional animal welfare office of the University of Tübingen. The experiments involving the *Xenopus laevis* frogs were approved by the animal ethical committee of the Friedrich Schiller University of Jena and by the Thüringer Landesamt für Verbraucherschutz. The respective protocols were performed in accordance with the approved guidelines. Extreme efforts were made to reduce the stress and to keep the number of frogs to a minimum.

cGMP analogues synthesis: Synthesis of cyclic nucleotide analogues was performed by Biolog Life Science Institute GmbH & Co. KG according to previously described methods [16] (https://patentscope.wipo.int/search/en/detail.jsf?docId=WO201801 0965).

In vitro PKG activation/inhibition assay: FLAG-Strep-Strep-tagged human PKG1α (2–671) Wt, human PKG1β (4–686) Wt and human PKG2 (1-762) Wt were expressed in HEK293T cells. Cells were transfected at 80% confluency in whole medium employing the transfection reagent polyethyleneimine (Polysciences Europe GmbH, Germany). The cells were lysed using 50 mM Tris-HCl (pH 7.3), 150 mM NaCl, 0.5 mM TCEP, 0.4 % Tween, protease and phosphatase inhibitors (Roche, Germany). For purification we employed Strep- Tactin® Superflow® resin (IBA GmbH, Germany). We included an additional washing step with 366 mM Na_2HPO_4, 134 mM NaH_2PO_4 (pH 7.3) and 0.5 mM TCEP at room temperature to release any remaining nucleotides from the respective nucleotide binding pockets. Strep-tagged proteins were eluted with 200 mM Tris-HCl (pH 8), 300 mM NaCl, 2 mM EDTA and 5 mM desthiobiotin (IBA GmbH, Germany) and subsequently stored at 4°C in 50 mM Tris-HCl buffer (pH 7.3) containing 150 mM NaCl and 0.5 mM TCEP.

PKG kinase activity was assayed *in vitro* using a coupled spectrophotometric assay originally described by Cook et al. [18] in a clear 384 well PS-MICROPLATE (Greiner Bio-One, USA) in a CLARIOstar plate reader (BMG LABTECH, Germany). The final assay mixture contained 100 mM MOPS (pH 7.0), 10 mM $MgCl_2$, 1 mM ATP, 1 mM phosphoenolpyruvate, 15.1 U/ml lactate dehydrogenase, 8.4 U/ml pyruvate kinase, 230 µM reduced nicotinamide adenine dinucleotide, 0.1 mg/ml BSA, mM β-mercaptoethanol and, as PKG substrate, 1 mM VASPtide (RRKVSKQE; GeneCust, Luxembourg). PKG Activation was determined with cGMP (Figure S1) and the cGMP analogues CN003, CN226, and CN238 (all Biolog Life Science Institute GmbH & Co. KG, Germany) in dilution series ranging from 100 µM to 5.1 nM. The kinase reaction was started with 5 nM of the corresponding PKG isoform. Inhibition studies were performed by adding each PKG isoform supplemented with 2 µM cGMP to the assay mix and the respective cGMP analogue in dilutions ranging from 100 µM to 5.1 nM. One to three independent protein preparations were used for each assay, which in turn were performed in duplicates.

Organotypic retinal explant cultures: Organotypic retinal cultures derived from C57, *rd10*, *rd1*, and C3H animals, were prepared as previously described [19,20] under sterile conditions. Post-natal day (P)5 *rd1*, P9 or P12 *rd10* animals were sacrificed, the eyes rapidly enucleated and incubated in R16 retinal culture medium (07491252A; Gibco; Waltham, Massachusetts, USA) with 0.12% proteinase K (21935025; ICN Biomedicals Inc., Costa Mesa, California, USA) for 15 min at 37 °C. Proteinase K activity was blocked by the addition of 20% foetal bovine serum (FCS) (F7524, Sigma) followed by rinsing in R16 medium. Afterwards, the anterior segment, lens, vitreous, sclera, and choroids were removed, while the RPE remained attached to the retina. The explant was cut into a four-wedged shape resembling a clover leaf and transferred to a culture membrane insert (3412; Corning Life Sciences) with the RPE facing the membrane. The membrane inserts were placed into six-well culture plates and incubated with complete R16 medium with supplements and free of serum and antibiotics [19], in a humidified incubator (5% CO2) at 37 °C. For the first 48h the retinae were cultured with complete R16 medium without any treatment to allow adaptation to culture

conditions. Afterwards, they were either exposed to different cGMP analogues (dissolved in water), each at [50 µM], or kept as untreated control. In both cases, medium was changed every second day with replacement of the full volume of the complete R16 medium, 1mL per dish, with fresh medium. The culturing paradigm was from P5 (explantation) to P11 (end of culture) for *rd1*. For the *rd10* model, two culturing paradigms were used: from P9 to either P17 or P19, and from P12 to P24. Culturing was stopped by 45 min fixation in 4% paraformaldehyde (PFA), cryoprotected with graded sucrose solutions containing 10, 20, and 30% sucrose and then embedded in Tissue-Tek O.C.T. compound (Sakura Finetek Europe, Alphen aan den Rijn, Netherlands). Tissue sections of 12 µm were prepared using Thermo Scientific NX50 microtome (Thermo Scientific, Waltham, MA) and thaw-mounted onto Superfrost Plus glass slides (R. Langenbrinck, Emmendingen, Germany).

Histology: For retinal cross-sectioning preparation, the eyes were marked nasally, and the cornea, iris, lens, and vitreous were carefully removed. The eyecups were fixed in 4% PFA, cryoprotected in sucrose, and sectioned as above. For retinal flat mount preparation, the eyes were enucleated and the anterior segment, lens, vitreous, sclera, choroids and RPE were removed. The retinas were fixed with 4% PFA and directly prepared for immunostaining.

TUNEL assay: The various cGMP analogues were tested for their effect on photoreceptor cell death, using terminal deoxynucleotidyl transferase dUTP nick end labeling (TUNEL) assay [21] (Sigma-Aldrich *in situ* Cell Death Detection Kit, 11684795910, red fluorescence). DAPI contained in the mounting medium (Vectashield antifade mounting medium with DAPI; Vector Laboratories, Burlingame, CA, USA) was used as nuclear counterstain.

Immunofluorescence: Immunostaining with primary antibody against rabbit RBPMS (1:500; Abcam, Cambridge, UK) was performed on 12 µm thick retinal explants cryosections by incubating at 4 °C overnight. Immunostaining with primary antibody against rabbit KCNA3 (1:200; Alomone labs), rabbit KCNA6 (1:300; Alomone labs) and mouse SMI32 (1:1000; Biolegend) was performed on 14 µm thick retinal cross-sections and retinal flat mounts by incubating at 4 °C overnight. Alexa Fluor 488 and 568 were used as secondary antibodies. Sections were mounted with Vectashield medium containing 4',6-diamidino-2-phenylindole (DAPI, Vector).

Microscopy and image processing: Images were captured using 7 Z-stacks with maximum intensity projection (MIP) on a Zeiss Axio Imager Z1 ApoTome Microscope MRm digital camera (Zeiss, Oberkochen, Germany) with a 20x APOCHROMAT objective. For more details about the characteristics of the filter sets for the fluorophores used see Table 1. For the quantifications of positively labelled cells, pictures were captured on at least six different areas of the retinal explant for at least four different animals for each genotype. Adobe Photoshop (CS5Adobe Systems Incorporated, San Jose, CA) was used for image processing.

Table 1: Fluorophores and microscope filters. Excitation (exc.) and emission (em.) characteristics of the TMR red, AF488 and AF568 and of the microscope filter sets used to visualize them.

Fluorophore	exc. max. / em. max. (nm)	exc. filter / em. filter (nm)
TMR red	540/580	538-562/570-640
AF488	495/519	450–490 /500-550
AF568	577/603	538-562/570-640

***Ex-vivo* retinal function test:** Prior to recording organotypic retinal cultures were kept dark for at least 12h, further manipulations were performed under dim red light. The retinas were divided into two equal halves, one of which was placed immediately on the electrode field of the recording chamber and kept in the dark. The second retinal half was used for histological preparation and immunofluorescence (see above). Two recordings were obtained from locations within the central retinal half. Retinal function tests were performed in R16 medium, and the recording chamber temperature was set to 37°C. Functional tests were performed in R16 medium, and the recording chamber temperature was set to 37°C. In contrast, experiments with acute retinal explants were caried out in ACSF-medium (Haq et al. 2018) and exposed either to the cGMP analogues CN238 and CN056, each at [50 µM], Margatoxin at [50 nM] or kept untreated as a control. Electrophysiological recordings and raw data preparation of the organotypic retinal cultures and the acute retinal explants were performed as following: To record the light-evoked retinal responses, a micro-electrode array system (MEA; USB-MEA60-Up-BC-System-E, Multi-Channel Systems; MCS; Reutlingen, Germany), equipped with HexaMEA 40/10iR-ITO-pr (60 electrodes = 59 recording and one reference electrode) was employed. The recordings were performed at 25.000 Hz sampling rate to collect unfiltered raw data. The trigger synchronized operation of the light stimulation (LEDD1B T-Cube, Thorlabs, Bergkirchen, Germany) and MEA-recording were controlled by a dedicated protocol implemented within the MC-Rack software (v 4.6.2, MCS) and the digital I/O – box (MCS). The light stimulation (white light LED, 2350 mW, MCWHD3, Thorlabs), guided by fiber-optic and optics, was applied from beneath the transparent glass MEA: five full field flashes of 500 ms duration with 20 s intervals. A spectrometer USB4000-UV-VIS-ES (Ocean Optics, Ostfildern, Germany) was employed to calibrate the intensity of the applied light stimulation (1,33E+14 photons/cm²/sec). For the analysis of the electrophysiology data, custom-developed scripts (MATLAB, The MathWorks, Natick, MA, USA) were used, if not indicated otherwise. MEA-recording files were filtered employing the Butterworth 2nd-order (MC-Rack, MC) to extract retinal ganglion cell spikes (high pass 200 Hz) and field potentials (bandpass 2 – 40 Hz). The field potentials recorded by the MEA system are referred as micro-electroretinogram (µERG), and largely correspond to the human electroretinogram (ERG) as described by [22]. The filtered data were converted to *.hdf files by MC DataManager (v1.6.1.0). Further data processing was performed in MATLAB (spike and field potential detection) as previously described [23,24].

For calcium-imaging of retinal ganglion cells acute retinal explants derived from *rd10* mice were loaded by the calcium-indicator fluorescent dye OGB1 (Oregon Green 488 BAPTA-1, Thermofisher, Germany, [25]. Recordings of the ganglion cell layer were performed utilizing an upright fluorescence microscope (BX50WI, Olympus, Germany) equipped with a 20X water immersion objective (LUMPlan FL, 40X/0.80W, ∞/0, Olympus), a polychromator

(VisiChrome, Till Photonics) and a CCD camera (RETIGA-R1, 1360×1024 pixel, 16 bit). Time stacks of the OGB1 fluorescence were acquired at 10 Hz (λexc= 470; Olympus U-MNU filter set, 30 ms exposure time, 8-pixel binning) using the VisiView software (Till Photonics). KCl stimulus [50 mM, 50 µl droplet] was bath applied in the vicinity of the objective via the Micro-Injection Syringe Pump (MICRO2T SMARTouch, World Precision Instruments, WPI, Florida USA), while the perfusion rate was set to 2 ml/min (Perfusion system of MCS).

Kinase activity profiling using multiplex peptide microarrays: Kinase activity profiling of retinal explant samples was analyzed on PamGene's Serine/Threonine Kinase (STK) Arrays, according to the manufacturer's instructions (PamGene International B.V., 's-Hertogenbosch, The Netherlands). The rd10 retinal explant samples treated with CN238 or untreated were lysed for 30 min on ice with M-PER Mammalian Extraction Buffer (Thermo Fischer Scientific, #78501) supplemented with protease and phosphatase inhibitor cocktails (Halt Phosphatase Inhibitor Cocktail, Thermo Fischer Scientific, #78420 and Halt Protease Inhibitor Cocktail EDTA free (Thermo Fischer Scientific, #87785), followed by centrifugation (16 000 x g, 15 min, 4 °C). The supernatant was immediately divided into aliquots and snap frozen at -80 °C. Protein quantification of the retinal lysates was performed by Bradford Assay, as per the manufacturer's instructions.

STK activity measurement was performed on PamChips®, where the chip comprises of four arrays, each with 142 Serine/Threonine-containing peptides. Briefly, each assay was performed in duplicate with an assay mix comprising of 0.25 µg of protein lysate, protein kinase buffer (proprietary, PamGene), 0.01% BSA, STK primary antibody mix (proprietary, PamGene), and 400 µM ATP. The PamChips® were first placed in PamStation® and blocked with 2% BSA. Subsequently, an assay mix was added and pumped back and forth through the PamChip® wells in order to facilitate interactions between the active kinases and the immobilized peptides. The phosphorylation of peptides by kinases present in the samples was detected by a FITC-conjugated secondary antibody targeting towards the primary STK antibody cocktail [26,27]. The images of the arrays were recorded at multiple exposure times and quantified by BioNavigator® software, version 6.3.67.0 (PamGene International B.V., 's-Hertogenbosch, The Netherlands).

Statistics:

1) **Analysis of PKG activation/inhibition assay:** data were analyzed using GraphPad Prism 8.0.1 (GraphPad Software, Inc, La Jolla, CA, USA). Activation (K_{act}) and inhibition (IC_{50}) data are presented as mean ± standard deviation (SD); *n* = at least 3 except CN226 (n=2).

2) **Analysis of retinal cell death:** The total number of TUNEL positive cells in the defined area of the outer nuclear layer (ONL) were estimated by dividing the ONL area by the average area occupied by a cell (*i.e.*, cell size). The number of positively labelled cells in the ONL was counted manually on pictures captured on at least six different areas of the retinal explant for at least four different animals for each genotype. Only cells showing a strong staining of the photoreceptor nuclei were considered as positively labelled.

Values obtained are given as fraction of total cell number in ONL (*i.e.,* as percentage) and expressed as mean ± SD.

3) **Analysis of ganglion cell survival:** An area of 1 mm^2 was divided by the product of the length of counting and the section´s thickness (12 µm). The number of RBPMS positive cells was counted manually. For statistical analysis in both 1) and 2) a one-way ANOVA testing followed by the Dunnett´s multiple comparison test as implemented in Prism 8 for Windows (GraphPad Software) was conducted.

4) **Analysis of functional-data:** (A) MEA data. Data of the organotypic retinal cultures and the acute retinal explants were analyzed as following: For the quantification of the PKG inhibitor effects on retinal light sensitivity, the photoreceptor (µERG) and ganglion cell (spikes) responses were considered: (1) Light responsiveness: This is represented by the percentage of light-dependent µERG detecting electrodes, to estimate the retinal light-sensitivity and to indirectly infer the density of functional photoreceptors in a given electrodes recording field. Note that a single MEA electrode captures the integrated signal of multiple photoreceptors within the recording field. The 59 MEA electrodes with 40 µm spacing together span an overall recording field of 340 X 280 µm, allowing to estimate the retinal light-sensitivity at 59 different positions. A µERG response upon light stimulation was counted as light-responsive if exceeding the respective threshold (response amplitude 1.75-fold ≥ calculated average of 500 ms control pre-stimulus baseline). (2) Deflection of the negative wave of the µERG: This measure reflects the strength of the light-evoked photoreceptor response – its hyperpolarization, equivalent to the a-wave in a conventional ERG – indicated by the initial negative deflection of the µERG (Figure 3 C, arrow). (3) Spike responses were accounted as light-stimulus correlated, if the post stimulus activity (average of 6 bin counts: 500 ms light duration and 100 ms post stimulation, 100 ms binning) exceeded the pre-stimulus activity (threshold: average of 5 bin counts pre-stimulus; 500 ms and 100 ms binning). Activity maps were generated to reflect the µERG recordings in their spatial context. Each pixel corresponds to a recording electrode of a MEA (center-center) and its surrounding recording area. The color encodes the negative deflection of the recorded µERG (-5 µV binning). For statistical analysis of the *rd10* data, one-way ANOVA followed by the Dunnett´s multiple comparison test was applied and for the WT dataset the Wilcoxon-Mann-Whitney test was utilized (MATLAB, The MathWorks).

5) **Analysis of STK data:** The microarray images taken at multiple exposure times were combined to a single value in BioNavigator® and log2 transformed. The differences in phosphorylation signal intensities (significant differences $p < 0.05$) between rd10 treated with CN238 and untreated retinal samples for each peptide (KCNA1_438_450, KCNA2_442_454, KCNA3_461_473, KCNA6_504_516) was determined by Unpaired t-test and visualized as Bar Plots (GraphPad Prism version 9.2.0). (B) Calcium-imaging data. Ganglion cell traces were extracted from calcium-imaging recordings (200 per recording) by encircling ganglion cells as region of interest (ROI, ~ 10-pixel diameter). The ROIs were drawn manually in ImageJ and the extracted traces values were imported and analyzed using Matlab (MATLAB, The MathWorks). For statistical analysis of the

functional data one-way ANOVA followed by the Dunnett´s multiple comparison test was applied (MATLAB).

Conflict of interests

R., F. S., and F.P.-D. have filed for three patents on the synthesis and use of cGMP analogues (PCTWO2016/146669A1, PCT/EP2017/066113, and PCT/EP2017/071859) and have obtained a European Medicine Agency orphan drug designation for the use of CN03 for the treatment of retinitis pigmentosa (EU/3/15/1462). F.P.-D. is shareholder of, or has other financial interest in, the company Mireca Medicines, which intends to forward clinical testing of cGMP analogues.

Acknowledgements

We thank Norman Rieger from the Institute of Ophthalmic Research (Tübingen). We would also like to thank Philipp Henning for his help in the generation of FSS-PKG constructs and Mathias Seeliger, Thomas Euler, Timm Schubert and Per Ekström for helpful discussions. This research was funded by grants from the European Union (transMed; H2020-MSCA-765441), the Baden-Württemberg Foundation (BWST-WSF_006), the Charlotte and the Tistou Kerstan Foundation and the German Ministry for Education and Research (BMBF; TargetRD, 16GW0267K, 16GW0269, 16GW0270).

Author contribution

Conceptualization FPD; methodology, AT, WH, AR, AR and AF; writing—original draft preparation, AT, WH, AR, AR, AF, FWH and FPD; writing—review and editing AT, WH, AR, AR, AF, FWH and FPD; supervision, FPD; funding acquisition, FPD.

References

1. Berger W, Kloeckener-Gruissem B, Neidhardt J: **The molecular basis of human retinal and vitreoretinal diseases**. *Prog Retin Eye Res* 2010, **29**:335-375.
2. Sahel JA, Marazova K, Audo I: **Clinical characteristics and current therapies for inherited retinal degenerations**. *Cold Spring Harb Perspect Med* 2014, **5**:a017111.
3. Arango-Gonzalez B, Trifunović D, Sahaboglu A, Kranz K, Michalakis S, Farinelli P, Koch S, Koch F, Cottet S, Janssen-Bienhold U, et al.: **Identification of a common non-apoptotic cell death mechanism in hereditary retinal degeneration**. *PLoS One* 2014, **9**:e112142.
4. Power M, Das S, Schütze K, Marigo V, Ekström P, Paquet-Durand F: **Cellular mechanisms of hereditary photoreceptor degeneration - Focus on cGMP**. *Prog Retin Eye Res* 2020, **74**:100772.
5. Han J, Dinculescu A, Dai X, Du W, Smith WC, Pang J: **Review: the history and role of naturally occurring mouse models with Pde6b mutations**. *Mol Vis* 2013, **19**:2579-2589.
6. Farber DB, Lolley RN: **Cyclic guanosine monophosphate: elevation in degenerating photoreceptor cells of the C3H mouse retina**. *Science* 1974, **186**:449-451.
7. Paquet-Durand F, Hauck SM, van Veen T, Ueffing M, Ekström P: **PKG activity causes photoreceptor cell death in two retinitis pigmentosa models**. *J Neurochem* 2009, **108**:796-810.
8. Kim JJ, Lorenz R, Arold ST, Reger AS, Sankaran B, Casteel DE, Herberg FW, Kim C: **Crystal Structure of PKG I:cGMP Complex Reveals a cGMP-Mediated Dimeric Interface that Facilitates cGMP-Induced Activation**. *Structure* 2016, **24**:710-720.
9. Browning DD: **Protein kinase G as a therapeutic target for the treatment of metastatic colorectal cancer**. *Expert Opin Ther Targets* 2008, **12**:367-376.
10. Canals S, Casarejos MJ, de Bernardo S, Rodríguez-Martín E, Mena MA: **Nitric oxide triggers the toxicity due to glutathione depletion in midbrain cultures through 12-lipoxygenase**. *J Biol Chem* 2003, **278**:21542-21549.
11. Canzoniero LM, Adornetto A, Secondo A, Magi S, Dell'aversano C, Scorziello A, Amoroso S, Di Renzo G: **Involvement of the nitric oxide/protein kinase G pathway in polychlorinated biphenyl-induced cell death in SH-SY 5Y neuroblastoma cells**. *J Neurosci Res* 2006, **84**:692-697.
12. Fallahian F, Karami-Tehrani F, Salami S, Aghaei M: **Cyclic GMP induced apoptosis via protein kinase G in oestrogen receptor-positive and -negative breast cancer cell lines**. *Febs j* 2011, **278**:3360-3369.
13. Leung EL, Wong JC, Johlfs MG, Tsang BK, Fiscus RR: **Protein kinase G type Ialpha activity in human ovarian cancer cells significantly contributes to enhanced Src activation and DNA synthesis/cell proliferation**. *Mol Cancer Res* 2010, **8**:578-591.
14. Lolley RN, Farber DB, Rayborn ME, Hollyfield JG: **Cyclic GMP accumulation causes degeneration of photoreceptor cells: simulation of an inherited disease**. *Science* 1977, **196**:664-666.
15. Butt E, Eigenthaler M, Genieser HG: **(Rp)-8-pCPT-cGMPS, a novel cGMP-dependent protein kinase inhibitor**. *Eur J Pharmacol* 1994, **269**:265-268.
16. Vighi E, Trifunovic D, Veiga-Crespo P, Rentsch A, Hoffmann D, Sahaboglu A, Strasser T, Kulkarni M, Bertolotti E, van den Heuvel A, et al.: **Combination of cGMP analogue and drug delivery system provides functional protection in hereditary retinal degeneration**. *Proc Natl Acad Sci U S A* 2018, **115**:E2997-E3006.
17. Zhao J, Trewhella J, Corbin J, Francis S, Mitchell R, Brushia R, Walsh D: **Progressive cyclic nucleotide-induced conformational changes in the cGMP-dependent protein kinase studied by small angle X-ray scattering in solution**. *J Biol Chem* 1997, **272**:31929-31936.

18. Cook PF, Neville ME, Jr., Vrana KE, Hartl FT, Roskoski R, Jr.: **Adenosine cyclic 3',5'-monophosphate dependent protein kinase: kinetic mechanism for the bovine skeletal muscle catalytic subunit**. *Biochemistry* 1982, **21**:5794-5799.
19. Belhadj S, Tolone A, Christensen G, Das S, Chen Y, Paquet-Durand F: **Long-Term, Serum-Free Cultivation of Organotypic Mouse Retina Explants with Intact Retinal Pigment Epithelium**. *J Vis Exp* 2020.
20. Caffé AR, Ahuja P, Holmqvist B, Azadi S, Forsell J, Holmqvist I, Söderpalm AK, van Veen T: **Mouse retina explants after long-term culture in serum free medium**. *Journal of Chemical Neuroanatomy* 2001, **22**:263-273.
21. Loo DT: **In situ detection of apoptosis by the TUNEL assay: an overview of techniques**. *Methods Mol Biol* 2011, **682**:3-13.
22. Stett A, Egert U, Guenther E, Hofmann F, Meyer T, Nisch W, Haemmerle H: **Biological application of microelectrode arrays in drug discovery and basic research**. *Anal Bioanal Chem* 2003, **377**:486-495.
23. Haq W, Dietter J, Bolz S, Zrenner E: **Feasibility study for a glutamate driven subretinal prosthesis: local subretinal application of glutamate on blind retina evoke network-mediated responses in different types of ganglion cells**. *J Neural Eng* 2018, **15**:045004.
24. Haq W, Dietter J, Zrenner E: **Electrical activation of degenerated photoreceptors in blind mouse retina elicited network-mediated responses in different types of ganglion cells**. *Sci Rep* 2018, **8**:16998.
25. Briggman KL, Euler T: **Bulk electroporation and population calcium imaging in the adult mammalian retina**. *J Neurophysiol* 2011, **105**:2601-2609.
26. Chirumamilla CS, Fazil M, Perez-Novo C, Rangarajan S, de Wijn R, Ramireddy P, Verma NK, Vanden Berghe W: **Profiling Activity of Cellular Kinases in Migrating T-Cells**. *Methods Mol Biol* 2019, **1930**:99-113.
27. Hilhorst R, Houkes L, Mommersteeg M, Musch J, van den Berg A, Ruijtenbeek R: **Peptide microarrays for profiling of serine/threonine kinase activity of recombinant kinases and lysates of cells and tissue samples**. *Methods Mol Biol* 2013, **977**:259-271.
28. Sahaboglu A, Paquet-Durand O, Dietter J, Dengler K, Bernhard-Kurz S, Ekström PA, Hitzmann B, Ueffing M, Paquet-Durand F: **Retinitis pigmentosa: rapid neurodegeneration is governed by slow cell death mechanisms**. *Cell Death Dis* 2013, **4**:e488.
29. Sancho-Pelluz J, Arango-Gonzalez B, Kustermann S, Romero FJ, van Veen T, Zrenner E, Ekstrom P, Paquet-Durand F: **Photoreceptor cell death mechanisms in inherited retinal degeneration**. *Mol Neurobiol* 2008, **38**:253-269.
30. Alarautalahti V, Ragauskas S, Hakkarainen JJ, Uusitalo-Järvinen H, Uusitalo H, Hyttinen J, Kalesnykas G, Nymark S: **Viability of Mouse Retinal Explant Cultures Assessed by Preservation of Functionality and Morphology**. *Invest Ophthalmol Vis Sci* 2019, **60**:1914-1927.
31. Berkelaar M, Clarke DB, Wang YC, Bray GM, Aguayo AJ: **Axotomy results in delayed death and apoptosis of retinal ganglion cells in adult rats**. *J Neurosci* 1994, **14**:4368-4374.
32. Osborne A, Hopes M, Wright P, Broadway DC, Sanderson J: **Human organotypic retinal cultures (HORCs) as a chronic experimental model for investigation of retinal ganglion cell degeneration**. *Exp Eye Res* 2016, **143**:28-38.
33. Rodriguez AR, de Sevilla Müller LP, Brecha NC: **The RNA binding protein RBPMS is a selective marker of ganglion cells in the mammalian retina**. *J Comp Neurol* 2014, **522**:1411-1443.

34. Roy A, Tolone A, Hilhorst R, Groten J, Tomar T, Paquet-Durand F: **Kinase activity profiling identifies putative downstream targets of cGMP/PKG signaling in inherited retinal neurodegeneration**. *Cell Death Discov* 2022, **8**:93.
35. Höltje M, Brunk I, Grosse J, Beyer E, Veh RW, Bergmann M, Grosse G, Ahnert-Hilger G: **Differential distribution of voltage-gated potassium channels Kv 1.1-Kv1.6 in the rat retina during development**. *J Neurosci Res* 2007, **85**:19-33.
36. Koeberle PD, Wang Y, Schlichter LC: **Kv1.1 and Kv1.3 channels contribute to the degeneration of retinal ganglion cells after optic nerve transection in vivo**. *Cell Death Differ* 2010, **17**:134-144.
37. Roy A, Groten J, Marigo V, Tomar T, Hilhorst R: **Identification of Novel Substrates for cGMP Dependent Protein Kinase (PKG) through Kinase Activity Profiling to Understand Its Putative Role in Inherited Retinal Degeneration**. *Int J Mol Sci* 2021, **22**.
38. Butt E, Pöhler D, Genieser HG, Huggins JP, Bucher B: **Inhibition of cyclic GMP-dependent protein kinase-mediated effects by (Rp)-8-bromo-PET-cyclic GMPS**. *Br J Pharmacol* 1995, **116**:3110-3116.
39. Atkinson EL, Iegre J, Brear PD, Zhabina EA, Hyvönen M, Spring DR: **Downfalls of Chemical Probes Acting at the Kinase ATP-Site: CK2 as a Case Study**. *Molecules* 2021, **26**.
40. Johnson LN: **Protein kinase inhibitors: contributions from structure to clinical compounds**. *Q Rev Biophys* 2009, **42**:1-40.
41. Wei JY, Cohen ED, Yan YY, Genieser HG, Barnstable CJ: **Identification of competitive antagonists of the rod photoreceptor cGMP-gated cation channel: beta-phenyl-1,N2-etheno-substituted cGMP analogues as probes of the cGMP-binding site**. *Biochemistry* 1996, **35**:16815-16823.
42. Fox DA, Poblenz AT, He L: **Calcium overload triggers rod photoreceptor apoptotic cell death in chemical-induced and inherited retinal degenerations**. *Ann N Y Acad Sci* 1999, **893**:282-285.
43. Paquet-Durand F, Beck S, Michalakis S, Goldmann T, Huber G, Mühlfriedel R, Trifunović D, Fischer MD, Fahl E, Duetsch G, et al.: **A key role for cyclic nucleotide gated (CNG) channels in cGMP-related retinitis pigmentosa**. *Hum Mol Genet* 2011, **20**:941-947.
44. Das S, Popp V, Power M, Groeneveld K, Yan J, Melle C, Rogerson L, Achury M, Schwede F, Strasser T, et al.: **Redefining the role of Ca(2+)-permeable channels in photoreceptor degeneration using diltiazem**. *Cell Death Dis* 2022, **13**:47.
45. Wang Y, Wang W, Liu J, Huang X, Liu R, Xia H, Brecha NC, Pu M, Gao J: **Protective Effect of ALA in Crushed Optic Nerve Cat Retinal Ganglion Cells Using a New Marker RBPMS**. *PLoS One* 2016, **11**:e0160309.
46. Beykin G, Norcia AM, Srinivasan VJ, Dubra A, Goldberg JL: **Discovery and clinical translation of novel glaucoma biomarkers**. *Prog Retin Eye Res* 2021, **80**:100875.
47. Lynch SK, Abràmoff MD: **Diabetic retinopathy is a neurodegenerative disorder**. *Vision Res* 2017, **139**:101-107.
48. Medeiros NE, Curcio CA: **Preservation of ganglion cell layer neurons in age-related macular degeneration**. *Invest Ophthalmol Vis Sci* 2001, **42**:795-803.
49. Yenice E, Şengün A, Soyugelen Demirok G, Turaçlı E: **Ganglion cell complex thickness in nonexudative age-related macular degeneration**. *Eye (Lond)* 2015, **29**:1076-1080.
50. Mueller-Buehl AM, Tsai T, Hurst J, Theiss C, Peters L, Hofmann L, Herms F, Kuehn S, Schnichels S, Joachim SC: **Reduced Retinal Degeneration in an Oxidative Stress Organ Culture Model through an iNOS-Inhibitor**. *Biology* 2021, **10**.
51. Neufeld AH, Sawada A, Becker B: **Inhibition of nitric-oxide synthase 2 by aminoguanidine provides neuroprotection of retinal ganglion cells in a rat model of chronic glaucoma**. *Proc Natl Acad Sci U S A* 1999, **96**:9944-9948.

52. Husain S, Abdul Y, Singh S, Ahmad A, Husain M: **Regulation of nitric oxide production by δ-opioid receptors during glaucomatous injury**. *PLoS One* 2014, **9**:e110397.
53. Bian K, Murad F: **What is next in nitric oxide research? From cardiovascular system to cancer biology**. *Nitric Oxide* 2014, **43**:3-7.
54. Howell GR, Soto I, Libby RT, John SW: **Intrinsic axonal degeneration pathways are critical for glaucomatous damage**. *Exp Neurol* 2013, **246**:54-61.
55. Vrabec JP, Levin LA: **The neurobiology of cell death in glaucoma**. *Eye (Lond)* 2007, **21 Suppl 1**:S11-14.
56. Pattamatta U, McPherson Z, White A: **A mouse retinal explant model for use in studying neuroprotection in glaucoma**. *Exp Eye Res* 2016, **151**:38-44.
57. Diem R, Meyer R, Weishaupt JH, Bahr M: **Reduction of potassium currents and phosphatidylinositol 3-kinase-dependent AKT phosphorylation by tumor necrosis factor-(alpha) rescues axotomized retinal ganglion cells from retrograde cell death in vivo**. *J Neurosci* 2001, **21**:2058-2066.
58. Koeberle PD, Schlichter LC: **Targeting K(V) channels rescues retinal ganglion cells in vivo directly and by reducing inflammation**. *Channels (Austin)* 2010, **4**:337-346.
59. Pinto LH, Klumpp DJ: **Localization of potassium channels in the retina**. *Prog Retin Eye Res* 1998, **17**:207-230.
60. Liu H, Prokosch V: **Energy Metabolism in the Inner Retina in Health and Glaucoma**. *Int J Mol Sci* 2021, **22**.
61. Wang L, Dong J, Cull G, Fortune B, Cioffi GA: **Varicosities of intraretinal ganglion cell axons in human and nonhuman primates**. *Invest Ophthalmol Vis Sci* 2003, **44**:2-9.
62. Pivovarov AS, Calahorro F, Walker RJ: **Na(+)/K(+)-pump and neurotransmitter membrane receptors**. *Invert Neurosci* 2018, **19**:1.
63. Hammond SM, Aartsma-Rus A, Alves S, Borgos SE, Buijsen RAM, Collin RWJ, Covello G, Denti MA, Desviat LR, Echevarría L, et al.: **Delivery of oligonucleotide-based therapeutics: challenges and opportunities**. *EMBO Mol Med* 2021, **13**:e13243.
64. Maguire AM, Bennett J, Aleman EM, Leroy BP, Aleman TS: **Clinical Perspective: Treating RPE65-Associated Retinal Dystrophy**. *Mol Ther* 2021, **29**:442-463.
65. Kitiratschky VB, Stingl K, Wilhelm B, Peters T, Besch D, Sachs H, Gekeler F, Bartz-Schmidt KU, Zrenner E: **Safety evaluation of "retina implant alpha IMS"--a prospective clinical trial**. *Graefes Arch Clin Exp Ophthalmol* 2015, **253**:381-387.

Supplementary information

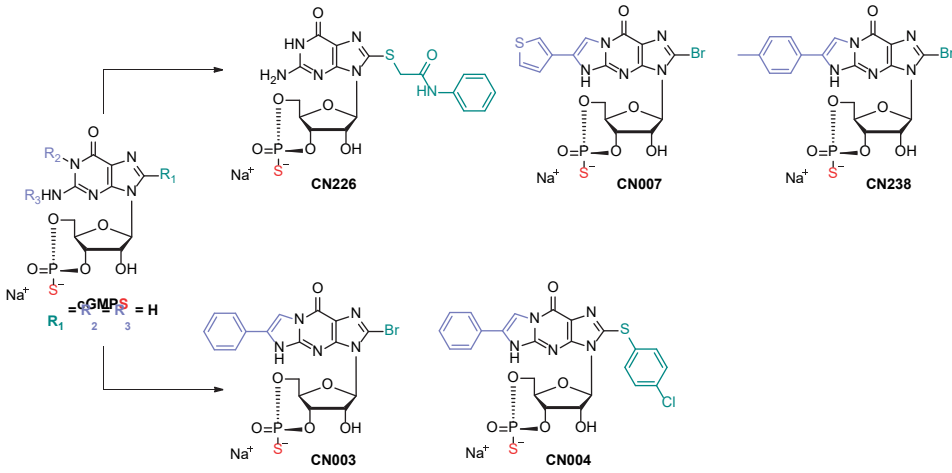

Figure S1: Structures of tested novel cyclic nucleotide analogues of cGMP and reference compounds. CN003: 8- Bromo- β- phenyl- 1, N^2- ethenoguanosine- 3', 5'- cyclic monophosphorothioate, Rp- isomer (Rp-8-Br-PET-cGMPS); **CN004**: 8- (4- Chlorophenylthio)- β- phenyl- 1, N^2- ethenoguanosine- 3', 5'- cyclic monophosphorothioate, Rp- isomer (Rp-8-pCPT-PET-cGMPS); **CN007**: 8- Bromo- (3- thiophen- yl- 1, N^2- etheno)guanosine- 3', 5'- cyclic monophosphorothioate, Rp- isomer (Rp-8-Br-(3-Tp)ET-cGMPS); **CN226**: 8- Phenylamidomethylthioguanosine- 3', 5'- cyclic monophosphorothioate, Rp- isomer (Rp-8-PAmdMT-cGMPS); **CN238**: 8- Bromo- (4- methyl- β- phenyl- 1, N^2- etheno) guanosine- 3', 5'- cyclic monophosphorothioate, Rp- isomer (Rp-8-Br-pMe-PET-cGMPS).

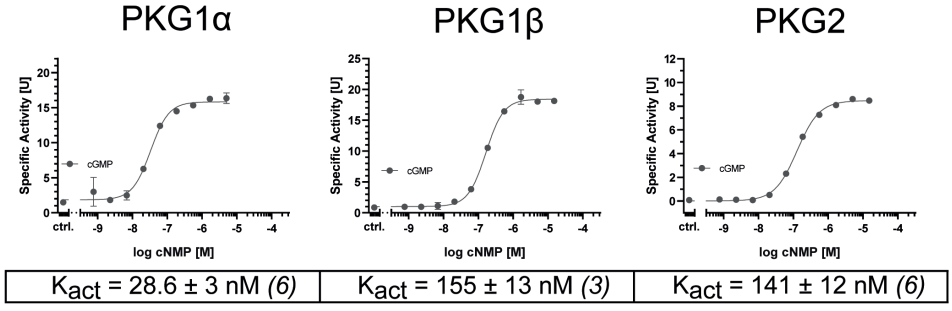

Figure S2: cGMP-dependent activation of the three distinct PKG isoforms. Activation curves of PKG1α, PKG1β, and PKG2 were obtained with cGMP dilution series ranging from 5 µM to 25.4 pm for PKG1α and from 15 µM to 762 pm for PKG1β and PKG2.

	PKG1α	PKG1β	PKG2
CN003	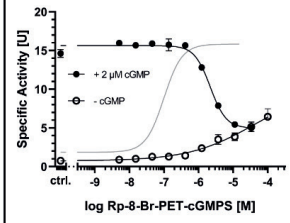	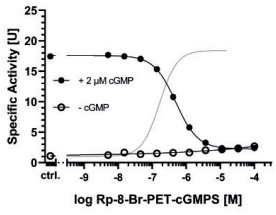	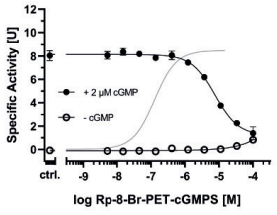
IC_{50}	1.9 ± 0.24 µM *(3)*	0.40 ± 0.09 µM *(3)*	5.8 ± 1.7 µM *(3)*
CN238	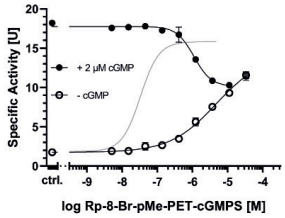	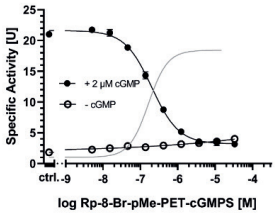	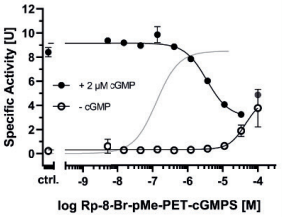
IC_{50}	1.1 ± 0.2 µM *(5)*	0.38 ± 0.22 µM *(3)*	4.6 ± 1.0 µM *(3)*
CN226	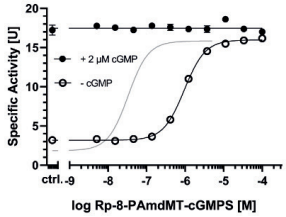	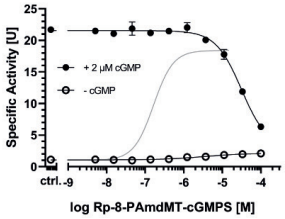	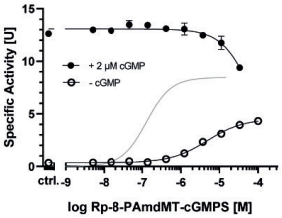
IC_{50}	-*(2)* (K_{act} = 0.87 ± 0.1 µM)	*(2)*	- *(2)*

Figure S3: Agonistic and antagonistic properties of the cGMP analogues CN003, CN238, and CN226. The activation of all PKG isoforms (grey solid line) was determined with cGMP (*cf*. supplementary figure 1). Activation/Inhibition curves of 5 nM PKG1α, PKG1β, and PKG2 were measured with the cGMP analogues CN003, CN238, and CN226. For each analogue first the activation was determined (open circles) and in a second approach the inhibition in the presence of 2 µM cGMP was measured (solid circles). IC_{50} values were calculated from cGMP analogue dilution series ranging from 100 µM to 5.1 nM obtained in 2-5 independent measurements.

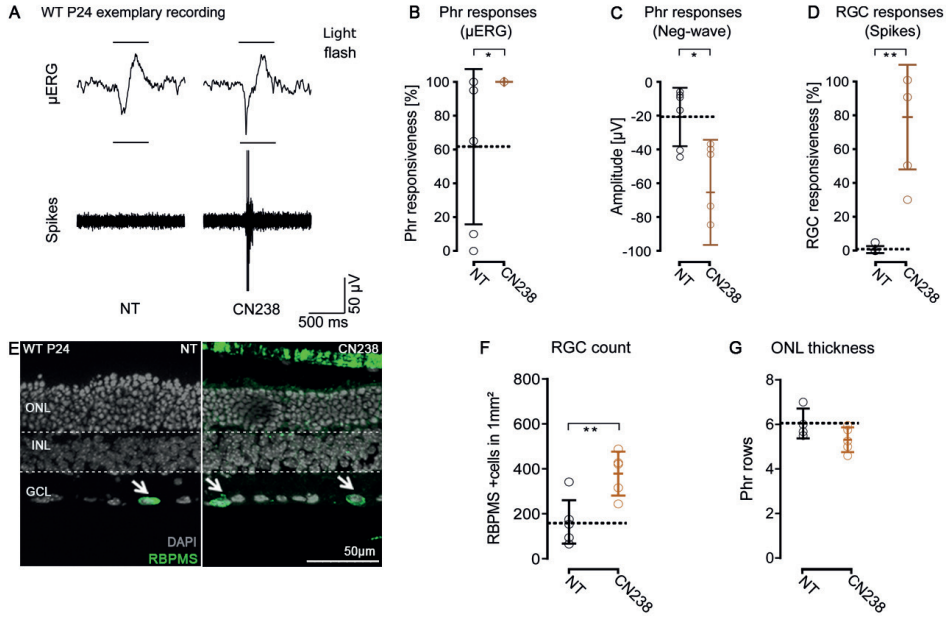

Figure S4: CN238 improves RGC viability and function in WT retinal explant cultures. (**A**) Representative light-correlated RGC spike recordings of WT P24 retinal explants treated from P14 to P24 with 50 µM CN238 and compared to NT. (**B**-**D**) Quantification of light-stimulus evoked retinal activity in NT and treated WT explants: (**B**) light responsiveness (percentage of MEA electrodes detecting light-correlated µERG activity). (**C**) Quantification of negative µERG amplitudes. (**D**) RGC activity expressed as percentage of MEA electrodes detecting light-correlated spike-activity. (**E**) Sections derived from recorded WT P24 retinal explant cultures stained with DAPI (grey) and RBPMS (green). (**F**) Quantification of RBPMS positive cells in WT P24 retinal explants sections NT or treated with CN238. (**G**) Quantification of photoreceptor rows in NT and CN238 treated WT explants. Error bars indicate SD; statistical analysis: unpaired Student´s *t*-test; levels of significance: $*P \leq 0.05$, $**P \leq 0.01$, $***P \leq 0.001$. ONL = outer nuclear layer, INL = inner nuclear layer, Phr = photoreceptor, µERG = micro-electroretinogram, GCL = ganglion cell layer, MEA = micro-electrode array.

7

Chapter 7

General discussion

Overview of the results and main findings

In spite of the high genetic and phenotypic heterogeneity in inherited retinal degenerative diseases (IRDs), several gene-based therapies have been successful in clinical trials and the first drug Luxturna (for the RPE64 specific gene mutation) has been FDA-approved in 2017. However, implementation of gene-based (or stem cell based) therapies is challenging as well as very expensive with a limited fit for a specific genetic defect. Therefore, it is crucial to find novel generic targets and develop a more common way for IRD treatment. As described in **Chapter 1,** in the last two decades a great amount of research has been carried out around the control of the 3',5'-cyclic guanosine monophosphate (cGMP) axis, its interplay with signal transduction and the role of the protein kinase G (PKG) family. Several European research collaborations (Drugsford, *trans*Med, TreatRP) have initiated the search into novel potent cGMP inhibitory analogues capable of targeting photoreceptor cell death pathways. In the present thesis the effect of these novel cGMP inhibitory analogues on PKG and its downstream targets was studied in several model systems using recombinant kinases, photoreceptor-derived cells and transgenic mice models mimicking pathophysiology of retinal degenerative diseases.

In **Chapter 2**, a literature review is presented to describe the key pathways involved in photoreceptor cell death and the analytical methods employed to study them. The initial studies focused on apoptosis of photoreceptor cells in the retina but research methods applied could not clearly differentiate between apoptotic and non-apoptotic cell death [1]. The therapeutic strategies based on inhibition of apoptotic pathways provided only limited success [2,3] and current research focus has shifted to non-apoptotic photoreceptor cell death pathways with new insights on the role of epigenetic factors, energy metabolism and/or the phototransduction cascade and the interplay with cGMP signaling. In the present thesis, studies were conducted with a focus on the role of the cGMP-PKG signaling axis in photoreceptor cell death. As described previously, phototransduction is regulated by changes in cGMP levels in photoreceptors and accumulation of cGMP has been demonstrated to damage photoreceptors and is a common feature in different IRD models [4,5]. This makes it important to study the cGMP-dependent signaling pathways in photoreceptor mediated cell death and to identify potential novel biomarkers for IRDs which is the main focus of this thesis. Chapter 2 also presents a discussion on several studies on gene expression (RT-qPCR and Microarrays) and protein expression (Western Blot, Enzyme-linked immunosorbent assays, Mass spectrometry, Immunohistochemistry and Multiplex peptide microarrays), and tools to assess cell metabolism (Clark electrodes, Warburg apparatus, Seahorse bioanalyzer) to study IRDs [6].

Recent accumulated evidences suggest that it is imperative to study cGMP-dependent photoreceptor degeneration mechanisms for identifying mutation-independent therapies. cGMP can either bind to cGMP-gated ion channels (CNGCs) and increase Ca^{2+} influx inside photoreceptors or it can bind to cGMP-dependent Protein Kinase G (PKG) which can phosphorylate several proteins and activate a plethora of biological pathways. The direct relationship between CNGCs and increased Ca^{2+} with photoreceptor cell death has not been clearly established [7–9], whereas PKG- specific inhibition has shown to significantly decrease photoreceptor cell death [10,11]. PKG as a serine/threonine kinase has two

isoforms, PKG1 and PKG2 and could have hundreds of potential targets about which limited information is available. Moreover, the current targets and mechanisms to explain the role of PKG (in)activation in the retina are not well known. Therefore, in **Chapter 3**, a new tool for the kinase activity profiling of the retina was applied using a multiplex peptide microarray technology and in this way novel and relevant PKG substrates could be identified. First the activity of recombinant PKG1 and PKG2 were assessed in the presence of known PKG activity modulators such as ATP, cGMP, cAMP and PKG activator/ inhibitors on microarrays containing 142 Serine/Threonine-containing peptides. Based on the phosphorylation response of these peptides, 50 PKG targets were identified as either specific and/or common for PKG1 and or PKG2. This information was thereafter applied to study the role of endogenous PKGs as present in the murine photoreceptor cell line 661W. The results suggested that in a complex cellular environment, PKG activators can cause an increase in PKG activity but the most prominent effect was seen in another, closely related kinase, PKA. According to literature, PKG2 is able to phosphorylate the catalytic subunit of PKA [12], which was also confirmed by our recombinant PKG study [13].

To shed more light on the possible interaction of PKG inhibitors in the retina and its critical phosphorylation targets and downstream pathways, murine retinal tissue and explants were used in **Chapter 4**. In this chapter, it was confirmed that the target-specific inhibition of PKG activity (through PKG inhibitor CN03) in organotypic retinal explants is able to strongly reduce the number of TUNEL positive dead cells, indicating a neuroprotective effect of CN03 on the retina. Investigation of the kinase activity after CN03 treatment also appeared to result in an overall decrease in phosphorylation of peptides in CN03-treated diseased retinal explants [14]. The designation of the peptides as PKG1- or PKG2- substrates was based on our studies in Chapter 3, where we ranked the peptides on the multiplex peptide microarray according to their preference for PKG1 and or PKG2 recombinant kinases. Out of twenty-two strongly altered peptides in CN03-treated *rd1* explants, fourteen are substrates for both PKG1 and PKG2, three for PKG1 only. Based on literature data, among those fourteen peptides, KCNA6, NCF1, GRIK2, VTNC, ADRB2, BRCA1, RYR1, KCNA3, and VASP have been confirmed to be present in the retina. In Chapter 4, the phosphorylated peptides were subsequently linked to the putative upstream kinases and found that kinase activity of particularly PKAα, Pim1, PKG1, PKG2, CaMK4 was suggested to be reduced by CN03 treatment in the retina explants. Notably, these were the same kinases that were predicted to be more active in the diseased *rd1* explants in comparison to WT explants, demonstrating the specific targeting by the drug candidate CN03. Major biological pathways such as Insulin resistance, mTOR, MAPK signaling, long-term potentiation, circadian entrainment, and HIF-1 signaling, determined to be potentially downregulated with the treatment were upregulated in the diseased condition. From these peptides and biological pathways found to be affected in their phosphorylating activity, six peptides were selected for further confirmation by immunohistochemical analysis (CREB1, KCNA3, KCNA6, TOP2A, F263, GRIK2) using *ex vivo* analysis of the retina. Here, we were able to confirm the presence of these proteins in different cell layers of the retina, which may play a crucial role in cGMP-PKG mediated photoreceptor degeneration.

The research in retinal tissue in the *rd1* model was followed by studying the uniquely phosphorylated proteins by PKG in the IRD model *rd10* by integration of kinome activity

and phosphor-proteomics analysis as described in **Chapter 5**. The *rd10* is another frequently used mice model to mimic retinal degeneration but degeneration happens at a slower rate so the retinal structure and (cell) functions are maintained over a longer period of time. In this study both multiplex kinome activity profiling (applying microarray analysis) and phosphoproteome profiling (applying Liquid Chromatography-Mass Spectrometry: LCMS analysis) were performed simultaneously in *rd10* retinal explants either treated or untreated with the PKG inhibitor (CN03). The CN03-mediated PKG inhibition showed an overall decrease in phosphorylation of peptides in multiplex kinome activity profiling with a significant decrease in phosphorylation of seven peptides. Out of the seven peptides, CAC1C, PLM, CREB1, PTK6, and TOP2A were identified as substrates for both PKG1 and PKG2, while RBL2 and STK for PKG2 only. Notably, a diverse phosphoproteomics profile was observed in CN03-treated *rd10* explants with both inhibited as well as activated phospho-peptides in the LC-MS data as compared to the untreated *rd10* controls. The highest-ranking network of kinases supposed to be downregulated with the treatment and common to both techniques (LC-MS and kinome activity), the AGC and CaMK families of kinases (*eg.* PKG1, PKG2, PKA, CaMKs, RSKs, AKTs, SGKs, and PKD1) were prominent. Intracellular signaling by second messengers, Calcium-induced signalling, Calmodulin-induced events, MAPK targets, CREB phosphorylation and RAS activation were amongst the major biological pathways which were affected by CN03 treatment in this *rd10* model. From the identified peptides and pathways that show reduced phosphorylating activity, 3 substrates (CREB, CaMK4 and CaMK2) were selected for further confirmation to assess their presence as well as activity by immunohistochemical analysis and immunoblotting using *ex vivo* analysis of the retina. Finally, we were able to confirm the presence and activity of three potential PKG targets where CaMK2 and CREB showed higher expression and phosphorylation in *rd10* whereas in contrast CaMK4 showed higher activity in *wild type* retinal explants.

In **Chapter 6**, the effect of a novel PKG inhibitor CN238 was studied in *rd1* and *rd10* retinal explants with a special emphasis on its effect on the K^{+}-channel $K_v1.6$. Photoreceptor viability and functionality was preserved in *rd10* retinal explants by both the promising PKG inhibitor CN238 and the reference compound CN03. Additionally, CN238 and CN03 also protected retinal ganglion cells from axotomy-induced rapid degeneration during the retinal explanation procedure and preserved their functionality. Further analysis of kinase activity-dependent protein phosphorylation patterns in CN238-treated *rd10* explants revealed an overall decrease in phosphorylation of peptides with a significant reduction in twenty-one peptides. Moreover, the Ca^{2+} imaging experiments identified the outward rectifying K^{+}-channel $K_v1.6$ as a possible mediator of PKG-dependent axotomy induced degeneration of ganglion cells. These results confirmed the significant neuroprotective capacity of cGMP analogues on both the photoreceptors and retinal ganglion cells, thereby broadening their potential applications for the treatment of retinal diseases and possibly neurodegenerative diseases characterized by axonal damage such as spinal cord injury and multiple sclerosis.

In summary, this PhD thesis confirmed the key role of cGMP and PKG activity in photoreceptor degeneration in retina and several novel targets downstream of cGMP-PKG signaling were identified in both photoreceptor cell cultures as well as in retinal explants. This is a remarkable step forward in the search of the downstream effects of new cGMP analogues which, up to now were studied mostly with a few, selected kinase substrates applying

immunohistochemistry staining in the retina. The novel potential PKG targets identified by multiplex peptide microarrays could further be validated by other protein expression techniques. Therefore, this approach and the findings could elucidate the role of PKG, especially of downstream targets in photoreceptor as well as ganglion cell degeneration.

General Discussion and future perspectives

PKG and its downstream targets

In **Chapter 3,** the multiplex peptide analysis of 661W cell lysates and recombinant PKGs and PKG identified several novel PKG targets. Depending on the peptide substrates, PKG1 and PKG2 showed similar kinase profiles, but also some isoform-specific substrate regulation. In addition to ten known substrates established from literature, about fifty new substrates specific to PKG1 and/or PKG2 were identified. This is a great advantage of multiplex peptide arrays, where one can study simultaneously more than 100 endogenous Serine/Threonine kinases and their downstream phosphorylation targets within a cell or tissue system. In this thesis, the unbiased kinome activity profiling approach identified interesting downstream interacting targets of PKG in retinal degeneration. For instance, cAMP response element-binding protein (CREB1) and calcium-calmodulin dependent protein kinase 2 (CaMK2) were identified as major targets potentially affected by PKG inhibition in *rd1* and *rd10* (Chapter 4 and Chapter 5). CREB1 is known to be overexpressed and constitutively phosphorylated in cancers and its pharmacological inhibition by compound 666-15 is well tolerated *in vivo* [15,16]. Interestingly, CREB1 is targeted by CaMK2 which is known to be overactivated in *rd1* photoreceptors [17,18]. It has also been reported that CaMK2-CREB signaling might be compromised in excitotoxic and axonal injuries in ganglion cells and reactivation of CaMK2 has protective effect on ganglion cells [19]. Moreover, the role of PKG activation in stimulation of the calmodulin/CaMK2 signaling cascade has also been confirmed in cardiomyocytes [20]. Therefore, PKG mediated CaMK2-CREB signaling looks like a promising target in photoreceptors as well as ganglion cell preservation. Another closely related kinase, CaMK4 which also targets CREB1, was identified to have potentially lowered activity upon CN03 treatment but validation experiments showed an increased signal intensity after the treatment. Further studies into CaMK2 and CaMK4 in regulation in different cell layers of the retina is recommended to determine if it is overexpressed in photoreceptors and/or other retinal cell layers.

Besides the determination of key PKG-specific downstream targets, a significant cross-talk within the cGMP-PKG-PKA signaling axis was observed in 661W cells which is known to express the phosphodiesterase 6 (PDE6) enzyme, essential to control the cGMP axis and both isoforms of PKG [21]. In addition to PKG, our results showed that PKA can also be activated by cGMP, albeit at higher concentrations, in the range of those needed to open CNG channels. Furthermore, In the 661W cells we demonstrated that PKA is also able to phosphorylate VASP, a known direct target of PKG. This cross talk between PKG and PKA as found in cells indicates that PKG is activated by cGMP and this step subsequently activates PKA, which might provide a plausible explanation for the clear effect of PKA via the cGMP axis. In this environment the common route of PKA activation (through the cAMP stimulus) might be bypassed by the cGMP route. This is confirmed by literature studies where PKG is

known to phosphorylate the regulatory subunit of PKA *in vitro* and *in vivo* which circumvents activation of PKA by cAMP [12]. In contrast, PKA could also elevate cGMP concentrations through Ca^{2+} mobilization or through cAMP and subsequently affect PKG signaling in ciliary cells [22]. Furthermore, along with PKGs, PKA was also amongst the major kinases with potentially lowered activity upon CN03 treatment in *rd1* and *rd10* retinal explants (see Chapter 3 and 4). Since, cGMP, cAMP, Ca^{2+}, PKG, and PKA-signaling pathways are closely interconnected, it is imperative to study this interplay of PKG-PKA further in retinal cells. As a follow up to the cell studies, kinome activity profiling was performed on *rd1* and *rd10* organotypic retinal explants treated with the PKG inhibitor CN03 (Chapter 4, Chapter 5). The major kinases with potentially lowered activity included PKGs but also other kinases such as PKAs, PKCs and CaMKs. Moreover, recent studies identified these same kinases as cGMP-interacting proteins with potentially higher activity in murine IRD retinas, which might be interesting to develop novel therapeutic targets, supplementary to the PKG axis [14,23].

Additionally, several voltage dependent potassium channels belonging to the K_v1 family ($K_v1.3$, $K_v1.6$) showed significantly reduced phosphorylation on treatment with CN03 in *rd1* and CN238 in *rd10* retinal explants (Chapters 4-6). $K_v1.3$ and $K_v1.6$ were also confirmed to be localized in different layers of the retina and MEA recordings showed that in addition to photoreceptors, they also preserved ganglion cells in *rd10* long-term retinal explant cultures. The K_v1 family has been identified to contribute to ganglion cell degeneration after optic nerve axotomy [24] and knockdown of either $K_v1.3$ or $K_v1.6$ has rescued ganglion cells *in vivo* [25]. Since, ganglion cell degeneration is not strictly related to IRDs but also a key feature of other retinal diseases such as glaucoma [26], diabetic retinopathy [27], and exudative or non-exudative age-related macular degeneration [28,29], these results broaden the applicability of PKG inhibition in diseases other than IRDs.

Quest for preclinical models to study IRDs

Single cell types are one of the simplest *in vitro* models to study retinal diseases. The cell lines used to study IRDs are derived from different cell types of the retina such as photoreceptors (661W, WERI-RB, Y79), retinal pigment epithelium (ARPE-19, D407) and ganglion cells (RGC-5) [30]. Cell lines allow quick and efficient screening of novel drugs as cell viability assays can be conveniently performed. However, cell lines are very systematic and uniform in nature and do not provide the diversity of a living tissue. Primary cell culture where cells are derived directly from the tissue of interest are considered to be closer to *in vivo* situation than established cell lines. Primary photoreceptor-like cell cultures derived from *rd1* murine eyes have been used as rapid *in vitro* compound screening system for several cGMP analogues to evaluate their effect on cell death [31]. Availability of tissues, complex and laborious cell culture and differentiation techniques, difficulty in reproducibility and having limited cell division and growth in culture media are some of the key issues associated with primary cell cultures. An *ex vivo* model system such as organotypic retinal explant culture recapitulates certain aspects of the *in vivo* retina very well including the retinal histology and presence of multiple cell types. Here, the retina is isolated and its physiology with multiple cell layers is preserved in cell culture for at least 2 weeks [32]. Retinal explant cultures are excellent models to study disease mechanisms, electrophysiology and drug screening [14,31].

Among animal models, murine models have been extensively used to determine proof of concept and act as a bridge between *in vitro* and *in vivo* studies. Murine models are available for 40% of human IRD-related genes which provide immense possibilities for research [33]. The photoreceptor cell loss phenotype in IRD murine models is similar to that in humans as degeneration of rods is followed up by cones and eventual blindness. Even though rate of photoreceptor degeneration in murine models is much quicker than that in human, it is helpful to use this model since it resembles pathogenesis and at the same time it reduces duration of studies and costs. Also, the model can be maintained under standard housing and breeding conditions and it is genetically manipulative. Nevertheless, in one of the best-characterized animal model of RP *rd1*, the photoreceptor degeneration overlaps with developmental apoptosis and rod cell death is almost completed by postnatal-day (P) 21 [34]. This is not the case in a slower degenerating model *rd10*, where rod cell death is completed by P45 and hence retinal structure and function is maintained over a longer time.

Even though mice IRD models serve as powerful tools to study etiology of human retinal degeneration, there are variations which can be strain-specific or due to different housing conditions for the mice. Laboratory mice are nocturnal and hence have a rod dominated retina which might be more interesting to study than the late photoreceptor degeneration process. They also do not have a macula which is present at the center of the retina and is responsible for visual acuity and most of the colored vision. Hence, macular dystrophies IRD studies are more relevant in large animals such as pigs, dogs, non-human primates [35]. They have high photoreceptor density including importantly cones, equivalent to the human macula [36,37]. Another advantage of large animals over laboratory murine models is similarity in their size of eye to the human eye [38]. This is very useful in development of translational therapy response because the surgical or drug delivery approaches will be almost similar and could be used later in human patients. For instance, the therapy development of the first FDA-approved gene therapy, Luxturna was performed in a dog model [39]. In spite of these advantages, generation of large experimental animals is expensive, slow and involves ethical concerns. Rate of photoreceptor degeneration is relatively slow which resembles closely to humans, which prolongs the duration and cost of studies

Recently, the culture systems for production of 3D tissue organoids from pluripotent stem cells from human IRD patients, have become an important tool to generate retinal tissues *in vitro* and reflect the *in vivo* disease development environment more closely. Retinal organoids provide a promising approach for rebuilding retina in patients with advanced retinal degeneration and are considered as a replenishable source of retinal progenitors building up neuroprotective strategies [40,41]. In a recent study, 3D retinal organoids were developed from induced pluripotent stem cells from a Retinitis Pigmentosa (RP) patient and the photoreceptor degeneration was successfully rescued by adeno-associated virus-mediated delivery of a specific gene [42] indicating great potential of this model in modelling photoreceptor degeneration and testing potential therapies in future.

Studying PKG signaling and its inhibition in IRD murine models

In this thesis, two murine IRD models were applied with different retina degeneration characteristics. The *rd1*, is probably the most extensively studied animal model for Retinitis Pigmentosa (RP). It is characterized by severe rod photoreceptor degeneration already during

retinal development where by postnatal day (P) 21 only cone photoreceptors remain [34]. In contrast, *rd10* is a slower degeneration model where PDE6B is still partially functional, which postpones complete rod cell death until P45 [34]. Since, rod photoreceptors remain viable for a longer period and photoreceptor degeneration does not coincide with developmental apoptosis, it has been postulated that *rd10* might resemble the human IRD condition more closely. Still in both the models, complete or partial non-functionality of PDE6 leads to an aberrant increase in cGMP which is toxic for photoreceptors [43]. This feature makes them state-of-the-art models to study mechanisms downstream of excessive cGMP signaling.

In both the models, application of PKG inhibitors (CN03 and CN238) showed a protective effect on photoreceptor cell death by significantly decreasing the number of TUNEL positive cells (Chapter 4-6). Effects of PKG inhibitor treatments showed a significant overlap in both *rd1* and *rd10*. The major common peptides with significantly decreased phosphorylation were CREB1 and TOP2A and kinases potentially involved in differential phosphorylation were PKG1, PKG2, and CaMK4. Still for the *rd10* model, CN03 treatment resulted in a lower number of peptides affected when compared to CN03 treatment in *rd1*. The difference in number of differentially phosphorylated peptides could be attributed to a distinctive rate of photoreceptor degeneration in *rd1* or *rd10* and the fact that the time point chosen for CN03 treatment was not identical in both models. A straightforward head-to-head comparison of PKG targets in both *rd* models is advised to investigate the expression of these potential PKG targets with time in degenerating *rd1* and *rd10* retinas. Since, for *rd10* at P18 still some residual PDE6 activity is left, this might be the reason why we did not observe significant changes in differential phosphorylation of peptides with CN03 treatment in the *rd1* retina at P10. These differences in time events between the two models should be addressed in future studies assessing retinal degeneration.

Suitability of multiplex peptide microarrays in identifying novel, potential kinase targets

Protein phosphorylation by kinases is one of the critical drivers of signal transduction which leads to diverse cellular events such as cell death, growth, differentiation, and apoptosis. Over 73 FDA approved kinase inhibitors for a single target also have affinity for multiple kinases which can shed light on signaling networks [44]. The kinase inhibitor drugs have limited success in clinical trials because of side effects which were not identified earlier. The high-throughput kinome profiling technologies are thus very important to study kinase inhibitors and identify the kinase signaling networks. Since a kinase can have multiple substrates, these multiplex peptide microarrays were used to identify 60 novel substrates for recombinant PKGs (Chapter 3). It was followed up by investigation of the effect of PKG inhibitors on endogenous kinase activity in retinal cells, tissue and explants (Chapters 4-6).

In this thesis, multiplex peptide array platforms with Serine/Threonine (STK) chips permitted simultaneous profiling of kinase activity for hundreds of protein kinases in retinal samples. Amongst the various kinome profiling methods available (*e,g*. Kinomescan, KinoBeads), the peptides microarray method has the advantage of its unique chip design allowing higher concentration of peptides which ultimately increases the signal sensitivity and reduces noise [44]. Also, to maximize binding kinetics and reduce reaction time, the samples are pumped back and forth through the array throughout the duration of the assay. The multiplex platform has been successfully deployed across multiple research domains and

generated actionable scientific insight in cancer biology [45,46] and neuroscience [13,14]. This permits assessment of samples with biological context, where the net effects of all the interactions between kinases and kinase regulating molecules are reflected in the results. However, reporter peptides on the microarray may be phosphorylated by multiple protein kinases, therefore, this requires sophisticated bioinformatic softwares to deconvolute kinome activity data and predict potential kinases responsible for phosphorylation pattern whilst these peptides are not described well enough in literature and bioinformatics database. Another, obvious limitation of the technology is that the chips are biased to the information available on the printed peptides on the chips. Also, it should be mentioned that non-specific binding of antibodies does occur during phosphorylation signal detection and this requires deconvolution methods to map upstream kinases to explain the variation of the phosphorylation signals. Even though these are notable limitations, this multiplex peptide array provides a powerful high-throughput profiling technique to measure kinome activity in complex biological samples [44,47].

The multiplex peptide microarrays allow generation of hypothesis of the kinases that might be involved in changes in peptide phosphorylation. However, since the human Serine/Threonine kinnases are represented by a limited number of 142 peptides on the microarrays, this also limits the accuracy of kinase prediction by their activity/specificity data available on these databases. To validate the hypothesis generated by microarrays and test the kinases that are actually involved, additional confirmatory experiments are required. The novel PKG target proteins identified in this thesis by peptide-based microarray technology were validated by antibody-based techniques such as immunohistochemistry and immunoblotting to confirm their presence and activity in retinal tissue and explants [14]. In future other techniques such as gene expression studies could also be employed for PKG target validation along with multiplex peptide microarrays. Gene expression analysis studies of three different IRD models at peak photoreceptor cell death have identified several differentially expressed cGMP-related genes and cGMP-PKG signaling pathways to be mostly affected [48]. In Chapter 5, kinome activity profiling by multiplex peptide microarrays was combined with phosphoproteomics which resulted in identification of PKG targets which were common to both the techniques. However, careful analysis is required to get a full picture of the phosphoproteome in all retina cell layers. Currently applied protein detection techniques and microarrays require no-prior knowledge of the target and are sensitive and quick, however they do use whole tissue lysates, which is a heterogenous mixture of all different cell types in the retina. Since the 3D structure of the retina is so important for its function, it is not easy to determine which cells in the retina are actually responsible for the change. New developments in mass spectrometry may provide single-cell resolution in future [49]. The same holds true for new developments in single cell next generation sequencing, which may help to unravel activated pathways on the cellular level [50,51].

The first application of assessing phosphorylating PKG targets in the retina comes from the work with VASP peptide which has been frequently used to localized the PKG activation in different cell types in the retina [31]. In the thesis, localization and phosphorylation signal intensity of several new proteins could be determined in different retinal cell layers, as described in Chapters 4-6. Even though IHC provides single cell resolution, IHC is also limited by availability of antibodies that specifically target a particular protein. Fluorescence

quenching, affinity chromatography are some other techniques that could be applied to determine if proteins are in closed proximity. In a study, to identify cGMP-interacting proteins in normal and degenerating retinas, affinity chromatography with immobilized cGMP analogs was used to enrich the retinal samples with cGMP-interacting proteins and followed up by mass spectrometry [23]. The proximity of identified novel proteins such as pCaMK2α, GSK3β, MAPK1/3 and EPAC2 *in situ* to cGMP in the photoreceptor layer seems thus a valid conclusion and was also confirmed by Proximity Ligation Assay.

In summary, multiplex peptide microarray technology, along with IHC and phosphoproteomics was applied successfully to extend the knowledge of PKG and its downstream targets in a multi cell layered retina. Nevertheless, studying single protein kinases will remain essential in biochemical validation studies and the application of next generation sequencing techniques may further help profiling of kinase events in retina in search for addressable gene targets.

Challenges to develop drug candidates targeting the PKG axis in retina

Over the last decades, cGMP analogues have been proposed as a valid target to intervene with signal transduction [52,53]. PKG inhibitors that target ATP-binding sites such as KT5823 or substrate-binding sites such as DT-2 on PKG lack specificity or potency *in vivo* [54,55]. On the other hand, cGMP analogues, and especially the new generation of analogues are a class of second messenger compounds that are able to activate or inhibit both isoforms of PKG [56]. The inhibitory cGMP analogues (Rp-cGMPS) bind to the cGMP-binding sites on PKG and prohibit the conformational change required for activation of the catalytic active subunit of PKG. These analogues are resistant to hydrolysis by PDEs which metabolizes *in vivo* cGMP to 5'-cGMP. The class of novel cGMP inhibitory analogues used in this thesis, also include additional β-phenyl-1,N^2-etheno-modification (PET) moiety in the Rp-cGMPS backbone which makes it an inhibitor of CNGCs too along with PKGs. Further alterations such as addition of sulphur-connected to aromatic ring or other substituents such as a bromine atom, strongly increased lipophilicity of these compounds as compared to cGMP, which resulted in enhanced membrane permeability [31]. It is possible that these cGMP inhibitory analogues in addition to their primary effects also cause elevation of cAMP and cGMP by indirectly inhibiting all the PDEs in the cells *eg.* CN03 (Rp-8-Br-PET-cGMPS) inhibits PDE1B/2/4/5/10 [56]. These analogues might also have different selectivity for PKGs *eg.* CN03 appears to be a more potent inhibitor of PKG1 (Ki= 35 nM) than PKG2 (Ki= 450 nM) [57,58] and could have multiple targets *eg.* CN03 can inhibit PKA but only at higher concentration of 11 μM [57]. Therefore, interpretations of effects of these novel cGMP inhibitory analogues should take into account their specificities and possible cross target activities in assessing recombinant kinases as a starting point.

The initial pre-clinical studies of these novel cGMP inhibitory analogues on IRD models *in vitro* and *in vivo* suggest their exciting potential as drug candidates [11,59]. However, how far these benefits will translate to patients remains to be investigated. To develop these compounds into a successful IRD treatment requires delivery of these compounds to photoreceptors in the retina. Different routes of local drug administration have been used such as suprachoroidal [60], subretinal [61], and intravitreal [62] injection. The local administration routes target the eye and hence limit exposure to the rest of the body. Even if

the drug leaks out of the eye, it gets diluted several orders of magnitude which significantly reduces the risk of adverse effects [63]. However, patient discomfort, need of well-trained doctors and possible intraocular inflammation hinder local application of the drug in the eye. These problems could be overcome by systemic drug administration routes but they will require very high drug dose in order to reach an effective concentration in the eye and drugs are also rapidly excreted by the urinary system [63,64]. Moreover, a restrictive physiological blood-retinal-barrier protects the retina and this also possess quite a challenge for therapeutic agents to reach photoreceptors. These issues could be avoided if the drug is encapsulated with a retina-target drug delivery system such as glutathione conjugated liposomes [65]. The cGMP analogue CN03, encapsulated in glutathione conjugated liposome has shown effective drug delivery in the retina enabling significant photoreceptor protection in IRD models [11]. Nonetheless, the feasibility of systemic retinal drug administration needs to be explored further in clinical settings as there is risk of potential systemic adverse effects. Thus, a careful analysis of drug administration routes for the cGMP inhibitory analogues and drug delivery systems which comply with regulatory requirements as well as further studies on potential systemic side effects are critical. Future research in the role of cGMP analogues should also take into account the issues with drug delivery into the retina early on and alter compound development as well as delivery systems accordingly. In addition, the stability of the drug and not being hydrolysable by PDEs in human body are some other properties that need to be investigated further. Pharmacokinetics and toxicological studies of these drugs and their liposomal encapsulated form could be done in higher animal models. Effect of the drugs on surrogate biomarkers could be studied in (target) tissue and/or in peripheral blood stream. The response of these potential biomarkers should first to be optimized and validated in animal models *in vivo* thereby offering the future possibility to compare and analyze the phenotypic outcome in clinical trials where these novel PKG targets could be quantitatively evaluated even in RP-patient blood samples as a biomarker.

In conclusion, the identification of novel PKG targets and the associated biological pathways using PKG inhibitors such as CN03 and CN238 as shown in this thesis is encouraging and merits further (pre) clinical research into the druggability of the target *in vivo*. The PKG inhibition studies in this thesis have clearly identified novel phosphorylated targets such as CaMKs and CREB which could provide a basis for understanding cGMP-PKG mediated photoreceptor degeneration mechanisms. These new PKG targets could eventually also be developed to serve as new (surrogate) biomarkers to study the effect of CN03 and CN238 in clinical trials.

References

1. Kraupp, Bettina Grasl, Branislav Ruttkay-Nedecky, Helga Koudelka, Krystyna Bukowska, Wilfried Bursch and RS: **In situ detection of fragmented DNA (TUNEL assay) fails to discriminate among apoptosis, necrosis, and autolytic cell death: a cautionary note.** *Hepatology* 1995, **21**:1465–1468.
2. Zeiss CJ, Neal J, Johnson EA: **Caspase-3 in postnatal retinal development and degeneration**. *Investig Ophthalmol Vis Sci* 2004, **45**:964–970.
3. Hafezi F, Abegg M, Grimm C, Wenzel A, Munz K, Stürmer J, Farber DB, Remé CE: **Retinal degeneration in the rd mouse in the absence of c-fos**. *Investig Ophthalmol Vis Sci* 1998, **39**:2239–2244.
4. Arango-Gonzalez B, Trifunović D, Sahaboglu A, Kranz K, Michalakis S, Farinelli P, Koch S, Koch F, Cottet S, Janssen-Bienhold U, et al.: **Identification of a common non-apoptotic cell death mechanism in hereditary retinal degeneration**. *PLoS One* 2014, **9**:1–11.
5. Lolley RN, Farber DB, Rayborn ME, Hollyfield JG: **Cyclic gmp accumulation causes degeneration of photoreceptor cells: Simulation of an inherited disease**. *Science (80-)* 1977, **196**:664–666.
6. Roy A, Hilhorst R, Groten J, Paquet-Durand F, Tomar T: **Technological advancements to study cellular signaling pathways in inherited retinal degenerative diseases**. *Curr Opin Pharmacol* 2021, **60**:102–110.
7. Kulkarni M, Trifunović D, Schubert T, Euler T, Paquet-Durand F: **Calcium dynamics change in degenerating cone photoreceptors**. *Hum Mol Genet* 2016, **25**:3729–3740.
8. Pawlyk BS, Li T, Scimeca MS, Sandberg MA, Berson EL: **Absence of photoreceptor rescue with D-cis-diltiazem in the rd mouse**. *Investig Ophthalmol Vis Sci* 2002, **43**:1912–1915.
9. Barabas P, Peck CC, Krizaj D: **Do calcium channel blockers rescue dying photoreceptors in the pde6b rd1 mouse?** *Adv Exp Med Biol* 2010, **664**:491–499.
10. Paquet-Durand F, Hauck SM, Van Veen T, Ueffing M, Ekström P: **PKG activity causes photoreceptor cell death in two retinitis pigmentosa models**. *J Neurochem* 2009, **108**:796–810.
11. Vighi E, Trifunovic D, Veiga-Crespo P, Rentsch A, Hoffmann D, Sahaboglu A, Strasser T, Kulkarni M, Bertolotti E, Van Den Heuvel A, et al.: **Combination of cGMP analogue and drug delivery system provides functional protection in hereditary retinal degeneration**. *Proc Natl Acad Sci U S A* 2018, **115**:E2997–E3006.
12. Haushalter KJ, Casteel DE, Raffeiner A, Stefan E, Patel HH, Taylor SS: **Phosphorylation of protein kinase a (PKA) regulatory subunit RI by protein kinase g (PKG) primes PKA for catalytic activity in cells**. *J Biol Chem* 2018, **293**:4411–4421.
13. Roy A, Groten J, Marigo V, Tomar T, Hilhorst R: **Identification of novel substrates for cGMP dependent protein kinase (PKG) through kinase activity profiling to understand its putative role in inherited retinal degeneration**. *Int J Mol Sci* 2021, **22**:1–17.
14. Roy A, Tolone A, Hilhorst R, Groten J, Tomar T, Paquet-Durand F: **Kinase activity profiling identifies putative downstream targets of cGMP/PKG signaling in inherited retinal neurodegeneration**. *Cell Death Discov* 2022, **8**:1–12.
15. Sakamoto KM, Frank DA: **CREB in the pathophysiology of cancer: Implications for targeting transcription factors for cancer therapy**. *Clin Cancer Res* 2009, **15**:2583–2587.
16. Li BX, Gardner R, Xue C, Qian DZ, Xie F, Thomas G, Kazmierczak SC, Habecker BA, Xiao X: **Systemic Inhibition of CREB is Well-tolerated in vivo**. *Sci Rep* 2016, **6**:1–9.

17. Hauck SM, Ekström PAR, Ahuja-Jensen P, Suppmann S, Paquet-Durand F, van Veen T, Ueffing M: **Differential modification of phosducin protein in degenerating rd1 retina is associated with constitutively active Ca2+ /calmodulin kinase II in rod outer segments**. *Mol Cell Proteomics* 2006, **5**:324–336.
18. Bito H, Deisseroth K, Tsien RW: **CREB phosphorylation and dephosphorylation: A Ca2+- and stimulus duration-dependent switch for hippocampal gene expression**. *Cell* 1996, **87**:1203–1214.
19. Guo X, Zhou J, Starr C, Mohns EJ, Li Y, Chen EP, Yoon Y, Kellner CP, Tanaka K, Wang H, et al.: **Preservation of vision after CaMKII-mediated protection of retinal ganglion cells**. *Cell* 2021, **184**:4299–4314.
20. Chai Y, Zhang DM, Lin YF: **Activation of cGMP-dependent protein kinase stimulates cardiac ATP-sensitive potassium channels via a ROS/calmodulin/CaMKII signaling cascade**. *PLoS One* 2011, **6**:e18191.
21. Mencl S, Trifunović D, Zrenner E, Paquet-Durand F: **PKG-dependent cell death in 661W cone photoreceptor-like cell cultures (experimental study)**. In *Retinal Degenerative Diseases*. . 2018:511–517.
22. Zagoory O, Braiman A, Priel Z: **The mechanism of ciliary stimulation by acetylcholine: Roles of calcium, PKA, and PKG**. *J Gen Physiol* 2002, **119**:329–339.
23. Rasmussen M, Welinder C, Schwede F, Ekström P: **The cGMP system in normal and degenerating mouse neuroretina: New proteins with cGMP interaction potential identified by a proteomics approach**. *J Neurochem* 2020, doi:10.1111/jnc.15251.
24. Koeberle PD, Wang Y, Schlichter LC: **Kv1.1 and Kv1.3 channels contribute to the degeneration of retinal ganglion cells after optic nerve transection in vivo**. *Cell Death Differ* 2010, **17**:134–144.
25. Koeberle PD, Schlichter LC: **Targeting KV channels rescues retinal ganglion cells in vivo directly and by reducing inflammation**. *Channels* 2010, **4**:337–346.
26. Beykin G, Norcia AM, Srinivasan VJ, Dubra A, Goldberg JL: **Discovery and clinical translation of novel glaucoma biomarkers**. *Prog Retin Eye Res* 2021, **80**:100875.
27. Lynch SK, Abràmoff MD: **Diabetic retinopathy is a neurodegenerative disorder**. *Vision Res* 2017, **139**:101–107.
28. Medeiros NE, Curcio CA: **Preservation of ganglion cell layer neurons in age-related macular degeneration**. *Investig Ophthalmol Vis Sci* 2001, **42**:795–803.
29. Yenice E, Şengün A, Soyugelen Demirok G, Turaçli E: **Ganglion cell complex thickness in nonexudative age-related macular degeneration**. *Eye* 2015, **29**:1076–1080.
30. Schnichels S, Paquet-Durand F, Löscher M, Tsai T, Hurst J, Joachim SC, Klettner A: **Retina in a dish: Cell cultures, retinal explants and animal models for common diseases of the retina**. *Prog Retin Eye Res* 2021, **81**:100880.
31. Vighi E, Trifunovic D, Veiga-Crespo P, Rentsch A, Hoffmann D, Sahaboglu A, Strasser T, Kulkarni M, Bertolotti E, Heuvel A Van Den, et al.: **Combination of cGMP analogue and drug delivery system provides functional protection in hereditary retinal degeneration**. *Proc Natl Acad Sci U S A* 2018, **115**:E2997–E3006.
32. Belhadj S, Tolone A, Christensen G, Das S, Chen Y, Paquet-Durand F: **Long-term, serum-free cultivation of organotypic mouse retina explants with intact retinal pigment epithelium**. *J Vis Exp* 2020, **2020**:1–13.
33. Collin GB, Gogna N, Chang B, Damkham N, Pinkney J, Hyde LF, Stone L, Naggert JK, Nishina PM, Krebs MP: **Mouse models of inherited retinal degeneration with photoreceptor cell loss**. *Cells* 2020, **9**:931.

34. Sancho-Pelluz J, Arango-Gonzalez B, Kustermann S, Romero FJ, Van Veen T, Zrenner E, Ekström P, Paquet-Durand F: **Photoreceptor cell death mechanisms in inherited retinal degeneration**. *Mol Neurobiol* 2008, **38**:253–269.
35. Pennesi ME, Neuringer M, Courtney RJ: **Animal models of age related macular degeneration**. *Mol Aspects Med* 2012, **33**:487–509.
36. Winkler PA, Occelli LM, Petersen-Jones SM: **Large Animal Models of Inherited Retinal Degenerations: A Review**. *Cells* 2020, **9**:882.
37. Mowat FM, Petersen-Jones SM, Williamson H, Williams DL, Luthert PJ, Ali RR, Bainbridge JW: **Topographical characterization of cone photoreceptors and the area centralis of the canine retina**. *Mol Vis* 2008, **14**:2518.
38. Petersen-Jones SM: **Drug and gene therapy of hereditary retinal disease in dog and cat models**. *Drug Discov Today Dis Model* 2013, **10**:e215–e223.
39. Acland GM, Aguirre GD, Ray J, Zhang Q, Aleman TS, Cideciyan A V., Pearce-Kelling SE, Anand V, Zeng Y, Maguire AM, et al.: **Gene therapy restores vision in a canine model of childhood blindness**. *Nat Genet* 2001, **28**:92–95.
40. Singh RK, Binette F, Seiler M, Petersen-Jones SM, Nasonkin IO: **Pluripotent Stem Cell-Based Organoid Technologies for Developing Next-Generation Vision Restoration Therapies of Blindness**. *J Ocul Pharmacol Ther* 2021, **37**:147–156.
41. Singh RK, Mallela RK, Cornuet PK, Reifler AN, Chervenak AP, West MD, Wong KY, Nasonkin IO: **Characterization of Three-Dimensional Retinal Tissue Derived from Human Embryonic Stem Cells in Adherent Monolayer Cultures**. *Stem Cells Dev* 2015, **24**:2778–2795.
42. Lane A, Jovanovic K, Shortall C, Ottaviani D, Panes AB, Schwarz N, Guarascio R, Hayes MJ, Palfi A, Chadderton N, et al.: **Modeling and Rescue of RP2 Retinitis Pigmentosa Using iPSC-Derived Retinal Organoids**. *Stem Cell Reports* 2020, **15**:67–79.
43. Paquet-Durand F, Marigo V, Ekström P: **RD Genes Associated with High Photoreceptor cGMP-Levels (Mini-Review)**. In *Retinal Degenerative Diseases*. . 2019:245–249.
44. Alganem K, Hamoud AR, Creeden JF, Henkel ND, Imami AS, Joyce AW, Ryan V WG, Rethman JB, Shukla R, O'Donovan SM, et al.: **The active kinome: The modern view of how active protein kinase networks fit in biological research**. *Curr Opin Pharmacol* 2022, **62**:117–129.
45. Görte J, Danen E, Cordes N: **Therapy-Naive and Radioresistant 3-Dimensional Pancreatic Cancer Cell Cultures Are Effectively Radiosensitized by β1 Integrin Targeting**. *Int J Radiat Oncol Biol Phys* 2022, **112**:487–498.
46. Deville SS, Silva LFD, Vehlow A, Cordes N: **C-Abl tyrosine kinase is regulated downstream of the cytoskeletal protein synemin in head and neck squamous cell carcinoma radioresistance and DNA repair**. *Int J Mol Sci* 2020, **21**:7277.
47. Bußmann L, Hoffer K, von Bargen CM, Droste C, Lange T, Kemmling J, Schröder-Schwarz J, Vu AT, Akingunsade L, Nollau P, et al.: **Analyzing tyrosine kinase activity in head and neck cancer by functional kinomics: Identification of hyperactivated Src family kinases as prognostic markers and potential targets**. *Int J Cancer* 2021, **149**:1166–1180.
48. Wei C, Li Y, Feng X, Hu Z, Paquet-Durand F, Jiao K: **RNA Biological Characteristics at the Peak of Cell Death in Different Hereditary Retinal Degeneration Mutants**. *Front Genet* 2021, **12**.
49. Slavov N: **Single-cell protein analysis by mass spectrometry**. *Curr Opin Chem Biol* 2021, **60**:1–9.
50. Voigt AP, Binkley E, Flamme-Wiese MJ, Zeng S, DeLuca AP, Scheetz TE, Tucker BA, Mullins RF, Stone EM: **Single-Cell RNA Sequencing in Human Retinal Degeneration Reveals Distinct Glial Cell Populations**. *Cells* 2020, **9**:438.

51. Sridhar, Akshayalakshmi, Akina Hoshino, Connor R. Finkbeiner, Alex Chitsazan, Li Dai, Alexandra K. Haugan KME et al.: **Single-cell transcriptomic comparison of human fetal retina, hPSC-derived retinal organoids, and long-term retinal cultures**. *Cell Rep* 2020, **30**:1644–1659.
52. Lohmann SM, Vaandrager AB, Smolenski A, Walter U, De Jonge HR: **Distinct and specific functions of cGMP-dependent protein kinases**. *Trends Biochem Sci* 1997, **22**:307–312.
53. Schwede F, Maronde E, Genieser HG, Jastorff B: **Cyclic nucleotide analogs as biochemical tools and prospective drugs**. In *Pharmacology and Therapeutics*. . 2000:199–226.
54. Burkhardt M, Glazova M, Gambaryan S, Vollkommer T, Butt E, Bader B, Heermeier K, Lincoln TM, Walter U, Palmetshofer A: **KT5823 inhibits cGMP-dependent protein kinase activity in vitro but not in intact human platelets and rat mesangial cells**. *J Biol Chem* 2000, **275**:33536–33541.
55. Gambaryan S, Butt E, Kobsar A, Geiger J, Rukoyatkina N, Parnova R, Nikolaev VO, Walter U: **The oligopeptide DT-2 is a specific PKG i inhibitor only in vitro, not in living cells**. *Br J Pharmacol* 2012, **167**:826–838.
56. Poppe H, Rybalkin SD, Rehmann H, Hinds TR, Tang XB, Christensen AE, Schwede F, Genieser HG, Bos JL, Doskeland SO, et al.: **Cyclic nucleotide analogs as probes of signaling pathways [1]**. *Nat Methods* 2008, **5**:277–278.
57. Butt E, Pöhler D, Genieser HG, Huggins JP, Bucher B: **Inhibition of cyclic GMP-dependent protein kinase-mediated effects by (Rp)-8-bromo-PET-cyclic GMPS.** *Br J Pharmacol* 1995, **116**:3110–3116.
58. Vaandrager AB, Edixhoven M, Bot AGM, Kroos MA, Jarchau T, Lohmann S, Genieser HG, De Jonge HR: **Endogenous type II cGMP-dependent protein kinase exists as a dimer in membranes and can be functionally distinguished from the type I isoforms**. *J Biol Chem* 1997, **272**:11816–11823.
59. Paquet-Durand F, Hauck SM, Veen T Van, Ueffing M, Ekström P: **PKG activity causes photoreceptor cell death in two retinitis pigmentosa models**. *J Neurochem* 2009, **108**:796–810.
60. Yeh S, Kurup SK, Wang RC, Foster CS, Noronha G, Nguyen QD, Do D V.: **Suprachoroidal Injection of Triamcinolone Acetonide, Cls-Ta, for Macular Edema due to Noninfectious Uveitis: A Randomized, Phase 2 Study (DOGWOOD)**. *Retina* 2019, **39**:1880–1888.
61. Ochakovski GA, Peters T, Michalakis S, Wilhelm B, Wissinger B, Biel M, Bartz-Schmidt KU, Fischer MD: **Subretinal injection for gene therapy does not cause clinically significant outer nuclear layer thinning in normal primate foveae**. *Investig Ophthalmol Vis Sci* 2017, **58**:4155–4160.
62. Meyer CH, Krohne TU, Charbel Issa P, Liu Z, Holz FG: **Routes for drug delivery to the eye and retina: Intravitreal injections**. *Retin Pharmacother* 2016, **55**:63–70.
63. Tolone A, Belhadj S, Rentsch A, Schwede F, Paquet-Durand F: **The cGMP pathway and inherited photoreceptor degeneration: Targets, compounds, and biomarkers**. *Genes (Basel)* 2019, **10**:1–16.
64. Coulson R, Baraniak J, Stec WJ, Jastorff B: **Transport and metabolism of N6- and C8-substituted analogs of adenosine 3',5'-cyclic monophosphate and adenosine 3'5'-cyclic phosphorothioate by the isolated perfused rat kidney**. *Life Sci* 1983, **32**:1489–1498.
65. Maussang D, Rip J, van Kregten J, van den Heuvel A, van der Pol S, van der Boom B, Reijerkerk A, Chen L, de Boer M, Gaillard P, et al.: **Glutathione conjugation dose-dependently increases brain-specific liposomal drug delivery in vitro and in vivo**. *Drug Discov Today Technol* 2016, **20**:59–69.

8

Chapter 8

Summary

Inherited retinal degenerative diseases (IRDs) are a group of rare diseases that lead to progressive vision loss due to photoreceptor degeneration and eventual blindness. They are characterized by diverse genetic and phenotypic heterogeneity which mandate the quest for designing generic treatments that will be amenable for a large cohort of patients. The 3',5'-cyclic guanosine monophosphate (cGMP)-mediated Protein Kinase G (PKG) signaling has been implicated as one of the major drivers leading to photoreceptor cell death. Therefore, a better insight into the downstream effects of PKG and its phosphorylation targets is necessary to design better PKG targeted therapies and novel treatment response-related biomarkers.

The aim of this thesis was to study the effect of novel PKG inhibitors on kinase signaling and photoreceptor viability in retinal cells, tissues and explants. This knowledge was applied to identify potential new PKG target proteins (surrogate biomarkers) and the biological pathways downstream of PKG, which might lead to photoreceptor degradation. **Chapter 1** provided an introduction to the topic. In **Chapter 2**, key pathways involved in photoreceptor cell death and their study by transcriptomics, proteomics and metabolomics techniques was described. Since, proteins targeted by PKG in the retina are still unknown, in **Chapter 3**, recombinant PKGs in the presence of PKG activity modulators were applied on multiplex peptide microarrays to identify 50 novel PKG substrates. When microarray methodology was applied on photoreceptor-derived 661W cells treated with PKG modulators, the results indicated prominence of another closely related kinase PKA, besides PKGs. Thus, interpretation of any effects of PKG activity modulators in a biological system should take their potential cross-target activities into consideration. The possible interactors of PKG in the retina were investigated further in **Chapter 4** using *in vivo* murine *rd1* retinal tissues and *ex vivo* organotypic cultured explants. PKG-specific inhibition by CN03 provided photoreceptor protection in *rd1* retinal explants. Kinase activity profiling results demonstrated an overall decrease in peptide-based substrate phosphorylation after CN03 treatment, with a significant decrease in 22 peptides. Based on PKG classification data from chapter 3, 14 of the significantly changed peptides were substrates for both PKG1 and PKG2 and 3 for PKG1 only. The major kinases predicted to have lowered activity with CN03 treatment were PKAα, Pim1, PKG1, PKG2, and CaMK4. The presence of six proteins corresponding to the peptides was confirmed in different cell layers of the murine retina. PKG is a serine/threonine kinase (STK) with likely several hundred potential phosphorylation target which makes it difficult to find targets or biomarkers relevant for photoreceptor cell death. To overcome this hurdle, in **Chapter 5**, the uniquely phosphorylated proteins by PKG were studied by combination of kinase activity profiling and phosphoproteomics techniques in the IRD murine model *rd10* in the absence and presence of the PKG inhibitor CN03. Similar to *rd1*, CN03 exhibited a neuroprotective effect on photoreceptors in *rd10* as well. Kinase activity profiling of rd10 retinal explants showed an overall decrease in peptide phosphorylation after CN03 treatment. Out of 7 significantly changed peptides, 4 were substates for both PKG1 and PKG2 and 2 for PKG only. The mass-spectrometry-based phosphoproteomics data showed diverse inhibited as well as activated peptides. Intracellular signaling by second messengers, Calcium-induced signalling, Calmodulin-induced events, MAPK targets, CREB phosphorylation and RAS activation were amongst the major biological pathways which were affected by CN03 treatment in this *rd10* model. Based on integration of data from both the techniques CREB, CaMK2 and CaMK4 were identified as key effected downstream

proteins of PKG and their presence was confirmed in retina by immunohistochemistry and immunoblotting. In **Chapter 6**, the effect of a novel PKG inhibitor, CN238 was studied in *rd1* and *rd10* retinal explants. Akin to CN03, CN238 preserved photoreceptor viability and functionality in both *rd1* and *rd10*. Further studies revealed that both CN03 and CN238 in addition to photoreceptors, also protected retinal ganglion cells. The kinome activity profiling and Ca^{2+} imaging experiments of CN238-treated *rd10* retinal explants identified the K^+-channel $K_v1.6$ as a possible mediator of PKG-dependent axotomy induced degeneration of retinal ganglion cells. Thus, these results broadened the potential application of PKG inhibitors in diseases characterized by axonal damage such as spinal cord injury or multiple sclerosis.

Altogether, this thesis confirmed the role of cGMP-PKG signaling in photoreceptor degeneration and also identified and validated the presence of novel PKG downstream targets in murine-based IRD models. These results will form the basis for further understanding of the biological pathways involved in IRDs and could be employed to develop new surrogate biomarkers during clinical development of novel PKG inhibitors.

A

Appendix

Acknowledgements

About the author

List of publications

Overview of completed training activities

Acknowledgements

All good things come to an end and so must my PhD. The last three and a half years were a roller coaster ride accompanied with growth, struggle, sad and happy tears. Finally, it is time to wrap up this chapter of my life and thank the wonderful people who were part of this beautiful journey.

First of all, I would like to thank my supervisionors: **Prof. Dr. Ivonne Rietjens**, **Prof. Dr. John Groten** and **Dr. Tushar Tomar**. Ivonne, thank you for always being very efficient, sharp and responsive. I am very grateful for your scientific advice and guidance at the crucial stages of my PhD. John, thank you for giving me the opportunity to be a part of this exciting Marie Curie project. You always pushed me to do my best and guided me in the right direction. Thank you for your feedbacks, patience, enthusiasm, and support during my PhD journey. Tushar, thank you for all the encouragement in these last two years. Your addition to the supervising team gave a new dimension to my thesis. Thank you for coming up with innovative ideas which broadened my knowledge about different topics as well. You were always a call away and very prompt and effective in your response. I am glad that I got to know and work with you.

Furthermore, I would like to extend my thanks to my previous supervisor **Dr. Riet Hilhorst**. You helped me get familiar with not only the project but also Netherlands. You were always very patient, supportive, and taught me a lot. Besides work, I am happy that I got to know you at the personal front as well. I enjoyed our long walks, biking trips, jam making sessions and dinners. You and Ton are like my family away from family. Thank you for always looking out for me.

I would also like to thank the members of the thesis committee for their invaluable time and effort to evaluate my thesis.

My sincere thanks to all the co-authors who contributed to this thesis, in particular the following people. Especial thanks to **Prof. Dr. François Paquet-Durand** and **Dr. Arianna Tolone** form Eberhard Karls University of Tübingen. Thank you for our beautiful collaboration and always helping us out in times of need particularly when we required more retina tissue samples. I am grateful to our collaborators from Lund University, **Prof. Dr. Per Ekstrom** and **Jiaming Zhou** for the fruitful Phosphoproteomics and Kinomics collaboration. I would also like to thank **Prof. Dr. Valeria Marigo** from University of Modena and Reggio Emilia for her advice regarding cell studies. To all the members of the *trans*Med consortium, thank you for the interesting collaborations and beautiful memories.

I would also like to express my gratitude to **Prof. Dr. Jacques Vervoort**. Unfortunately, he is no longer with us but I am glad that I got to know and work with him on LC MS.

To everyone at PamGene, thank you for always being so kind and helpful. **Liesbeth**, thanks for always answering my questions with a smile, checking my experiment setups, and also helping me with the crucial experiments in the lab. **Lies,** I will always be indebted to you

for setting up the Western Blot with my student **Merijn**. Thank you Merijn for providing me interesting Western Blot data as additional conformation technique and best wishes for future endeavors. **Monique**, thank you for explaining me new lab rules and always helping me find reagents in the lab! The entire **BioAssay Team**, thank you for the advice and constructive feedback on my project. **Rik**, **Peter** and **Dirk**, thank you for helpful discussion on data analysis; **Savi**, thanks for helping me with BioNavigator-related questions and always being very cheerful and kind.; **Frank, Dragan and Faris**, I enjoyed our fun conversations, which made me forgot about all the stress; **Hans**, thanks for being very prompt with fixing the technical IT issues; **Piek** and **Inge**, thank you for all the administrative help and the nice conversations.

I was also blessed to work with the wonderful people at Tox! **Nico**, **Hans B.**, and **Nynke**, thanks for the interesting conversations during coffee breaks. To the 'backbone' of Tox: **Laura**, **Sebas**, **Bert**, **Hans**, **Nacho**, **Wouter**, **Naomi**, **Marco**, your support in the lab is indispensable. Sebas, thank you for all the help with LC MS struggles and always being in a fun mood, which made those struggles less frustrating. Laura, thank you for all the advice regarding cell studies; Bert, you were very kind to me and I really enjoyed our long talks; Nacho, thanks for always helping me out. **Lidy**, **Gerda**, **Carla** and **Letty**, thank you for your support with the administrative issues.

In the Tox family, my friends were an important part of support in my laboratory work and daily life. Special thanks to my awesome paranymphs, **Aafke** and **Veronique**! Thank you for helping me out with Defense-related things despite your busy schedules. Aafke, you are just too kind, considerate, funny, and helpful. You are the only person who always likes whatever I cook and we have so many great memories together (the Zumba class was the best one)! Veronique, thank you for patiently listening to all my PhD related issues. You are never scared to learn something new and I am so proud that you are now a pro in R! Thank you both for being my Paranymphs and I wish you best of luck with everything in life!

Qianrui, thank you for always giving me delicious Chinese snacks! We had a great time in Spain and several joyful moments in the office and gym. We both would talk about anything and everything! Thank you for being someone I could rely on. **Chen**, you are a very easygoing and friendly person. I miss our fun banter, gym and bike sessions. Thank you for always giving me the best advice! **Biyao**, I very much appreciate your constant help and support through everything. You were always very prompt and kind. **Shivani**, I met you just about a year back but thanks for all the fun as well as serious conversations. Also, our 'dinner dinner' group, Aafke, Chen, Biyao, **Menno**, and **Merel**, thank you for all the entertaining talks and hanging out with you guys always made me very happy. I wish we meet soon! To my officemates (Dames 4034), Aafke, Veronique, Qianrui, **Katja**, **Yiming,** and **Germaine**, thanks for being great companions! I would also like to extend my gratitude to all the current and former PhDs and Postdocs at Tox: Aafke**, Annelies, Aziza,** Biyao**,** Chen**, Danlei, Diana, Diego, Donovan, Edith, Felicia, Frances,** Germaine**, Georgia, Ghaliya, Hugo, Isaac, Ixchel, Jiaqi, Jing, Jingxuan, Katharina, Liang, Marta, Maartje, Matteo,** Menno**,** Merel**, Nina, Qianrui, Qiuhui, Shivani, Suparmi, Tessa, Thijs,** Veronique**, Weijia, Wisse, Xiyu, Yasser,** Yiming**.** Thank you for nice time in the lab and wonderful memories of PhD trips, Christmas dinners, and Sinterklaas celebrations.

I would also like to give my warmest thanks to my closest friends. **Rachana**, thanks for being just a call away and a patient listener; **Arianna**, thanks for lifting and cheering me up whenever I felt down; **Jessy**, thanks for being a very considerate friend; **Tamara** and **Goran**, thanks for always motivating me to do my best; **Saurabh** thank you for checking on me from time to time; **Anvita** and **Sudhanshu**, I am forever grateful to both of you for introducing me to my future husband!

My family has been an unwavering support system for me throughout my life. My dearest **Mummy** and **Papa**, thanks for your endless love and encouragement, which made this journey from India to Europe possible; my **Nana** and **Nani**, whatever I am today is because of your teachings since I was a little child; my **Bhaiya** and **Bhabhi**, I am grateful for your guidance and support; and my **Mama** and **Mami**, thank you for all the love. Last but not the least, my fiancé **Janoo**, I am short of words to express my love and gratitude to you. You always have my back and I cannot wait to start our beautiful life together.

Sincere apologies to all those I have unintentionally missed in this section.

I will definitely recall my PhD life as a great teacher that taught me to keep going and never give up!

About the author

Akanksha Roy was born on 27th July, 1992 in Bihar, India. She studied Biotechnology at Banasthali University, India and obtained her Bachelor of Technology in 2015. Subsequently she moved to Munich, Germany to obtain her Masters degree in Biology from Ludwig Maximilian University, and obtained Master of Science in 2018. Thereafter, Akanksha started her PhD in November 2018 in the Netherlands as an Early Stage Researcher of the Marie Sklodowska-Curie European Training Network *trans*Med. During her PhD, she followed the post-graduate program in Toxicology and training program at EU *trans*Med consortium. For her interesting translational research on retinal diseases, she received travel award for presenting her work at XXIV International Symposium on Retinal Degeneration in Nashville, USA. Since Oct 1, Akanksha is working as Commissioning Editor at the publishing company Springer Nature.

List of publications

Roy, A., Groten, J., Marigo, V., Tomar, T., & Hilhorst, R. (2021). Identification of novel substrates for cGMP dependent protein kinase (PKG) through kinase activity profiling to understand its putative role in inherited retinal degeneration. *International journal of molecular sciences, 22*(3), 1180. https://doi.org/10.3390/ijms22031180

Roy, A., Hilhorst, R., Groten, J., Paquet-Durand, F., & Tomar, T. (2021). Technological advancements to study cellular signaling pathways in inherited retinal degenerative diseases. *Current Opinion in Pharmacology, 60*, 102-110. https://doi.org/10.1016/j.coph.2021.07.002

Roy, A., Tolone, A., Hilhorst, R., Groten, J., Tomar, T., & Paquet-Durand, F. (2022). Kinase activity profiling identifies putative downstream targets of cGMP/PKG signaling in inherited retinal neurodegeneration. *Cell death discovery, 8*(1), 1-12. https://doi.org/10.1038/s41420-022-00897-7

Roy, A., Zhou, J., Nolet, M., Welinder, C., Zhu, Yu, Paquet-Durand, F., Groten, J., Tomar, T., & Ekström, P. (2022). Integrative kinase activity profiling and phosphoproteomics of retinal explants during cGMP dependent retinal degeneration (Submitted)

Tolone, A., Haq, W., **Roy, A.**, Fachinger, A., Rentsch, A., Herberg, F., Schwede, F., Tomar, T., Groten, J., & Paquet-Durand, F. (2022). Retinal degeneration: Multilevel protection of photoreceptor and ganglion cell viability and function with the novel PKG inhibitor CN238 (Submitted)

Overview of completed training activities

Courses		
From the clinic to the lab	Lund, Sweden	2018
The problem of drug delivery	Prague, Czech Republic	2019
Practical hands-on training on the making of drug delivery systems	Prague, Czech Republic	2019
Compound synthesis and development	Modena, Italy	2019
Practical hands-on training on retinal cell culture	Modena, Italy	2019
Scientific writing and presentation	TOX-WUR	2019
From the lab to the clinic	Reykjavik, Iceland	2020
Career planning and job hunting	Virtual course	2020
Turning science into business	Virtual course	2021
Clear, engaging and persuasive- scientific writing to stand out	Virtual course	2021
Pharmaceutical development and clinical trial design	Virtual course	2021
Meetings		
XIX International Symposium on Retinal Degeneration	Hybrid event, Nashville, USA	2021
Young Researcher Vision Camp	Leibertingen, Germany	2019
*trans*Med conferences	Sweden, Czech Republic, Italy, Iceland, and Virtual events	2018-2021
Other activities		
Preparation of research proposal	TOX-WUR	2018
Scientific presentations	TOX-WUR, PamGene	2018-2022

The research described in this thesis was financially supported by the European Union Horizon 2020 Research and Innovation Programme- *trans*Med under the Marie Curie grant agreement No. 765441 (*trans*Med; H2020-MSCA-765441).

Financial support from Wageningen University for printing this thesis is gratefully acknowledged.

Layout and printing by ProefschriftMaken | proefschriftmaken.nl